RAIN ATTENUATION MODELING FOR OUTAGE PREDICTION OF FREE SPACE OPTIC LINK UNDER TROPICAL WEATHER

BY

SURIZA AHMAD ZABIDI

A thesis submitted in fulfilment of the requirement for the degree of Doctor of Philosophy

Kulliyyah of Engineering
International Islamic University Malaysia

MARCH 2014

ABSTRACT

In present world, optical fiber is the most emerging and prominent high speed medium of communication. However, optical communication can also be established without fiber and it is known as Free Space Optics (FSO). FSO has attracted a lot of attentions for a variety of applications in telecommunications field. FSO is a line of sight technology allowing optical connectivity without requiring fiber cable or security spectrum licenses. Compare to fiber optic, FSO provides lower cost and shorter time of deployment. Whereas comparing to microwave, FSO offers higher speed, broader and unlimited bandwidth with unlicensed spectrum. Since the transmission of FSO is through atmosphere, there is a variety of detrimental features of the atmospheric channel that may lead to serious signal fading and even complete loss of signal altogether. For FSO signal, the most important obstruction is local weather condition such as fog, snow, cloud, haze and rain. In temperate region, numerous studies and experiments have been conducted and the most limiting factors are found fog and snow. In tropical region with the absence of fog and snow, rain and haze are considered to be the limiting factors. ITU-R has recommended FSO attenuation models which are based on data acquired mainly from temperate climate. Hence to investigate those prediction models using tropical data measurement is required urgently to implement FSO in tropics. Therefore, the focus of this research is to propose new specific rain attenuation parameters that best represent tropical weather condition and to investigate the link availability. A FSO link with 850nm wavelength and 6mW transmit power was installed at International Islamic University Malaysia with 800m link distance. A real time rain intensity and visibility measurement system were installed synchronously with FSO link. Laser power was monitored concurrently with rain intensity and haze. From the concurrent measurement, the effects of rain and haze on FSO link were investigated. Based on one year measurement, modified regression coefficients for ITU-R specific rain attenuation model have been proposed. Preliminary analysis on the effect of haze on FSO and availability of FSO link in tropical climate has been done based on measured data. From the observation, link availability of 99.99% can be achieved for a link distance of 1.25km and fade margin of 25dB. The outcome of this research is expected to give a foundation for the design and development of a long range FSO link under tropical weather condition.

ملخّص البحث

في العالم الحاضر ، والألياف البصرية هي الوسيلة الأكثر سرعة عالية الناشئة وبارز للاتصال. ومع ذلك، يمكن أيضا أن تنشأ الاتصالات البصرية دون الألياف و كما هو معروف البصريات المساحة الحرة (FSO) . وقد اجتذب FSO الكثير من الانتباه لمجموعة متنوعة من التطبيقات في مجال الاتصالات السلكية واللاسلكية . FSO هو خط الأفق التكنولوجيا البصرية مما يسمح لل اتصال دون الحاجة إلى كابل الألياف أو تراخيص الطيف الأمن . مقارنة الألياف البصرية، FSO توفر تكلفة أقل و وقت أقصر من النشر. بينما مقارنة مع الميكروويف ، FSO يقدم سرعة أعلى وأوسع و عرض النطاق الترددي غير محدود مع الطيف غير المرخص . منذ انتقال FSO هو من خلال الغلاف الجوي، و هناك مجموعة متنوعة من الميزات الضارة المترتبة على قناة الغلاف الجوي التي قد تؤدي إلى يتلاشى إشارة خطيرة وحتى فقدان كامل لل إشارة تماما. لل إشارة FSO ، و عرقلة الأكثر أهمية هو حالة الطقس المحلية مثل الضباب والثلوج و السحب ، الضباب و المطر. في المنطقة المعتدلة ، وقد أجريت العديد من الدراسات والتجارب وتوجد أهم العوامل التي تحد الضباب و الثلوج . في المنطقة الاستوائية مع عدم وجود الضباب و الثلج، وتعتبر الامطار والضباب لتكون العوامل التي تحد . وقد أوصى ITU- R نماذج توهين FSO التي تقوم على البيانات التي حصل عليها أساسا من المناخ المعتدل . وبالتالي للتحقيق في تلك نماذج التنبؤ باستخدام مطلوب قياس البيانات الاستوائية على وجه السرعة لتنفيذ FSO في المناطق المدارية . وبالتالي، فإن التركيز في هذا البحث هو اقتراح المعلمات توهين المطر محددة الجديدة التي تمثل أفضل حالة الطقس الاستوائي والتحقيق من توافر الارتباط. تم تثبيت وصلة FSO مع الطول الموجي nm850 و MW6 نقل الطاقة في الجامعة الإسلامية العالمية ماليزيا مع M800 مسافة الارتباط. تم تركيب كثافة الأمطار و قياس مدى الرؤية نظام الوقت الحقيقي بشكل متزامن مع وصلة FSO . تم رصد قوة الليزر بالتزامن مع شدة المطر والضباب . من قياس متزامنة، وقد تم التحقيق من آثار المطر والضباب على وصلة FSO . على أساس قياس سنة واحدة ، تم اقتراح تعديل ل معاملات الانحدار ITU- R محددة المطر نموذج التوهين . وقد تم ذلك تحليل أولي عن تأثير الضباب على FSO و توافر الرابط FSO في المناخ الاستوائي استنادا إلى بيانات قياس . من الملاحظة، يمكن أن يتحقق من توافر الارتباط 99.99 ٪ لمسافة رابط km1.25 وتتلاشى هامش DB25 . ومن المتوقع أن تعطي الأساس ل تصميم وتطوير وصلة FSO بعيدة المدى في ظل حالة الطقس الاستوائي نتائج هذا البحث.

APPROVAL PAGE

The thesis of Suriza Ahmad Zabidi has been approved by the following:

_____
Wajdi Al Khateeb
Supervisor

_____
Md Rafiqul Islam
Co-supervisor

_____
Khalid A.S. Al-Khateeb
Internal Examiner

_____
Syed Alwee Aljunid b Syed Junid
External Examiner

_____
Shamah b Mohd Supa'at
External Examiner

_____
El-Fatih Abdullahi Abdelsalam
Chairman

DECLARATION

I hereby declare that this thesis is the result of my own investigations, except where otherwise stated. I also declare that it has not been previously or concurrently submitted as a whole for any other degrees at IIUM or other institutions.

Suriza Ahmad Zabidi

Signature …… Date ……..

INTERNATIONAL ISLAMIC UNIVERSITY MALAYSIA

DECLARATION OF COPYRIGHT AND AFFIRMATION OF FAIR USE OF UNPUBLISHED RESEARCH

RAIN ATTENUATION MODELING FOR OUTAGE PREDICTION OF FREE SPACE OPTIC LINK UNDER TROPICAL REGION

Affirmed by Suriza Ahmad Zabidi

---------- ----------

Signature Date

ACKNOWLEDGEMENTS

In the name of Allah, the Most Gracious and the Most Merciful

Alhamdulillah, all praises to Allah for the strengths and His blessing in completing this thesis. Special appreciation goes to my supervisor, Assoc. Prof. Dr Wajdi Al-Khateeb, and co-supervisors, Prof Dr Rafiqul Islam and Assoc. Prof Dr Ahmed Wathik Naji for their supervisions, encouragement, guidance and constant support. Also sincere thanks to Prof. Dr. Khalid A.S. Al-Khateeb for his valuable critics and comments.

I would like to express my appreciation to the Dean, Kulliyah of Engineering, Prof Emeritus Dato' Wira Dr Md Noor b Salleh, Deputy Dean of Postgraduate Study, Prof. Dr. Erry Yulian Triblas Adesta and Head of Electrical and Computer Engineering Department, Prof. Othman O.Khalifa for their support and help towards my postgraduate affairs. My acknowledgement also goes to all the technicians and office staffs of Kulliyah of Engineering for their co-operations. Also to MIMOS Bhd. for making this project a successful project with the collaboration between both parties MIMOS Bhd. and IIUM.

Sincere thanks to all my dear friends for their kindness, moral support and prayer during my study. Thanks for the friendship and memories.

Last but not least, my deepest gratitude goes to my beloved husband and children; Dr. Sany Izan b Ihsan, Muhammad b Sany Izan, Zubair b Sany Izan, Muaz b Sany Izan, Sofwan b Sany Izan and Yaasir b Sany Izan for their endless love, prayers, understanding and encouragement. To those who indirectly contributed to this research, your kindness means a lot to me. Thank you very much.

TABLE OF CONTENTS

LIST OF TABLES

LIST OF FIGURES

LIST OF ABBREVIATIONS

FSO	Free Space Optics
IR	Infrared
LAN	Local Area Network
MAN	Metropolitan Area network
RF	Radio Frequency
ITU-R	International Telecommunication Union Sector
GHz	GigaHertz
GLM	Generalized link margin
BER	Bit Error Rate
MODTRAN	Moderate resolution atmospheric Transmission
OptSim	Optical Simulation
FFDI	Fiber Distributed Data Interface
ATM	Asynchronous transfer mode
ESCON	Enterprise System Connection
MMW	Milimeter Wave
GUI	Graphical User Interface
Gbps	Gigabit per second
ML	Maximum-likelihood
MLSD	Maximum-likelihood sequence detection
MVR	Meteorological Visual Range
MMS	Meteorological Services Malaysia
MATLAB	Matrix laboratory

HgCdTe	Heterastructural photodiode
OSI	Open System Interconnection
cPolSK	Circular Polarization Shift Keying
BDF	Bit detect and forward
ABDF	Adaptive Bit Detect and Forward
ADF	Adaptive Decode and Forward
APD	Avalanche photo diode
WDM	Wavelength division multiplexing
VCSEL	Advanced vertical cavity surface emitting laser
SNR	Signal-to-noise-ratio
SONET	Synchronous Optical Networking
CO2	Carbon dioxide molecules
H2O	Water vapour molecules
N2	Nitrogen molecules
O2	Oxygen molecules
CDF	Cumulative distribution function
QKD	Quantum Key Distribution
BB84	Bennett and Brassard 1984 (Quantum Key Distribution scheme)
LOS	Line of sight
PC	Personal Computer
USB	Universal Serial Bus
SSE	Sum of square error
SST	Sum of square total
MOR	Meteorological optical range
TX	Transmitter

RX	Receiver
EXCO	Extinction coefficient
RFC	Request for Comment
IP	Internet Protocol
GigE	Gigabit Ethernet
USB	Universal Serial Bus
MTBF	Mean time between failures
IPv4	Internet Protocol version 4
UDP	User Datagram Protocol

LIST OF SYMBOLS

$N(r)$	Number of water drops
N_0	Rain dependent constant
r	Radius
γ	Rain dependent constant
A_s	Rain specific attenuation
Q	Scattering cross section
D	Drop size
λ	Wavelength
m	Water drop
N(D)	Drop size distribution
k	Power law parameter
α	Power law parameter
d_o	Equivalent rain cell
L, d	Path length
$L_{EFF,}$ d_{eff}	Effective path length
r ,δ	Path reduction factor
R	Rain intensity
$\gamma_{0.01}$	Specific attenuation at 0.01%
C	Probability level
m	Depends on the radio link path and its frequency
β	Best fit equation

$C(L)$	Coefficient
ρ	Distance of decaying rain rate
R_{eff}	Effective rain intensity
μm	Micrometer
mrad	Miliradian
G	Geometric loss
d_r	Receive aperture diameter (m)
d_t	Transmit aperture diameter (m)
θ	Beam divergence (mrad)
L	Distance between transceiver (km)
$erfc$	Error function
Q	Q-factor
π	Pi
$\tau(\lambda, L)$	Transmittance of the atmosphere at wavelength λ
P_R	Received optical power at distance L
P_T	Optical power at the optical source
$\gamma(\lambda)$	Total attenuation/extinction coefficient (m^{-1})
$\beta_{m,a}$	Molecular and aerosol scattering coefficients
$\alpha_{m,a}$	Molecular and aerosol absorption coefficients
V	Visibility
ε	Transmittance
q	Particle size distribution
ε	Residual error (in regression analysis)
R^2	Coefficient of determination

CHAPTER 1

INTRODUCTION

1.1 FREE SPACE OPTICS (FSO) OVERVIEW

Theory of optics started back in 1011 to 1021 by Abu Ali Hasan Ibn Al Hasan Al Haytham or frequently referred to as Ibn Al Haytham. An Unknown scholar at the end of the 12th century or the beginning of the 13th century translated his most famous seven volume book, "Book of Optics", into Latin. In 1572, Friedrich Risner, a German Mathematician, printed Ibn Haytham "Book of Optics" with the title "Opticae Thesaurus" (Wikipedia).

Free space optics (FSO) technology or optical wireless started as early as Claude Chappe's optical telegraph in the 18th century (Bouchet et. a., 2006). In 1880, Alexander Graham Bell patented the photo phone, which modulated light reflected from the sun with a voice signal and transmitted that across free space to a solid-state detector (Korevaar et al., 2003).

In the 1960s with the invention of the laser it facilitated the revolutionized of free space optics. Beside that military organization were particularly interested and boosted the development of free space optics. The technology however lost market momentum when the installation of optical fiber networks for civilian uses was at its peak.

Terminologically, FSO refers to the transmission of infrared (IR) beams or modulated visible beams through the air to obtain optical communications. Similar to fiber optics, free space optics use lasers to transmit data. FSO operates in the infrared (IR) range around 850 and 1550 nm (frequencies around 200 THz) (fSona 2001).

In the industry, cable free optical communication systems is another definition for FSO system (Ricklin et al., 2006). It is a line-of-sight optical technology where voice, video, and data propagate on low-power light beams at speeds of megabytes or even gigabytes per second. A free-space optical link consists of two optical transceivers precisely align to each other with a clear line-of-sight. These transceivers consist of a laser transmitter and a detector to provide full duplex capability. Normally, the optical transceivers mount on building rooftops or behind windows. The working distance of FSO is over several hundred meters to a few kilometres (Bloom et al., 2003).

Table 1.1
Comparison of attributes of free space optics and other technology

	Coaxial Cable	**Microwave Radio**	**Satellite**	**Optical Fiber**	**FSO**
Transmission Speed	500 Mbps	275 Mbps	90Mbps	100 Mbps – 100 Gbps	Varies
Ease of installation	Moderate	Difficult	Difficult	Difficult	Easy
Cost	Moderate	Moderate	Moderate (exclude satellite costs)	High	Low
Advantages	Vulnerable to interference, speed	Speed	Speed, availability	Security capacity, speed,	Cost, bandwidth, speed
Disadvantages	Bulky, difficult to work with	Can be intercepted	Propagation delay, can be intercepted	Difficult to splice and terminate	Highly dependent on local weather
Security	Good	Poor	Poor	Excellent	Fair
Notes	Broadband use is more maintenance intensive	Requires radio license from the FCC	Private Systems not common	Higher speed always on the horizon	New technology

In telecommunications technology, from years to years, show improvement in the telecommunication systems with their own strengths and limitation. Table 1.1 illustrates the comparison of existing technology and FSO system (Baker, 2008).

Some of the advantages of FSO system are as listed below (Bloom, 2002)

- Offer higher speed, broader and unlimited bandwidth
- Most cost effective solution (low cost of deployment)
- Can be deployed within the shortest time frame
- Unlike radio and microwave systems, FSO is an optical technology
- No spectrum licensing or frequency coordination with other users is required
- The transceivers can transmit and receive through windows and mount inside the buildings
- Simplifying wiring and cabling
- Permitting the equipment to operate in a very favorable environment
- Laser beam cannot be detected with a spectrum analyzer or RF meters
- Laser transmission is optical and travel along a line of sight path that cannot intercepted easily
- Laser beams are narrow and invisible, making them harder to find and even harder to intercept and crack
- Data can be transmitted over an encrypted connection.

1.2 APPLICATIONS

Several applications of FSO system are as listed below

- LAN-to-LAN connections on campuses at Fast Ethernet or Gigabit Ethernet speeds.

- LAN-to-LAN connections in a city. Example, Metropolitan area network.
- To cross a public road or other barriers which the sender and receiver do not own.
- Speedy service delivery of high-bandwidth access to optical fiber networks.
- Converged Voice-Data-Connection.
- Temporary network installation (for events or other purposes).
- Reestablish high-speed connection quickly (disaster recovery).
- As an alternative or upgrade add-on to existing wireless technologies.
- As a safety add-on for important fiber connections (redundancy).
- For communications between spacecraft, including elements of a satellite constellation.
- The light beam can be very narrow, which makes FSO hard to intercept, improving security. In any case, it is comparatively easy to encrypt any data traveling across the FSO connection for additional security. FSO provides vastly improved EMI behavior using light instead of microwaves.

Despite of growing interest in the terrestrial FSO application, however, the performance of FSO link is highly dependent on different weather conditions. Local weather condition is the major limiting factor on FSO link propagation. Furthermore, deployment distance and availability of FSO link greatly affected by atmospheric effects therefore not all geographical sites are suitable for FSO link broadband solution (Davide et al., 1986). The outage of the link depends on the link length and on the persistence of adverse weather conditions.

A lot of studies, analysis, and experiments on the effect of weather on FSO link performance conducted in temperate weather condition. The result of weather analysis in temperate region agrees that fog and snow as the main cause of attenuation. In

tropical region, however, various studies, analysis, and experiment are required on the feasibility of deployment FSO link system. Furthermore, this is the region where rain is present throughout the year and haze occurs occasionally without the presence of fog and snow as in temperate regions. Besides that, data from temperate region employ to formulate available specific rain attenuation parameters may overestimate or underestimate the attenuation in tropical region.

It is the aim of this research to analyze, to do simulation, and to use experimental data to predict the specific rain attenuation modeling for FSO link under tropical weather condition by considering the effect of direct rain effect on the link. The other aim is to predict the availability of an FSO link operating in tropical region. Beside that is to investigate the performance of deploying FSO link for a long-range link. The result will give a foundation of designing a long-range FSO link under tropical weather conditions.

1.3 CHALLENGING ISSUES

In the telecommunication system, fiber optics provide an excellent solution for high bandwidth, low error and can serve as the backbone of the internet infrastructure (Willebrand, 2001) However, the cost of deployment is very expensive and time consuming. Furthermore, it is quite impossible to re-deploy the fiber optic cable if the customer relocates or switches to a rivalry service provider.

While for radio frequency (Muhammad et al., 2005), require immense capital investments to acquire spectrum licenses (Ken, 2003). RF technology however cannot scale to optical capacities of several gigabytes. The current RF bandwidth ceiling is 622 megabits. Compared to FSO, RF does not make economic sense for service providers looking to extend optical networks. Furthermore, for a mature technology as

RF, the spectrum already congested and service to provide broadband for high-speed application may no longer be sufficient (Acompora et al., 1999; Chinlon et al., 2001).

Another mature technology is copper. Copper infrastructure is available almost everywhere and the percentage of buildings connected to copper is much higher than fiber. It is still however, not a viable alternative for solving the connectivity bottleneck (Cablefree, 2000). The biggest barrier is bandwidth scalability. Copper technologies may ease some short-term pain, but the bandwidth limitations of 2 megabits to 3 megabits make them a marginal solution.

Due to the above arguments, free space optics has more advantages compare to fiber optics, RF or other wireless systems. Some of the challenging issues of FSO are as follows:

- Actual transmission rates are weather dependent.
- Weather attenuations are variable and hard to predict.
- Distance is limited
- Vendor maximum range specifications can be misleading.
- Lack of standards as of August 2004 ITU still working on 802.16g (Coexistence in License-Exempt bands).
- FSO may not work well in some locations
- Fog, haze, dust storms, scintillation
- Compared to fiber optic higher launch power is required to get useful distance

1.4 FRAMEWORK OF THE RESEARCH

1.4.1 Problem Statement

Regardless of the fact that FSO plays an important role in the built up of high capacity networks require to support the growing bandwidth demand however there are still

limitation due to weather attenuation on the link. The basis of deployment of FSO communication link in tropical region especially in Malaysia is statistical value only without any analysis on the performance and availability done on the link.

In temperate regions, fog and snow are the two limiting factors for FSO link propagation, however, in tropical regions, with the absence of fog and snow, the limiting factor is expected to be rain, and haze. The prediction model for FSO in tropical weather condition using measure data does not exist. There is also no correlation between simulation and real data measurement under tropical weather condition.

Depending on the technical data provides by the manufacturer of FSO equipment, the deployment of short distance FSO link is achievable, therefore, a long link distance of an FSO system need to be analyzed.

Hence, the significance of this research is to provide a useful analysis on the effect of weather, with a focus on rain effect, on FSO link propagation under tropical region. Furthermore, prediction and propose specific rain attenuation model that best represents tropical region will enable the design and enhancement of FSO product according to tropical region weather condition. The specific rain attenuation model also will become a resource for designers of FSO link under tropical weather conditions and in particular in Malaysia; since the deployment of FSO in Malaysia by vendors' base on statistical data without concrete facts on the transmission availability of the FSO. Furthermore, the analysis on the performance of an FSO link in tropical region will improve the equipment reliability and link availability of the future FSO technology in Malaysia for even longer FSO link.

1.4.2 Research Objective

The objectives of the research are as follows

- To predict and propose a new specific rain attenuation prediction parameter specifically for a tropical region
- To perform analysis on the effect of rain intensity variation on FSO link propagation
- To predict the outage/availability of an FSO link under tropical weather condition
- To perform analysis on FSO link performance and long distance FSO link

1.4.3 Research Question

- How well the temperate region attenuation model can work for tropical region?
- How does the rain intensity affect the FSO link under tropical weather?
- How does the variation of rain intensity affect rain attenuation on FSO link?
- How long can we have a successful transmission in tropical weather condition?
- How does available prediction software can predict the performance and availability of tropical weather condition?
- What are the limiting factors in deploying a long-range FSO link?
- What is the availability for a long distance deployment of FSO?

1.4.4 Research Hypothesis

Free Space Optics (FSO) becomes one of the most attractive solutions for high speed, broader bandwidth, shorter deployment time, and low cost communication technology. It is capable of providing data transmission similar to fiber optics, however, only the medium of transmission is different.

An extensive data collection is needed in order to analyze FSO system performance and availability in tropical regions. Real time attenuation modeling can produce accurate attenuation value that best represents tropical weather condition. The non-uniform distribution of rainfall over the link will predict different specific rain attenuation. Furthermore, the non-uniform distribution affects the link distance.

Available specific rain attenuation model might not present an accurate outcome of tropical weather condition since the research performs with temperate region data. Besides that, to evaluate the system performance and to improve the link availability the atmospheric attenuation phenomena should be control.

1.4.5 Research Scope

The scope of the research is to predict and propose empirically specific rain attenuation using measure data for FSO under tropical weather condition. The prediction will be considering the effect of rain intensity variation on FSO. The parameters to consider are the effect of rain and haze on FSO link. Whereas no coverage of scintillation effects in this thesis since the distance deploy is only a short distance. The analysis will use theoretical, calculated and experimental data to propose the specific rain attenuation prediction. Other important factor to consider is the availability or outage of the link operating in tropical region. Besides that, the research also will cover the performance and long distance deployment feasibility of an FSO link.

1.4.6 Research Methodology

Research methodology begins with a comprehensive literature review about the work done in the FSO area in temperate and tropical region, by considering their FSO

parameters evaluation, weather effects parameters, availability analysis and region of deployment. The stages of research methodology are as illustrated below

- Mathematical formula and theoretical analysis
- Site location search
    a. Using Google Earth
    b. Visit site location
- Configuration setup:
    a. FSO system

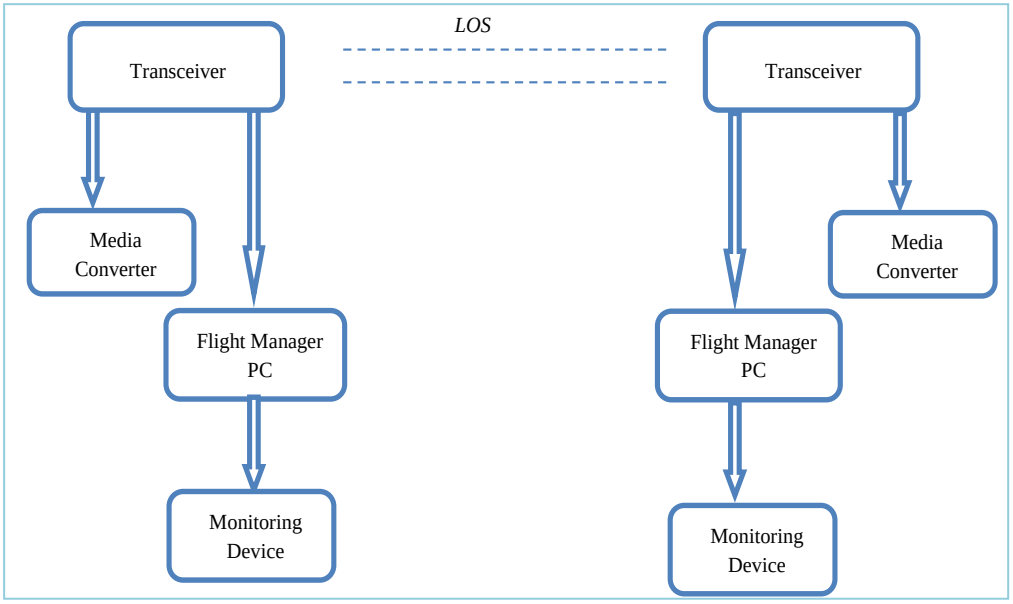

Figure 1.1. FSO system setup configurations

b. Rain measurement equipment

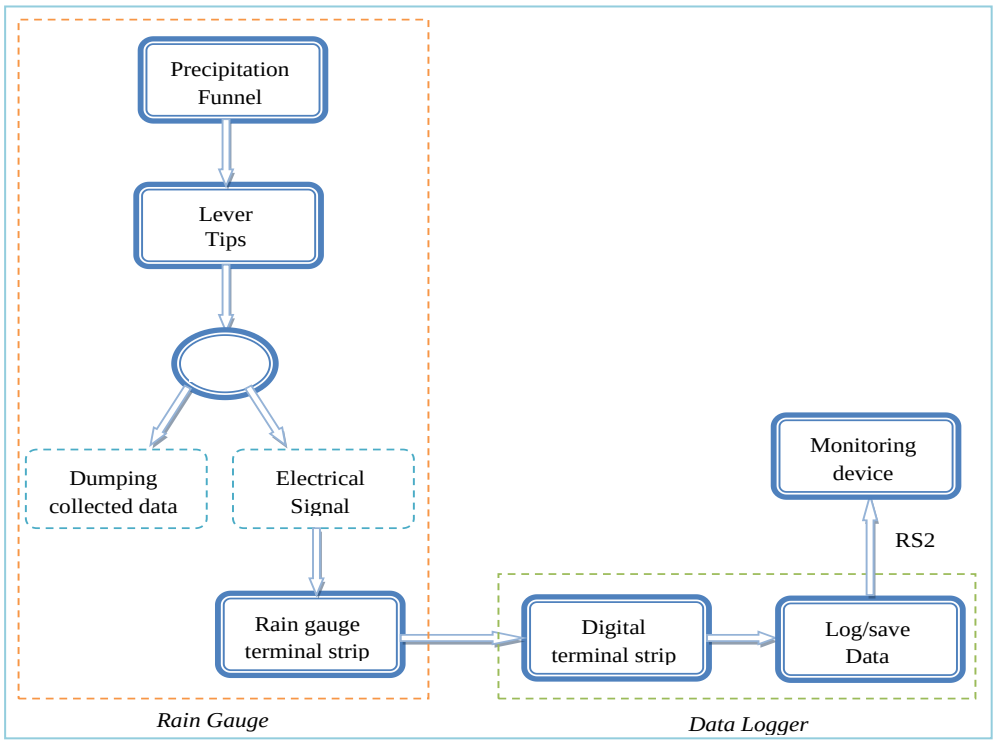

Figure 1.2. Rain intensity meter configuration

c. Visibility meter

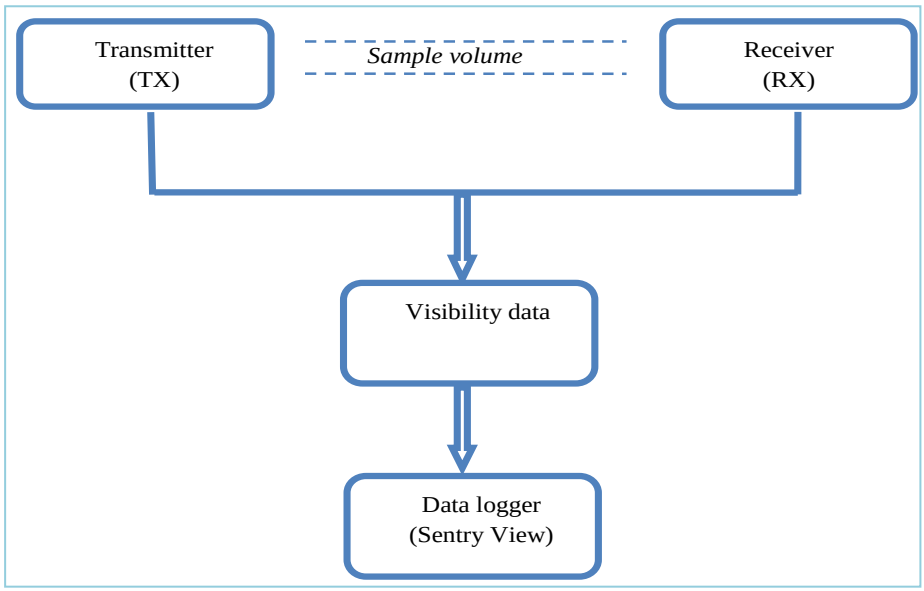

Figure 1.3. Visibility meter configuration

- Integration of rain intensity data, visibility meter and FSO link attenuation to monitor real time attenuation
    a. Rain intensity measurement
    b. Rain attenuation measurement
    c. Visibility measurement
- Rain data and variation result and analysis
    a. Calculation analysis
    b. Experimental analysis
- Outage prediction and availability result and analysis
    a. Simulation analysis
    b. Calculation analysis
- FSO link performance and long distance result and analysis
    a. Calculation analysis
    b. Simulation analysis
    c. Experimental analysis

1.4.7 Expected Outcome

The expected outcome of the research is to predict and propose specific rain attenuation model that best represent the tropical region weather condition. Other outcomes are to have prediction model that can facilitate a broad assessment of FSO deployment under tropical weather condition with the analysis of availability/outage of the link.

The correlation between simulated and experimental data will provide better results in term of system performance and availability under local weather condition.

Base on the measure data and performance analysis, the outcome of long distance deployment is achievable and practicable.

1.5 THESIS ORGANIZATION

This thesis is arranged into six (6) chapters. The introductory chapter covers the overall background of FSO system and the content of the whole research report. In the chapter includes the problem statement, research objectives, research question, research hypothesis, research scope, research methodology and expected outcome.

Second chapter discusses on the review of the available specific rain attenuation models, which is the focus of the research. This chapter also covers review related to modeling specific rain attenuation such as effective path length and reduction factor. Another focus of this chapter is the fundamental of FSO system technology and attenuation. The strength and limitations of the previous works critically reviewed and summarize in a table for easier view.

Third chapter comprises of detail explanation on experimental setup, data measurement and data analysis of FSO system, rain intensity meter, rain intensity variation and visibility meter. Rain intensity variation is discussed in term effective path length and reduction factors for FSO link. Besides that, this chapter discuss on the fundamental of BER analysis and long distance setup.

Fourth chapter explains in detail on the methodology of finding the specific rain attenuation parameters that best represent the tropical region. Validation and benchmarking of the propose parameters is another focal point of this chapter.

Fifth chapter provides analysis on the outage prediction and availability measurement analysis during rain and during haze. Another analysis on this chapter is on the deployment of long distance FSO link.

Sixth chapter concludes this thesis. The conclusion is about the overall findings of this project. For future work, we suggest some recommendations.

1.6 SUMMARY

Some overviews and backgrounds of FSO are highlighted in previous few sub-sections. The introduction of the FSO just to give some insight on what FSO is all about. This chapter discusses on the objectives and motivation on engaging in this research scope.

To justify on the importance of this research, we need to have knowledge of the theory, work done and area of other researchers works. In the following chapter, we present the discussion of literature review to stress on the foundation, theory and previous work on FSO that will be the foundation of our research endeavours.

CHAPTER 2

LITERATURE REVIEW

2.1 INTRODUCTION

In the era of limited bandwidth but faster speed connectivity is needed, free space optics (FSO) emerge as one of the most viable alternatives. Technologically, FSO is similar to fiber optic communication. The medium of transmission for FSO is atmosphere while fiber optic is through fiberglass in the fiber cable. Since their technologies are similar, they share the same advantages such as higher speed, unlimited bandwidth and protocol independent. However, in terms of cost and time for deployment, FSO is cheaper and the deployment time is shorter since no cable needed for FSO link, which reduce the time and cost significantly. Despite of all the advantages, weather condition is the limiting factor of an FSO link since its use atmosphere as the medium of transmission.

In tropical regions, with the absent of fog and snow, rain and haze are expected to be the major restrictive aspect in FSO link transmission. Various rain rate and specific rain attenuation models have been developed and used in communication systems especially in terrestrial microwave and satellite system (Mandeep et al., 2007).

The prediction of rain attenuation model can be done in two methods (Ojo et al., 2008) - empirical method or analytical method. The empirical method is based on regression model that provide the best fit between observed attenuation distribution and observed rain-rate distribution with 1-minute integration (Crane et al., 1997; Zhou et al., 2009). The calculation of rain prediction is using analytical method from the cumulative distribution of the mean annual rainfall. Empirical method is the most

commonly useful methods for specific rain attenuation prediction from available rain intensity data (Zhou et al., 2009; Moupfouma, 1985).

In FSO communication system, prediction of specific rain attenuation models developed with data measured in temperate regions proved inaccurate for tropical rain (Bryant, 1998; Dijk et al., 1983; Paraboni et al., 1997)

This chapter will discuss on the available specific rain attenuation model in microwave, satellite and FSO area. Accurate specific rain attenuation prediction needs to consider the effective path length on which the area the rain falls on the propagation link. Once knowing the rain attenuation, outage prediction can be determined. This chapter also cover the discussion on long distance FSO deployment and view of general design of FSO system and technology.

2.2 SPECIFIC RAIN ATTENUATION MODEL IN MICROWAVE / SATELLITE COMMUNICATION

Rainfall exists due to non-selective scattering, which is wavelength independent (Achour, 2002b). Rain attenuation is generally does not affected a system with signal frequencies below 10 (Achour, 2002a). However, rain attenuation takes effect on a system with signal frequencies above 10GHz, which is in the case of FSO system (Hasan et al., 2011).

Specific rain attenuation models accepted worldwide are ITU-R model and Crane model. Moupfouma model is among other available model. Models that relate closely to tropical rain attenuation are Jafri model and Mandeep model. The following sub-section will discuss on the available specific rain attenuation model in for microwave and satellite link.

2.2.1 ITU-R Model

ITU-R method (ITU-R P.530-13, 2009) is based on rain rate at R0.01 exceeded in 0.01% of the time. The integration time is 1 minute. ITU-R formula for specific rain attenuation model is as in Equation (2.1)

$$A = aR^b \tag{2.1}$$

Where a and b are functions of frequency and rain temperature and computed from interpolating of values given in ITU-R 838 (ITU-R P.838, 2005). R is rain rate of $R_{0.01}$ (obtain at 1-minute integration time with rain rate exceeded at 0.01% of the time).

The accuracy of rain attenuation prediction requires consideration of the effective path length. The effective path length computed by multiplying the actual path length and by a reduction factor

$$r = \frac{1}{1+{}^{d}/_{d_0}} \tag{2.2}$$

Where d is the actual length and d_o is as in Equation (2.3) and (2.4)

For $R_{0.01} \leq 100$ mm/h $\quad d_o = 35\, e^{-0.015R_{0.01}}$ (2.3)

For $R_{0.01} > 100$ mm/h $\quad d_o = 35\, e^{-1.5}$ (2.4)

Therefore, estimation of rain attenuation for 0.01% becomes

$$A_{0.01} = Ad_{eff} = Adr \quad (dB) \tag{2.5}$$

In other percentage of time, Equation (2.6) represented as

$$\frac{A_p}{A_{0.01}} = 0.12p^{((0.546+0.043\ \log_{10} p)} \tag{2.6}$$

Where p are values in the following range 1%, 0.1%, 0.01%, and 0.001% which give the following factor 0.12, 0.39,1, and 2.14 respectively.

2.2.2 Crane Model

Crane model is a well-known model for specific attenuation due to rainfall. Regression coefficient and the rain rate of interest are used to determine specific rain attenuation (Crane, 1996).

Equation (2.7) is a Crane attenuation model

$$A = kR^{\alpha}(e^{y.\delta} - 1)/y \text{ dB} \quad 0 < \text{d} < \delta(\text{R}) \text{ km} \tag{2.7}$$

And

$$A = kR^{\alpha}\left(\frac{e^{y.\delta}-1}{y} + \frac{(e^{zd} - e^{z}\delta(R).e^{0.83-0.17\ln(R)}}{z}\right) \quad \text{dB} \tag{2.8}$$

$$\delta(R) < d < 22.5\ km$$

Where $\delta(R)$ is a function of rain rate

$$\delta(R) = 3.8 - 0.6\ln(R) \quad km$$

And d is link distance in km, while y id defines as

$$y = \alpha\left(\frac{0.83-0.17\ln(R)}{\delta(R)} + 0.26 - 0.03\ln(R)\right) \tag{2.9}$$

And

$$z = \alpha(0.026 - 0.03\ln(R) \tag{2.10}$$

2.2.3 Moupfouma Model

The empirical relationship of kR_p^{α} by Olsen (Olsen, 1978) is the foundataion of Moupfouma model (Moupfouma, 2009). The rain rate under consideration is $R_{0.01}$ (mm/hr) exceeded in 0.01% of the time. The specific rain attenuation is represented by $\gamma_{R_{0.01}}$ on the microwave link and is shown below

$$\gamma_{R_{0.01}} = kR_{0.01}^{\alpha} \tag{2.11}$$

Where k and α is managed by radio link functioning frequency.

To overcome the non- uniformity of rainfalls along the propagation link, the equivalent path length, L_{eq} is used rather than the actual path length. Therefore the induce attenuation $A_{0.01}$ exceeded for 0.01% of time can be deduced as follows

$$A_{0.01} = \gamma_{R_{0.01}} \times L_{eq} \tag{2.12}$$

and

$$L_{eq} = l\, r \tag{2.13}$$

Where l is the actual path length and r is the reduction factor.

The detailed discussion on reduction factor is in section 3.3.1.

2.2.4 Jafri Din Model

Jafri Din's model (Jafri Din, 1997) use Drop Size Distribution measurement to formulate the specific rain attenuation parameters. The calculation of the specific rain attenuation model is as follows

$$A_s = 4.343 * 10^3 \frac{\lambda^2}{\pi} \sum Re\left[S_{H,V}(0)\right] N(D) \Delta D \tag{2.14}$$

Where λ (m) is the wavelength, *N(D)*Δ (per cubic meter) is the drop size distribution and $S_{H,V}(0)$ is the amplitude of forward scattering. $S_{H,V}(0)$ is from numerical calculations. Whereas A_s depends directly on *N(D)* which can be obtained from distrometer measurement on the ground or by radar, satellite or microwave indirectly measurement.

Equation (2.14) – (2.16) presented the relationship between drop size distribution *N(D)* parameters and rain rate (R),

$$N_t = a_0 R^{b_0} \tag{2.15}$$

$$\mu = a_\mu + b_\mu \ln R \tag{2.15}$$

$$\sigma^2 = A_\sigma + B_\sigma \ln R \tag{2.16}$$

Where μ is the mean of *ln(D)*, σ are the standard deviation of *ln(D)* and N_t is the total number of drops for every diameter interval. Rain rate (R) can be calculated from *N(D)* using Equation (2.17)

$$R = 6\pi * 10^{-4} \int V(D) D^3 N(D)\, dD \qquad (2.17)$$

Where $V(D)$ (m/s) is the raindrops terminal velocity, D is the drop diameter and $N(D)$ is the drop size distribution. Regression analysis use to obtain Equation (2.14), (2.15) and (2.16).

Therefore, using Equation (2.14), (2.15) and (2.16), for any path length we can determined rain attenuation but with a constraint, that rain falls uniformly along the propagation path.

2.2.5 Mandeep Model

The model (Mandeep, 2011) is based on a modified model of ITU-R with data 3 years data measurement. The acquire data is on rainfall rate and rain attenuation in USM Nibong Tebal from satellite SuperBird-C.

The formula for other percentage of time is as shown in Equation (2.18).

$$A_p = A_{0.01} \left(\frac{p}{0.01}\right)^{-0.3061 + 0.0524 \ln(p) + 0.045 \ln\left(A_{0.01}\right) + \beta(1-p)\sin\theta} \text{ dB} \qquad (2.18)$$

Where

$$\beta \begin{cases} 0 & if\ p \geq 1\% \\ -0.005(|\varphi| - 36 & if\ p < 1\% \end{cases}$$

And p is the percentage probability (except for 0.01%), β can be determined by φ (the latittude of the earth station), θ is the elevation angle of antenna and $A_{0.01}$ is the rain

attenuation exceeded at 0.01% of the time. It can be calculated from the following equation

$$A_{0.01} = \gamma_R L_E \text{ dB} \tag{2.19}$$

Where

$$\gamma_R = kR_{0.01}{}^{\alpha} \tag{2.20}$$

And L_E is the effective path length

$$L_E = L_R V_{0.01} \text{ km} \tag{2.21}$$

Where $V_{0.01}$ is the vertical adjustment reduction factor and can be calculated as in Equation (2.10)

$$V_{0.01} = \frac{1}{1+\sqrt{sin\theta\,(31\left(1-e^{-(\theta/(1+x))}\right)\frac{\sqrt{L_R Y_R}}{f^2}-0.45)}} \tag{2.22}$$

In (Mandeep et al., 2007), the value of k and α is given as

$$A = 0.1245R^{1.058} \text{ dB/km} \tag{2.23}$$

Where R (mm/hr) is the rain rate.

2.3 SPECIFIC RAIN ATTENUATION MODEL IN FREE SPACE OPTICS COMMUNICATION

In FSO, there are two models of specific rain attenuation recommended by International Telecommunication Union Sector (ITU-R) (ITU-R P.1814, 2007). In Table 2.1 presents specific rain attenuation model of ITU-R and other few prediction models used for FSO in temperate region (Bouchet et al., 2006).

Table 2.1
Rain attenuation prediction model for FSO recommended by ITU-R

Model	Origin	Author	k	α	Note
Carbonneau	France	ITU-R	1.076	0.67	Temperate region
Japan	Japan	ITU-R	1.58	0.63	Temperate region
J.Joss	Switzerland	Bouchet	0.509	0.63	Temperate region Drizzle or light rain (R<3.8 mm/hr)
J.Joss	Switzerland	Bouchet	0.319	0.63	Temperate region Mean rain (3.8<R<7.6 mm/hr)
J.Joss	Switzerland	Bouchet	0.163	0.63	Temperate region Convective rain (R>7.6 mm/hr)
Marshal & Palmer	Canada	Bouchet	0.365	0.63	Temperate region

2.3.1 Japan Model

Rain particles can cause excess attenuation by causing the angular redistribution of the incident flux; known as scattering. The physical size of the scatters with respect to the transmission laser wavelength determined the scattering type. Particle with larger than the wavelength, the scattering is wavelength independent which is the case of raindrops. This model use raindrop size distribution to calculate the attenuation due to rain (Aburakawa, 2002). Equation 2.24 shows mathematically the relation of drop size distribution due to rain on the propagation link (ITU-R F.2106-1, 2010).

$$A_{tt_{rain}} = 27.29 \times 10^5 \int_0^\infty r^2 . fl \, dr \qquad (2.24)$$

Where r is the diameter of raindrops (m). fl is given by the statistical data of rainfall rate and given as presented in Equation (2.25).

$$fl = B \exp(CR^k r) \qquad (2.25)$$

Based on Marshal and Palmer model: B = 0.16 C = -82 k = -0.21

The rain attenuation is then as presented in Equation (2.26)

$$A_{tt_{rain}} = \alpha \times R^{\beta} \quad (2.26)$$

The Japan specific rain attenuation parameter (ITU-R P.1814, 2007) is as stated in Equation (2.27)

$$A = 1.58 \times R^{0.63} \quad (2.27)$$

2.3.2 Carbonneau Model

Specific rain attenuation power law is given by (ITU-R P.1814, 2007)

$$\gamma_{rain} = k.R^{\alpha} \quad (2.28)$$

Where k and α depend on the rain characteristic and R (mm/hr) is the rain rate. The pluviometers or weather radar can measured rain intensity, R (mm/hr) directly.

We can estimate the attenuation coefficient from the raindrop size distribution of Marshal and Palmer. The model is as mentioned in section 2.2.1. The attenuation coefficient for Carbonenau (Carbonneau et. al., 1997) is as shown in Equation (2.29)

$$A = 1.076 \times R^{0.67} \quad (2.29)$$

2.3.3 Marshal and Palmer Model

Rain attenuation is most severe and greatly dependent on raindrop-size distribution (Ishii et al., 2010). The most commonly used raindrop size distributions are Marshal and Palmer (Marshal et al., 1948). Marshal and Palmer distribution proposed renowned empirical expression by fitting their data and the Laws and Parsons data (Laws et al., 1943). Equation (2.30) presented Marshal and Palmer distribution.

$$N(r)=N_0 e^{-\gamma r} \quad (2.30)$$

Where, $N(r)dr$ is the number of water drops per unit volume whose equivalent radius lies between r and $r+dr$. N_0 (in m^{-3} mm^{-1}) with accepted value of $N_0 = 16 *$

$10^3 m^{-3} mm^{-1}$ and γ (in mm^{-1}) are experimentally determined constant and they depend on the type of rain under consideration (Bouchet et al., 2006). Accepted values for $\gamma = 8.2R^{0.21} mm^{-1}$ where R is the rain intensity, mm/hr. Specific rain attenuation A in dB/km is calculated by integrating all of the raindrop-size as

$$A = 4.323 \int Q(D, \lambda, m) N(D) dD \quad (2.31)$$

Where Q is the attenuation cross section that is a function of the drop diameter, D is the wavelength of the radio wave λ, and the complex refractive index of the water drop m, which is a function of the frequency and the temperature, and $N(D)$ is the drop size distribution (Harrold, 1967). From the given equation, the calculation of specific rain attenuation in either microwave or FSO is the same and it is globally accepted. A power law as shown in Equation (2.32) represents rain specific attenuation

$$A = kR^{\alpha} \quad (2.32)$$

Where R is the rain rate in mm/hr, k & α are power law parameters. The power law parameters depend on frequency, raindrop size distribution and rain temperature. For calculating the attenuation, it is adequate to assume that raindrops have a spherical shape. This assumption makes k & α independent of polarization (Zhang et al., 1999).

The attenuation coefficient for Marshal and Palmer is as in Equation (2.33)

$$A = 0.365 \times R^{0.63} \quad (2.33)$$

2.3.4 J.Joss Model

Joss (Bouchet et al., 2006; Joss et al., 1968; Olsen et al., 1978) model uses drop size distribution to find k and α values pertinent to rainfalls in the widespread and convective rain. Joss divides the rain into three type's namely convective rains,

continuous rain and drizzle. Joss uses negative exponential distribution obtained by fitting the average size spectrum of very light widespread rain or drizzle (composed mostly of small drops). The value of N_0 and γ for the Joss model parameter is derived according to the rain type as shown below

Convective rain $N_0 = 28 * 10^2 m^{-3} mm^{-1}, \gamma = 6R^{0.21} mm^{-1}$ (2.34)

Continuous rain $N_0 = 14 * 10^3 m^{-3} mm^{-1}, \gamma = 8.2R^{0.21} mm^{-1}$ (2.35)

Drizzle $N_0 = 6 * 10^4 m^{-3} mm^{-1}, \gamma = 11.4R^{0.21} mm^{-1}$ (2.36)

The attenuation coefficients for J.Joss model are as in Equation (2.37) – (2.39)

For R<3.8 mm/hr $A = 0.509 \times R^{0.63}$ (2.37)

For 3.8<R<7.6 mm/hr $A = 0.319 \times R^{0.63}$ (2.38)

For R>7.6 mm/hr $A = 0.163 \times R^{0.63}$ (2.39)

From the listed rain intensity, it is shows that J.Joss Marshal is not comparable to the high rain intensity under tropical weather condition.

In order to have an accurate prediction of specific rain attenuation, we need to consider the effective path length. Effective path length can be analyzed in term of reduction factor. The following section will focus on rain locality discussion on the available model of reduction factor.

2.4 RAIN LOCALITY CONSIDERATION

Development of specific rain attenuation prediction required 3 steps as mention in Crane (Crane, 1996);

i. At the percentage of time of interest, the rainfall rate in mm/hr need to be determined

ii. At the selected rainfall rate, the specific attenuation of the signal in dB/km needs to be calculated

iii. The effective length of the propagation needs to be carefully estimated

Non-uniformity of rain rate along the propagation path reduces the effective path length. One definition of effective path length is the average length of the intersection between the path and the rain cell (Silva Mello et al., 2006). The effect of the non-uniform rainfall along the propagation path represent by a rain cell which is an equivalent cell of uniform rainfall rate and length, d_o. Interception can occur to the propagation of the link by equivalent rain cell at any position with equal probability. In non-technical language, the effective path length is the area in which the rain falls on the propagation link. The rain might not fall on the entire propagation path, but it falls on the area that we call effective length of the link. Demonstration of the terminology is as in Figure 2.1.

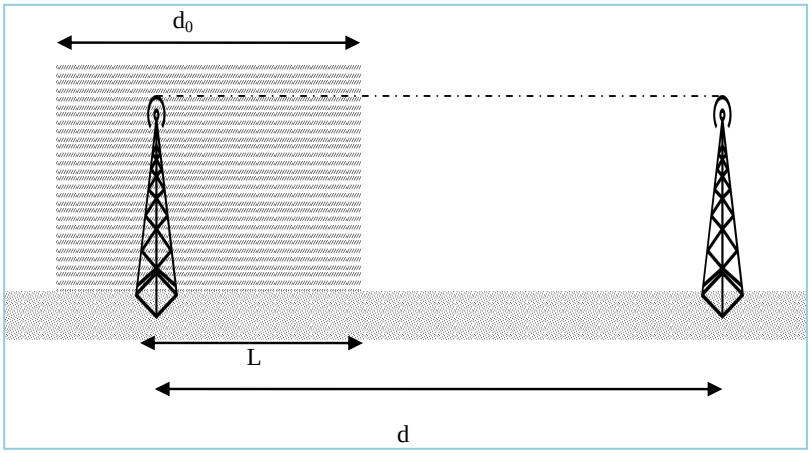

Figure 2.1. Effective path length

Empirically, the equivalent rain cell, d_o, is derived from the path length, d and experimental data. In (Pontes et al., 2007) it states that the equivalent raincell d_o depends on the long-term point rainfall rate measured in the region. In the above model d_o is an exponentially decaying function of the point rainfall rate R (mm/hr).

Mathematically, L_{eff} is presented as (Silva Mello, 2007):

$$L_{eff} = \frac{1}{d_o + d} \int_{d_0}^{d} L(x)dx = r.d = \frac{1}{1+{}^{d}/_{d_o}} d \tag{2.35}$$

where $$d_o = 119R_{0.01}^{-0.244}$$

The simplest model of L_{eff} is stated in ITU-R (ITU-R P.530-8, 1999) as

$$L_{eff} = r \times d \tag{2.36}$$

Equation (2.36) stated that effective path length, L_{eff} depends on the reduction factor, r and actual path length, d, Based on ITU-R recommendation, the rain specific attenuation (Olsen et al., 1978) is presented as in Equation (2.37)

$$A = A_s L_{eff} \tag{2.37}$$

Where A_s is the rain specific attenuation as in Equation (2.38)

$$A_s = kR^{\alpha} \tag{2.38}$$

Where k and α are regression coefficient obtained after carrying out regression on the raindrop size distribution with known calculated values of specific attenuation for certain range rain rate.

From Equation (2.39), effective path length, L_{eff}, depend on the path length, d and the reduction factor, r, as shows in Equation (2.39) (Perez Garcia et al., 2004)

$$r = \frac{L_{eff}}{d} \tag{2.39}$$

The model can be used to predict the corresponding value of rain attenuation of $A_{0.01}$ At the rainfall rate exceeded at 0.01% of the time, $R_{0.01}$ as presented in Equation (2.40)

$$A_{0.01} = \gamma_{0.01} d_{eff} = k(R_{0.01})^{\alpha} . \frac{d}{1+d/d_o(R_{0.01})} \tag{2.40}$$

Where $\gamma_{0.01}$ is the specific attenuation and k and α are parameters of specific attenuation. If no measured value of k and α is available, the value given by ITU-R can be used.

2.4.1 Reduction factor models

The analysis of reduction factor is due to the effect of rain on the propagation link is discussed in microwave (Khamis, 2005), radar (Khamis et al., 2005) and satellite signal (Abdulrahman et al., 2010). Analysis on the effective path length is required to predict accurately the specific rain attenuation. As mentioned in the previous section, the effective path length depends on the reduction factor and the actual path length.

Some of available and widely utilize reduction factor analysis and models are Lin Model, Moupfouma Model, Assis Model, Dissanayake and Allnutt Model, ITU Model, Silva Mello model (Silva Mello et al., 2007) and Abdulrahman model (Abdulrahman et al., 2011). In FSO however, there exist no model for reduction factor analysis. The available mathematical reduction factor formula is utilized for the purpose of the analysis in this thesis

2.4.1.1 Lin Model

Lin model (Lin, 1977) is as presented in Equation (2.41), it takes into account the factor for the partially correlated rain variations along the propagation path of

length, L,

$$r = \frac{1}{1+\frac{L}{L(R)}} \tag{2.41}$$

and $$L(R) = \frac{2636}{R-6.2} \text{ (km) for R>10 mm/hr} \tag{2.42}$$

$L\ (R)$ is approximately calculated base on distribution measurement of five (5) minute point rain rates from August 1973-July 1974 with rain attenuation is at 11 GHz on the 42.5 km path. Partially correlated rain variations along the propagation path is related to the diameter of a rain cell in such that non-linear factor in Equation (2.41) equals one half when $L= L\ (R)$. Lin model, however, largely overestimates the measured values at higher rain rates.

2.4.1.2 Moupfouma Model

Moupfouma model (Moupfouma, 1984) derived from experimental data obtained from 30 terrestrial links in the 7-38GHz band range. The links located in Congo, Japan, U.S. and Europe with path length up to 58 km. Equation (2.43) shows the Moupfouma reduction factor model.

$$r = \frac{1}{1+CL^m} \tag{2.43}$$

C depends on the probability level of interest, P (percent), and m depends on the radio link path and its frequency. Therefore, Moupfouma path reduction factor can be represented as

$$r = \frac{1}{1+0.03\left(\frac{P}{0.01}\right)^{-\beta}.L^m} \tag{2.44}$$

and $$m(f,L) = 1 + 1.4 * 10^{-4} f^{1.76} \log_e L \tag{2.45}$$

where f(GHz) is the frequency, L is the actual path length (km), and β coefficient is given as a result of best fit by

For $L \leq 50$ km

$\beta = 0.45$ for $0.001 \leq$ P(percent) ≤ 0.01

$\beta = 0.6$ for $0.01 <$ P(percent) ≤ 0.1

For $L > 50$ km

$\beta = 0.36$ for $0.001 \leq$ P(percent) ≤ 0.01

$\beta = 0.6$ for $0.01 <$ P(percent) ≤ 0.1

Moupfouma calculation considered the frequency of the equipment in GHz, while FSO equipment is in Terahertz that gives unreasonable results when calculating the r. The revised Moupfouma model (Tusubira et al., 2003), however, is employed for Terahertz equipment. Revised Moupfouma model using empirical data derives from the distribution extension introduced the value of m = 1.02286. The empirical data collected over a period of six months and the distribution technique used to extend the data to cover the recommended minimum one-year measurement period.

Equation (2.46) presented the revised Moupfouma model

$$r = \exp\left(\frac{-R_{0.01}}{1+C(L)*R_{0.01}}\right) \quad (2.46)$$

Where $C(L) = -100$ for $L \leq 7$ km

$C(L) = \left(\frac{44.2}{L}\right)^{0.78} - 100$ for $L > 7$ km

2.4.1.3 Assis Model

Assis model (Assis, 1990) established on the assumption of the exponential distribution attribute of the rain cell and is presented as in Equation (2.47)

$$r = \frac{1}{y}[1 - e^{-y}] \quad (2.47)$$

Where $= bL/2\rho$, ρ is the distance at which the rain rate decays by a factor of 1/e in an exponential rain cell model and b is actually the value of α, the parameter given in

Equation (2.36). The path length L is limited to L < 20.7 km and ρ for a tropical region is as presented in Equation (2.48)

$$\rho = 65.4R^{-0.695} \tag{2.48}$$

2.4.1.4 Dissanayake and Allnutt Model

Dissanayake and Allnutt model (Dissanayake et al., 1992) based on lognormal rain rate, path attenuation distribution and neglects frequency dependence. This reduction factor model is applicable for each region defined by ITU-R distribution rain regions and as expressed in Equation (2.49)

$$r = \frac{1}{1+y+x\sqrt{A_S L}} \tag{2.49}$$

Where L (km) is the path length, A_s (dB/km) is specific attenuation and x, y, are coefficients that largely depends on the rain rate distribution, the rain spatial correlation function and percentage of time concerned. The value use of terrestrial path at 0.01% of time for x and y are x = 0.194 and you = -0.372.

2.4.1.5 ITU-R Model

ITU-R model (ITU-R P.530-8, 1999) derived reduction factor by the considering rain rate, $R_{0.01}$, for 0.01% of time.. This model is valid for a path length up to 60 km. The ITU-R model is a shown in Equation (2.50)

$$r = \frac{1}{1+\frac{L}{L_o}} \tag{2.50}$$

Where L (km) is the actual path length and L_o corresponds to

$$L_o = 35e^{-0.015R_{0.01}} \qquad \text{for } R_{0.01} \leq 100\text{mm/hr}$$

$$L_o = 35e^{-1.5} \qquad \text{for } R_{0.01} > 100\text{mm/hr}$$

2.4.1.6 Silva Mello Model

Silva Mello model (Silva Mello et al., 2007) proposed a new semi-empirical prediction method to address the problems found in current ITU-R method. Equation (2.51) illustrates the derive model of reduction factor.

$$r = \frac{1}{1+({}^{d}/_{d_o})} \tag{2.51}$$

Where

$$d_o = 119R^{-0.244} \tag{2.52}$$

The concept of an effective rainfall is introduced by Silva Mello model to avoid inconsistencies and retain the general expression for the effective path length, d_{eff}. The cumulative distribution of rain attenuation obtains from the distribution of rainfall rate in the links region by

$$A_p = \gamma . d_{eff} = k[R_{eff}(R_{p,d})]^{\alpha} . \frac{d}{1+{}^{d}/_{d_o(R_p)}} \tag{2.53}$$

and

$$R_{eff} = 1.763R^{0.753+0.197/d} \tag{2.54}$$

Using the full rainfall rate distribution, the rain attenuation distribution can be expressed as shown in Equation (2.55)

$$A(p) = k\left[1.763.R_p^{0.753+\frac{0.197}{d}}\right]^{\alpha} . \frac{d}{1+d/(119R_p^{-0.244})} \tag{2.55}$$

k and α is from ITU-R if local measured data about specific rain attenuation data is not available.

2.4.1.7 Abdulrahman Model

Abdulrahman model (Abdulrahman et al., 2011) proposed the path reduction factor as adopted by ITU-R. The relationship between the equivalent rain cell diameter (d_o) and

the path reduction factor at 0.01% of the time $\delta(R_{0.01}, d)$ is as in Equation (2.56)

$$\delta(R_{0.01}, d) = \frac{1}{1+d/d_o} \quad (2.56)$$

And

$$d_o = 2.6379 R_{0.01}^{0.21} \quad (2.57)$$

The effective path length, L_{eff} as in Equation (2.58) can be derived by substituting Equation (2.57) into Equation (2.56) and multiplying by the path length of the link

$$L_{eff}(R_{0.01}, d) = \frac{d}{1+\left(\frac{d}{2.637 R_{0.01}^{0.21}}\right)} \quad (2.58)$$

2.5 FSO SYSTEM PARAMETERS

The atmosphere of the earth comprises of a series of concentric gas layer as shown in Figure 2.2 (Wikipedia).

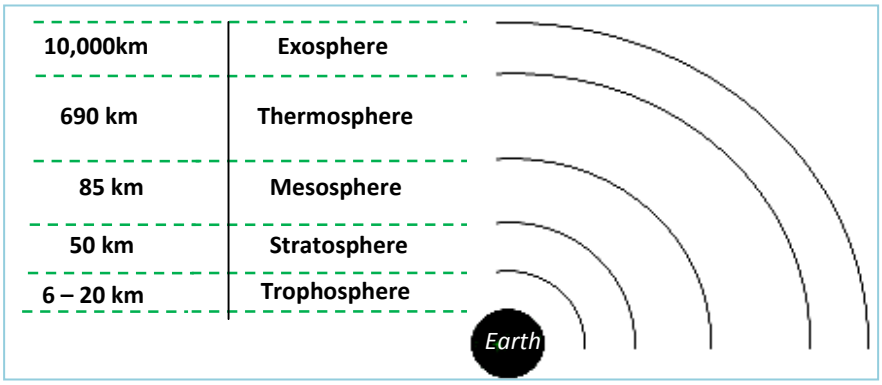

Figure 2.2.Atmospherics layers

In FSO telecommunication, the troposphere layer is the one where most of the weather phenomena occur. The influences of propagation of light in the troposphere are: (Bouchet et al., 2005):

The gas composition of the atmosphere

- Presence of aerosol, that is small particles of variable size (ranging from 0.1 to 100µm) in suspension in the air
- Hydrometeors such as rain, snow, and hail
- Lithometeors such as dust, smoke and sand
- Modifications of the gradient and refractive index of the air (propagation medium) are at the source of scintillation and turbulence.

Atmospheric effects that affected FSO link propagation are low clouds, heavy rain, fog, alignment, building sway, line-of-sight obstruction and scintillation. The summary of the effect is as shown in Figure 2.3

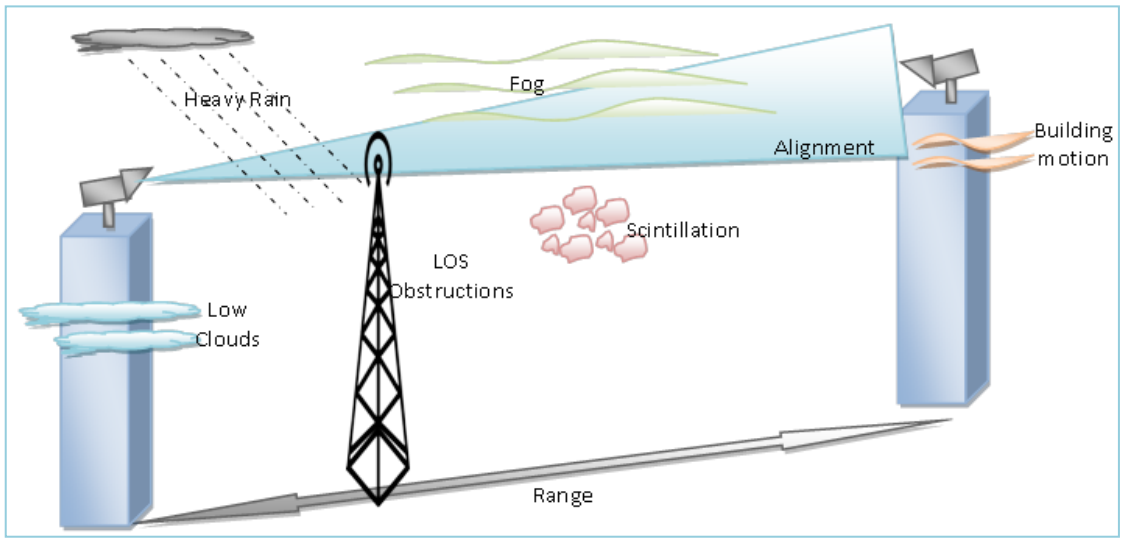

Figure 2.3. Environmental effect on FSO link

Before going into details on the atmospheric effect on the FSO link, it is important to take into consideration of several FSO system parameters. There are two different categories of the parameters (Bloom et al., 2003): internal parameters and external parameters. Internal parameter is related to the design of an FSO system which include optical power, transmission bandwidth, wavelength, optical loss on the transmit side, divergence angle, receiver sensitivity and bit-error-rate. External parameter or non-system-specific parameters are atmospheric attenuation, scintillation,

deployment distance, window loss, pointing loss and visibility. The schematic in Figure 2.4 detail out the internal and external FSO system design parameters (Lightpointe, 2009a):

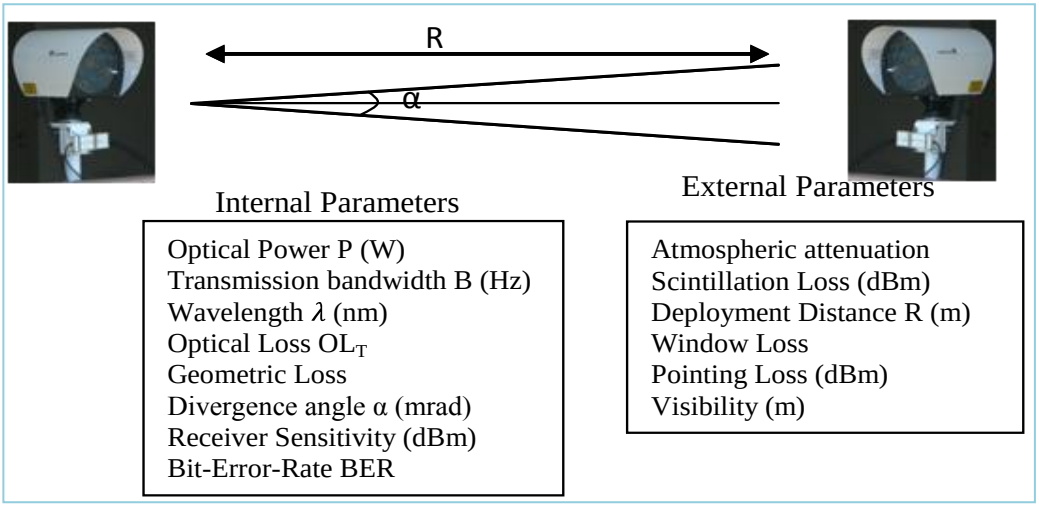

Figure 2.4. External and Internal Parameters of FSO

However, we need to address the overall system performance of a link first and then follows with the parameters that will affect the performance of FSO link. Link margin or link budget quantified the overall system performance.

2.5.1 Link Margin

Link margin is the prediction calculation of how much margin or extra power is available in a link under any particular set of operating condition (Bloom et al., 2003). The integration of the link margin and model of atmospheric attenuation used to calculate expected availability base on the losses from both scattering and scintillation. The calculation of link margin will have the following inputs: transmit power, receive sensitivity, optical losses, geometric losses and miss-point or alignment loss.

The amount of energy transmitted by the FSO system is called the transmit power. Receiver sensitivity is the amount of optical energy that received by the FSO system for a specific error rate. In other word, receiver sensitivity is a measure of how faint the signal successfully received by the receiver. The lower the power that the receiver can successfully process defines better receiver sensitivity (Tropos, 2007). Optical system losses include scatter, surface reflection, absorption, and overfill losses. Geometrical loss is a loss that occurs due to the spreading of the transmitted beam between the transmitter and receiver.

The expression of link margin is as stated in Equation 2.59 (Bouchet et al., 2005; Kolka et al., 2007):

$$Link\ Margin,\ L_M(dB) = P_R - S_r \tag{2.59}$$

Where P_R is power received (dBm) and S_r is sensitivity (dBm)

The power received is as shown below:

$$Power\ received\ (dBm) = P_T - Loss_{Tot} \tag{2.30}$$

Where P_T is power transmitted (dBm) and $Loss_{Tot}$ is total loss. With FSO, total losses are geometrical loss, optical loss, equipment loss and atmospheric attenuation loss.

Therefore link margin can be represented as

$$Link\ Margin\ (dB) = P_T - S_r - Loss_T \tag{2.31}$$

In order to examine the effect of the above parameters on the availability of the FSO system, internal and external parameters of the link evaluated and compared with the available link margin.

2.5.2 Internal Parameter

As shown in Figure 3.3, internal parameters are geometric loss, divergence angle, optical power, optical loss, transmission bandwidth and wavelength, receiver sensitivity and bit error rate.

2.5.2.1 Geometric Loss

Geometric loss occurs due to the divergence of the optical beam along the propagation link. As a result, not the entire beam hits the receiver's telescope, and cause the geometrical loss. Figure 2.5 shows the geometrical loss (gray area) (Chen, 2002).

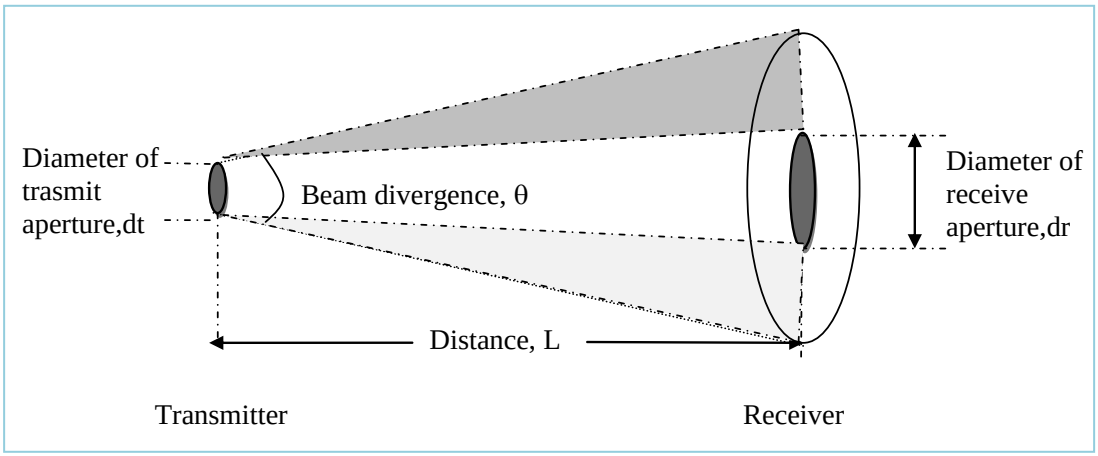

Figure 2.5. Geometrical Loss

Geometrical loss depends on the beam divergence, transmitter aperture, receiver aperture diameter and the range of the link. The loss is equal to the area of the receiver collecting optics in the area of the beam at the receiver.

Equation 2.33 is the formula of Geometrical loss (Bloom et al., 2003):

$$Geometric\ loss, G(dB) = \left[\frac{d_r}{d_t + (\theta L)}\right]^2 \quad (2.33)$$

Where

d_r = Receive aperture diameter (m)

d_t = Transmit aperture diameter (m)

θ = Beam divergence (mrad)

L = Distance between transceiver (km)

For FSO link system, geometrical loss is always present due to the nature of FSO transmission. Geometrical loss does not vary with time like atmospheric attenuation. We need to consider it since it is a fixed loss of an FSO system with the loss value depending on the system.

2.5.2.2 Divergence Angle

Beam divergence angle, θ, as shown in Figure 3.4, is beams transmitted angle. The beam is spread or extends in diameter as it reaches towards the receiver. The shape of the beam is a cone-like shape. A cone angle or divergence angle determines how much the beam would spread as it travels through the atmosphere. The beam will spread further from the terminal and by the time it gets to the receiving terminal, the beam diameter may be several meters wide. Consequently, not all of the light in the beam would hit the receive aperture, rather, a big portion of the beam would be wasted around the sides of the terminal (Lightpointe, 2009b). It is as presented in Figure 2.6

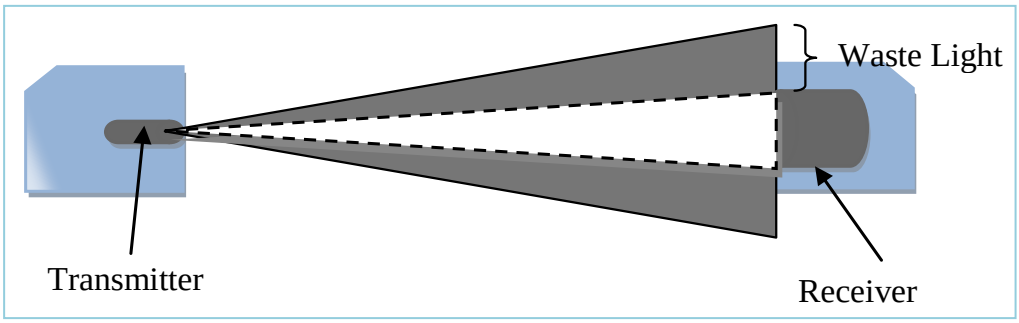

Figure 2.6. The impact of divergence on the light beam

In order to reduce the geometric loss and allow more light to concentrate on the receivers' aperture area, it is important to minimize the beam divergence angle. However, by minimizing divergence angle, it is more difficult to keep the beam aligned with the line of sight between the two transceivers. Building motions, mount vibration, strong winds and certain weather conditions will cause the terminal or the beam to move and may sometimes lead to beam completely missing the receiver's aperture area. This can cause errors in the transmission, or result in complete loss of link. Due to this fact, the wider beam divergence the greater possibility of the beam to hit the receiver aperture area (Husagic, 2009). One solution for this design deficiency is by using tracking system. The tracking system automatically or manually allows the alignment between the terminals. Most of the commercial FSO transceivers already have built-in tracking systems and this eases the alignment problems.

2.5.2.3 Optical Power

By transmitting, more transmit power to the receiver side; more power will reach and receive at the receiver side. The beam can penetrate further and achieve longer ranges from having more transmitted power. Higher power can handle weather that is more difficult and increases the availability of the link. As each transmitter designed to comply with the maximum transmits power regulations, it is not that simple to transmit more power. The regulations exist for safety purposes so that the power release does not give any harm to living creatures.

Even if we ignored these restrictions, increasing power without boundaries does not always help the signal. Addition of power beyond the saturation level makes no impact on the signal strength, and therefore, when designing the transmitter, saturation level must be determined and taken into consideration. Another issue with transmit

power limit is the cost, the more power means more cost, and in communication, as cost effective equipment as possible is desired.

Furthermore, many FSO manufacturers include space divergence within the transmitter. This means that more transmitting optics situated about the transmitter in order to ensure that the signal beam received even if one of the sent beams absorbed by the atmosphere or becomes misaligned due to the refractions and reflections.

2.5.2.4 Optical Loss

Optical loss in FSO is due to imperfect lenses and other optical elements such as coupler (Willebrand et al., 2001). Each optical component that the light beam must go through may involve an external window as well being absorbed, reflect or scatter which reducing the total received power.

Although lenses increase, the overall signal strength by focusing the light beam still reflect and absorb some of the transmitted light. The quality of lenses and mirror and their physical interface with an optical signal influence optical loss (Wainright et al., 2005). Optical loss identified by measuring or deriving from the manufacturer optical components. In (Willebrand et al., 2001), optical loss is given as a 4dB reduction in signal power. The number is not a significant number that can cause availability of the link.

2.5.2.5 Transmission Bandwidth and Wavelength

Optical transmission wavelength is in visible light spectrum. The diagram of the electromagnetic spectrum as shown in Figure 2.7 (Kidouchim, 2007) and Figure 2.8 (Kidouchim, 2007) indicating the wavelength and frequency of visible light:

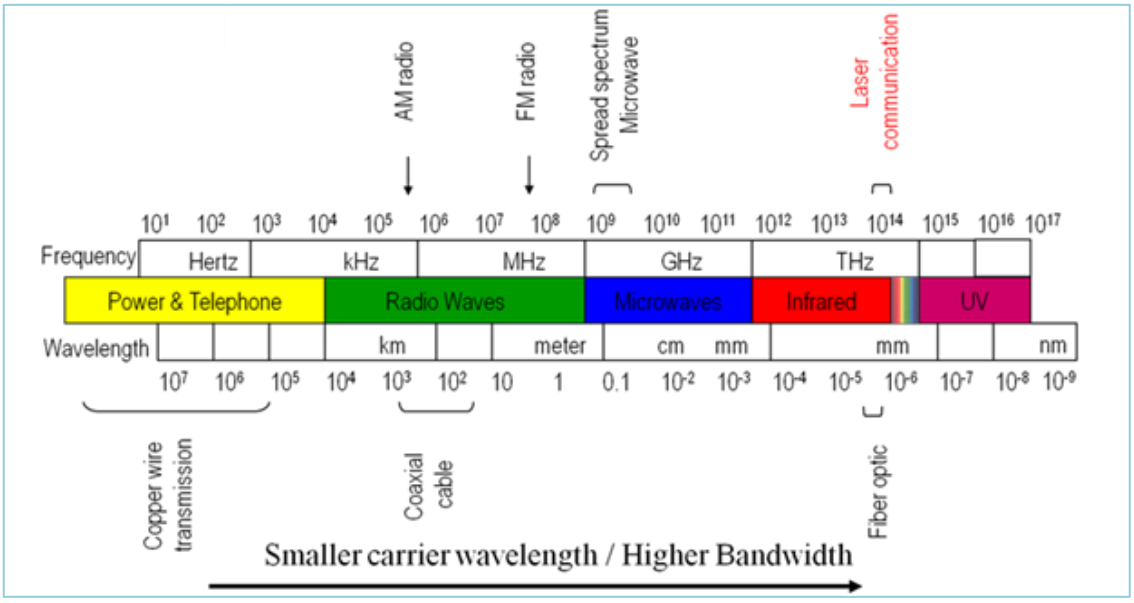

Figure 2.7. Electromagnetic Spectrum (Kidouchim, 2007)

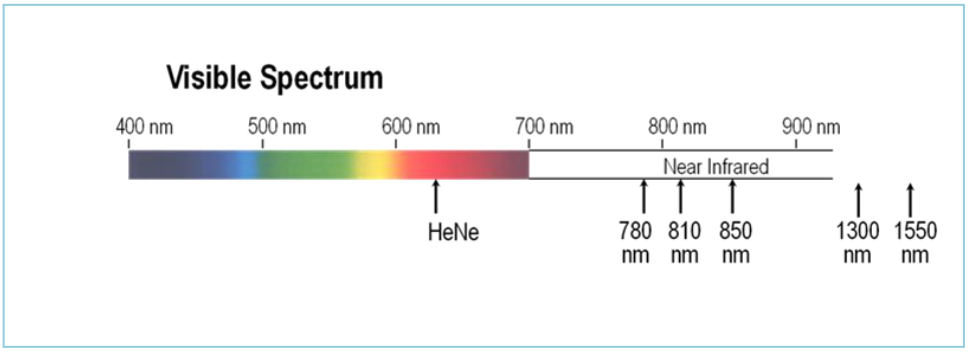

Figure 2.8. Visible Spectrum (Kidouchim, 2007)

The commercially available FSO equipment operates in the near-IR wavelength. The range of the wavelength is between 700nm and 1600nm (Zhuanhong et al., 2006). In the visible and near-IR, the physic and transmission properties of optical energy are similar as it travels through the atmosphere. However, there are several factors influencing the chosen wavelength (fSona, 2001).

Standard use of FSO system wavelengths are of 850nm, 1310nm and 1550nm that is in the low atmospheric attenuation windows (Lightpointe, 2009a). These

attenuation windows coincide with the standard transmission windows of optical fiber communications system. Therefore, FSO system designers can use the components that operated at the standard of fiber optic communication system. 1310nm band, however, does not have acceptable attenuation properties for use in transmission through free space, the two remaining wavelengths to considered are 850nm and 1550nm.

Therefore, to ensure the highest performance of an FSO system, it is important to choose a wavelength within these two atmospheric windows. Between the two wavelength windows, FSO system must have the following characteristic in order to be a suitable transmitter for a telecommunication system (Hudson Jr, 1969):

Operation at higher power levels (important for longer FSO system)

Favourable high-speed modulation characteristic (important for high speed FSO system)

Components small on footprint and low in power consumption (important for overall system design and system maintenance)

The capability to operate over a wide temperature range without showing major performance decay or degradation (important for outdoor system installation)

Mean time between failure (MTBF) operation exceeding 10 years.

Some of the characteristics of 850nm and 1550nm are as shown in Table 2.2:

Table 2.2

Characteristic of 850nm and 1550nm wavelength equipment

850nm	1550nm
Low attenuation	Low attenuation
Reliable	Reliable
Inexpensive transmitter and detector components	High quality transmitter and detector components
Widely use by today's service provider	New technologies amplifiers to boost transmission power
Highly sensitive avalanche photo diode (APD) detector technology	Development of wavelength division multiplexing (WDM) is feasible in this range
Advanced vertical cavity surface emitting laser (VCSEL)	Very high speed semiconductor laser technology

Figure 2.9 shows an illustration of the transmission window created with MODTRAN developed by the Air Force Research Laboratory (Bloom et al., 2003). The figure shows several transmission windows that are nearly transparent; with attenuation less than 0.2dB/km and it is within 700 nm – 10,000 nm wavelength range. These windows are located around specific wavelengths; with the majority of FSO system design operate in the window of 780-850 nm and 1520-1600 nm.

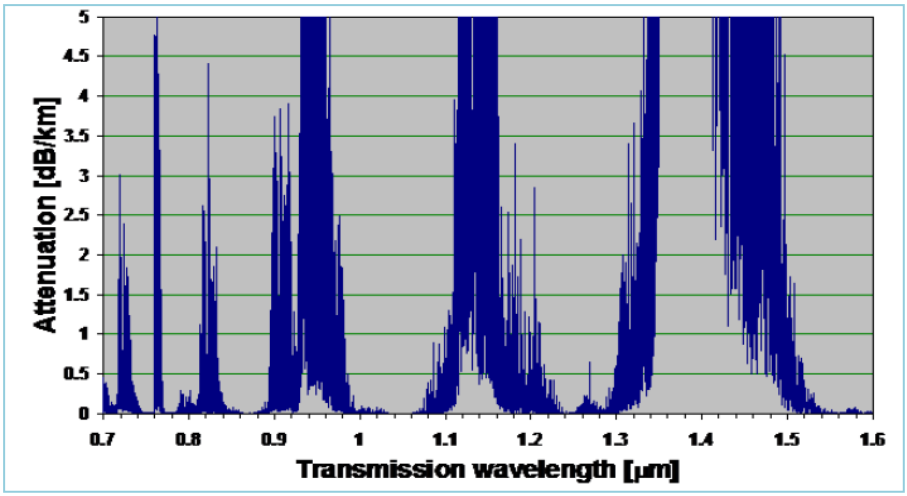

Figure 2.9. Transmission properties of the atmosphere in the near infrared wavelength range under clear weather conditions (Bloom et al., 2003)

2.5.2.6 Receiver Sensitivity

Receiver sensitivity is the measure of how well the signal detection circuitry can make use of the received power level. In FSO system, since it uses a simple binary encoding and on-off keying, therefore the receiver must be able to detect these two different binary states.

Receiver sensitivity is also a measurement on how low the signal power can be and still be visible above the background noise. The source of background noise comes from several sources, such as ambient light, shot noise (caused by random fluctuation) in the motion of charge carrier in a conductor, and thermal noise (noise generated by thermal agitation of electrons in a conductor)

The receiver sensitivity is also a function of modulation speed of the incoming signal. Higher speed signal (shorter bit in time) contains less photons that receiver detect; making it more difficult to resolve a "1" and "0" states. Different receiver designs approach this limit with varying degree success.

2.5.2.7 Bit Error Rate

For analogue systems, signal-to-noise-ratio (SNR) is a standard measurement for laser communication performance. For digital communications, there is another meaningful measurement (Arun, 2008). In digital transmission, bit-by-bit (binary encoding) is the basis of the transmission of digital bits over the optical link also known as bit error rate (BER). Definition of BER is the probability of error may occur in a bit in pulse train; "1" bit turns into a "0" bit or vice versa. We can also observe BER for link under current operating condition within a window of 10 seconds divided by the total number bits received during those 10 seconds (Chen, 2002).

It is suggested that (S. Bloom et al., 2003), the industry adopt the standard metric "Average Required Power at the Receiver Aperture for 10^{-9} Bit Error Rate" (Leitgeb et al., 2009). Extrapolating to other error rates is pretty straight forward, with 10^{-12} approximately corresponding to 1 dB less sensitivity and 10^{-6} approximately corresponding to 1 dB more sensitivity.

The specified receiver sensitivity will apply to a specific BER. The effect of noise causes increases in the BER until it exceeds some specific and predefined threshold. The threshold chose depends on the specific application, for high rate data transmission, a BER threshold of better than $1x10^{-10}$ is often used.

In any digital communication system, the ultimate function of the physical layer is to transport bits of data through a medium such as copper cable, optical fiber or free space in an accurate and quick as possible. Two basic measurements applied to measure physical layer performance which are the speed the data can be transported (data rate) and the integrity of the data arrived at the destination. Data integrity measurement called bit error rate or BER.

There are two levels in most digital protocols require BER performance. Telecommunications protocols, such as SONET require a BER of one error in 10^{10} bits (i.e. BER = $1/10^{10}$ = 10^{-10}). For data communications, protocols like Fiber Channel and Ethernet commonly specify a BER of better than 10^{-12} using shorter bit patterns. In some system, the specification requires about 10^{-16} or lower.

In digital transmission, eye diagram is a tool use for qualitative analysis of the signal. Eye diagram provides evaluation of system performance and can offer insight into the nature of channel in-perfection. The examination of signal integrity in the purely digital system such as optical transmission also use eye diagram as the analysis tool. Besides that, the high-speed communication systems also use eye diagram

analysis. Commonly use criterion in the analysis of the performance of a communication system is its BER measured at the receiver. However, BER is pass/fail in nature and it conveys nothing more. Eye diagram serves as an additional testing procedure, to analyze the system behaviour. It is accomplished by giving the opportunity to know how much the timing margin is available at the receiver or how much noise the signal can tolerate before there is a significant increase in BER.

One parameter in eye diagram is the measurement of Q-factor. In optical communication, the error rate depends on signal to noise ratio determined by Q-factor (Nadeem et al., 2009). Equation 2.34 shows the relationship between BER and Q factor.

$$BER = \frac{1}{2} erfc(\frac{Q}{\sqrt{2}}) \quad (2.34)$$

Where

$$erfc(x) = \frac{2}{\sqrt{\pi}} \int_{x}^{\infty} e^{-v^2} \quad (2.35)$$

If Q-factor of the system or design increases then BER decrease means signal received with small noise factor at receiver.

Q-factor is a parameter that directly reflects the quality of a digital optical communication signal. Q-factor measure of overall system quality therefore, the higher the Q-factor; the better the quality of the optical signal.

2.5.3 External Parameters

The medium of transmission for an FSO link is atmosphere. Many factors that attenuate, distort, divert or interfere with an optical beam, comparatively with transmission through an optical fiber. Atmospheric attenuation that causes the absorption and scattering are the main challenge to implement FSO link (Nadeem et

al., 2009). Local weather conditions affected FSO link performance. The interaction between atmosphere and optical beam produces a wide variety of phenomena: frequency selective absorption, scattering and scintillation (ITU-R P.1817, 2007). A brief description of this phenomenon is as illustrated in Table 2.3

Table 2.3
Effect of the interaction of atmosphere and optical beam

– Frequency selective absorption of specific optical wavelengths results from the interaction between the photons and atoms or molecules that leads to the extinction of the incident photons, elevation of the temperature, and radiative emission.
– Atmospheric scattering results from the interaction between the photons and the atoms and molecules in the propagation medium. Scattering causes an angular redistribution of the radiation with or without modification of the wavelength.
– Scintillation results from thermal turbulence within the propagation medium that results in randomly distributed cells. These cells have variable sizes (10 cm-1 Km), temperatures, and refractive indices causing scattering, multipath and variation of the angles of arrival.

A detail discussion on the effect of atmospheric attenuation of the transmission of an FSO link discuss in next sub-section.

2.5.3.1 Atmospheric Attenuation

In the atmosphere, even under a clear weather condition, there is no term as "free space" since it is composed of oxygen, nitrogen molecules and other particles. The atmosphere also can contribute large amount of water vapour especially in polluted region. Infrared photon propagation in the atmosphere can be scattered or absorb by these particles (Ricklin et al., 2006). Scattering, absorption and turbulences are the dominant mechanisms of signal loss and distorted (Achour, 2002b). This scattering causes portions of the light beam travelling from a source to deflect away from the intended receiver.

It is impossible to change the physics of the atmosphere, but it is possible to take advantage of optical atmospheric windows by choosing the transmission wavelengths accordingly. As discussed previously in the *3.4.2.5. Transmission Bandwidth and Wavelength* section, FSO equipment commercially available operates in the near IR spectral windows located around 850nm and 1550nm. Other windows exist but they are limited in use by the availability of devices and components; they are difficult in practical implementation (Crane, 2003)

The atmospheric attenuation is described by Beer's Law equation (Gagliardi et al., 1995):

$$\tau(\lambda, L) = \frac{P_R}{P_T} = exp\ (-\gamma(\lambda).L) \qquad (2.36)$$

Where

$\tau(\lambda, L)$ = Transmittance of the atmosphere at wavelength λ

P_R = Received optical power at distance L

P_T = Optical power at the optical source

$\gamma(\lambda)$ = Total attenuation/extinction coefficient (m^{-1})

The attenuation coefficient, $\gamma(\lambda)$, depends on four individual parameters in a function of wavelength; which are molecular and aerosol absorption coefficient, β, and molecular and aerosol scattering coefficients α. Mathematical representation of the parameters is as follows:

$$\gamma(\lambda) = \beta_m(\lambda) + \beta_a(\lambda) + \alpha_m(\lambda) + \alpha_a(\lambda) \qquad (2.37)$$

Where $\beta_{m,a}$ = Molecular and aerosol scattering coefficients

$\alpha_{m,a}$ = Molecular and aerosol absorption coefficient absorption

2.5.3.2 Molecular Absorption

Absorption occurs when there is an interaction between the propagating photons and molecules present in the atmosphere along its path (Popoola et al., 2009). Molecular absorption occurs due to the interaction between the optical radiation, atoms and molecules of the medium such as N_2, O_2, H_2O, CO_2, O_3, Ar etc. (ITU-R P.1817, 2007). This will lead to the disappearing of the incident photon and an elevation of temperature. The type of gas molecules and their concentration are the base of absorption coefficient (Naboulsi et al., 2003). Molecular absorption is a selective phenomenon with results in a spectral transmission of the atmosphere presenting transparent zones, called atmospheric transmission window. The transmission windows are in the optical range (Chabane et al., 2004) as presented below

Table 2.4
Transmission windows in the optical range

Transmission Windows	Range
Visible and very near IR:	from 0.4 to 1.4 µm
Near IR to IR I :	from 1.4 to 1.9 µm and 1.9 to2.7 µmz
Mean IR or IR II:	from 2.7 to 4.3 µm and 4.5 to 5.2 µm
Far IR or IR III:	from 8 to 14 µm
Extreme IR or IR IV:	from 16 to 28 µm

Absorption by atmospheric gases defines the atmospheric windows (Middleton, 1952),(Hudson Jr, 1969). Typical absorption spectrum is as presented in Figure 2.10 (Willebrand et al., 2001). The vibration and rotation of the particle lead to absorption in many bands. Distinguished window appears between 0.72 µm and 15 µm in the atmospheric windows. Water vapour dominated the region from 0.7-2.0 µm a combination of water and carbon dioxide dominated the absorption in the region from 2.0-40 µm is dominated (Willebrand et al., 2001).

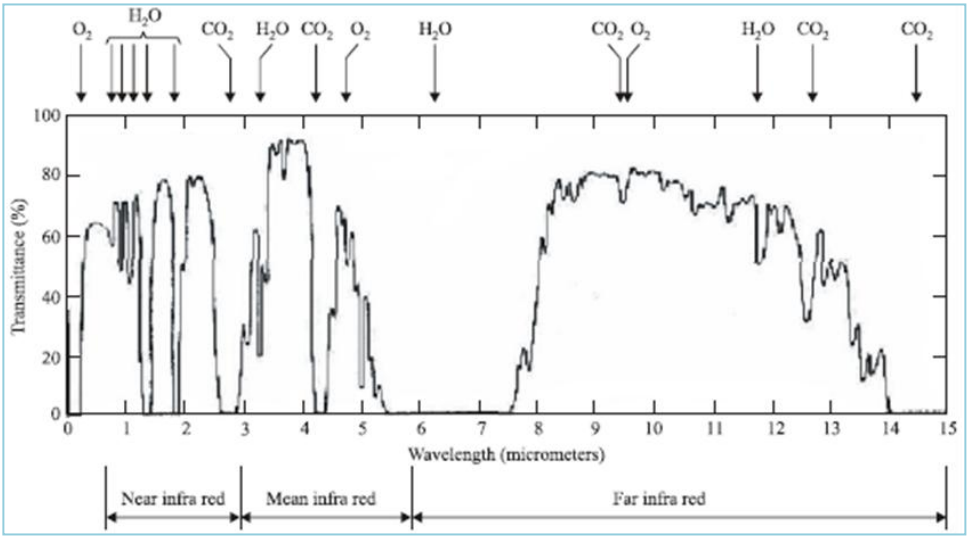

Figure 2.10. Transmittance of the atmosphere due to molecular absorption (Willebrand et al., 2001)

Overall, the profile of each absorption line determines the collision effect due to the interaction of the moving molecules relative to the incident wave. These phenomena lead to a spectral widening of the natural line of each molecule. For carbon dioxide (CO2) molecules, water vapour (H2O), nitrogen (N2) and Oxygen (O2), the absorption line profiles can extend sufficiently far from each central (ITU-R P.1817, 2007). In (ITU-R F.2106-1, 2010), it is illustrated values of specific molecular absorption according to wavelength (nm). The values are as illustrated in Table 2.5

Table 2.5
Specific molecular absorption values

Wavelength (nm)	A_{sp} **= Specific molecular absorption (dB/km)**
550	0.13
690	0.01
780	0.41
850	0.41
1550	0.01

Total molecular attenuation is as presented in Equation (2.38)

$$A_{mol}\ (dB) = A_{sp}(\lambda) * d \qquad (2.38)$$

Where d is the link distance (km).

FSO equipments, however, the wavelength used are 690, 780, 850 and 1550 nm; which located in transmission windows where molecular absorption is negligible. It is negligible owing to the fact that these particles are very small in this region of the spectrum (Naboulsi et al., 2004),(Harris, 1995; Wainright et al., 2005)

2.5.3.3 Molecular Scattering

We can define scattering as a redirection or redistribution of light that can lead to a significant reduction of receiving light intensity along the propagation path (Zhuanhong et al., 2006). The scattering model calculated by taking into consideration of the particle radius and the incident wavelength. There are three distinct cases exist (Wainright et al., 2005)

- The particle radius is much smaller than the incident wavelength ($r \ll \lambda$)
- The particle radius is much larger than the incident wavelength ($r \gg \lambda$)
- The particle radius is approximately the incident wavelength.

Molecular scattering is occurring in the first case above. In general, we can classify scattering of light into three types (Achour, 2002b): Rayleigh scattering, Mie scattering and Non-selective scattering. Molecular scattering is Rayleigh scattering and the discussion is in this section while other scattering phenomena will be touched in other sub-section.

Another definition (ITU-R P.1817) of molecular scattering is the interaction of light with atmospheric particles whose sizes are smaller than the wavelength of the

incident light resulting in molecular scattering. Molecular scattering or Rayleigh scattering contributes to the total attenuation of the electromagnetic radiation.

FSO systems operating in the longer wavelength near infrared waveband range; however, the impact of molecular scattering of the transmitted signal is negligible (Willebrand et al., 2001). Molecular scattering is primarily significant in the ultraviolet to visible wave range (Achour, 2002b).

2.5.3.4 Aerosol Absorption

Aerosol is extremely fine solids or liquid particles suspended in the atmosphere with very low fall speed by gravity (ice, dust, smoke, etc.) (Bouchet et al., 2005),(ITU-R P.1817, 2007),(M.Chabane et al., 2004). The size of these particles lies between 10^{-2} to 100 μm and example of aerosols are fog, dust and maritime spindrift particles.

The concentration, size and chemical natures of aerosol influenced the condition in the atmosphere. The chemical composition determines the aerosol refractive index. The same as molecular scattering, aerosol scattering also is negligible in the near infrared and visible waveband. It is because the imaginary part of the refractive index of these particles is very small in this region of the spectrum (M.A. Naboulsi et al., 2004).

By the above discussion on the molecular absorption, molecular scattering and aerosol absorption; the attenuation coefficient, $\gamma(\lambda)$ depends only with aerosol scattering, which will be elaborate further in next sub-section.

2.5.3.5 Aerosol Scattering

When the particle sizes are of the same order of magnitude as the light wavelength of the transmitted wave, aerosol scattering occurs. The scattering coefficient in this case computed using the Mie scattering model or Kruse formula.

Mie scattering occurs when the particle radius is in the order of the incident wavelength. The major contributors to the Mie scattering process in the near infrared wavelength range are fog, haze and pollution (aerosols) particles. Fog is the key opponent for FSO beam since the infrared wavelengths and the average radius of fog particle is about the same size. On the other hand, rain and snow particles are larger and have less effect on the beam.

Since FSO operating system operates in this near infrared spectrum region, attenuation coefficients are only approximately by the coefficient of aerosol scattering, $\beta_a(\lambda)$, The attenuation coefficient as in Equation 2.39 can be reduced as follows:

$$\gamma(\lambda) \cong \beta_a(\lambda) \tag{2.39}$$

This is based on the assumption that (Bohren & Huffman, 1983)

The scattered light has the same wavelengths as the incident light

Only single scattering occurs while the multiple scattering effects are neglected

The particles are spherical in shape and are acting independently with a complex refractive index in space.

To comply with the theory of Mie scattering of atmospheric particles is very complicated since the atmosphere have complex shapes and orientations. Therefore, the attenuation due to scattering will be used based on a reported empirical formula (Kruse et al, 1962), (Weichel, 1990). Visibility ranges in kilometres often been used to express the empirical equations. The visibility range can be defined as the distance

that a parallel luminous beams travels through in the atmosphere until its intensity drops to 5% of its original value (Willebrand et al., 2001). A straightforward definition of visibility is the distance at which human eye can see the distinction between a white and black boundary.

The empirical model (Kim et al., 2001) is as stated below:

$$\gamma(\lambda) \cong \beta_a(\lambda) = \frac{3.912}{V}\left(\frac{\lambda}{550}\right)^{-q} \quad (\text{km}^{-1}) \tag{2.40}$$

Where

V = Visibility (km)

λ = Transmission/incident wavelength

q = Particle size distribution coefficient

The Koschmeider law is used to calculated visibility and as in Equation (2.41) (Prokes, 2009)

$$V = \frac{3.912}{\gamma_{550nm}} \tag{2.41}$$

Meteorological visibility, V, defined as a distance at which transmittance falls to a certain value ε. Koschmieder proposes a value of ε = 0.02 and we can calculate this value using the atmospheric attenuation coefficient:

$$\gamma(\lambda) = \frac{-\ln(\varepsilon)}{V} \tag{2.42}$$

However, the World Meteorology Organization later proposed the value of 0.05 because it ensured the requirement for reliability resolving a black object against the horizon in daylight at a wavelength of 550nm, where the human eye has the highest sensitivity. Therefore the atmospheric attenuation coefficient now become

$$\gamma(\lambda) = \frac{-\ln(0.05)}{V} = \frac{3}{V} \tag{2.43}$$

In other words, the attenuation calculation for V is based on the threshold contrast (Naboulsi et al., 2004). In fact, the value of 3.912 based on the assumption that the threshold contrast is 2%. While the value of V = 3 is based on the threshold contrast of 5%.

However, the value of threshold contrast of 5% is more valid for fog attenuation calculation. Since, we are considering the tropical weather condition; fog is not the limiting factor for FSO link. Haze expected to have some effect on the FSO link. Visibility measurement can represent haze attenuation as in the calculation of fog attenuation. The difference between haze and fog is the visibility of haze is higher 1000m than fog. Their composition and size distribution varies strongly. In the following table, Table 2.6 shows the International visibility code (ITU-R P.1817, 2007) with the differentiation of visibility and attenuation in haze and fog and other weather conditions.

Table 2.6
Transmission windows in the optical range (ITU-R P.1817, 2007)

Weather conditions	Precipitation		mm/h	Visibility (m)	Attenuation (dB/Km)
Dense Fog				0	
Thick Fog				50	315
Moderate Fog				200	75
Light Fog				500	28.5
Very Light Fog	**Snow**	Storm	100	770	18.5
				1000	13.8
Light Mist		Strong Rain	25	1900	6.9
				2000	6.6
Very Light Mist		Average Rain	12.5	2800	4.6
				4000	3.1
		Light Rain	2.5	5900	2
				10000	1.1
Clear Air		Drizzle	0.25	18100	0.6
Very Clear Air				20000	0.54
				23000	0.47
				50000	0.19

A few standards model used to define the coefficient of particle size distribution, q, in the atmospheric attenuation condition. One model is Kruse model that is widely used in the calculation to determine an FSO equipment link budget. The attenuation coefficient, $\gamma(\lambda)$ and Kruse model predict the attenuation for any meteorological conditions; the attenuation will increase with increasing wavelength which implies a preference for equipment working at 1550 nm compared to the other

wavelengths suggested for FSO equipment (Carbonneau et al., 2000),(Szajowski et al., 1998)

Kruse model of particle size distribution is:

$$q = \begin{cases} 1.6 & if\ V > 50km \\ 1.3 & if\ 6km < V < 50km \\ 0.585V^{1/3} & if\ V < 6km \end{cases} \quad (2.44)$$

The evaluation of the parameter q using Kruse model for visibility lower than 6 km ($0.585V^{1/3}$) is not collected in dense fog. Therefore, the visibility, V < 1 km, its significance is in doubt (Middleton, 1952). Because of that, a recent study proposed another expression for the parameter q, which is called Kim model (Kim et al., 2001):

$$q = \begin{cases} 1.6 & if\ V > 50km \\ 1.3 & if\ 6km < V < 50\ km \\ 0.16V + 0.34 & if 1km < V < 6km \\ V - 0.5 & if\ 0.5km < V < 1km \\ 0 & if\ V < 0.5km \end{cases} \quad (2.45)$$

For tropical region which no fog attenuation to consider, only haze attenuation to be calculated, Kruse model is good enough since we do not need to consider for V < 1 km.

2.5.3.6 Rain Attenuation

There are three types of atmospheric scattering:

- Rayleigh scattering (molecular scattering)
- Mie scattering (aerosol scattering)
- Non – selective scattering (geometric scattering)

Non-selective scattering occurs when the particles drop size is much larger than the wavelength (Achour, 2002a) and it is wavelength independent. It is exists due to rainfall (Achour, 2002b).

In a country that experience high rainfall rate throughout the year such as in Malaysia; we expected rain to be the main factor of atmospheric attenuation. The outage time of the communication system can occur either due to equipment failure or propagation constraint. The propagation restraint especially the rain attenuation is so severe since rainfall can give up to several decibels of total attenuation (Shahrul Kamal, 2000).

The formation of rain is based on the water droplets in the atmosphere whose form and numbers is variable in time and space. The droplets considered spherical until a radius of 1 mm. Beyond that radius, the droplets known as oblate spheroids (flattened ellipsoid of revolution). In the calculation, the equivalent radius is used i.e. the radius of the sphere that has the same volume (Chabane et al., 2004).

International Telecommunication Union (ITU) has divided the world into fifteen rain climate zone with rainfall intensity exceeded (mm/hr) for each region. Malaysia categorized under region P. The division of the region is as illustrated in Table 2.7

Table 2.7
Rainfall Intensity Exceeded (mm/hr) for various regions

Outage Percentage of Time (%)	A	B	C	D	E	F	G	H	J	K	L	M	N	P	Q
1	<0.1	0.5	0.7	2.1	0.6	1.7	3	2	8	1.5	2	4	5	12	24
0.3	0.8	2	2.8	4.5	2.4	4.5	7	4	13	4.2	7	11	15	34	49
0.1	2	3	5	8	6	8	12	10	20	12	15	22	35	65	72
0.03	5	6	9	13	12	15	20	18	28	23	33	40	65	105	96
0.01	8	12	15	19	22	28	30	32	35	42	60	63	95	145	115
0.003	14	21	26	29	41	54	45	55	45	70	105	95	140	200	142
0.001	22	32	42	42	70	78	65	83	55	100	150	120	180	250	170

Equation (2.46) is to calculate rain attenuation

$$A\ (dB/km) = kR^{\alpha} \tag{2.46}$$

Where k and α is specific rain attenuation parameter and can be determined as discussed in detail in Chapter 2. R (mm/hr) is the rain intensity measured with a 1-minute integration time.

According to ITU Recommendation for determining specific rain attenuation model, the knowledge needed is the attenuation for 0.01% of the time (point rainfall rate of 0.01% of time) and then scaling this to the other percentage of time (ITU-R P.618-6, 1999).

2.5.3.7 Haze Attenuation

In temperate regions, fog is the main influenced by FSO link availability. In tropical region, however, the fog is not the main issue since the fog is not present. Rain and haze are two main causes of atmospheric attenuation in tropical region.

Internationally, we can define fog as a visibility of less than 1 km, while haze is visibility between 2 km to 5 km. Fog principally is composed of water droplets. Haze is an atmospheric phenomenon where dust, smoke and other dry particles obscure the

clarity of the sky. Haze is denser than water clouds because heavier substances are present in it, which causes haze to hang near the ground and keeps the air at higher elevations, relatively diminishes visibility.

In meteorology, visibility is the term for fog and haze measurement (Tim, 2006). Visibility is weather parameters used to estimate FSO link attenuation due to haze, fog and low cloud attenuation (Achour, 2002b). Transmissometers and scatter meters are instruments used to measure visibility.

2.5.3.8 Scintillation

Scintillation is the temporal & spatial variation in light intensity cause by atmospheric turbulence. Such turbulence creates pockets or air with rapid varying intensities and therefore fast-changing indices of optical refraction. These air pockets act like a prism and lenses with time varying properties. The amplitude and frequency of scintillation depend on the size of the cell compared to the diameter of the beam.

At ITU-R as shown in Figure 2.11 to 2.13, illustrated the effect as well as the variation (amplitude, frequency of the received signal (ITU-R P.1817, 2007):

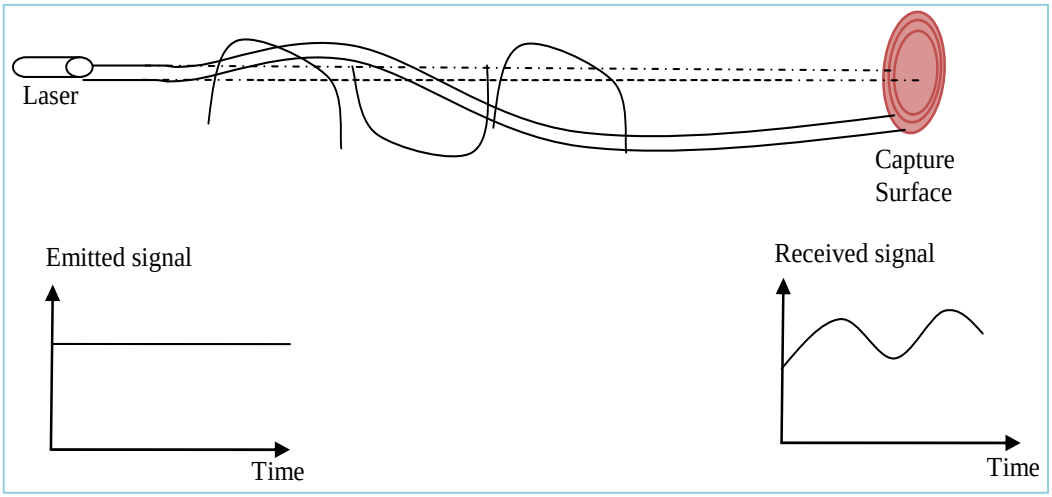

Figure 2.11 Derivation of the beam under the influence of turbulence cells larger than the beam diameter

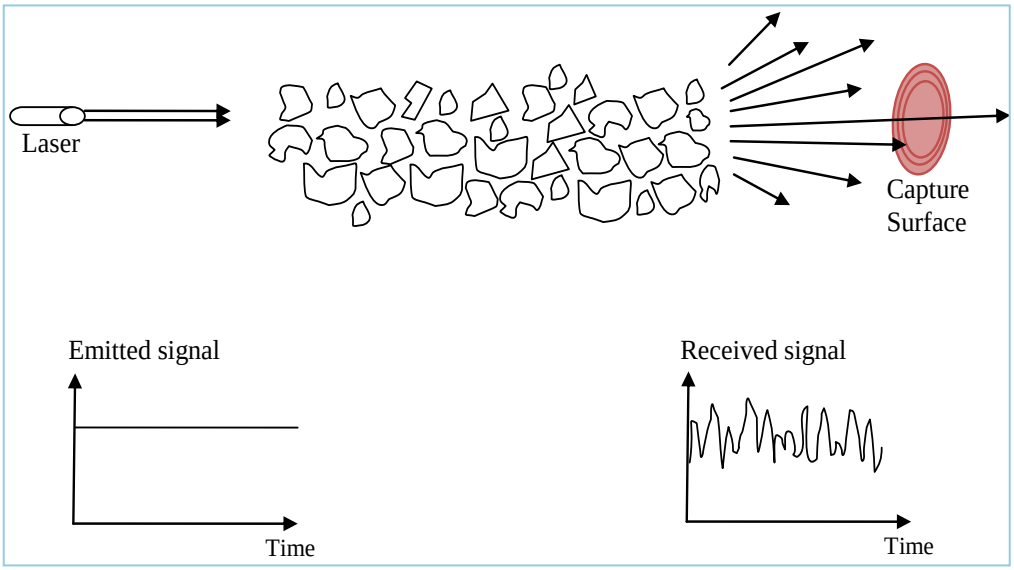

Figure 2.12. Derivation of the beam under the influence of turbulence cells smaller than the beam diameter (widening of the beam)

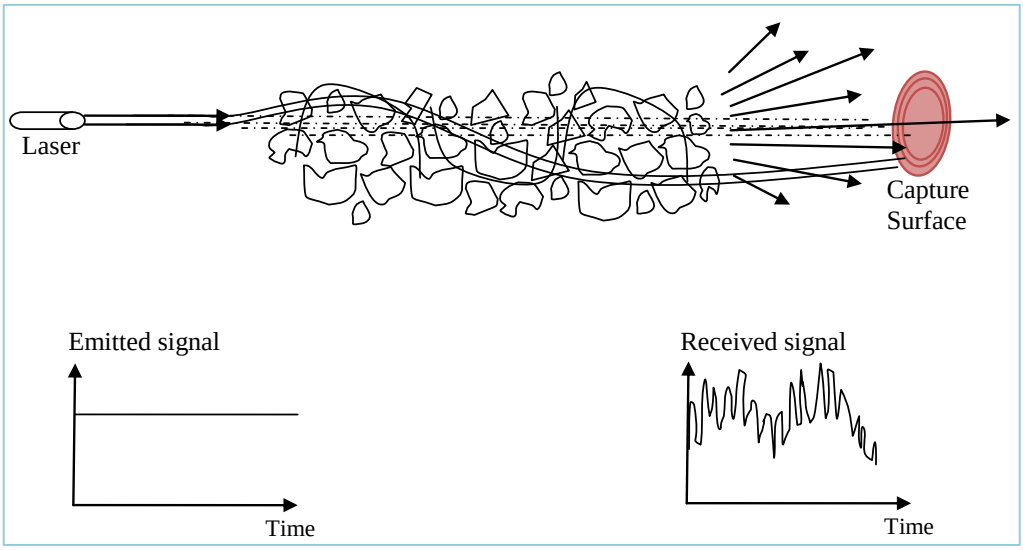

Figure 2.13. Effects of different size heterogeneities on laser beam propagation (scintillation)

A research is conducted that revealed very successful geometric solution to decrease the effect of scintillation significantly (Korevaar et al., 2003). One of the strategies is by using multiple transmission beams that sufficiently separated in space when they leave the transmission plane. By separating multiple transmitters and by making receiver optics sufficiently large (or sufficiently separating smaller receiving lens) different parts of the receiver lenses illuminated when the beam propagates through different air cells and reducing the effect of scintillation. In (Abtahi et al., 2006) also mention about multi transmitters and/or receivers provide diversity and large aperture receiver are two methods used in the commercials FSO system to mitigate the scintillation effect. They are not, however, for long distance link range.

Even though scintillation physically not correlated with visibility, scintillation under low visibility conditions usually neglected due to involving wet and cool weather. For high visibility conditions that typically occur on hot and sunny days, one has to reserve the maximum loss for scintillation in the link budget analysis.

In (Chen, B.,2002), it is mentioned that if the FSO link is installed outdoors, a 2 dB scintillation effect needs to be added to the losses when calculating the link margin.

2.5.3.9 Pointing Loss

Perhaps the distance between the transmitter and receiver is large enough that during installation of the link, it is difficult to see the far side. On the other hand, perhaps the tracking system contains errors. If either of these conditions exists, additional loss can incur because the transmitter does not point accurately enough at the receiver. Typically, these effects take place for distances in excess of 3 km, at which point we might subtract an additional dB of power from the link budget. Therefore, if the distance is less than 1 km, we can consider pointing loss insignificant and can set to 0 dB.

2.6 OUTAGE PREDICTION (AVAILABILITY)

The parameters of FSO link and the statistical properties of the atmosphere determine the availability of FSO link. The manufacturer gives the FSO link parameters and atmospheric parameters depend on the local weather condition. Atmospheric parameters have already discussed in previous sub-section.

In temperate regions, main atmospheric parameters are fog (Kim et al., 2001). In tropical regions, atmosphere parameter expected to be the limiting factor in FSO link availability is heavy rain, haze and turbulence (scintillation).

In carrier-class availability expected to be in the range of 99.999% which is 0.001% throughout the year. In enterprise-class, however, 99.99% availability is good, which the outage is 0.01% of the year (Kim et al., 2000). In (Chen, B., 2002), it is mentioned that the availability required by telecommunication operator is higher than

required by enterprise users. The telecommunication operator requires availability from 99.99% to 99.999% while the enterprise user is from 99.9% to 99.99%.

The availability is calculated based on clear weather condition and during the presence of weather effect such as rain and haze if we consider tropical weather condition via the following steps (Chen, B., 2002):

Calculate available link margin during clear weather condition

Determine atmospheric attenuation over 1 km distance for the desired availability

Determine atmospheric attenuation for transmission other than 1 km

Added any other available losses

Determined either desired availability is achievable

Many researchers do studies and analysis of FSO link availability since it is one of important analysis of service providers. Some of previous work on the availability of an FSO link presented below.

(Akbulut et al., 2005) worked on the characteristic of an experiment outdoor FSO and combination with radio frequency (RF) link for higher availability and uninterrupted communication link. The experiment carried out using a developmental design of FSO / RF systems for a one (1) year period. The experiment conducted in continental climate where weather conditions do not change significantly for the same seasons over the years. The result shows that a snowstorm is the most significant weather effects on the availability of FSO communication. The experiment, however, conducted in continental climate where snow as the major effect on FSO link. In tropical regions, snow is not the problem. Only mathematical formula use to calculate the attenuation of snow on the FSO link without any real data analysis of the effect.

(Gebhart et al., 2003) discuss on an analysis of reliability and availability of FSO link, theoretically and experimentally. Result obtains from commercial available FSO and self-developed optical point-to-point and point-to-multipoint FSO system. Parameters evaluated are atmospheric effect, link margin, geometrical loss, scattering, turbulence (scintillation), visibility and BER in winter. The distance is 2.7 km in Graz, Austria. The influence of turbulence is also investigated, which gives the duration of scintillation. From the investigation, Mie scattering is the one that influence FSO transmission and not Rayleigh scattering. The measurement time is four (4) years. The result shows that the unavailability of the FSO link is due to fog and attenuation is strongly depending on the season, climate and daytime. With the comprehensive evaluation, however, the measurement conducted under the temperate region where fog is present but absence in tropical region. The influence on the availability of the link is different in tropical region. There is no specification on the wavelength of the FSO link in the paper.

The paper (Bouchet et al., 2005) introduces a quality of service software prediction. The software with quiet comprehensive GUI taking into consideration installation sire of FSO link, FSO systems specification, link distance, weather effect, side effect like material of the wall, floor, e.t.c. The result will provide the attenuation due to atmospheric attenuation, all the losses, link margin and link availability. The data, however, based on temperate region which rain and snow attenuation are considered as one attenuation. The prediction software is mean for France region. It will be more useful if it is included function to produce results in other regions.

The focus of the discussion on this paper is the availability test done on commercial available FSO system (Korevaar et al., 2003). Parameters evaluated are link availability based on visibility collected at the airport area. Attenuation parameters

under investigation are fog and drizzle. The simulation result accomplishes using MODTRAN program while for scintillation analysis is done theoretically. Equations also develop to calculate link margin for scintillation fade, which depends on location, time of day and weather condition. The paper also introduces a model to calculate the probability of encountering a given attenuation in an average sense (to compare different FSO system). The result, however, is analyzed using theoretical and simulation with visibility data from airport are in temperate weather condition. Visibility data gather at the airport area and the attenuation condition may be different from those experiences in the city.

A research on the availability of FSO and hybrid FSO/RF system is discussed (Kim et al.,2001). The research is examining on the limitation of distance of FSO system for carrier and enterprise application. The paper introduces the first map of FSO link distances contour over North America. The map eventually will evolve into an attenuation map for predicting FSO performance. The basis of availability analysis is on historical visibility data from the international airport. Two methods use to calculate the availability of FSO link. For enterprise-class FSO link, visibility data are used and for carrier-class FSO link, FSO link budget and the worst possible weather or attenuation conditions are used. The finding show that hybrid FSO/RF system can provide carrier-class availability of 99.999% across much longer ranges than on FSO-only system. The parameter consider in the research, however, is valid for a temperate region, which the presence of fog. In tropical regions, fog is absent. The visibility data also come from the airport area. Under the influence of fog, the availability of FSO link is only for a very short distance whereas the area without fog, it will show different results. Contour map is only valid in North America.

This paper (Florex, 2010) describes the results obtained from the analysis of FSO propagation in a contaminated atmosphere and on the availability of the link. The paper discussed on the estimation method of the availability of FSO system knowing the distance of the link and some physical characteristics of the atmosphere. The modulation scheme is Circular Polarization Shift Keying (cPolSK). The method, however, utilize mathematical analysis base on empirical formula for link attenuation and link availability calculation. The weather effect on FSO does not measure experimentally and the link distance does not stated in the paper.

The paper (Kolka et al., 2007) discussed on the availability of FSO estimated using visibility records collected from 210 European airports. Long-term visibility records represent an invaluable source of data for the estimation of the quality of service of FSO link. The result evaluated for Italy, France and Germany.

The paper analyzes the availability of FSO link by changing distance of the FSO link head (Sporik et al., 2010). The influence of atmospheric attenuation measured at the receiver is in the form of received signal strength. The distances of an FSO link are set to 50 m, 100 m, 150 m, 200 m, 300 m and 400 m. The availability recorded for 3 months and 1year. The study shows the influence of shortening of a distance on the availability of FSO link and, in addition, decreasing in random atmospheric attenuation. Atmospheric attenuation taking into consideration is medium fog.

Long-term atmospheric attenuation from meteorological visibility and turbulence used to calculate the availability of an FSO link is presented in this paper (Kvicala, 2007). Monitored received signal use to calculate total atmospheric specific attenuation. The availability predicted using meteorological visibility data in the Czech

Republic for the period of 1 year. The probability of certain values of atmospheric attenuation that influence the link unavailability also analyzed.

2.7 LONG DISTANCE MEASUREMENT PROPERTIES AND LINK PERFORMANCE

Free Space Optics (FSO) is a line-of-sight communication system. A few factors affected the transmission of the beams. All these factors affected the received power at the receiver, which determines the availability of the link. The received power of an FSO system depends upon several conditions like deployment distance, atmospheric loss, scintillation, pointing loss, geometrical loss, equipment loss and rainfall. Atmospheric effect makes it worse with longer distance and degraded link availability.

The range of the deployment distance will raise effect on the power received at the receiver. One of it is atmospheric loss. For an FSO link system, Mie scattering will have the most effect on the link. The major contribution of Mie scattering is fog and haze. For tropical region, however, the fog is absent, so haze is the only factor to consider.

Scintillation builds up as the air heat up due to the ground heats up in the sun. This will cause air pockets to develop and it can change the propagation path of the FSO beams. These air pockets can change the index of refraction at random since it is not stable in time or in space, resulting in receiver saturation or signal loss (Bloom, 2003). The longer the link the higher the scintillation index will be.

Pointing loss is a loss due to building sway. This loss is considered in the calculation since the experiment is done at the top level of both buildings. In the study (Bloom, 2003), its mention that for the link less than 1 km, the pointing loss can be considered insignificant and can be set to 0.

Geometrical loss is one of the greatest losses for FSO link propagation. It occurs due to the divergence of the optical beam along the propagation link and further discussion on this is in Chapter 3. It is the most considered loss that will affect greatly on the receive power at the receiver.

The manufacturer provides equipment loss value. The last effect to consider is rain attenuation.

This paper (Sandalidis et al., 2008) investigates the error rate performance of FSO links over strong turbulence channels with pointing error effect. Turbulence model used is K distribution. From the study, the researcher derives a multiplicative statistical channel model, fading conditions mention previously and a closed-form BER expression. The result concludes that atmospheric turbulences and building sway (pointing loss) are the two dominant factors affecting the performance of optical wireless. The result, however, is an assumption from FSO system model. The model is derived from analytical expression and mathematical calculation without the presence of real data analysis. The calculation also needs to take into consideration of geographical contour of the installation site since some places; building sway is not a problem at all.

The paper (Loschnigg et al., 2009) discussed on the long-term performance observation of FSO link in term of availability of the optical link under the influence of fog. The distance of FSO link is 300m. Data collection is from April 2008 until end of November 2008. Wavelengths investigated are 550 nm, 850 nm and 950 nm. The availability measurement, however, done in the Ethernet layer and not in the physical layer of the FSO link. Whereas, the carrier class availability measurement is at the physical layer. Furthermore, the link distance is short (300 m) and data are measured in temperate region with fog is the limiting factor.

This paper (Singh et al., 2011b) studied on receiving optical power performances of FSO link. A simulation analysis conducts on the optical aperture size that achieves the best average BER given the same amount of transmitted power. The wavelength of FSO is 1550 nm with beam divergence is 3 mrad and link distance is 500 m. The analysis, however, use simulation only and the atmospheric attenuation effect is crucial in determining the performance of FSO link. The distance of the study is just a short distance, which makes the performance higher compare to longer distances and the atmospheric effect lesser.

A discussion on bit error rate of an FSO link using different optical windows is the focus in this paper (Singh et al., 2011a). Optical windows under investigation are 780 nm, 850 nm, 1310 nm, 1550 nm and 1610 nm. The basis of analysis, however, is using simulation method and atmospheric turbulence on assumption value without any real data.

The paper (Nazmi et al., 2012) evaluated pointing error for practical Bit Error Rate. The evaluation is for FSO link under different weather condition with 1.55 µm wavelength. Parameter under evaluation is scattering effect. The evaluation, however, perform with the simulation analysis using an empirical formula of power received, atmospheric attenuation coefficient and scattering. The simulation investigates on the effect of fog on FSO whereas fog is not the restraining factor in tropical region. Therefore, the result of the analysis is not for tropical users or designers.

2.8 GENERAL REVIEW OF FSO TECHNOLOGY AND SYSTEM

The specific rain attenuation prediction is model base on the effect of rain attenuation on FSO link propagation. This section will focused on the effect of atmospheric on FSO link. Detail discussion on the FSO system and framework will be in Chapter 3.

2.8.1 Atmospheric Effects and Attenuation

The paper (Colvero et al., 2007) presented an experiment of comparison about three optical transparency windows of the Earth's atmosphere along a period of 1 year. The three optical windows are 0.78 μm, 1.55 μm and 9.1 μm. The result proposes two methods for recording real time measurements of visibility for effects of fog, haze scattering, raindrop size and distribution for FSO link. Online monitoring of visibility measurement together with receives power data allowing a precise comparison of the links for wide range visibilities. The paper present a very comprehensive study of the attenuation, however, the assumption that the method proposed can be adapted in different region with different operation wavelength; the equipment for others to conduct the experiment are quiet expensive. The researcher does not mention the link distance of an FSO link under investigation, since link distance also plays an important role in term of link availability.

This paper discusses on several understanding of the physical processes underlying optical extinction and optical turbulence-induced signal loss (Ricklin et al., 2006). A comprehensive discussion on optical turbulence models and difference available model is the focus in this paper. The inspection on the difference available optical turbulence models is for estimation of the anticipated range of optical turbulence for a particular geographic location and time. The analysis, however, is theoretically performing with data from the temperate region weather. No detail discussion specify on the technique to mitigate the effect of optical turbulences.

This paper (Prokes, 2009) focus on the atmospheric effects of FSO system with emphasize on link parameters and atmospheric scattering (in term of meteorological visibility). The calculation is done by comparing internal parameter of the commercial available FSO system. Power loss by turbulence that cause scintillation effect and link

availability calculated from collecting visibility data at the airport area. The result shows that the turbulence effect on FSO is for relatively long distances. We can see a significant reduction on scintillation effect by increasing the receiver aperture or multi-optical transmitter. The source of atmospheric effect analysis, however, using data in temperate regions. The atmospheric condition analyzes for link availability is visibility data collected at airport area, which, does not presented the local weather condition.

The paper (Kim et al.,2000) discussed on comparison between the propagation of laser beam with 785 nm and 1550 nm wavelengths under fog and haze condition. The differences of Rayleigh scattering, Mie scattering and non-selective or geometrical scattering is presented. The calculation of the total scattering or attenuation coefficient is by applying mathematical model. The investigation result shows that fog attenuation does not depend on the wavelength. In the case of haze, the attenuation of haze is higher at 785 nm wavelength compared to 1550 nm wavelength. The paper also introduces Kim's attenuation coefficient and the size distribution of the scattering particles. The researchers propose a new part of the equation for the atmospheric attenuation. The propose model, however, is based on a mathematical model without experimental verification. The atmospheric attenuation develops considering the weather condition in temperate region with the present of fog as the limiting factors for FSO link availability.

This paper (Kim et al., 1999) explained on the experimental analysis of atmospheric scintillation for 785nm and 1550nm laser beam transmission. The fluctuation in received optical power at terrestrial range of 1.2 km and 2.2 km is measured experimentally. The result of the experiment indicates that scintillation fades are more of a problem at 1550 nm wavelength compared to 785 nm. The experiment conducted, however, on the wavelength of 785 nm and 1550 nm. Most of

the available FSO system uses 850nm wavelength. The necessary to investigate the effect of scintillation on 850 nm by taking into account the link distance of the FSO link. Furthermore, scintillation effect measurement under temperate weather condition might give different result compare to the scintillation effect in tropical region.

The paper discuss on the propagation of optical and infrared waves with the focus on the transmission of light in the atmosphere (Naboulsi, 2003). Models discuss are Beer Lambert Law, Kim Model, Kruse Model and Al- Naboulsi Model, Carbonneau Model, snow attenuation model and scintillation attenuation model. The methodology of analysis is by conducting an experiment on 850 nm wavelength, FSO equipment and measurement of visibility in the presence of fog. The experiment performed, however, is only to measure the effect of fog in term of visibility. The raw data then is inserted in the mathematical equation to calculate the attenuation but not by real time monitoring on the effect of fog on the link. Other analysis is for existing mathematical model and the experiment accomplishes in temperate regions.

This paper introduces a series of attenuations regarding simulation of FSO atmospheric propagation (Zhuanhong et al., 2006). Atmospheric attenuation under investigation is absorption, scattering and scintillation. The focus of the simulation is on the evaluation of the effect of fog and rain attenuation on FSO link. The results show that fog attenuate the link more than rain. From the simulation result also indicates that rain effect can be negligible. In tropical region, however, with the presence of heavy rain throughout the year we cannot omit the effect of rain from the analysis of FSO link propagation.

This paper (Popoola et al., 2009) reported about atmospheric channel effects on the terrestrial FSO link. Atmospheric parameter under study is Mie scattering. Available empirical model by Kim and Kruse apply in the mathematical calculation to

find the scattering value. The effect of scintillation is discussed in term of BER. The analysis, however, focuses on fog event occur for 1-day in Milan. The period of investigation is very short to come out with a concrete result of the weather effect on FSO link.

The effect of meteorological visibility on the link range is analyzed using Kim and Kruse models in this paper (Dordova et al., 2009). Empirical equation of Kim and Kruse models are used in the calculation of atmospheric attenuation. Wavelengths under consideration are 850 nm and 1550 nm. The result shows that 1550 nm experience lower atmospheric attenuation compared to 850 nm. Nevertheless, for atmospheric turbulence, the 850 nm wavelength system has more advantages compare to 1550 nm wavelength system. The analysis, however, is only taking care of one parameter of weather effect on FSO link, which is visibility. The experiment also conducted in temperate region with calculation of attenuation using Kim and Kruse model without real data measurement.

This manuscript (Grabner et al., 2007) explains about the analysis on the effect of atmospheric visibility on optical wave in order to predict the performance of the FSO communication link. Available models described the relationship between visibility and optical attenuation due to fog. The experiment conducted on FSO link with wavelength of 830 nm and 100 m long link operate in Praha, Czech Republic. The period of two days in November 2006 required monitoring receiver power and visibility. Least square fitting of measured data become the basis of the new model proposed. The experiment, however, conducted for a very short period under temperate region weather condition. To propose and predict model accurately, at least a year visibility data require considering the variation of the weather-changing event.

The discussion in this paper (Srinivasan et al., 2010) is on the effect of climate on line-of-sight (LOS) in FSO communication. Climate under investigation are fog and turbulence. Fog attenuation is calculated using Kruse and Kim formula. By comparing link margin and link loss, the availability of the link calculated. The period of data collection is between 2002 and 2005. The visibility data, however, collected in temperate region where fog is the major attenuation effect on FSO link. The place and weather condition of the installed FSO link determines the availability of the link.

The impact of weather on the optical pulse propagation in FSO investigated in this paper (Awan et al., 2009). Weather impacts under investigation are fog, rain and snow. The impact of transmitting optical signal evaluated by their behaviour based on measured data collected at four different places in Austria for several months. Beam loss due to scattering is calculated with empirical formula, which the transmitted optical intensity reduced 5% of its original value. The evaluation concludes that for optical wireless link in troposphere, fog is the most limiting factor as compared to rain and snow. To have a concrete result, however, more attenuation data on the FSO link required. A minimum of one-year data is needed. Since the measured data conducted in temperate regions, fog is the limiting factor; whereas in tropical region with the absence of fog, rain and haze are expected to be the limiting factor.

Channel modeling is the discussion in (Muhammad et al., 2005) with the focus on the terrestrial FSO link. The research evaluated the effect of fog, rain, snow and scintillation. These effects are evaluated using empirical formula. A channel modeling based on temperate weather condition is presented (in term of GUI) which provide the basic platform to investigate the effect of weather. It will be more useful if the modeling procedure incorporate the location of the installation site and weather condition from different regions. .

Fog attenuation prediction for optical and infrared waves discussed in (Naboulsi et al., 2004) in term of an empirical and theoretical point of view. The researcher proposed a fast transmission relationship based on an exact Mie theory calculation valid in the 0.69 μm to 1.55 μm spectral band. The propose method reduce the use of heavy computer code to predict fog attenuation according to visibility. The model to predict fog attenuation, however, needs to be checked by experimental analysis since the propose model does not take into account all distribution of attenuation presence in the weather. Furthermore, fog is applicable for a temperate region analysis, while in tropical region, haze is a valid measurement of attenuation cause on FSO link.

The analysis on the effect of haze on FSO under Malaysia environment accomplished and presented in this paper (Naimullah et al., 2007). Focused of the analysis are scattering coefficient and atmospheric attenuation effects on low visibility. Visibility data used is from the Meteorological Department of Malaysia for Subang's airport area, in the year of 2000. Although the analysis is under Malaysia's weather condition, however, the calculation of attenuation based on empirical formula of Kim and Kruse Models without any physical installation of FSO link to observe the effect of haze on the link.

The paper (Naimullah et al, 2008) presented the comparison of wavelength propagation for FSO communication. Atmospheric attenuation especially haze attenuation is selected to be used as the parameter for comparison of which wavelength performed better during a hazy condition. Wavelengths under consideration are 780 nm, 850 nm and 1550 nm. The result demonstrates that under severe low visibility, wavelength 1550 nm shows less effect on scattering coefficient. The result, however, concluded based on theoretical and mathematical calculation using available models.

Experimental analysis with physical installation of FSO link or at least lab-simulated analysis needed to verify the assumption.

The paper (Achour, 2002a) introduces a series of publication regarding simulation of FSO atmospheric propagations. This paper has focused on attenuation due to rainfall. The researcher classifies input information to model FSO atmospheric propagation into three categories deployment parameters, FSO system parameters and weather parameters. Categories of atmospheric attenuations are absorbing, scattering which are Rayleigh scattering, Mie scattering and non-selective scattering. Weather parameters under revision are Meteorological Visual Range (visibility), absolute humidity, saturation, dew point and relative humidity. Non-selective scattering occurs is due to rainfall. The analysis of rainfall attenuation starts with derivation of raindrop distribution function using Simulight software. The simulation model includes modeling the raindrop distribution based on the raindrop diameter size as well as the speed at which raindrops fall on the ground. The paper, however, presented only theoretical models without any test performed on the real FSO link. Rainfall intensities base on rain event in temperate region will have different rain intensity and raindrop size distribution compare to tropical region.

The paper (Achour, 2002b), focus on haze, fog and low cloud attenuation. The paper also discuss in detailed about the physics of atmospherics. Beer's Law describes haze, fog and cloud attenuation and atmospheric parameters discussed are absorbing, scattering in where haze, fog and low cloud reside. Method of analysis is a simulation and theoretical analysis. Wavelengths investigated are 550 nm, 850 nm and 1550 nm. The reviewer, however, focussed more on fog and low cloud whereas haze is left out from the explanation. Fog is a parameter considered in temperate region, but haze is

parameter valid for investigation in tropical region. The method is lacking in experimental analysis for verification.

A field study performs in area of Milan, Italy to investigate the effect of visibility and turbulence (D'Amico et al., 2003). The field test is for measurement of 195 m and 3160 m link distance. Working in parallel are FSO links operating at 840 nm and 1550 nm wavelength for long path measurements and wavelength 850 nm for short path measurement. The period of data collection is from 2001 until 2002. The finding introduces correction coefficient for correlating between measurement and estimation. Visibility data, however, converted into estimated specific attenuation by applying the relation proposed as Beer's law without real attenuation measurement on the FSO link. A long distance measurement of scintillation effect required instead of a short distance FSO link.

This paper (Le-Minh et al., 2010) explain about the experimental result perform on FSO link employing a different modulation scheme under the influence of atmospheric scintillation. The experiment performs in the laboratory scale with a chamber to simulate the turbulence effect. Length of the chamber is 5.5 m. The demonstration is to investigate the performance of an FSO link under the effect of turbulence by expressing it in term of BER. The analysis is perform in a controlled environment, however, cannot simulate real link installation in the turbulent prone area. The distance of the link is very short since the turbulence effect (scintillation) will affect more on longer link range. Besides that, the atmospheric effect is not the only caused by turbulence. For better conclusion on the effect of atmospheric attenuation on a different modulation scheme of FSO link, other atmospheric affect need to be included in the investigation since the atmosphere is the major factor of FSO link availability.

The paper (Vitasek et al., 2011) focuses on atmospheric turbulence in FSO channel. The wavelengths uses for FSO link are 850 nm and 1550 nm. The simulation method using OptiSystem conducted and comparison of the result with available atmospheric turbulence attenuation (Andrew's method). The analysis, however, performs by simulation and mathematical calculation using available equation. Without physical measurement of the effect of turbulence on FSO link, no concrete result can be constructed. The investigation on the distance of the link is also important to investigate the effect of turbulence on FSO link.

The researcher conducted three-month trial in Singapore to study the scintillation effect for rain and non-rain period (Ananda, 2002). Scintillation caused laser beam deformation due to changes in refractive index of the medium. The experiment data collected on the effect of three FSO link with 1 km link distance installed on open ground. The analysis of data is executing using MATLAB. Measurement of raw scintillation data for morning, midday and evening during rain and the non-rain event is carry out. The result demonstrates that scintillation effect is small on tropical environment; the effect of rain is higher and more significant. Although the study of scintillation execute in tropical region, however, the result reveals that another factor affects FSO link propagation more than scintillation. It might be due to the link distance under investigation is only 1 km. The experiment also does not give the specification of the FSO equipment under investigation. No complete internal parameters of the link discuss in the paper.

The paper (Davidsona et al., 2003) presented a report on the result of experimental measurement of scintillation on 980 nm link propagate through the turbulent atmosphere on a horizontal optical path up to 100 m in length. The experiment conducted on a plane normal to the direction of the laser beam. The light

propagated through the turbulent atmosphere as a function of retro-reflector. The experiment, however, conducts in a very short link distance under a controlled-environment. Scintillation effect is more crucial for a longer link range of FSO. The wavelength use in the experiment is a good candidate for the system under investigation only.

The paper discusses on the optical power margin or fade margin for a standard 1 km link in clear weather condition (Duncan, 2001). A mathematical formula to calculate fade margin is established. Atmospheric attenuation tabularize for common weather condition. This short report, however, does not include the region of the common weather condition. Different region will have different values for atmospheric attenuation especially region with fog, haze and heavy rain which will make the fade margin approaching to threshold (outage of the link) during the worst weather condition.

The paper (Sporik et al, 2010) discusses on the impact of distance of FSO's head at the level of the received signal. Parameters of optical attenuation under investigation are absorption and scattering of light, optical intensity fluctuation, background radiation and short-term interruption (e.g. flying bird). Link budget, the power received and geometrical attenuation presented in calculation form. Influence of atmospheric shows on Received Signal Strength Indication (RSSI), which measure the received power. The FSO link distance is set up at 200 m and the maximum distance is 425 m. The results, however, base on a calculation of the theoretical model of FSO. Availability of 3 months then scales up for year availability with an assumption that is no failure of the rest of the year. The availability analysis does not take into consideration real value of atmospheric attenuation.

Rain attenuation at Terahertz link is the focus of the discussion in this paper (Ishii et al., 2010). In millimetre-wave and terahertz wave system, raindrop-size distributions are severely and greatly attenuate the system. The paper also discuss on a few available raindrop size models. The specific rain attenuation model is predicted from raindrop size distribution with method recommended by ITU-R. The experiment conducted in the central part of Europe for 2 months with 1 km link distance. The purpose of the experiment is to collect rain data and from it rain attenuation is calculated. The experiment shows that the highest rain intensity is 12 mm/hr. The rain data collected, however, base on temperate region with lower rain rate compare to high rain rate in tropical region. The effect of higher rain intensity on the FSO link will be a major concern in tropical region. The prediction model develop base on 2 months data collection that does not cater all variations of rain throughout the year; therefore, a year of data needed to have a valid predictive model.

This paper analyzed the effect of rain intensity in Jakarta and Tangerang on the FSO system performance (Bouna et al., 2011). There exist no physical installation of FSO link and empirical model developed base on measurement in Jakarta Meteorological Department. The laser wavelength is 650 nm and 3 months data measurement. The distance of the FSO link under investigation, however, does not mention. The result accomplished by fictitiously assuming the installation of FSO system between two buildings. Rain data from the Meteorological Department usually measured in an hour interval. The hourly interval lost the information on the exact time when the rain really occurs. Prediction of empirical model required longer data measurement period and longer link distance.

The Capsoni's paper (Capsoni, 2006) discusses on the attenuation due to rain on FSO link. Rain parameters under consideration are the size distribution of

raindrops, the terminal velocity and the scattering cross section. The experiment setup is constituted of the commercial optical link with the transmit data up to 155 Mbps and wavelength 785 nm. Beam divergence is 2.5 mrad, sampled every 1 second and link distance is 319 m. Two (2) years of rain data collected from Meteorological Station. Although the investigation is conducted on FSO link, however, the measurement is done in temperate region where the rain intensity is lower than the rain intensity in tropical region. Furthermore, the link under investigation is very short.

The thesis (Sarpinah et al, 2004), explores the FSO link propagation due to weather condition. The weather condition in the focus is rain and haze. Rain and haze data collected throughout the year 2000 in Subang airport area. The collection of rain and haze data however, is from Malaysia Meteorological Department at Petaling Jaya branch. The data is in mm/hr format, which is the cumulative of the rain for one hour. The cumulative data is signified the losses of data when the rain is actually occurring and for how long it is occurring. There is no direct measurement of the attenuation of the FSO link.

The paper (Rahman et al., 2008) discuss on a preliminary result and activities of a research on rain attenuation in the Perlis region. There are two FSO products with maximum link transmission of 2500 m and 4500 m. The wavelength of the product is 785 nm and laser power 70 mW. The researcher uses ITU Recommendation to calculate specific rain attenuation. The ITU Recommendation however, is for microwave link that consider the polarization of vertical and horizontal link. Analysis of rain attenuation use existing specific rain attenuation model, which formulate using data from temperate regions. OptiSystem Software is used for the verification analysis and although the researcher mentions about measuring data but no indication of any measurement data available in the manuscript.

The paper reports on the study of a simulation of FSO transmission due to attenuation effect on Petaling Jaya area, Malaysia (Fatin et al., 2010). FSO parameters evaluate are link margin, geometrical attenuation, atmospheric attenuation and other system dependent losses. The data for evaluation is visibility data obtain from the Meteorological Department of Malaysia and input to the OptSim Software for simulation result. Receive signal performance is presented in term of eye diagram, Bit-Error-Rate (BER) and optical spectrum analysis. Although the result is obtained however, it is by simulation only without experimental analysis on the physical FSO link. The visibility data under consideration is only for a month, which does not represent the variation in weather conditions. A minimum of a year visibility data requires for a more substantial result.

Fatin's paper (Fatin et al, 2011) presents the effect of rain attenuation on FSO transmission in Kuala Lumpur. The experiment is done for 700 m link distance and 820 m wavelength with 3 mrad beam divergence. Local measurement of rain intensity and rain attenuation is calculated using k and α value based on Japan location. The data are then simulated and OPTsim Software utilize to analyse BER. The result stipulates, however, with real rain intensity but calculated rain attenuation using empirical values available in temperate regions. There exist no raw data for rain attenuation on FSO link under investigation. Furthermore, the calculation of rain attenuation achieve with parameters from Japan since k and α value for FSO link are not available in tropical region.

The author (Amandeep et al., 2012) discusses on link margin optimization of FSO under the impact of varying Meteorological conditions. Predictable attenuations and unpredictable attenuations are the two divisions of the FSO parameters. The discussion is focused on unpredictable attenuation, which are atmospheric attenuation,

rain attenuation, scintillation and snow attenuation. With the equation for unpredictable attenuation, link margin is calculated and plotted for different weather conditions. Wavelengths under investigation are 850 nm, 1300 nm and 1500 nm. Al though the analysis is done in tropical region, however, the analysis is conducted by calculating the values using empirical equations without any real experimental data. In the paper also, FSO equipment parameters are available. The assumption that they had formulated link margin equation for FSO performance evaluation is fictitious since the same equation used in ITU-R (ITU-R P.837-5, 2007). The robustness of the system also doubtful since the equipment specifications are unknown and only base on assumptions.

2.9 SUMMARY TABLE

Table 2.8
Summary of literature review

Year	Author	Title	Strengths	Limitations
1978	Olsen, R.L. Roger, D. Hodge, D.	The aRb relation in the calculation of rain attenuation	• A comprehensive set of k and α values in the frequency range from 1 GHz – 1000 GHz • Compute values with logarithmic regression to Mie scattering calculation • Apply drop size distribution analysis for "widespread" and "convective" • Theoretical comprehensive explanation	• Calculation analysis only and no real data measurement to find k an α • Temperate rainfall events
1984	Moupfouma, S.H.	Improvement of a rain attenuation prediction method for terrestrial microwave links	• Propose an empirical model of rain attenuation prediction on a terrestrial path using the effective path length method • Measured rain falls and rain attenuation (1minute interrogation time) • Proposed model reveals better agreement with experimental data than the CCIR (now ITU-R) • In good agreement with some of 30 terrestrial radio link attenuation data	• The effect of rain is analyzed on radio link • The effect of rain on communication medium that depends on different frequencies compare to FSO which does not depend on frequency • Temperate region measurement data which might give different attenuation on link in tropical region
1997	Carbonneau, T.H Wisley, D.R.	Opportunities and challenges for optical wireless: the competitive advantage of free space telecommunications link in today's crowded	• Explained on opportunities and challenges for optical wireless • Illustrated advantages of wire line and wireless last-mile technologies with some parameters of comparisons	• Weather effect on FSO link discussed is based in temperate regions • Fog is the limiting factor of FSO propagation • Other parameters of weather effect and

		marketplace.	• Presented on the transmission properties of the atmosphere, power budget and availability • Introduce k and α value for FSO link	region of installed FSO need to put into consideration for the availability or unavailability of the link analysis
1997	Jafri Din	Influence of rainfall drop size distribution on attenuation at microwave frequencies in tropical region	• Investigate the drop size distribution for Malaysia rain drops • Finding the best fit rain fall drop size distribution especially at higher rates • Compare results from rain gauge and radar • Tropical weather condition	• Microwave links that have different frequencies while FSO frequency is not considered • Base of drop size distribution calculation only • No comparison between measured and calculated rain attenuation

1998	Kim, Isaac I. Stieger, Ron A.Koontz, Joseph Moursund, Carter Barclay, Micah Adhikari, Prasanna Schuster, John Korevaar, E	Wireless optical transmission of Fast Ethernet, FDDI, ATM, and ESCON protocol data using the TerraLink laser communication system	• Analyze wireless optical transmission with some communications protocol data
			• Multiple transmit beam and large receive aperture of FSO transceivers
			• Atmospheric attenuation under evaluation is atmospheric scattering and atmospheric turbulence.
			• FSO link is tested for fast Ethernet, Fiber Distributed Data Interface (FFDI), asynchronous transfer mode (ATM) and Enterprise System Connection (ESCON) protocols.
			• Conclusion
			  ○ wireless lasercom as a very attractive alternative
			  ○ can provide a reliable and cost effective backup to existing fiber optic
				• Weather effect and availability are based on visibility measurement
				• Visibility measurement represents fog only
				• Measurement of weather attenuation is in temperate regions
				• The tropical region weather effect is different from temperate regions

1999	Kim, I. I. Mitchell,M. Korevaar, E	Measurement of scintillation for free-space laser communication at 785 nm and 1550 nm	• Experimentally measured atmospheric scintillation for 785nm and 1550nm laser beam transmission • Link ranges are about 1.2 km and 2.2 km.	• The common practice of available FSO system use 850 nm wavelengths, the experimental work on 785 nm and 1550 nm.

			• Scintillation fades are more of a problem at 1550 nm wavelength compared to 785 nm	• The effect of scintillation on 850nm need to be investigated • Does not stress on link distance in the discussion • Scintillation effect is measured under temperate weather condition • Scintillation effect is different in tropical region
1999	Zhang, W. Moayeri, N.	Power-law parameters of rain specific attenuation	• Divided rain rate into low and high • Two sets of power law for the two rain rate categories • Low rain rate: Analyze use Marshal and Palmer (M-P) rain drop size distribution • High rain rate: Analyze use Gamma, Lognormal and Law and Parson (L-P) rain drop size distribution	• Theoretical and calculation only • No real data measurement • Based on a drop size distribution calculation to develop specific rain attenuation power law • For rain rate 0 mm/hr to 150 mm/hr
2000	Kim, I. I. McArthur, B. Korevaar, E.	Comparison of laser beam propagation at 785 nm and 1550 nm in fog and haze for optical wireless communications	• Investigate the effect of fog and haze on FSO link and compare it with the propagation of laser beam with 785 nm and 1550 nm wavelengths. • Define Rayleigh scattering, Mie scattering and non-selective or geometrical scattering • Calculation of total scattering is done by mathematical modeling • Fog attenuation does not depend on the wavelength. • Attenuation of haze is higher at 785 nm compared to 1550 nm wavelength. • Introduces Kim's attenuation coefficient and the size distribution of the scattering particles	• The result is based on a mathematical model without experimental verification • Develop atmospheric attenuation with data in temperate regions • In temperate regions, fog is the limiting factors for FSO link availability.
2001	Kim, I. I.	Availability of free-space optics	• Present on availability of FSO and FSO/RF	• Parameter considers is valid for a

	Korevaar,E.	(FSO) and hybrid FSO/RF systems	system • Introduce the first map of FSO link distances contour over North America. • Use historical visibility from international airport area to analyze the availability • Two methods to calculate availability , for enterprise-class, and for carrier-class FSO link • Hybrid FSO/RF system can provide carrier-class availability of 99.999% across much longer ranges than FSO-only system	temperate region (presence of fog) • Visibility data taken from the airport area • Under the influence of fog, the availability of FSO link is only for a very short distance whereas the area without fog the result will be different • Contour map is only valid in North America.
2001	Duncan, W.	Optical Power Margin or "Fade Margin"	• Reported on optical power margin or fade margin • The fade margin is defined for a standard 1 km link in clear weather condition • Mathematical Formula to calculate fade margin is established • Atmospheric attenuation is tabulated for common weather condition	• Does not include the region of the common weather condition • Different region will have different values for atmospheric attenuation especially region with fog, haze and heavy rain • Fade margin approaching to threshold (outage of the link) during the worst weather condition
2002	Bloom, S.	The Physics of Free-Space Optics	• Explain and clarify design issues of FSO technologies using real collected data • Discussed features associated with FSO that can be considered performance enhancing • Parameters discussed are link margin, BER and wavelength • Tracking system, reducing scintillation effect, power control and eye safety are suggested as FSO system enhancement parameter	• Theoretical analysis only • Lacking simulation or experimental data • The assumption by the researcher on FSO link distance limit have not supported by any analysis • No analysis on FSO link availability for different weather condition and different climate condition
2002a	Achour, M.	Simulating Atmospheric Free-Space Optical Propagation: Part	• Introduce a series of publication regarding simulation of FSO atmospheric	• Presented only theoretical models without any test performed on the real FSO link

		I, Rainfall Attenuation	propagations • Focused on attenuation due to rainfall • Classified input information to model FSO atmospheric propagation into three categories deployment parameters, FSO system parameters and weather parameters • Atmospheric attenuations investigated are Rayleigh scattering, Mie scattering and non-selective scattering • Weather parameters under revision are Meteorological Visual Range (visibility), absolute humidity, saturation, dew point and relative humidity. • Derived rainfall attenuation using Simulight software	• Rainfall intensities are based on rain event in temperate region with different rain intensity and raindrop size distribution in tropical region
2002b	Achour, M.	Simulating Atmospheric Free-Space Optical Propagation, Part II: Haze, Fog and Low Clouds Attenuations	• Focused on haze, fog and low cloud attenuation • Discussed in detail physics of atmospherics • Atmospheric parameters discussed are absorbing, scattering • Method of analysis is a simulation and theoretical analysis • Wavelengths investigated are 550 nm, 850 nm and 1550 nm.	• Focussed on fog and low cloud whereas haze is left out of the explanation • Fog is a parameter to be considered in temperate region, but the haze is parameter valid for a tropical region to be investigated with the absence of fog • The method is lacking in experimental analysis for verification.
2002	Ramasarma, V.	Free Space Optics: A Viable Last-Mile Solution	• Give an overview of FSO technology, its capabilities and limitations, case of FSO within the last-mile broadband wireless arena, core applications, and deployment architectures • Describes factors that drive the interest in FSO technology: economic drivers and service drivers	• The paper only gives an overview on the FSO system without any analysis on any of the parameters • The installed equipment is not tested on the availability or unavailability of the link (install without analysis).

2002	Aburakawa, Y. Otsu, T.	Experimental evaluation of 800 nm band optical wireless link for new generation mobile radio access network	• Analyze applicability of optical wireless links to Radio Access Networks (RANs) • Analyze the atmospheric properties due to fog and rain • Investigate the availability of the optical wireless link • Estimate the attenuation coefficient due to rain with 10 minutes interrogation time with $k = 4.9$ and $\alpha = 0.63$	• Estimation value properties • Availability investigated based on meteorological data of visibility and rainfall rate • Rainfall rate is at the lower rate (highest 40 mm/hr) which is incomparable with rain rate in tropical region
2003	Gebhart, M. Leitgeb, E. Bregenzer, J.	Atmospheric effects on optical wireless links	• Analyze of reliability and availability of FSO link • Evaluate atmospheric effect, link margin, geometrical loss, scattering, turbulence (scintillation), visibility and BER • Link distance 2.7 km • 4 years data measurement • Mie scattering have more influence on FSO link and not Rayleigh scattering	• An experiment done in temperate regions • Measurement of atmospheric attenuation in temperate region has a different effect as in tropical region • Does not specify wavelength use for FSO link
2003	Korevaar, E Kim, I. I. McArthur, B.	Atmospheric Propagation Characteristics of Highest Importance to Commercial Free Space Optics	• Evaluate link availability base on visibility data collected at the airport area • Parameter evaluated are fog, drizzle and scintillation • Use MODTRAN software to simulate the result • Introduce model to calculate the probability of encountering a given attenuation in an average sense	• Theoretical and simulation analysis only • Analysis under temperate weather condition • Visibility collected at the airport will have different weather attenuation compared to measured in the city
2003	Naboulsi, M.A. Sizun, M. Fornel, F.	Propagation of optical and infrared waves in the atmosphere	• Discuss on propagation of optical and infrared waves on the atmosphere • Models discuss are Beer Lambert Law, Kim Model, Kruse Model and Al-	• The experiment only measures the effect of fog on the in term of visibility • Method of analysis is mathematical modeling

			Naboulsi Model, Carbonneau Model, snow attenuation model and scintillation attenuation model.	• No simulation or experimental verification of the method • Experiment accomplishes in temperate regions
2003	Bloom, S. Korevaar, E. Schuster, J. Willebrand, H.	Understanding the performance of Free Space Optics	• Explain some of the design issues surrounding FSO systems • Provide sufficient information to allow potential users to evaluate the suitability of a specific FSO system for a particular application • Extensive explanation on parameters considered	• Explanation and overview of the parameters only • No measurement or experiment on the mention parameters • Suggestion on what parameters should be considered that capable of delivering 99.9% or better performance at 500 to 1000 m link distance • Required real data analysis for a reliable conclusion since weather is the most important factors on FSO link availability
2003	Ananda, E.S.	Free Space Optics (FSO) Links in Singapore: Scintillation Effects	• Conducted 3 month trial in Singapore to study the scintillation effect for rain and non-rain period • Scintillation caused laser beam deformation due to changes in refractive index of the medium • The experiment data collected on the effect of three FSO link with 1 km link distance installed on open ground • Data analysis tool is MATLAB • Measured raw data of scintillation in the morning, midday and evening during rain and non-rain • Scintillation effect is small on tropical environment; the effect of rain is higher and more significant.	• Although the study of scintillation is done in tropical region the result reveals that another factor affects FSO link propagation more than scintillation • It might be due to the link distance under investigation is only 1 km • No specification of FSO equipment under investigation • No information on internal parameters of the link
2003	Davidsona,F.M.	Scintillation Measurements of	• Experimental measurement of scintillation	• The experiment performed in a very short

	Bucaillea, S. Gilbreathb, C. Ohb, E.	Broadband 980nm Laser Light in Clear Air Turbulence	on 980 nm link propagate through the turbulent atmosphere on a horizontal optical path up to 100 m in length • The experiment conducted on a plane normal to the direction of the laser beam • The light propagated through the turbulent atmosphere as a function of retro-reflector	FSO link distance under a controlled-environment • Scintillation effect is more crucial for a longer link range of FSO • The wavelength use in the experiment is a good candidate for the system under investigation only
2004	Naboulsi, M.A. Sizun, H. De Fornel, F.	Fog attenuation prediction for optical and infrared waves	• Fog attenuation prediction is discussed for optical and infrared waves • Empirical and theoretical point of view reviewed fog attenuation in the visibility and the IR region • Proposed fast transmission relationship based on an exact Mie theory calculation valid in the 0.69 μm to 1.55 μm spectral band • The propose method reduce the use of heavy computer code to predict fog attenuation according to visibility	• The model to predict fog attenuation need verification by experimental analysis • The propose model does not take into account all distribution of attenuation presence in the weather • Fog is valid for a temperate region, while in tropical region, haze is expected to be a valid measurement of attenuation cause of the FSO link.
2004	Sarpinah, B.S.N.	Effect of Rainfall Rate and Visibility on Free Space Optical Communications in Malaysian Environment	• Consider rain and haze effects on FSO under local weather condition • One year data of rain and haze	• Malaysia Meteorological Department data • Collected in term of mm/hr interrogation time • Losses the information on when the rain is really occurring and the time it is occurring • Does not do a direct measurement analysis of the rain intensified and rain attenuation
2005	Bandera, P, FSona, C.C	Defining a Common Standard for Evaluating and Comparing Free-Space Optical Products	• Explain basic concept of FSO link • Describe key performance of FSO link • Introduced Generalized Link Margin (GLM) for evaluating FSO equipment; independent of specific range or weather condition for evaluating and comparing	• No analysis of the stated atmospheric weather effect on the link • Focus only on the reliability of the equipment not on the availability of the link

			FSO products	
2005	Akbulut, A. Ilk, H. G. Ari, F.	Design, availability and reliability analysis of an experimental outdoor FSO/RF communication system	• Work on the characteristic of an experiment outdoor FSO and combination with radio frequency (RF) link • The objective is for higher availability and uninterrupted communication link • Design and develop an FSO / RF system • The period of experiment is 1 year • The snow storm is the most significant weather effects on the availability of FSO communication	• The experiment conducted in continental climate with snow as the major effect on FSO link • In tropical regions, snow is not the problem • The attenuation of snow on the FSO link is calculated using a mathematical formula • Missing real data analysis of the snow effect on the link
2005	Khamis, N.H.H. Jafri, D. Tharek, A.R.	Derivation of path reduction factor from the Malaysia Meteorological Radar data	• The result confirms that rain cell in Malaysia is highly convective and heavy rainfall in an area about 1.2 km (diameter) • Propose reduction factor from Malaysian Meteorological radar data • Radar ranges from 1 – 10 km	• Collected data only for 3 months • Taking into consideration only for $R_{0.01}$ in the study
2005	Bouchet, O. Marquis, T. Chabane, M. Alnaboulsi, M. Sizun, H.	FSO and Quality of Service Software Prediction	• Introduce quality of service software prediction • The software with quiet comprehensive GUI taking into consideration most aspects of parameters of FSO system • Provide result on the attenuation due to atmospheric attenuation, all the losses, link margin and link availability.	• The data are based on temperate region which rain and snow attenuation are considered as one attenuation • The prediction software is mean for France region only • Need to include function to perform analysis for other regions
2006	Ricklin, J. C. Hammel, S. M. Eaton, F. D. Lachinova, S. L.	Atmospheric channel effects on free-space laser communication	• Provide understanding of the physical process underlying optical extinction and optical turbulence-induced loss • Optical turbulence models are discussed comprehended	• Theoretical analysis only • Lack of discussion on the technique to mitigate the effect of optical turbulences

2006	Zhuanhong, J. Qingling, Z. Faliang, A.	International Conference on Communication Technology 2006 (ICCT'06)	• Introduces a series of attenuations regarding simulation of FSO atmospheric propagation • Investigate on absorption, scattering and scintillation. • Simulate the effect of fog and rain on FSO link • Results show that fog attenuate the link more than rain • Rain effect can be negligible)	• The simulation is done under temperate region data • In tropical regions, without the presence of fog, heavy rain experiences throughout the year • Rain is expected to be the major effect on FSO link propagation and cannot ne negligible
2006	Robeiro, W. Tan, R.	Free Space Optical Laser Communication Link	• Discussed on the development of a full-duplex FSO analogue/digital transceivers • Design and developed FSO laser communication link • The transceivers are capable of simultaneously transmitting and receiving either analogue or digital information • The selection is controlled by two switches	• The developed model lack of test on the environmental effect on the link • Local weather attenuations are the major effect therefore need to be taken care off
2006	Capsoni, C. Nebulosi,R. D'Amico, M.	Attenuation due to rain on FSO	• Discussed attenuation due to rain on FSO • Rain parameters under consideration are the size distribution of raindrops, the terminal velocity and the scattering cross section • The equipment of optical link with transmit data up to 155 Mbps and wavelength 785 nm • Beam divergence is 2.5 mrad • Sampled every 1 second • Link distance is 319 m • Rain data are taken from Meteorological Station for a period of 2 years	• Although the investigation is conducted on FSO link, the measurement is done in temperate regions • Rain intensity is lower than the rain intensity in tropical region • The link under investigation is very short
2007	Grabner, M. Kvicera, V.	On the relation between atmospheric visibility and	• Analyzed effect of atmospheric visibility	• The experiment conducted in temperate

		optical wave attenuation	on optical wave, to predict the performance of the FSO communication link • Available models are used to describe the relationship between visibility and optical attenuation due to fog • The experiment is done on FSO link with wavelength of 830 nm and 100 m long path • Receiver power and visibility is monitored for two days in November 2006 • A proposed new model based on the least square fitting of data	regions • Very short FSO link distance • Very short time data measurement • To propose and predict model accurately, at least a year visibility data require considering the variation of the weather changing event
2007	Naimullah, B.S.S. Hitam, S. Shah, N.S.M. Othman, M. Anas, S.B.A. Abdullah, M.K.	Analysis of the Effect of Haze on Free Space Optical Communication with the Malaysian Environment	• Analysis on the effect of haze on FSO under Malaysia environment • Focused of the analysis are scattering coefficient and atmospheric attenuation effects on low visibility • Visibility data used is from the Meteorological Department of Malaysia for Subang's airport area (year of 2000)	• Although the analysis is under Malaysia's weather condition, it is based on a calculation • Attenuation is calculated via an empirical formula of Kim and Kruse Models • No physical installation or FSO link to see the effect of haze on the link
2007	Colvero, C. P. Cordeiro, M. C. R. von der Weid, J. P.	FSO systems: Rain, drizzle, fog and haze attenuation at different optical windows propagation	• Presented in experimental comparison of three optical transparency windows • Period of 1 year • The three optical windows are 0.78 μm, 1.55 μm and 9.1 μm • Proposes two methods for recording real time measurements of visibility • Online visibility measurement together with received power data are monitored, allowing a precise comparison of the links for a wide range visibilities	• It is assumed that the method can be used at other region and different wavelength • The equipment to conduct the experiment in different region with different operation wavelength is expensive • Does not specify the link distance of the experiment conducted • Where link distance plays an important role in term of link availability
2007	Silva Mello, L.A.R. Pontes, M.S.	A new method for the prediction of rain attenuation in	• Proposed new method for the rain attenuation prediction	• Purely empirical method • Uses one single point of the rainfall rate

	De Souza, R.S.L	terrestrial links using the concept of effective rainfall rate	• Method use is an effective rainfall rate and the full rainfall rate cumulative distribution • Defined the expression of effective rain intensity • Cover mostly all percentages of time exceeded • Simple to apply	distribution to predict the attenuation distribution • Cannot be physically justified of the reduction factor and extrapolation function because it is frequency dependent
2007	Kolka, Z. Wilfert,O. Biolkova, V.	Reliability of digital FSO links in Europe	• An analysis of a very huge visibility record collected from 210 airports • Four year data collection period in European area • Analyze the link availability • Link availability is between 0.1 – 1% which mean a total of one to two day outage for a period of 1 year	• Not locally measured, but collected at the airport area • Evaluating fog as the limiting factor of link propagation, whereas, in tropical region fog is absent • Use available model to compare with the measured data • Temperate weather condition
2007	Kvicala, R. Kvicera, V. Grabner, M. Fiser, O.	BER and availability measured on FSO link.	• Deal with the problem of measuring the BER of FSO system • Implementing of BER tester with E1 interface system • Atmospherics under investigation are dense fog, moderate fog, thin fog and haze • Proposed Forward Error Correction algorithm to enhance transmission property of FSO link	• Data is meteorological data which are no locally measured • Temperate weather condition • Investigating fog as the cause of FSO link interruption while no fog in tropical weather condition • Four month data collection period
2008	Naimullah, B. S. Othman, M. Rahman, A. K. Sulaiman, S. I. Ishak, S. Hitam, S. Aljunid, S. A.	Comparison of wavelength propagation for Free Space Optical Communications	• Discuss on comparison of wavelength propagation for FSO communication • Atmospheric attenuation especially haze attenuation is selected to be used as the parameter for comparison • Wavelengths under consideration are 780 nm, 850 nm and 1550 nm • Under severe low visibility, wavelength	• The outcome is concluded based on theoretical and mathematical calculation using available models • The theory need to be proved by lab-simulated event and experimental analysis with real FSO link to verify the assumption

			1550 nm shows less effect on scattering coefficient.	
2008	Sandalidis, H. G. Tsiftsis, T. A. Karagiannidis, G. K. Uysal, M.v	BER Performance of FSO Links over Strong Atmospheric Turbulence Channels with Pointing Errors	• Investigate the error rate performance of FSO links over strong turbulence channels with pointing error effect • Turbulence model used is K distribution • Derived a multiplicative statistical channel model for fading conditions and a closed-form BER expression • Atmospheric turbulences and building sway (pointing loss) are the two dominant factors affecting the performance of optical wireless	• The result is verified by the assumption of an FSO system model • A model derived from analytical expression and mathematical calculation without the presence of real data analysis • Does not taking into consideration of geographical contour of the installation site since some places, building sway is not a problem at all
2008	Awan, M. S. Leitgeb, E. Marzuki, Khan, M. S. Nadeem, F. Capsoni, C.	Evaluation of fog attenuation results for optical wireless links in free space	• Evaluated different fog • The attenuation evaluated for five and two winter months respectively and eight summer days in Nice • Method of investigation is an experiment • The wavelengths of the link are 850 nm and 950 nm • The FSO link distance is 79.8 m and 650 m	• Measurement accomplished in temperate region with a short link distance • Since it is in temperate regions, only fog is considered, whereas in tropical region fog is absent
2008	Husagic, A. Al-Khateeb, W	Effect of Weather Conditions on Quality of Free Space Optics Links (with focus on Malaysia).	• Discussed on the quality of an FSO link in term of link margin and power received at the receiver. • Covers the specific weather condition under Malaysia environment • Method of link performance analysis is simulation • Rain and haze data are taken from the Meteorological Department of Malaysia	• Method analysis is calculation and simulation only • The analysis lacking on the existent attenuation on physical FSO installed under Malaysia environment • Rain and haze data taken from meteorological department, that loss the information on instantaneous rain time • Scintillation effect is discussed in brief
2008	Rahman, A. K.	Study of rain attenuation	• Focussed on rain attenuation for the local	• ITU Recommendation values of specific

	Anuar, M. S. Aljunid, S. A. Junita, M. N.	consequence in free space optic transmission	weather condition • Under tropical weather condition • 2 products of FSO which have a maximum range of 2500 m and 5000 m • The wavelength is 785 NM • Laser power is 70 nm • Use ITU Recommendation for calculating specific rain attenuation	rain attenuation are for use by microwave link by considering the horizontal and vertical link • Analysis is based on temperate region model • Validate the analysis using OptiSys Software • No direct measurement of rain and haze effect on the FSO is made
2009	Moupfouma	Electromagnetic wave attenuation due to rain: a prediction model for terrestrial or L.O.S. SHF and EHF radio communication	• Propose new approach for rain attenuation prediction modeling • Prediction is based on the percentage of time at any time rain attenuation will be exceeded, provided that the rain rate $R_{0.01}$ (mm/hr) is available • Propose new expression for effective path length analysis that will best fit the prediction model	• Temperate region data analysis • The effect of rain on the microwave link that need to consider the polarization which is not the case of FSO • Theoretical and calculation and derivation of specific rain attenuation not based on direct measurement of rain intensity and rain attenuation
2009	Prokes, A.	Atmospheric effects on availability of free space optics systems	• Discuss on atmospheric effects on FSO system • Focus on link parameters and atmospheric attenuation • Parameters under investigation are scattering, internal parameter power loss, and link availability • The longest distance of an FSO link suffers more turbulence effect	• Atmospheric effect is based on temperate region • Visibility collected at the airport area • No info available on the distance of FSO link • Visibility is not locally measured on its effect on FSO link
2009	Popoola, W. O. Ghassemlooy, Z. Awan, M. S. Leitgeb, E.	Atmospheric channel effects on terrestrial free space optical communication links	• Atmospheric parameters under study is Mie scattering • Methodology use is a mathematical calculation using available empirical model by Kim and Kruse • Times profile of visual range and specific	• The analytical focus on fog event occur for 1-day only • The period of investigation is very short • A concrete result of the weather effect on an FSO link is unattainable

			attenuation is presented for the 1 - day event • The effect of scintillation is discussed in term of BER	
2009	Leitgeb, E. Awan, M.S. Brandl, P. Plank, T. Capsoni, C. Nebuloni, R. Javornik, T. Kandus, G. Muhammad, S. S. Ghassemlooy, F. Loschnigg, M. Nadeem, F.	Current Optical Technologies for Wireless Access	• Study system requirement parameters for optical wireless evaluation • Parameters discuss are link specification/data rate, response time, timelines data throughput, availability and reliability • To increase the availability of an FSO link; a hybrid system of FSO and microwave is the solution	The result is based on calculation and empirical equation To have a tangible result, field test on an FSO system concerning the local atmospheric condition is necessary The only atmospheric condition taking into consideration is fog
2009	Dordova, L. Wilfert, O.	Free space optical link ranges determination on the basis of meteorological visibility	• Determine FSO link range with the effect of meteorological visibility • Calculation of atmospheric attenuation using empirical equations of Kim and Kruse model • Wavelengths consider are 850 nm and 1550 nm • 1550 nm experience lower atmospheric	• Consider visibility parameter only for the effect of weather • The experiment conducted in temperate regions • Calculation of attenuation using Kim and Kruse model • Lack real data measurement of the atmospheric attenuation on the link

			attenuation compared to 850 nm • For atmospheric turbulence, the 850 nm wavelength system has more advantages compare to 1550 nm	
2009	Awan, M. S. Marzuki, Leitgeb, E. Nadeem, F. Khan, M. S. Capsoni, C.	Weather Effects Impact on the Optical Pulse Propagation in Free Space	• Weather impacts under investigation are fog, rain and snow • Data collected at four different places in Austria for several months • Beam loss due to scattering is calculated by empirical formula • Optical wireless link in troposphere, fog is the most limiting factor as compared to rain and snow	• Require more attenuation data on the FSO link to have a concrete outcome • A minimum of one year data is needed and not just a few months • Data measurement conducted in temperate region therefore fog is the limiting factor • Whereas in tropical region with the absence of fog, rain and haze are expected to be the limiting factor
2009	Loschnigg, M. Mandl, P. Leitgeb, E.	Long-term performance observation of a Free Space Optics link	• Discussed on the long-term performance observation of an FSO link in term of availability of the optical link under the influence of fog • The distance of FSO link is 300m • Data collection is from April 2008 until end of November 2008 • Wavelengths investigated are 550 nm, 850 nm and 950 nm	• The availability measurement is done in the Ethernet layer and not in the physical layer of the FSO link • Whereas, the carrier class availability is measured in the physical layer • Short link distance (300m) of FSO transmission • Measured data in temperate region with fog is the limiting factor
2009	Karimi, M. Nasiri-Kenari, M	BER Analysis of Cooperative Systems in Free-Space Optical Networks	• Explained in the BER analysis of cooperative systems in FSO networks • Setting up 3-ways FSO communication and applying cooperative protocol • Numerical analysis and mathematical model are presented in the proposed cooperative system • Performance analysis is based on bit detect and forward (BDF), Adaptive Bit Detect and Forward (ABDF) and Adaptive	• Analyzed based on numerical results only, to conclude which cooperative system is best deployed • Does not taking into consideration atmospheric attenuation on the link

			Decode and Forward (ADF)	
2010	Fatin, H.H. Abu, S.M.S. Farah, D.M.	Simulation of FSO Transmission at Petaling Jaya due to Attenuations Effect	• Simulation using OptSim Software on FSO transmission due to attenuation effect • FSO parameters evaluate are link margin, geometrical attenuation, atmospheric attenuation and other system dependent losses. • Visibility data obtain from the Meteorological Department of Malaysia and input to the • Receive signal performance is presented in term of eye diagram, Bit-Error-Rate (BER) and optical spectrum analysis.	• The result is from simulation analysis only without experimental analysis on the physical FSO link • The visibility data are taken only for a month • Visibility data do not represent the variation in weather conditions. • To have a concrete result, 1 year data are required
2010	Dordova, L. Wilfert, O.	Determination of atmospheric transmission media properties in optical spectrum of analysis of optical beam profile	• Introduce a quick determination characteristic of the atmospheric transmission media in the optical band • Optical intensity profile explains the characteristic of atmospheric transmission media • Determine volume of turbulence and calculation of attenuation by aerosol in atmosphere • The method provides promptness for determining characteristics of atmospheric transmission media	• The method is based on mathematical analysis using available empirical equation of Kim and Kruse • Absent of experimental verification • Accuracy of the method needs to be verified by experimental analysis
2010	Srinivasan, R. Sridharan, D.	The climate effects on line of sight (LOS) in FSO communication	• Discussed on the effect of climate on line-of-sight (LOS) in FSO communication • Investigated fog and turbulence • Fog attenuation is calculated using Kruse and Kim formula • Availability of the link is calculated by comparing link margin and link loss caused	• The visibility data collected in temperate region where fog is the major attenuation effect on FSO link • In a tropical region haze is expected to be the limiting factor • Visibility data collected at the airport area • Availability varies in depend on the local

			by attenuation of fog on the link • Visibility data collected at airport area in year 2002 and 2005	weather condition • Installation site is important to analyze FSO link availability
2010	Le-Minh, H. Ghassemlooy, Z. Ijaz, M. Rajbhandari, S. Adebanjo, O. Ansari, S. Leitgeb, E.	Experimental study of bit error rate of free space optics communications in laboratory controlled turbulence	• Experimental results performed on FSO link employing a different modulation scheme under the influence of atmospheric scintillation • Laboratory scale with a chamber to simulate the turbulence effect • Length of the chamber is 5.5 m • Express the investigation result in term of BER	• Analysis in a control environment cannot simulate real link installation in the turbulent prone area • The distance of the link is very short since the turbulence effect (scintillation) will affect more on longer link range • Beside that the atmospheric effect is not only caused by turbulence • Required consideration on other atmospheric effect for better result
2010	Henniger, H. Wilfert, O.	An introduction to Free-space Optical Communications	• Overview of the challenges a system designer has to consider while implementing on FSO system • Discussed on selected optical modulation scheme • Overall system performance can be quantified using link margin, without and with atmospheric disturbance • Discussed in detail the influence scintillation effect	• Consider only one aspect of disturbance on FSO link • Other important atmospheric parameters need to be considered based on local weather condition • Method of investigation is by means of available empirical formula and calculation only
2010	Ishii, S. Sayama, S. Mizutani, K.	Rain Attenuation at Terahertz	• In milimeter-wave and terahertz wave system, raindrop-size distributions are severe and greatly attenuate the system • Discussed on a few available raindrop size models • Predicted a specific rain attenuation based on raindrop size distribution analysis using the method recommended by ITU-R • The experiment has been conducted in the	• Rain data measured in temperate regions • Rain rate is lower compared to high rain rate in tropical region • The effect of higher rain intensity on the FSO link will be a major effect compared to temperate regions • The prediction model has been developed for data collection only for 2 months, which does not cater all variations of rain

			central part of Europe for 2 months with 1 km link distance • The experiment is to collect rain data and rain attenuation is calculated • The highest rain intensity measured is 12 mm/hr.	throughout the year
2010	Florex, S. A. J.	Circular polarization and availability of free space optics (FSO) communication systems	• Describes the results obtained from the analysis of FSO propagation in a contaminated atmosphere and on the availability of the link • Presented on method to estimate the availability of FSO system knowing the distance of the link and some physical characteristics of the atmosphere • The modulation scheme is Circular Polarization Shift Keying (cPolSK)	• Method of analysis is a mathematical calculation based on empirical formula • Weather effect on FSO does not measure experimentally • Does not stated link distance •
2010	Šporik, J. Tejkal, V.	The increase of availability of an FSO link by reducing the distance of FSO's Heads	• Discussed on the impact of distance of FSO's head on the level of the received signal • Investigate absorption and scattering of light, optical intensity fluctuation, background radiation and short-term interruption (e.g. flying bird) • Link budget, the power received and geometrical attenuation presented in calculation form • Received Signal Strength Indication (RSSI), used to monitor measured received power • The FSO link distance is set up at 200 m and the maximum distance is 425 m	• Results are based on a calculation of the theoretical model of FSO • Availability of 3 months then scales up for a year availability with an assumption that is no failure of the rest of the year • The availability analysis does not take into consideration real value of atmospheric attenuation
2010	Saquib, Nazmus	Free space optical connectivity	• Discussed on using FSO as a last mile	• Lacking of real data analysis on the

	Sabbir Rahman Sakib, Md Saha, Apurba Hussain, Mustafa	for last mile solution in Bangladesh	solution in Bangladesh • Give overviews of other available telecommunication technologies • Discussed internal parameter, external parameter of FSO system, link budget, the power received and geometrical loss.	weather effect on FSO link under Bangladesh environment • The conclusive result of the availability of an FSO link under Bangladesh environment is unreachable • Only is focused on an overview of FSO systems in general
2011	Plank, T. Czaputa, M. Leitgeb, E. Muhammad, S. S. Djaja, N. Hillbrand, B. Mandl, P. Schonhuber, M.	Wavelength selection on FSO-links	• Analyzed on the stability of different optical wavelengths • Wavelength selections are dependent on the desired application, atmospheric effects, availability of receiver and transmitter components • Investigate fog attenuation • Wavelengths studied are 10 μm, 850 nm, 1064 nm, 1300 nm and 1550 nm • Most significant optical frequency bands are in the 850 nm, 1550 nm and 10 μm band	• The conclusion is based on calculation from the empirical equation without real test on the effect of atmospheric attenuation on selected wavelengths • Measurement conducted in temperate regions • Only the fog is considered in the analysis
2011	Vitasek, J. Latal, J. Hejduk, S. Bocheza, J. Koudelka, P. Skapa, J. Siska, P. Vasinek, V.	Atmospheric turbulences in Free Space Optics channel	• Focused on atmospheric turbulence in FSO channel • Wavelengths are 850 nm and 1550 nm • Method of analysis is through OptiSystem stimulation • The result is compared with available atmospheric turbulence attenuation (Andrew's method).	• The analysis is performed by simulation and mathematical calculation using available equation • Without physical measurement of the effect of turbulence on FSO link • A concrete result cannot be constructed • Link distance is another important parameter to consider for effect of turbulence on FSO link
2011	Abdulrahman, A. Y. Rahman, T. A. Rahim, S. K. A. Ul Islam, M. R.	Empirically Derived Path Reduction Factor for Terrestrial Microwave Links Operating at 15Gz in Peninsula Malaysia	• Describe the technique of deriving path reduction factor from experimental rain rate and rain attenuation data • Measured over seven Digi Mini-Link	• Tropical region analysis of the effect of rain on microwave link • The rain attenuation on the ink might give a different value comparable to on FSO

			operating at 15 GHz in Malaysia • Proposed empirical path reduction factor and comparison with ITU-R model • Data collection from January 2001 until May 2005 in Kuala Lumpur area • Long-term hourly precipitation data (12 years) are obtained from Meteorological Services Malaysia (MMS) and converted the hourly data to the equivalent one-minute rainfall rate	link • To develop a concrete prediction model, recommended by ITU-R, one-minute rain intensity interval is required • Meteorological Department usually collected based on an hourly basis, therefore, it lacks on the information at the real time the rain really falls during that one hour
2011	Bouna, R. W. L. Uranus, H. P.	Analysis of the effect of rainfall intensity in Jakarta and Tangerang to the performance of free space optics communication system	• Reported on the analysis of the effect of rainfall intensity in Jakarta and Tangerang to the performance of FSO system • The FSO link is assumed to be installed in a building • An empirical model is developed based on measurement in Jakarta and rainfall data from Meteorological Department • The laser wavelength is 650 nm • The data are measured for 3 months	• Does not mention the link distance of an FSO link under investigation • Fictitiously of assuming FSO system is installed between two buildings • Rain data from the Meteorological Department usually measured in an hour interval • The hourly interval lost the information on the exact time when the rain really occurs • Required longer data measurement to develop an empirical prediction model
2011	Fatin, H.M. Abu Sahmah, M.S. Nachimani, C.	Effect of Rain Attenuations on Free Space Optic Transmission in Kuala Lumpur	• Presented the effect of rain attenuation on FSO transmission in Kuala Lumpur • The experiment is done for 700 m link distance and 820 m wavelength with 3 mrad beam divergence • The measurement of rain intensity is done locally • Rain attenuation is calculated using k and α value based on Japan location • The data are then simulated and BER is analyzed in OPTsim Software	• The result stipulates with real rain intensity but calculated rain attenuation using empirical values available in temperate regions • There exist no raw data for rain attenuation on FSO link under investigation • Rain attenuation is calculated with parameters from Japan • k and α value for FSO link are not available in tropical region

2011	Mandeep, J.S. Ooi Wen, H.	Modified ITU-R rain attenuation model for equatorial climate	• Modified ITU-R rain attenuation model improved the rain attenuation prediction error in tropical climates • Three years measurement data from satellite SuperBird-C	• New proposed of vertical adjustment reduction factor that consider the elevation angle cannot be applied to the FSO system • It is only applicable to satellite evaluation of rain attenuation measurement
2011a	Singh, M.K. Kapoor, V. Sharma, N. Goswami, A.	Bit Error Rate Analysis of Free Space Optical Link Using Different Optical Windows	• Presented in the bit error rate analysis of an FSO link using different optical windows • Optical windows under investigation are 780 nm, 850 nm, 1310 nm, 1550 nm and 1610 nm • Bit error rate for each optical window is analyzed using simulation methods	• The analysis is based on simulation method • Atmospheric turbulence is based on assumed values without real data • No physical installation of FSO system
2011b	Singh, M.K. Kapoor, V. Sharma, N. Goswami, A.	Power Budget Performances of Free Space Optical Link using Direct Line of Sight Propagation	• Study on receives optical power performances of FSO link • Analyzing the optical aperture size that achieves the best average BER given the same amount of transmitted power • A method of analyzing is simulation • The wavelength of FSO is 1550 nm • Beam divergence 3 mrad • Link distance is 500 m	• The analysis is based on simulation only • The atmospheric attenuation effect is crucial in determining the performance of FSO link • The distance of the study is just a short distance, which makes the performance higher compare to longer distances and the atmospheric effect lesser
2012	Nazmi, A.M. Amr, S.E. Mostafa, H.A.	Pointing Error in FSO Link under Different Weather Conditions	• Evaluate pointing error for practical Bit Error Rate • Evaluation for FSO link under different weather conditions at 1.55 µm • Evaluate the scattering effect on the link	• Evaluation is done with the simulation analysis using an empirical formula of power received, atmospheric attenuation coefficient and scattering only • Simulation is performed for a fog effect on FSO whereas fog is not the restraining factor in tropical region • Analysis is not meant for tropical users or designers
2012			•	•

2.10 SUMMARY

The review of previous work by other researchers as summarized in Table 2.9 motivates us to do research on this area. From the summary table we can conclude that for FSO system, no specific rain attenuation model available for tropical region. Existing and standard use of specific rain attenuation parameters based on data measured in temperate regions. Specific rain attenuation available for the tropical weather condition has measured data with attenuation on the satellite link or microwave link and not on the FSO link. The result might not give an accurate measurement for tropical region where the rain rate is higher.

In order to predict accurate specific rain attenuation parameters, we need to analyze effective path length that considers reduction factors. From literature review, a lot of analysis on path reduction factor available in another medium of transmission but not for FSO link.

Since FSO link affected strongly from fog attenuation, which is a condition in temperate regions, in the literature clearly stated that most of the availability measurements considered fog or visibility measurement. While in tropical region, fog is the absence of the factor that attenuate the FSO link but rain and haze expected to affect the availability of FSO link.

Therefore, the aim of this research is to develop and propose new specific rain attenuation parameters for FSO under tropical weather condition using direct measurement of rain intensity and rain attenuation with 1-minute integration time. In order to have the accurate prediction model, we need to analyzed effective path length. The analysis is in term of effective path length to focus on the reduction factor. Another aim of this research is to predict the availability of an FSO link under tropical weather condition. With all the data that we have, we can perform analysis on the FSO

link signal performance in term of BER analysis and analyze a long distance range of FSO.

CHAPTER 3

EXPERIMENTAL SETUP, DATA MEASUREMENT AND DATA ANALYSIS

3.1 INTRODUCTION

The methodology of this research is experiment and data analysis. This chapter explain about the experimental setup of all the equipment use for this research. Along with the experimental setup is the data measurement and data analysis.

The structure of this chapter, firstly, the discussion is on FSO system and setup, follow with FSO data measurement. The following section will discuss on rain intensity meter setup and data measurement. The last section is on the visibility meter setup and data measurement. All the discussion with comprise of data analysis.

3.2 FSO SYSTEM SETUP AND DATA MEASUREMENT

FSO system is a line of sight system with receiver and transmitter unit. Since both equipments transmit and receive signal at both sides, the term use to describe it is transceiver. Rain attenuation is the measurement of the effect of rain on the link. The attenuation is acquired by monitoring and logging the level of power receives on the FSO unit. The following subsection will discuss on the FSO system setup and rain attenuation measurement on the link.

3.2.1 FSO System Setup

The basic FSO system is rather simple as shown in Figure 3.1 (Tom et al., 2005)

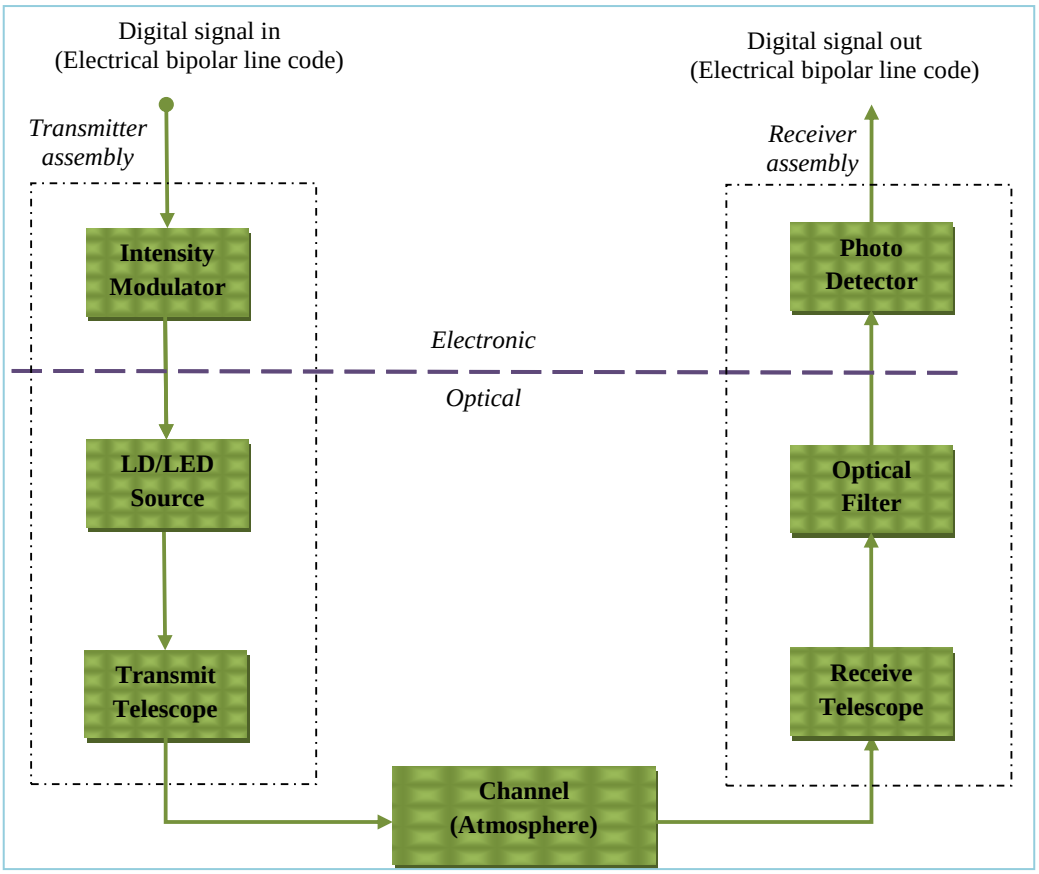

Figure 3.1. Basic FSO system

The FSO communication technology uses light to transmit information through an atmospheric medium (Davide et al., 1986). The light use is a low power infrared beam, which does not harm the eyes. FSO and fiber equipment can be combined without intermediate conversion since both the air and the material used for fiber cables have a good transmittance in the established wavelength. To ensure the highest performance of an FSO system, it is important to choose a wavelength that has the following characteristic in (Hudson Jr, 1969):

- Operation at higher power levels (important for longer FSO system)
- Favourable high-speed modulation characteristic (important for high speed FSO system)

- Components small on footprint and low in power consumption (important for overall system design and system maintenance)
- The capability to operate over a wide temperature range without showing major performance decay or degradation (important for outdoor system installation)
- Mean time between failure (MTBF) operation exceeding 10 years.

The suitable ranges of wavelength are 850 nm and 1550 nm. Some characteristics of the wavelength are as shown in Table 3.1. Our FSO system adopts 850 nm wavelengths.

Table 3.1
Characteristic of 850nm and 1550nm wavelength equipment

850nm	1550nm
Low attenuation	Low attenuation
Reliable	Reliable
Inexpensive transmitter and detector components	High quality transmitter and detector components
Widely use by today's service provider	New technologies amplifiers to boost transmission power
Highly sensitive avalanche photo diode (APD) detector technology	Development of wavelength division multiplexing (WDM) is feasible in this range
Advanced vertical cavity surface emitting laser (VCSEL)	Very high speed semiconductor laser technology

Table 3.2 shows the specification of the FSO equipment. Since the transmission of the FSO link comprises of sending and receiving for each link head, the term to describe it is a transceiver. There are four transmitters and four receivers on both transceivers. It is 850 nm wavelength equipments (Lightpointe). Detail specification of FSO link is in Appendix A. The bit rate is quite low for current communication system. It is because this research starts with the collaboration between

International Islamic University Malaysia (IIUM) and MIMOS Berhad (MIMOS). Initially, the collaboration is for a project of Quantum Key Distribution on FSO links (QKD). Therefore, the purchase of the equipment need to accommodate the transmit bit rate of quantum key using BB84 protocol.

Table 3.2
Specification of FSO transceivers

Item	Description
Beam Divergence	2 mrad
Output wavelength	850 nm
Transmit power	6 mW
Transmit Lens	2.5 cm
Receiver sensitivity	-45 dBm
Receiver lens	8 cm
Number of receivers	4
Number of transmitters	4
Bit Rate	155Mbps

The installation of FSO transceivers are at two sites within IIUM district, which are at Kulliyah of Engineering and Ruqayyah's hostel (*Mahallah* Ruqayyah) where there exist line of sight between both places. The distance of both transceivers is 800m. The site info of both transceivers is as shown below.

Table 3.3
Location of FSO transceivers

Location A		Location B
Latitude	3°15'10.15"N	3°15'35.50"N
Longitude	101°43'52.77"E	101°43'56.09"E
Elevation	80 m	102 m
Range	800 m	

FSO system works when there is a line of sight (LOS) and Figure 3.2 is showing the path profile for the two locations of FSO transceivers. Location for the first transceiver is on the rooftop of engineering building (location A) and the second transceiver is on the hostel site, *Mahallah* Ruqayyah Block G, (location B).

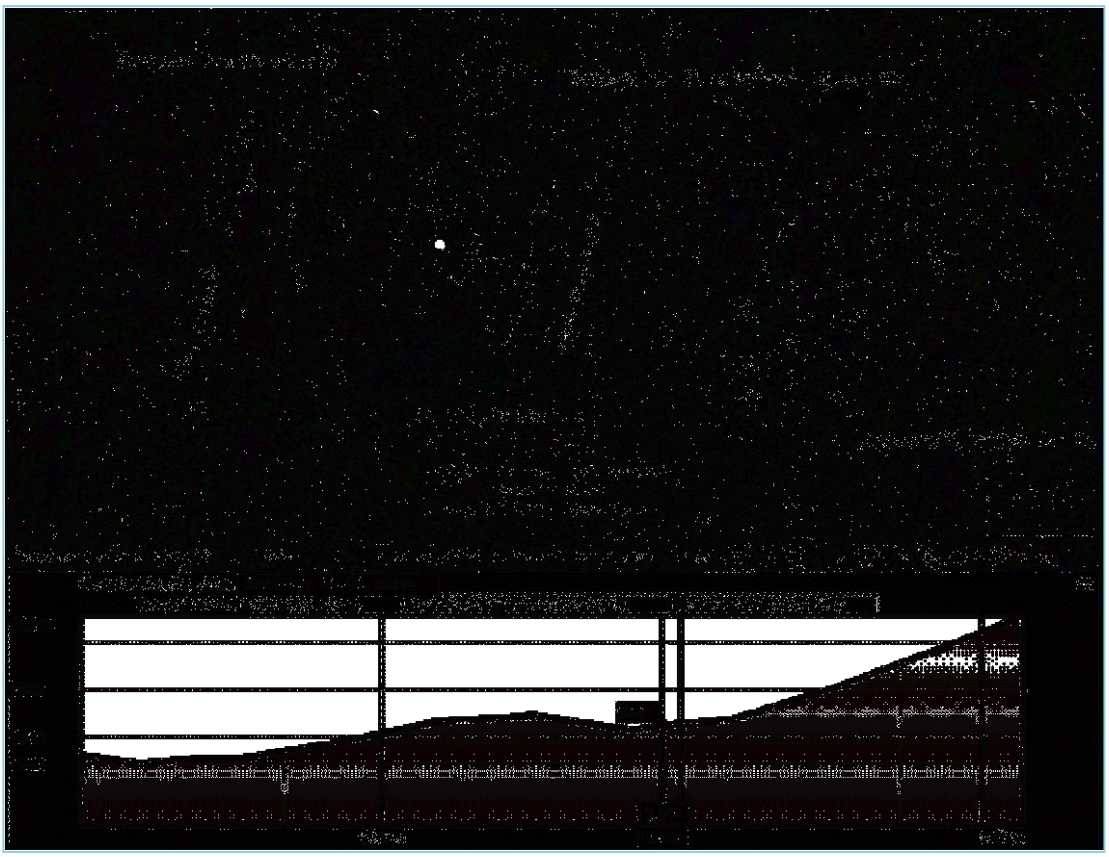

Figure 3.2. Location of FSO installation site from Google Earth

From Figure 3.2, the two FSO transceiver install for experimental analysis have a clear line of sight as required for FSO link transmission availability. Figure 3.3 shows a complete setup of FSO equipments for location A and B. A multi patch cable connects between the management points of the link head to the monitoring device via PC interface. The source of data transmission is from the data point of the link head and media converter. The other side of the transceiver is loop backed using fiber cable.

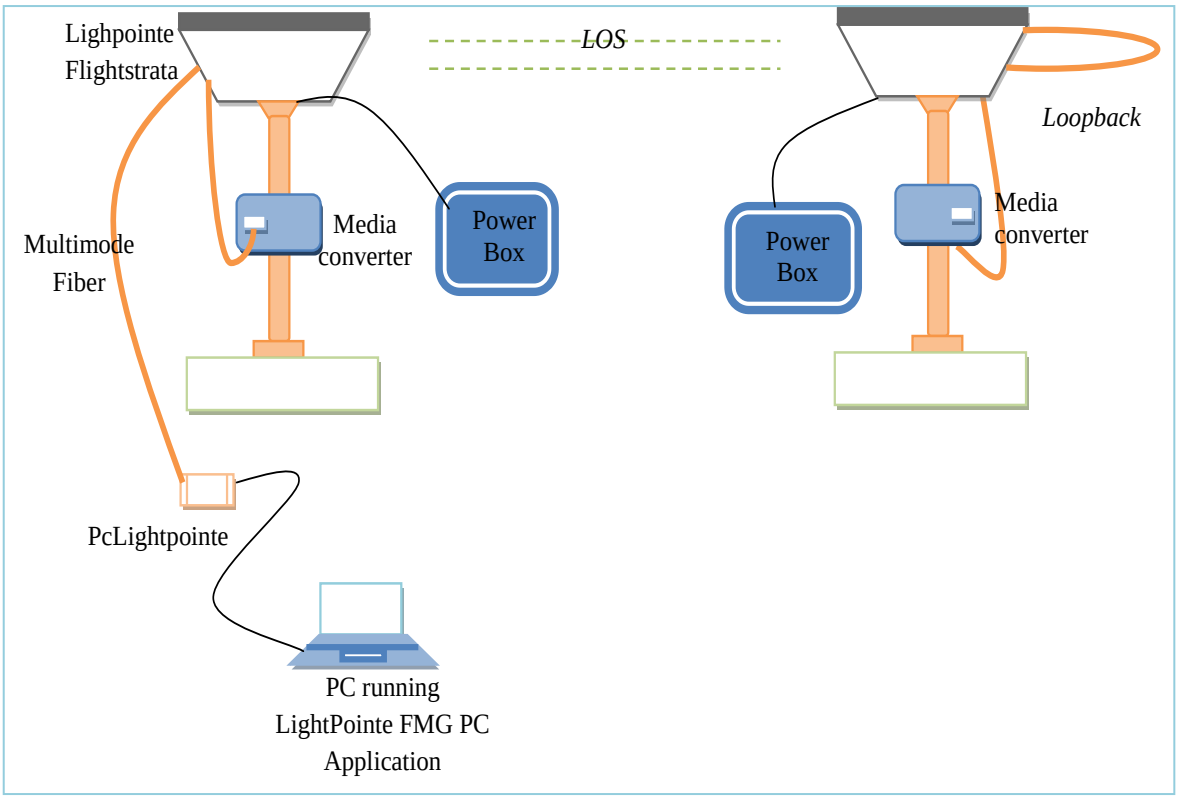

Figure 3.3. Complete setup of FSO equipments for location A and B

The physical setup of the equipments for both sites is as shown in the following figure.

Figure 3.4. Installation site of FSO links head at location A and location B

FSO link transmission is in the form of receiving level signal, monitored in location A, while looped back connection is for location B. In location A, PCLightpointe interfaced to the link head via optical wires and to the monitoring

device via Universal Serial Bus (USB) and serial connection. For a complete configuration of the monitoring device parameters, refer to Appendix B.

3.2.2 Data Measurement

During rain period, data is monitored and logged into the computer in the form of power receive level of an FSO link. Sample of rain effect on FSO link, which is the rain attenuation on the link, is as shown in Figure 3.5. Every 10 seconds the logger takes to log data into the computer in 24 hours time and a new data set will begin at 0.00 hour the next day.

Figure 3.5. Sample of attenuation of FSO link during rain on 2 October 2011

Figure 3.5 shows rain falls on FSO link for 1 hour and 25 minutes. The power received level before rain is -25 dBm and drop until around -39 dBm due to rain

intensity. The lowest dBm is associated with high rain intensity and next subsection will touch on this matter in details. Power receives level is extracted out of the log data every one minute. Sample of monitoring power-received data is as shown in Table 3.4.

Table 3.4
Sample of power received measured on 2 October 2011

Time (minute)	Power received (dBm)
4.56	-27
4.57	-28
4.58	-31
4.59	-31
5	-28.5
5.01	-28
5.02	-27
5.03	-27
5.04	-27
5.05	-30
5.06	-34
5.07	-37
5.08	-37
5.09	-38
5.1	-38
5.11	-38
5.12	-39

Table 3.4 shows an example of receive power measurement of the FSO link and it is a representative of the attenuation on the link. We extract rain attenuation values for a year rain event. Next subsection discusses about rain intensity setup and data measurement.

3.3 RAIN INTENSITY SYSTEM SETUP AND DATA MEASUREMENT

Rain intensity is a measured of the amount of rain per unit time. Rain gauge is the equipment to measure rainfalls. Rain gauge also known as an udometer or a pluviometer of an ombrometer or a cup (Wikipedia). There are several types of rain gauge and some of it is as listed below

- Standardized rain gauge
- Weighing precipitation gauge
- Tipping bucket rain gauge
- Optical rain gauge
- Acoustic rain gauge

Our rain intensity measurement equipment is tipping bucket rain gauge. Although tipping rain gauge is not as accurate as the standard rain gauge, however, the advantage of the tipping is that it is easier to capture the characteristic of the rain the rain is light, medium or heavy.

3.3.1 Rain Gauge System Setup

The tipping bucket rain gauge consists of a funnel that collects the precipitation into a small seesaw-like container. The rain travels down the funnel and drops into one of the two seesaw buckets balances on a pivot. The top bucket held in place by a magnet until it has filled to the calibration amount. After the amount of precipitation equal to the rain gauge resolution, the bucket tips, dumping the collected water. The schematic of the mechanism is as shown in Figure 3.6

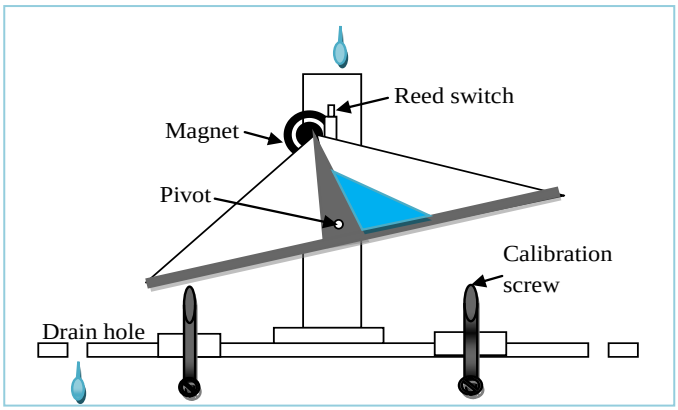

Figure 3.6. Schematic of the tipping bucket mechanism

When the bucket tips, it triggers a reed switch or sensor and sending electrical signals to the rain gauge terminal. The block diagram on the functionality of the rain gauge is as shown in Figure 3.7. The collected rainfall data at the rain gauge are sending through electrical signal to the digital terminal of data loggers (the specification is in Appendix B.)

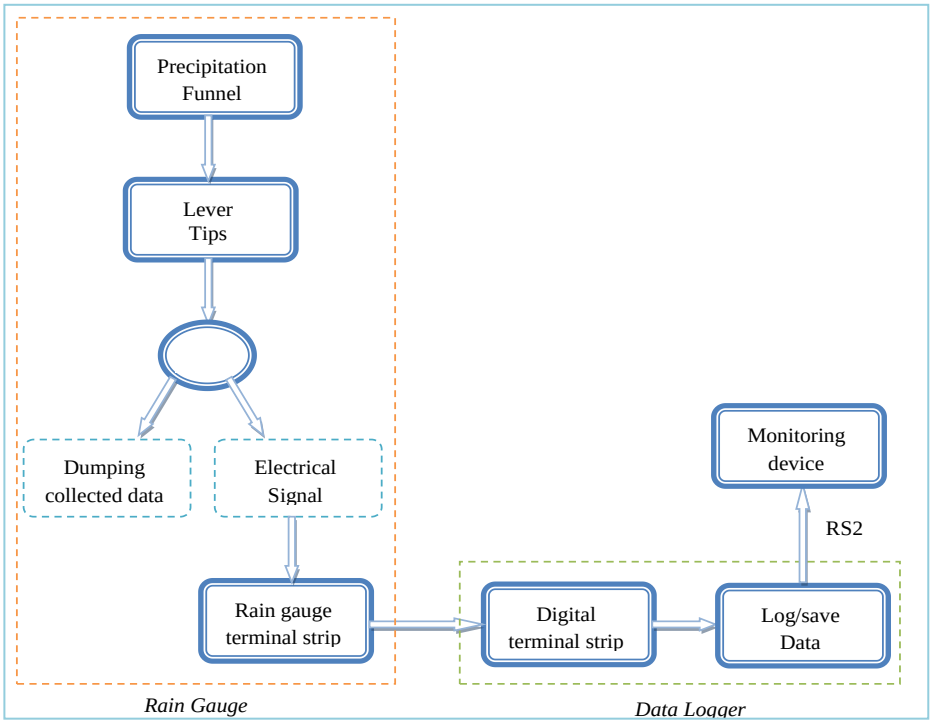

Figure 3.7. Rain gauge block diagram

The sample of rainy condition logged by data logger is as in Figure 3.8 for the 3 days rainy event in the year 2010.

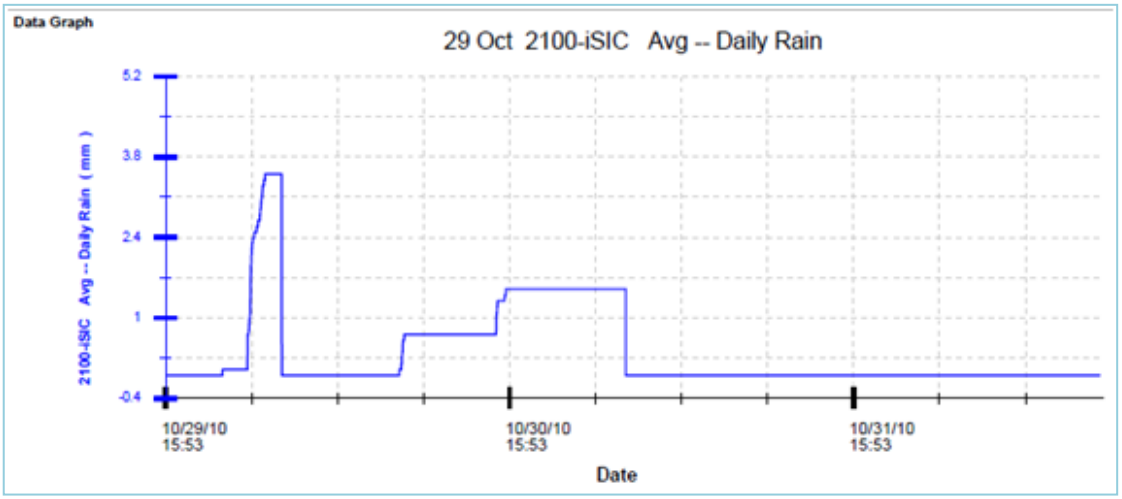

Figure 3.8. Sample of rain events for 3 days of 29 until 31 October 2010

The data logger log rainfall to the monitoring device with one-minute integration time (NexSens Technology). Sample of rain data is as shown in Table 3.5.

For our experiment, the rain gauge used is a Young Rain Gauge (YOUNG) and the logger is NexSens iSIC Data logger with iChart software (Nexsens Technology). Beside the rain gauge that we used which is 0.1mm/tip resolution rain gauge, there is another rain gauge installed earlier with 0.2 mm/tip (Casella Rain Gauge) resolution in the same building as we installed our FSO link system. Both are tipping bucket rain gauge and rainfall data will be stored in the data logger before transmitted to the monitoring device.

Table 3.5
Sample of rain data measured on 2 October 2011

Time (minute)	Rain Amount (mm)
16:56:00	0.2
16:57:00	1
16:58:00	0.8
16:59:00	0.8
17:00:00	0.8
17:01:00	0.6
17:02:00	0.2
17:03:00	0.2
17:04:00	0.2
17:05:00	0.6
17:06:00	0.4
17:07:00	0.4
17:08:00	0.4
17:09:00	0.2
17:10:00	0.2
17:11:00	0.6

Table 3.6 shows the specifications for both rain gauges. Detail specification of R.M. Young rain gauge is in Appendix C and Casella rain gauge is in Appendix D.

Table 3.6
Rain gauge specification

Specification	R.M. Young	Casella
Catchment area	200 cm^2	200 cm^2
Resolution	0.1 mm per tip	0.2 mm per tip
Accuracy	2% up to 25 mm/hr	1% up to 26 mm/hr
Output	Magnetic reed switch	Contact Closure
Contact rating	24 V DC 500 mA	24 V DC 500 mA

The setup of the rain gauge is as in Figure 3.9. The site of the rain gauge installation is outside of the engineering building and the data logger situated a few

meters away in the laboratory on the same level. The rainfall data from the rain gauge transmitted to the data logger and logged to the monitoring device where installed location of iChart software.

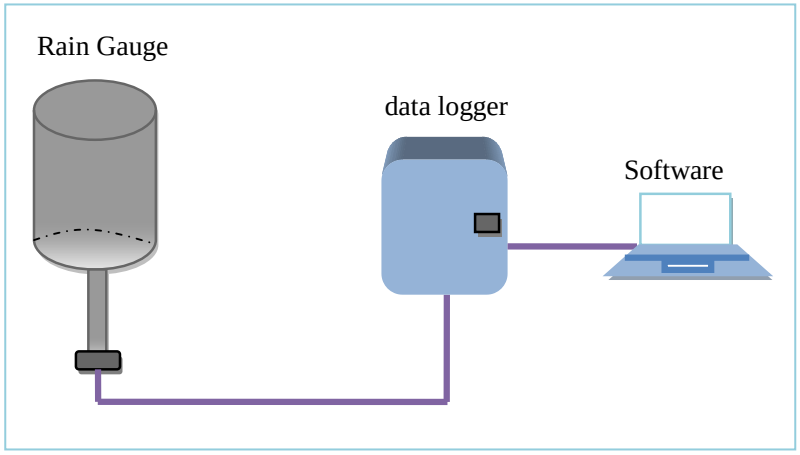

Figure 3.9. Rain gauge setup

Figure 3.10 shows the physical installation site of the rain gauge and data logger. To ensure the rain event captured correctly, integration of rain data saved with one-minute interval.

Figure 3.10. Rain gauge installation site and data logger

To accommodate the cumbersome a year of data processing, a program is developed using MATLAB. The GUI of the program is as shown below.

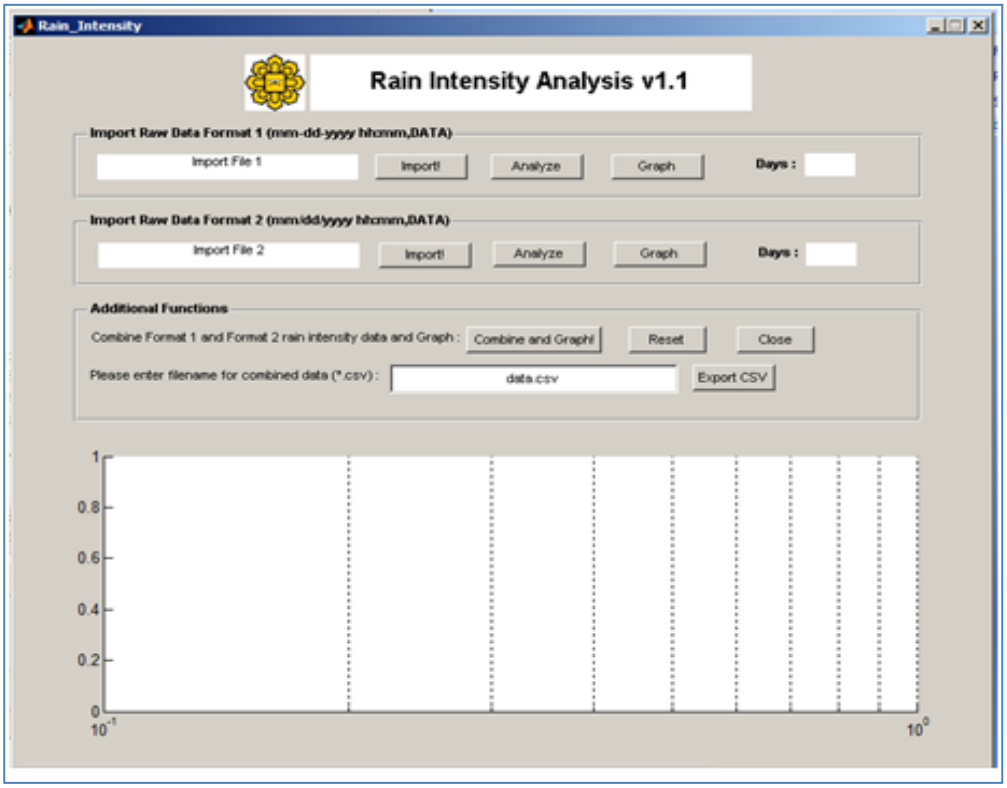

Figure 3.11. GUI rain intensity analysis

In this program, we have two input date format for the rain raw data. One is in the form of dd-mm-yy while the other half in the form of dd/mm/yy, which is too cumbersome to convert it to a single format. To overcome the problem we have two input formats to the program. Refer to Appendix E for the algorithm of the program.

Besides Rain Intensity program, we also develop programs to cater for a year cumulative data. To analyze one (1) year data for specific rain attenuation prediction of k and α values, we need to combine all the data and find cumulative distribution for a year for both rain intensity and rain attenuation. From rain intensity and rain attenuation cumulative distribution, we produce equiprobability plots for the k and α

prediction using regression analysis. To do this bulky job we run the data in Rain Data Analysis as shown in Figure 3.12

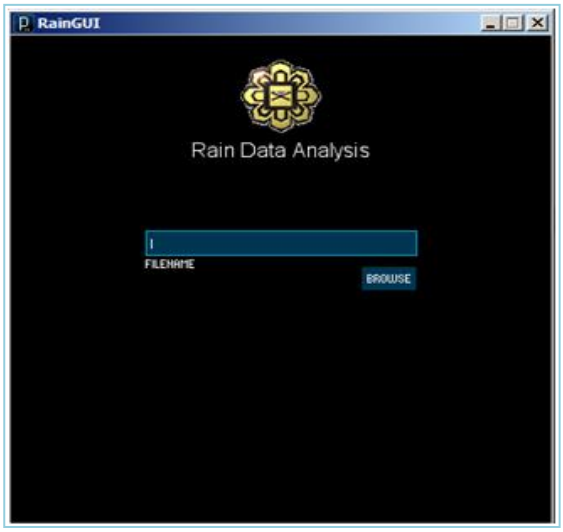

Figure 3.12. GUI of rain data analysis

The program will produce the following output by combining, sorting and counting the occurrence of rain intensity for the whole year and the output is as illustrated in Table 3.7.

Beside the rain attenuation, another focus is on rain intensity variation. The rain intensity variation analysis will determined either the rains fall uniformly throughout the link under investigation. Next section will focus on the setup and measurement of rain intensity variation.

Table 3.7
Sample output from Rain Data Analysis program

Rain Intensity mm/hr	Number of Times Occurrences
168	2
162	1
156	3
150	1
144	3
132	3
126	1
120	8
108	20
96	21
90	1
84	45
78	6
72	87
66	17

3.4 RAIN INTENSITY VARIATION SETUP AND MEASUREMENT

In order to predict accurately the attenuation due to rain, we need to consider the non-uniformity of the rainfall along the propagation path.

The verification of the uniformity of rain throughout out link, we setup second rain gauge on location B of the FSO link transceivers. The location of second rain gauge is as shown in Figure 3.13.

Rain data collected for a month and we analyze both sides rain event to clarify our assumption that for link less than 1 km rain will fall uniformly throughout the link.

Figure 3.13. Location of second rain gauge

3.4.1 Experimental Results of Reduction Factor

FSO transceivers are located in the engineering building and hostel buildings in link distance of 0.8 km. We installed the second rain gauge on the hostel's *Musolla* located about 40m from the FSO link head. Rain data collected for a month of April 2012 for both experimental sites of FSO link.

We analyzed and plotted cumulative distribution of both sites for comparison. Figure 3.14 shows the comparison of rainfall in engineering and hostel.

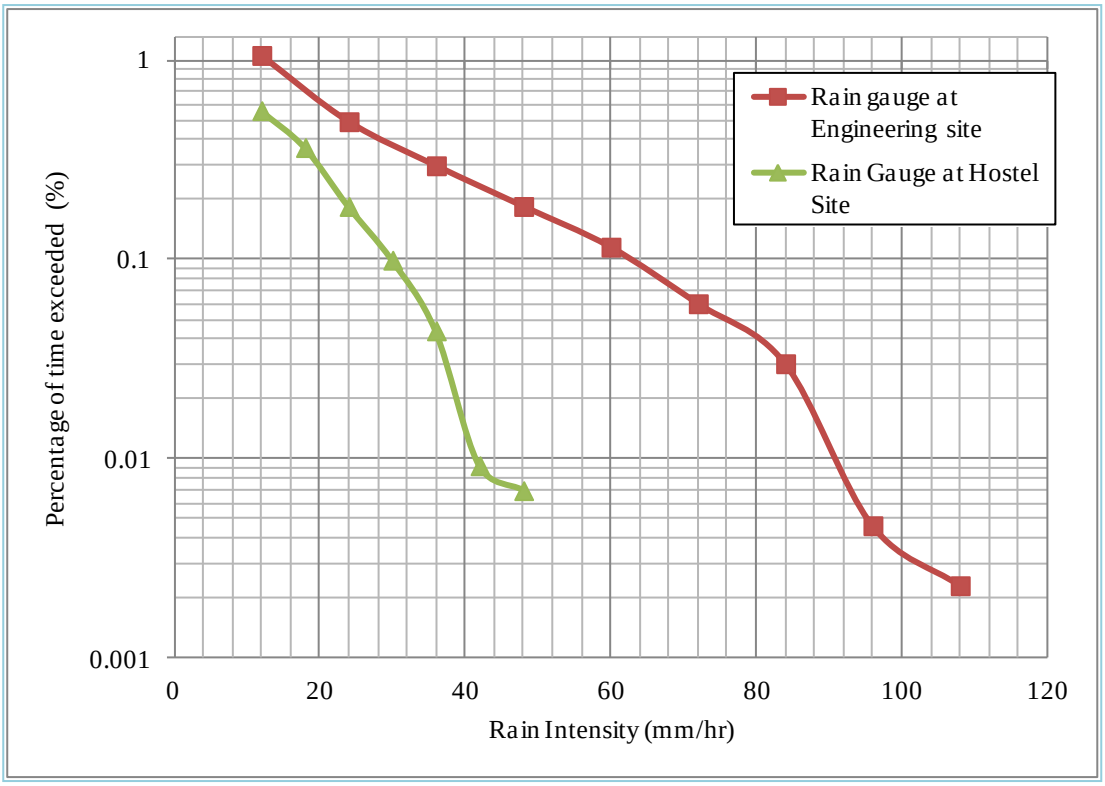

Figure 3.14. Comparison of rainfall on FSO link for April 2011 rain event

Figure 3.14 shows the results of two rain gauges in engineering and hostel building. The result shows that rainfall does not fall uniformly on the FSO link. The result does not comply with the theoretical analysis and universal analysis, which shows that for terrestrial link less than 1 km, the rain falls uniformly throughout the link. According to researchers doing the measurement of a rain cell (Houze R.A, 1997; Khamis, et al., 2005; Pan et al., 1994), in tropical region rainfall are mainly convective and occur in a relatively short period as compare to wide spread rain. In tropical regions, the rain cell effective diameters can be as small as 1 km. According to (Khamis et al., 2004), the diameter of a rain cell in km for 99.99% of time would be 1.65 km. Therefore, according to previous work, for link range below 1 km, rain should be uniform throughout the link.

The result of our experiment does not agree with the theory might due to the fact that, the rain cell does not cover both site of the link for the whole one month of April. To formulate the distribution of rain cell size using a rain gauge would require many such devices to be installed. This would be very difficult and expensive. An alternative approach is to use radar data which it out of the scope of this research. Another argument on the disagreement of the result, there might be a technical problem with the second rain gauge, since the rain on engineering site comparing between two rain gauge give almost good in agreement between both measurements. Due to the experimental result, the analysis of rain locality consideration is conducted with theoretical and calculation method and the detail discussion is as in the following section.

3.4.2 Reduction Factor Analysis

Reduction factor is determined by dividing the actual attenuation (predicted by model or measured) by the product of the actual path length and the specific attenuation (Akuon et al., 2011). Since so far there is no derivation of the reduction factor for FSO link, we select Abdulrahman method (Abdulrahman et al., 2011) for the calculation of reduction factor. Abdulrahman method derived from terrestrial link in tropical region. Therefore, it is a good basis to calculate FSO link reduction factors. The equation used for reduction calculation is as expressed below

$$r_p = \frac{A_p}{(kR_p^{\alpha})d} \tag{3.1}$$

R_p is the rain rate at p different percentage of time and d is the distance which is d = 0.8 km for FSO link. Equation (2.6) is used to calculate attenuation at the interest percentage, A_p with measured values of specific rain parameters as tabulated in Table 5.22 with ranges of rain intensity and the related value of k and α. The plot of the reduction factor for different percentages of time is presented in Figure 3.15; using prediction methods proposed by Abdulrahman. Figure 3.16 shows the plot using prediction proposed by Silva Mello.

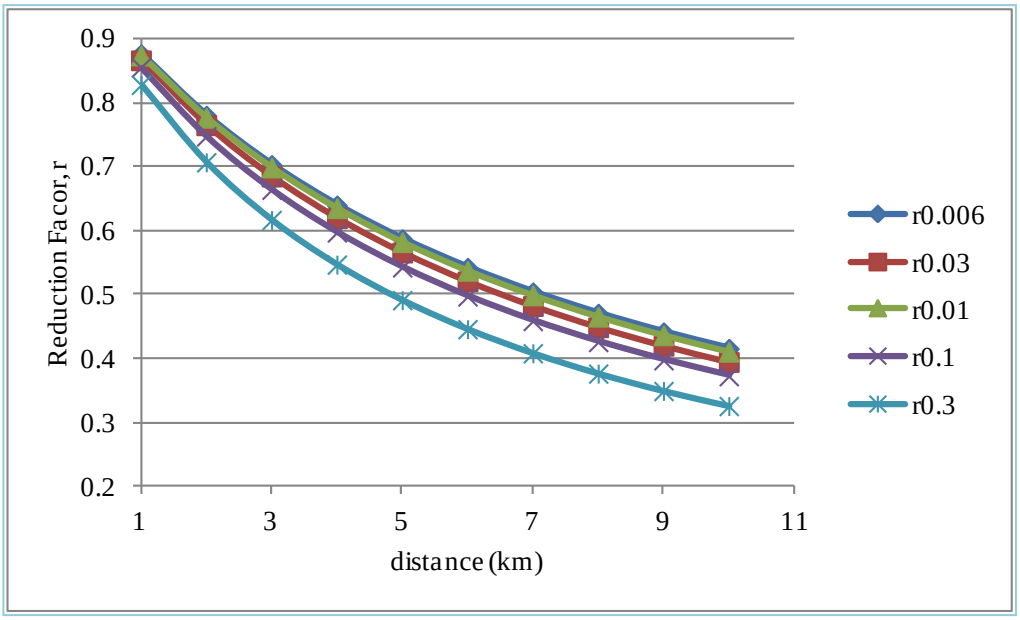

Figure 3.15. Variation of r with prediction methods proposed by Abdulrahman

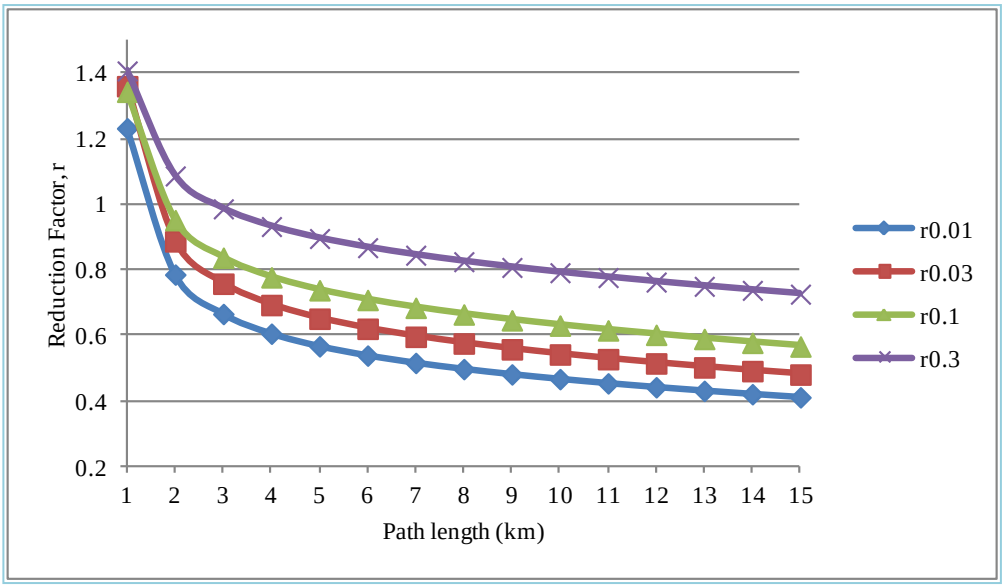

Figure 3.16. Variation of *r* with prediction method proposed by Silva Mello

Figure 3.15 and Figure 3.16 show the result for 1 km link range and the reduction factor is around one (1). The variation of r is not large for every kilometer and it is almost constant for different percentages of time at the same link distance. Therefore, we can assume that rain falls uniformly throughout the link for 0.8 km FSO link. Our assumption for proposing specific rain attenuation based on measured rain intensity and rain attenuation is valid (Suriza et al., 2011).

3.4.3 Comparison of Reduction Factor Model

Figure 3.17 illustrated plot of different reduction factor models with varying link distance.

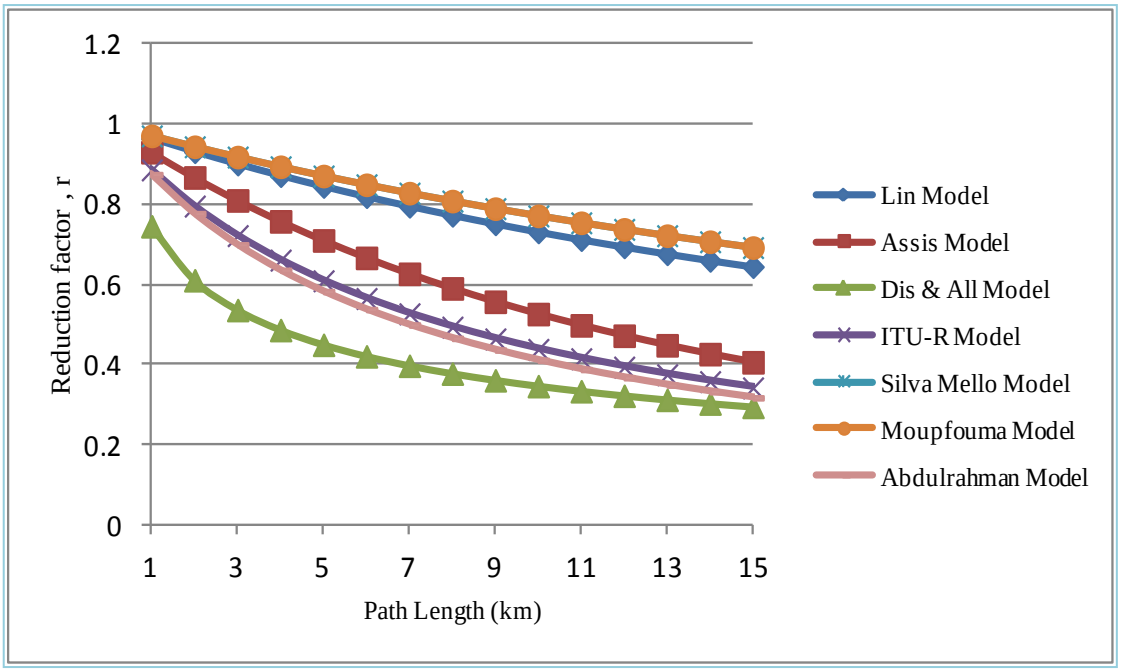

Figure 3.17. Calculating variation of calculated r proposed by many authors and ITU-R with link's path length

Figure 3.17 shows clearly among the entire model studied, the reduction factor is close to 1 on 1 km link, except for Dissanayake and Allnuts model. The calculation of reduction factor is based on 0.01% of the time exceeded with measured values of $R_{0.01}$ on the FSO link. Therefore the result is another way of proving that for FSO 0.8 km link the rain will be uniform throughout the link.

In Figure 3.17 also shows that reduction factors are decreasing with the path length and point rainfall rate as mention in (Silva Mello et al., 2007). Abdulrahman Model agreed closely with ITU-R model, which reduction closed to one (1) at 1 km. Abdulrahman Model is based on ITU-R Model for reduction factor calculation but with a different rain cell diameter, $d_{o,}$ analysis.

3.4.4 Attenuation at Different Percentage of Time

Abdulrahman method (Abdulrahman et al., 2011) derived path reduction factor from experimental rain rate and rain attenuation data for terrestrial link in Malaysia. The study demonstrated that ITU-R model may not be appropriate for predicting rain attenuation for tropical Malaysia Climate.

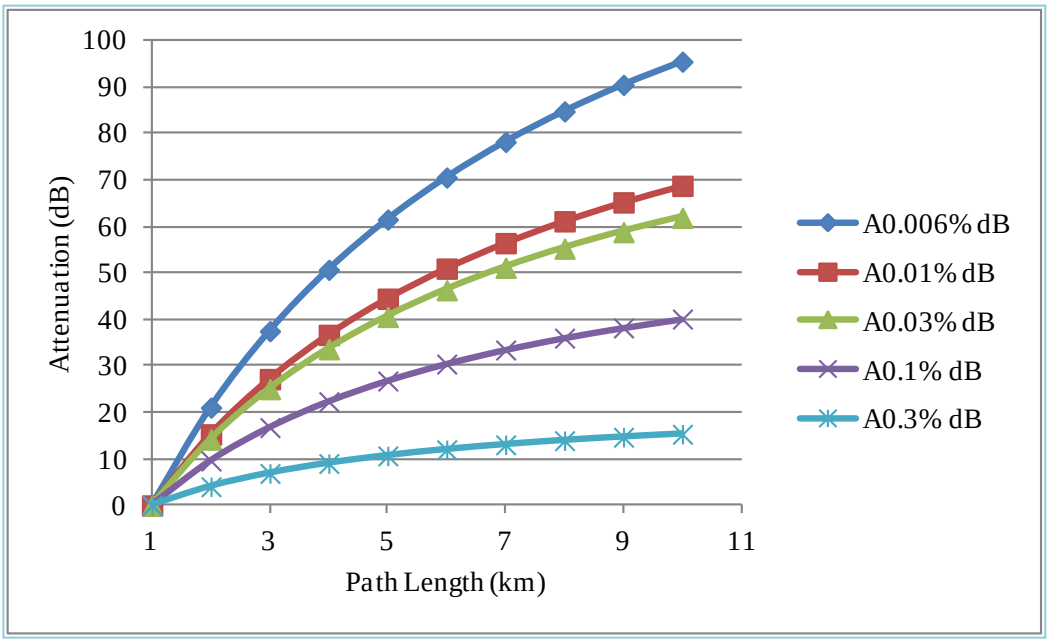

Figure 3.18. Total attenuation for different percentages of time using the model proposed by Abdulrahman and specific attenuation dB/km measured locally

Figure 3.18 illustrates total attenuation based on measured of rain attenuation on FSO link at different selected percentages of time. The figure shows that for low rain intensity the attenuation for different path length are almost constant. In our study, the lowest rain intensity of 0.5 % is 12 mm/hr. The total attenuation increase with the increase of path length or rain intensity of 0.006% of the time, which is the rain rate, is 113 mm/hr. The total attenuation increase quite sharply for the first 3 km and increase slowly with the increase in path length. For 0.3 % (18 mm/hr) attenuation

is 10 dB for 5 km link and increase slightly for longer length. For 0.1% (48 mm/hr) attenuation varies from 25 – 40 dB for any length longer than 5 km. It clearly indicates that all rainfall events with low intensities 48 mm/hr, rain intensity distributed uniformly up to few km only whereas the heavy rain extended up to longer distances. From the graph, we can achieve the availability of 99.99% at 3 km of link with link margin of 26 dB and 5 km with 40 dB and 10 km with 70 dB.

Beside the effect of rain on the FSO link, another expected limiting factor in tropical region is haze (represented in visibility measurement). Next section will discuss on the visibility setup and it measurement.

3.5 VISIBILITY METER SETUP AND DATA MEASUREMENT

Visibility defined for meteorological purposes as a quantity estimated by a human observer. Many subjective and physical factors affect the estimation of visibility. The essential meteorological quantity is transparency of the atmosphere and represent by meteorological optical range (MOR).

EnviroTech, (EnviroTech Sensors, 2009b) define the visibility as the greatest distance that a large dark object can be seen and recognized against a light sky background. The obstruction of vision classifies into two classes, hydrometers and lithometeors. Hydrometeors that are wet and example of it are rain, snow, fog, mist, drizzle and spray. While lithometeors are dry like salt, pollen, smoke and dust.

The propagation of light through the atmosphere is attenuated by absorption and scattering. The Beer-Lambert law gives the relationship between the attenuation of light by scattering and absorption. The fraction of light loss to scattering and absorption per unit distance in a participating medium identified as the extinction coefficient, σ and the standard unit of measure of extinction coefficient is km^{-1}.

Extinction coefficient directly related to the visual air quality. It represents the optical characteristics of the pollutant along the optical path that contribute to visibility impairments.

A different algorithm developed to convert extinction coefficient to visibility, one for daytime and one for day night. Koschmeider's law use for measurement of visibility in the daytime that relate to the viewing of dark objects against a light sky as previously mentioned.

$$V = 3/\sigma \tag{3.2}$$

Night time visibility relates to the distance at which we can notice a point source of light of known intensity. For measurement of visibility at night, Allard's Law presented in Equation (3.3)

$$V = e^{-\sigma V} / 0.00336 \tag{3.3}$$

The equipment to measure the visibility is Sentry Visibility meter. The Sentry visibility meter uses the principle of forward scattering. It utilizes a high power infrared light at a wavelength of 880 nm (EnviroTech Sensors, 2009a). The IR light is beam formed into a collimated cone of light at a nominal angle of 42 degrees to the axis of the receiving optics as shown in the Figure 3.19.

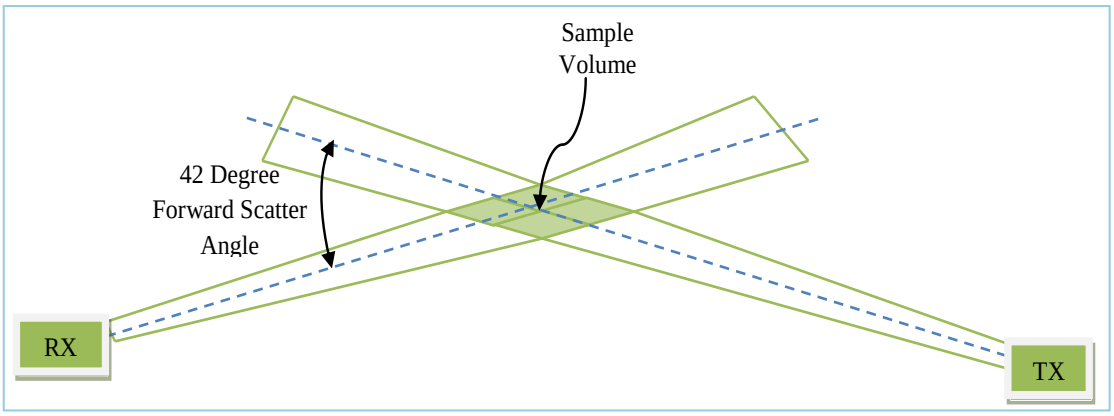

Figure 3.19. Forward Scattered Geometry

The mechanism on how the Sentry Visibility meter works on measuring the visibility locally is as follows,

- The optical system designed such that the infrared light projected from the transmitter (TX).
- The projected light intersects with the field of view of the receiver (RX)
- The TX and RX are angled with forward angle 42^{o}
- The intersection area is sampled volume.
- The extinction coefficient is calculated based on the scattered light in the sample volume

The 42^{o} forward angle ensures performance over a wide range of particle sizes in the sample volume including smoke, dust, haze, fog, rain and snow. In the sample volume, primarily give a local reading of the density of scattering particles that we can convert to visibility under the assumption that the density is homogenous. The particles can be divided into small suspended particulates such s fog, haze and smoke; while larger particles such as rain, snow, ice pellets, drizzle and mist.

The measurement of extinction coefficient (EXCO) by visibility sensor is a measure of the reduction of transmitting light. EXCO related directly to the visual air quality. It represents the optical characteristics of the pollutants along an optical path that contribute to visibility impairment. Furthermore, EXCO is the sum of scattering coefficient and the absorption coefficient. Since absorption is usually small, the EXCO is approximately equal to the scattering coefficient. Visibility used the formula as shown in Equation (3.2 and 3.2) to convert EXCO into as a measurement of visibility. The infrared light source and intelligent technology the measurement of EXCO are unaffected by other light sources. At good visibility, the extinction coefficient is near to zero and it increases as the visibility decreases.

3.5.1 Measurement Setup

The specification of Sentry Visibility meter is as presented in the following table (Gerard, 2008).

Table 3.8
Sentry Visibility Meter Specifications

Items	Specification
Visibility Range	30 m – 16 Km
Accuracy	+/- 10% RMSE
Scatter Angle	42 degree nominal
Extinction Range	100 -0.1863 Km^{-1} standard
	300 – 0.30 Km^{-1} optional
Source	880 nm LED
Weight	8 kg

The configuration of the experimental setup illustrated in Figure 3.20 and a distance between the TX head and RX head of the visibility detector is about 0.5 m. Therefore, the measurement is local.

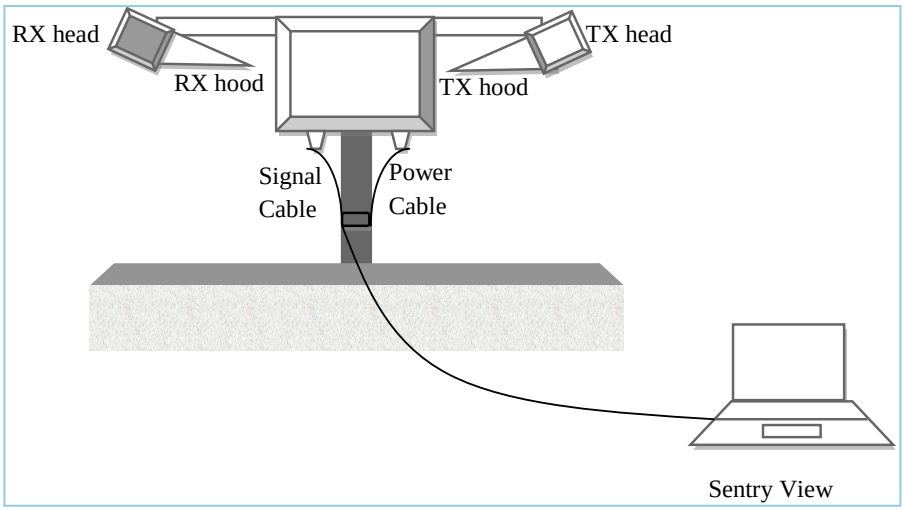

Figure 3.20. Configuration setup of Sentry visibility meter

Sentry view is the software where the visibility data is saved and it is resides in the monitoring device via RS232 cable. Table 3.9 shows a sample of data logged in the data logger.

Table 3.9:
Sample of visibility data logged on 28 Apr 2011

Date	Time	EXCO	Visibility (Km)
4/28/2011	0:00:00	0.239	12.52
4/28/2011	0:00:23	0.239	12.5
4/28/2011	0:00:30	0.239	12.51
4/28/2011	0:00:53	0.24	12.47
4/28/2011	0:01:00	0.242	12.38
4/28/2011	0:01:23	0.247	12.09
4/28/2011	0:01:30	0.249	12.03
4/28/2011	0:01:53	0.248	12.05
4/28/2011	0:02:00	0.247	12.12
4/28/2011	0:02:23	0.241	12.4
4/28/2011	0:02:30	0.24	12.46
4/28/2011	0:02:53	0.24	12.47
4/28/2011	0:03:00	0.241	12.43
4/28/2011	0:03:23	0.245	12.22
4/28/2011	0:03:30	0.247	12.13
4/28/2011	0:03:53	0.25	11.97

Complete specifications of Sentry data logger is as in Appendix F. The visibility versus link range and regional historical visibility data (Kim et al., 1998) is the parameter to estimate availability of FSO link. For our analysis, however, we measured visibility data locally, which is under tropical weather condition.

Another experimental setup done in this research is Bit Error Rate (BER). The following sub-section is the discussion on BER setup and measurement.

3.6 BIT ERROR RATE SETUP PROCEDURE

Free Space Optics (FSO) link that we have is in physical layer communication system. The manufacturer of FSO system does not provide any procedure for BER testing. Due to that, we developed our own procedure for BER testing. The configuration of the testing is as shown in Figure 3.21. Received level signal monitored at one site while the other site is loop backed. The BER tested by reducing the received power level.

Without any button to control the power, we reduced the power level using a mask that covers the front face of the link head. BER tester is used to measure the error rate.

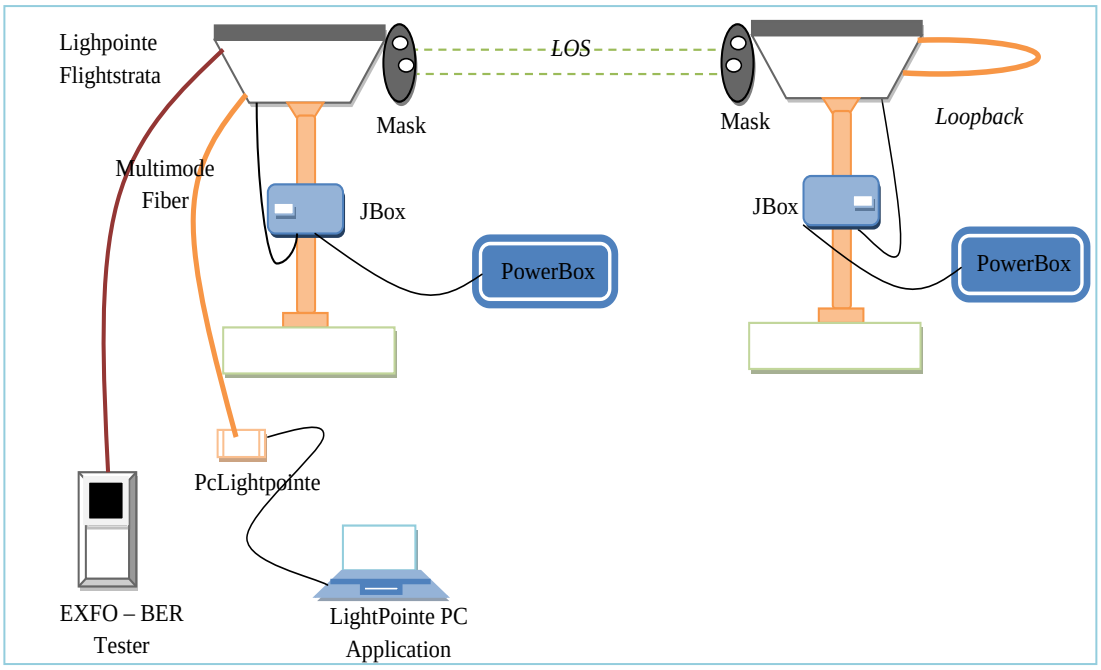

Figure 3.21. Configuration setup of BER testing

Figure 3.22 shows the view of the front face of the link head with all labels for the receivers, transmitter and alignment telescope.

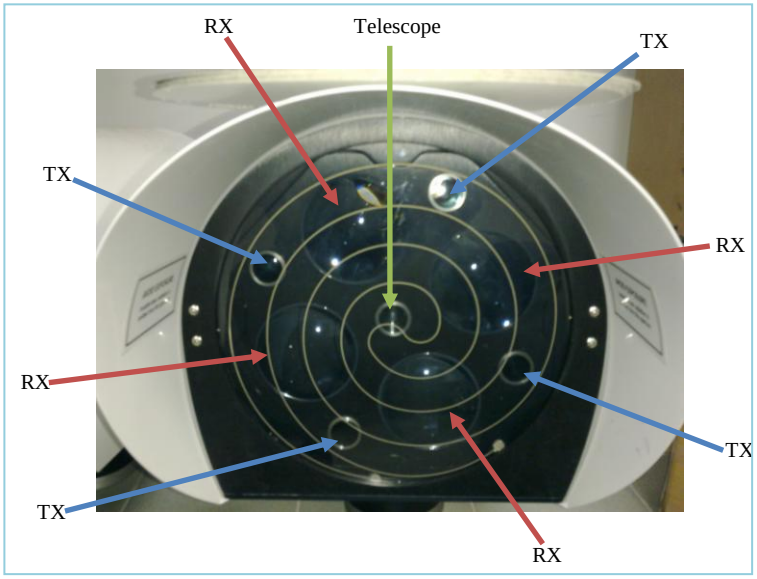

Figure 3.22. Actual photo of front view of FSO link head

To reduce the powers receive the signal of the FSO link by covering the front face of link head with a mask. An example of the mask is as shown in Figure 3.23.

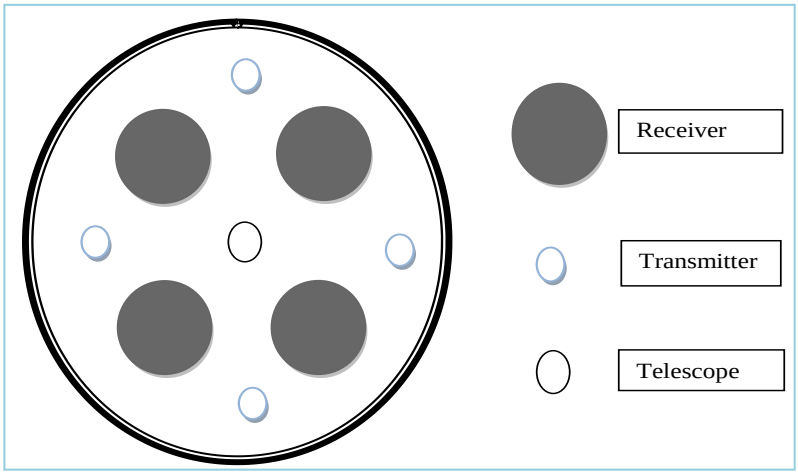

Figure 3.23. Block diagram of front view of FSO link head

A hole is made for every transmitter and receiver on the link head. For every test, we cover both sides of the link head with a mask, for example that have only one opening for the receiver. The next test will be for two (2) receivers. An example of the mask that use to cover the link head with one (1) receiver and one (1) transmitter, two (2) receivers and two (2) transmitters and so on as shown in Figure 3.24

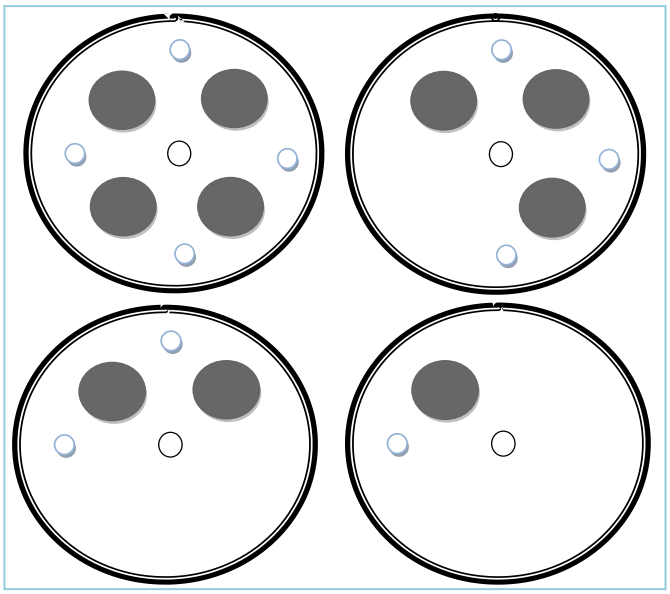

Figure 3.24. The mask that use to cover the link head with different configuration

Figure 3.25 shows the actual front views of link head with mask over it. For the test mask of a dark-colored material used for, it absorbs infrared light better than the light-color materials.

Beside dark-color mask, we also use layers of transparencies to block the signal. The process is by adding the layer of transparencies in front face of the link head, one layer after another.

Figure 3.25. Mask from a dark-colored material

3.6.1 Bit Error Rate Tester Configuration

The model of our BER tester is AXS-850 EXFO. Specification of BER tester is as in Table 3.10. Refer to Appendix G for full specification of BER tester (EXFO).

Table 3.10
BER tester specification

Features	Notes
Testing	Up to layer 4
Industry-standard range of tests	Throughput, back-to-back, frame loss and latency
Intelligent auto discovery	Find multiple remote AXS-200/850 units and loop them up or down for loopback testing
Smart Loopback	Loopback incoming test traffic up to layer 4
Optical power measurement	Optical power readings available during all testing phases

This model support BER, Request for Comment (RFC), and IP Connectivity up to Ethernet 10/100/1000 Electrical and GigE Optical Test. It uses standard USB and RJ-45 interfaces. It comes with 512MB of internal Flash memory (with USB up to 2GB), rechargeable batteries, semi-rigid carrying case and quick reference guide.

The availability test for a long distance link is conducted during a clear weather condition only. The experimental distances of the FSO link selected are 3 km and 6 km. The following subsection focus and explain in details about the experiment setup and configuration of the experiment.

3.7 LONG DISTANCE DEPLOYMENT SETUP AND MEASUREMENT

Two field experiments for 3 Km FSO link distance and 6 Km FSO link distance is carried out between two locations.

3.7.1 Three (3) Km FSO Link Field Test

Site location for 3 km filed test location is as illustrated in Table 3.11.

Table 3.11
Three (3) km field test location

	E1, Engineering	Kristal height
Latitude	3°15'10.29"N	3°15'12.07"N
Longitude	101°43'52.81"E	101°42'15.32"E

Figure 3.26 shows the location of both sites as see from Google Earth with its path profile and the distance is 3.01 km.

Figure 3.26. Location and path profile of 3 km sites viewed in Google Earth

Configuration setup for both sides is as shown in Figure 3.27. The monitoring device connected to the FSO link head at the Engineering's site while at Kristal Height's site it is loop backed.

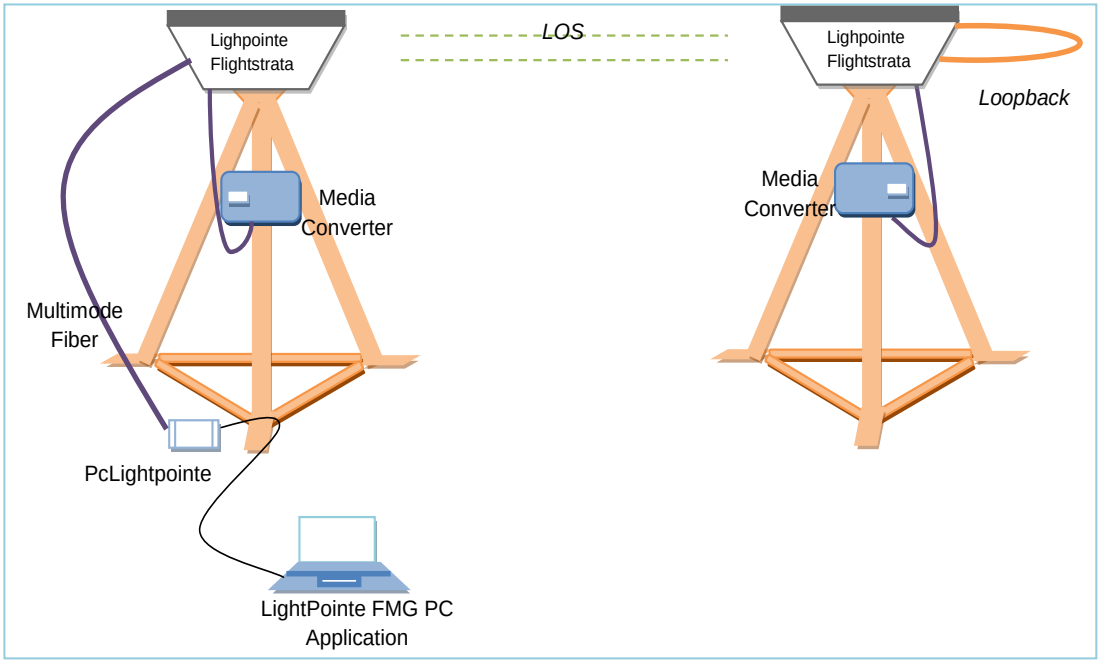

Figure 3.27: Configuration for E1, Engineering (left) and Kristal Height (right)

The test procedure is as in the following steps:

- Both FSO link head needs to be aligned to the same position; meaning realign to the position of each other. The re-align is done manually by finding the location through the alignment telescope on the FSO link head.
- Turn on the link head.
- Press test button (both sides need to press the test button at the same time).

The location of test button is as shown in Figure 3.28.

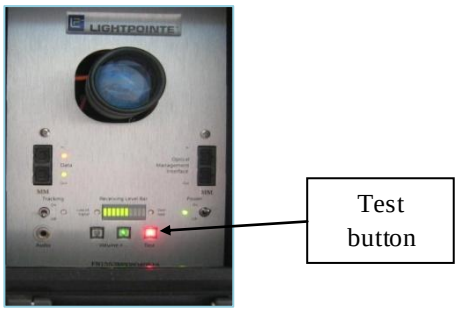

Figure 3.28. Position of test button

- The pathfinder of the link head will find the best location of each other.
- Once the best position is located, connect the data cable to the data management slot and monitor the received power level.

3.7.2 Six (6) km FSO Link Test

Site information for 6 km field test location as presented in Table 3.12

Table 3.12
Six (6) km field test location

	Sri Suajaya Condominium	**Kristal Height Condominium**
Latitude	3°12'1.55"N	3°15'12.44"N
Longitude	101°41'28.53"E	101°42'15.24"E

The location of both sites as see from Google Earth with its path profile is shown in Figure 3.29.

Figure 3.29: Location and path profile of 6 km sites viewed in Google Earth

Configuration of test setup for the 6 km test is as presented in Figure 3.30

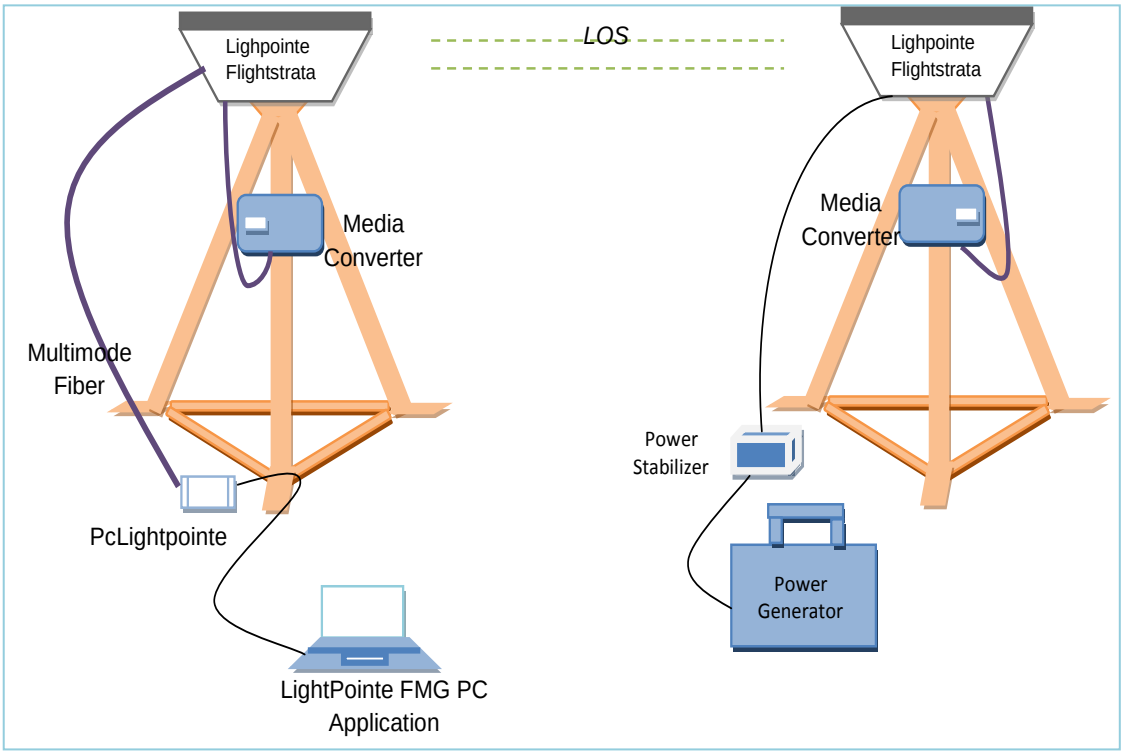

Figure 3.30. Configuration for Kristal Height (left) and Suajaya Condominium (right)

3.8 SUMMARY

This chapter discusses on the experimental setup, data measurement and data analysis method conducted for the research in this thesis. The experimental setup, field test configuration, instruments, measurement procedures and analysis techniques are among the discussion in this chapter.

In the following chapter, the specific rain attenuation modeling will be presented and further explain.

CHAPTER 4

SPECIFIC RAIN ATTENUATION MODELING

4.1 INTRODUCTION

In tropical regions, the limiting factor on Free Space Optics (FSO) link propagation and availability is rain since there is no fog or snow present in tropical region. Data measured in temperate region is the base for the currently available specific rain attenuation model of FSO link attenuation due to rain. The available model like Carbonneau Model is measured under France weather condition and Japan Model is measured under Japan weather condition. Temperate region rain intensity and their drops size distribution might be different from tropical weather condition. Therefore, the aim of this research to develop and propose a new specific attenuation model for FSO system base on the data directly measured under tropical region.

The structure of this chapter started with the detail flow chart on the methodology of specific rain attenuation modeling. The modeling starts with the rain intensified and rain attenuation measurements. Therefore, the rain intensity system and measurement; and FSO system and measurement are discussed in this section. Measured rain intensity and rain attenuation are processed and correlated. Then equal probability method is applied before k and α can be deduced using power regression analysis. Statistical validation and direct measurement validation are the two methods apply for the validation analysis.

4.2 MODELING FLOWCHART

A modeling flowchart of the whole procedure is as presented in Figure 4.1

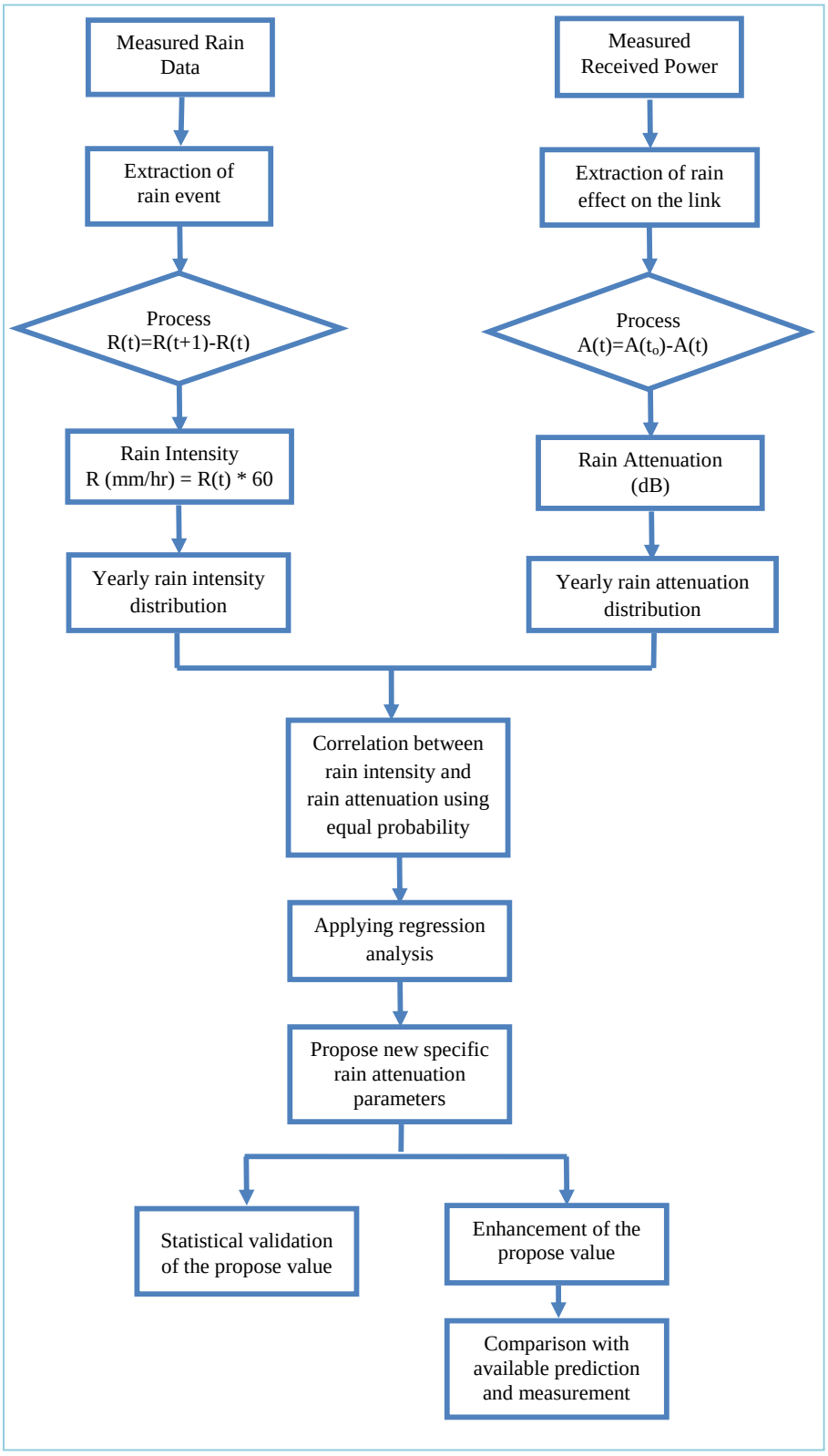

Figure 4.1. Flowchart of the modeling methodology

4.3 RAIN INTENSITY MEASUREMENT

As discussed in Chapter 3, section 3.2, the rainfall data collected using a tipping bucket rain gauge. The modeling of specific rain attenuation is performed by taking into consideration of a year rain data (from January 2011 until December 2011). Table 4.1 shows a sample of rain data collected on the 5th of February 2011 with 1-minute integration time.

Table 4.1
Sample of data collected on 5 of February 2011

Date/Time (mm/dd/yy) / hour	Average Rain (mm)
02-05-11 18.25	0.7
02-05-11 18.26	0.8
02-05-11 18.27	0.9
02-05-11 18.28	1
02-05-11 18.29	1.2
02-05-11 18.30	1.5
02-05-11 18.31	1.7
02-05-11 18.32	2.3
02-05-11 18.33	3
02-05-11 18.34	3.7
02-05-11 18.35	4.3
02-05-11 18.36	4.7
02-05-11 18.37	5.1
02-05-11 18.38	5.4

Using a simple equation as in Equation (4.1), rain intensity (mm/min) is extracted from the collected rain data that has been logged cumulatively about 24 hours for every month. Rain intensity in mm/min then represented in the form of mm/hr to be used in the calculation of rain attenuation. The data is as shown in Table 4.2.

$$R(t) = \big(R(t+1) - R(t)\big) * 60 \qquad (4.1)$$

Where $R(t)$ is rain intensity (mm/hr)

Table 4.2
Sample of rain data with rain intensity calculation

Date/Time (mm/dd/yy) / hour	Average Rain (mm)	Rain Intensity (mm/min)	Rain Intensity (mm/hr)
02-05-11 18.25	0.7	0.1	6
02-05-11 18.26	0.8	0.1	6
02-05-11 18.27	0.9	0.1	6
02-05-11 18.28	1	0.2	12
02-05-11 18.29	1.2	0.3	18
02-05-11 18.30	1.5	0.2	12
02-05-11 18.31	1.7	0.6	36
02-05-11 18.32	2.3	0.7	42
02-05-11 18.33	3	0.7	42
02-05-11 18.34	3.7	0.6	36
02-05-11 18.35	4.3	0.4	24
02-05-11 18.36	4.7	0.4	24
02-05-11 18.37	5.1	0.3	18
02-05-11 18.38	5.4	0.3	18

A sample of rain intensity fall during one rain event is as shown in Figure 4.2, the rain occurred on 19 May 2011 with a 1-minute integration time.

Figure 4.2 shows the lowest rain rate of one rain event on 19 May is 12 mm/hr while the highest rain rate is about 144 mm/hr. The rain seems to occur for 45 minutes and the integration time is a 1-minute.

The process is repeated for all one-year data. The output of the process is a cumulative distribution of the year rainfall data. As discussed in chapter 3, section 3.2.3 to accommodate the cumbersome of the process, we use a MATLAB program to find the cumulative distribution of rain intensity and rain attenuation. From rain intensity and rain attenuation cumulative distribution, we produce equal probability plots for the k and α prediction using regression analysis.

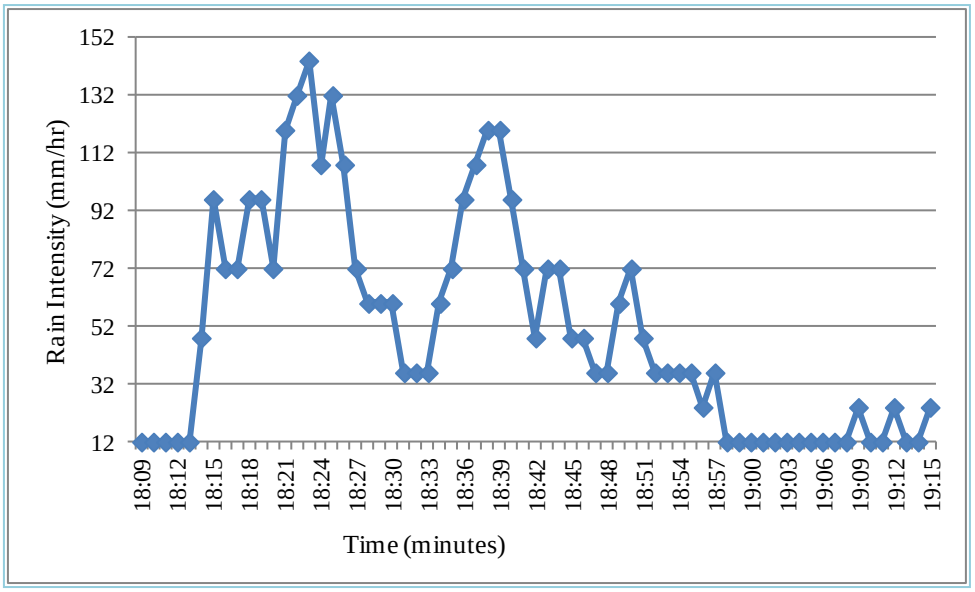

Figure 4.2. Example of one rain event on 19 May 2011

Examining the result of rain intensity closely, the cumulative distribution show that the rain intensity of 0.1 mm per tip resolution rain gauge can rise to more than 300 mm/hr for 0.001% of time as shown in Figure 4.3.

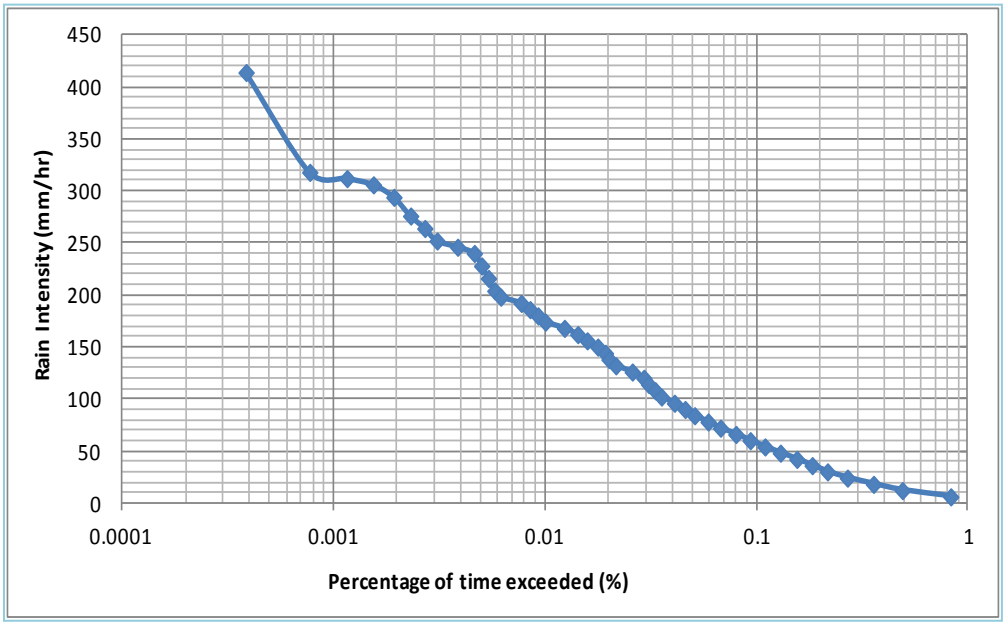

Figure 4.3. Cumulative distribution of rain rate measured for a year

This measurement is not possible even in high rain intensity of tropical. In (Islam et.al, 2000), (Yagasena et. al., 2003), (Khamis et. al,2005), it is stated that at 0.001% of the time, the rain rate is below 200 mm/hr or to be specific 190mm/hr (Yagasena et. al.,2003) and 194 mm/hr (Islam et.al, 2000) under Malaysian tropical environment.

The measurement uses 0.2 mm per tip resolution and the data collected from different research group from the year 2010 until 2012. The specification and data sheet of the rain gauge is in Appendix D. Due to the technical error in 0.1 mm rain gauge of our rain intensity measurement, we are going to opt to 0.2 mm per tip rain intensity for our analysis. To verify the practical by using 0.1 mm per tip resolution of rain gauge or 0.2 mm per tip resolution for our measurements, we carry out a comparison of measured rain intensity and rain attenuation. We compare the rain intensity of 0.1 mm per tip resolution against 0.2 mm per tip resolution rain gauge and the rain attenuation. A sample of the comparison is as shown in Figure 4.4 and a complete comparison is in Appendix H

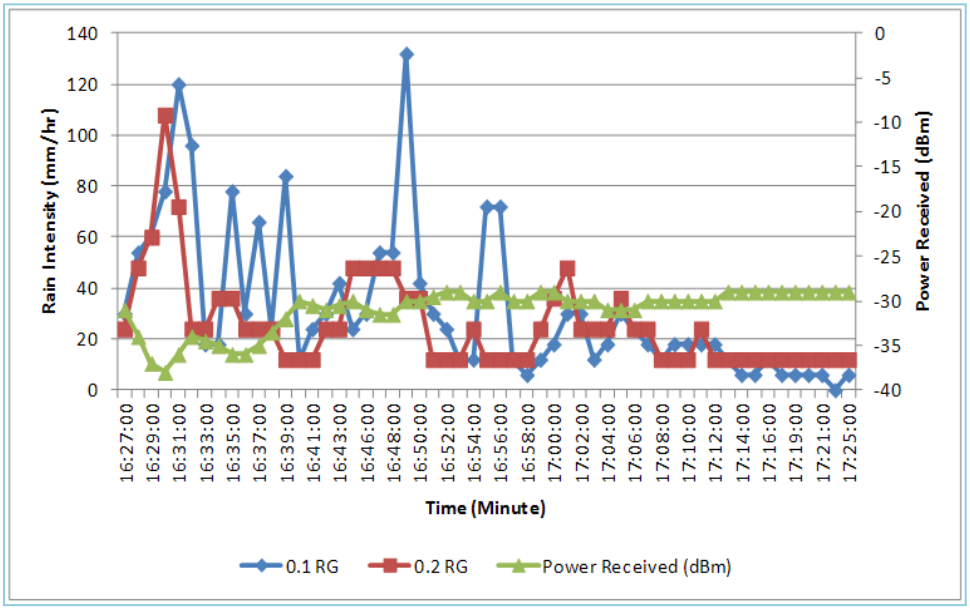

Figure 4.4. Comparison of 0.1 mm/tip, 0.2 mm/tip resolution rain gauge and power received level taken on 3 May 2011

Figure 4.4 shows that measurement of rain intensity using 0.1 mm per tip seems to shoot up at different places and does not really match the rain attenuation on the FSO link, indicate with power receives level. While the 0.2 mm per tip rain gauge measurement seem to have strong agreement with the rain attenuation on the FSO link.

By quantitatively analyzing the comparison data of 0.1 rain gauges and 0.2 rain gauges, the argument for using the 0.2 mm per tip resolution is more practicable. Analyzing all 30-comparison data, by focusing on the occurring of the peak of the rain intensity for each event, we generate the following Table.

Table 4.3 illustrates the peak occurring of 0.1 rain gauges and 0.2 rain gauge measurement with corresponding rain attenuation (representing by power receives level of the FSO link). The quantitative analysis is done by comparing how many percent the peak of rain intensity occurring at the same power received level showing the lowest value. Table 4.4 shows the summary of the analysis.

The result in Table 4.4 shows that, 25 data out of 30 data that represent 83.33% of the peak rain intensity occurring at the same time the highest rain attenuation-taking place on the FSO link. 0.2 rain gauges are evidence for more accurate data. For 0.1 rain gauge measurement, only 13.33% it occurs when the rain rate and rain attenuation are the highest.

Due to result of the analysis, 0.2 mm-per-tip rain intensity measurement selected for modeling of specific rain attenuation.

Table 4.3
Quantitative analysis of 0.1 rain gauge and 0.2 rain gauge measurement

Time Occuring (hour)	0.1 RG (mm/hr)	Received Power (dBm)	Time Occuring (hour)	0.2 RG mm/hr	Received Power (dBm)	Lowest Attenuation dB
7:53	66	-25.00	7:56	84	-34.00	-34.00
5:17	30	-28.00	5:14	24	-29.00	-29.00
19:38	36	-32.00	19:39	48	-33.00	-33.00
17:43	30	-31.00	17:40	36	-32.00	-32.00
18:32	42	-32.00	18:33	48	-33.00	-33.00
16:49	132	-30.00	16:30	108	-38.00	-38.00
3:34	48	-30.00	3:32	48	-31.00	-33.00
19:47	84	-28.00	11:31	36	-29.00	-29.00
18:29	294	-44.00	18:30	144	-44.00	-45.00
15:17	246	-29.00	15:15	48	-31.00	-31.00
18:48	240	-30.00	18:51	84	-33.00	-36.00
17:44	42	-29.00	17:49	48	-28.00	-30.00
16:00	150	-27.50	16:03	36	-28.00	-28.00
16:58	144	-26.00	16:50	24	-27.00	-27.00
23:52	132	-29.00	23:42	48	-30.00	-30.00
19:02	72	-31.00	19:07	108	-45.00	-45.00
18:00	78	-27.50	17:59	24	-28.00	-28.00
23:20	120	-31.00	23:10	48	-33.00	-33.00
13:46	48	-28.00	13:44	24	-29.00	-29.00
20:03	414	-38.00	1:12	108	-39.00	-40.00
12:43	24	-31.00	12:43	36	-31.00	-31.00
12:29	162	-28.00	12:33	60	-30.00	-30.00
12:17	84	-27.50	12:17	36	-27.50	-27.50
13:29	180	-28.00	13:40	48	-29.00	-29.00
14:18	252	-27.00	14:10	36	-29.00	-29.00
15:29	360	-31.00	15:32	84	-38.00	-38.00
14:03	400	-42.00	14:31	120	-41.00	-42.00
17:15	330	-34.50	17:12	144	-44.00	-44.00
19:23	48	-29.00	19:24	48	-30.00	-30.00
6:54	60	-28.50	7:04	36	-29.50	-29.50
16:35	24	-28.00	16:32	24	-28.00	-28.00

Table 4.4:
Summary of the quantitative analysis

	Percentage
0.1 rain gauge	13.33%
0.2 rain gauge	83.33%

4.4 RAIN INTENSITY MEASUREMENT USING 0.2 RAIN GAUGE

Figure 4.5 shows the cumulative distribution of rainfall for the year of 2011 using 0.2 mm per tip resolution rain gauge measurement.

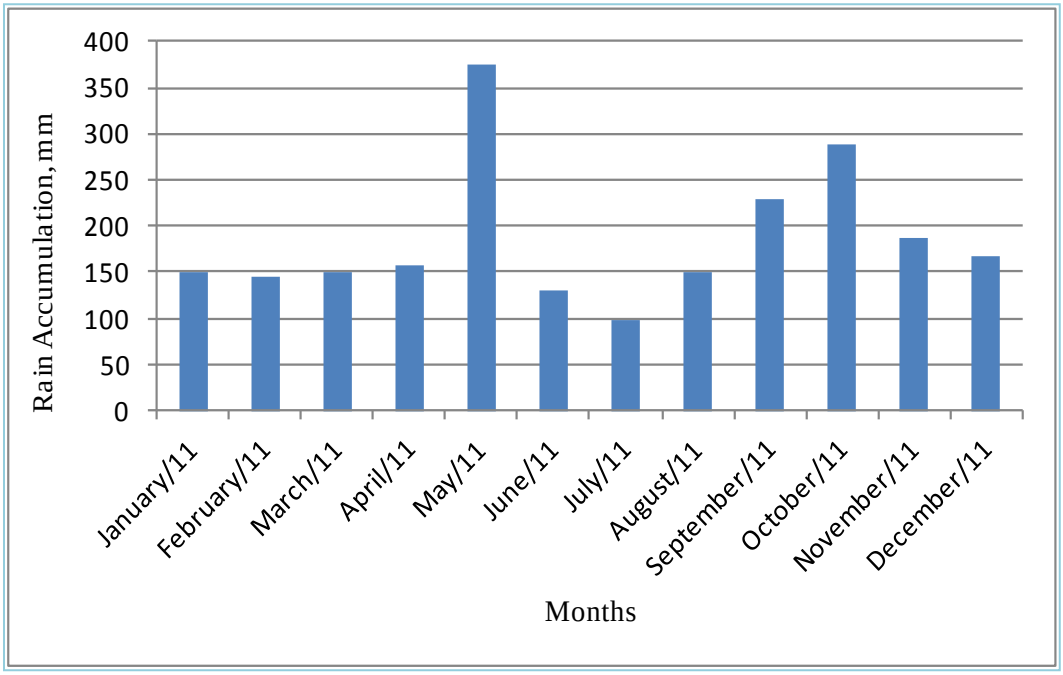

Figure 4.5. Year 2011 cumulative distribution

Figure 4.5 shows a cumulative distribution for a year measured by the highest cumulative rain in 2011 is around 375 mm in May. The lowest cumulative rain is on July 2011 with around 98 mm of rain.

A sample of rain intensity fall during one rain event is as shown in Figure 4.6, the rain occurred on 14 July 2011 with a 1-minute integration time.

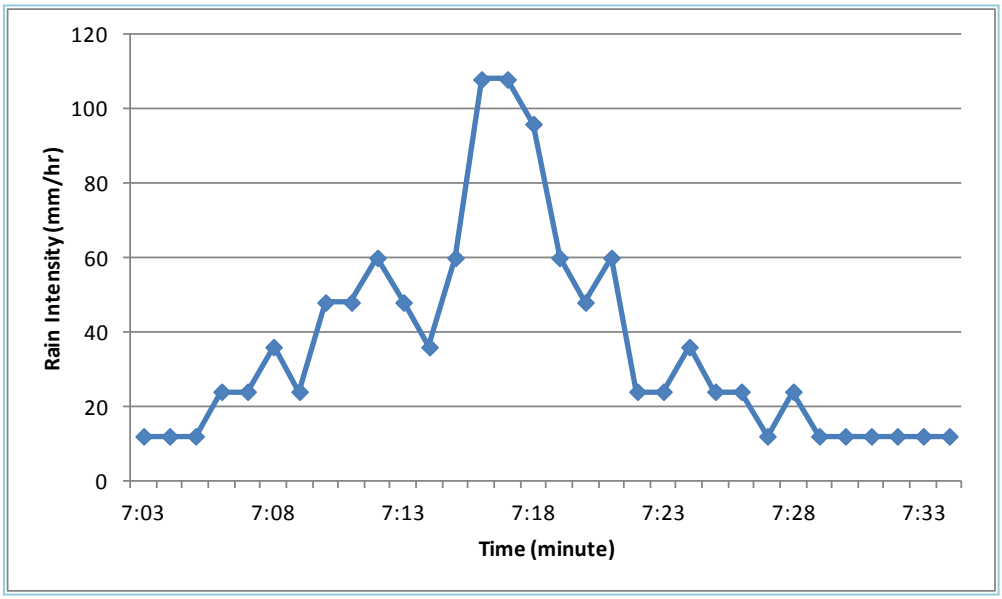

Figure 4.6. Example of rain event on 14 July 2011

Figure 4.6 shows the lowest rain rate of rain event on 14 July is 12 mm/hr while the highest rain rate is about 108 mm/hr. The rain last for about 35 minutes and occurring at 7.03 AM with 1-minute integration time.

The process is considering one-year measured rain data. The output of the process is a cumulative distribution of the year rainfall data. As discussed in chapter 3, section 3.2.3 to accommodate the cumbersome of the process we develop a MATLAB program to find the cumulative distribution of rain intensity and rain attenuation. From rain intensity and rain attenuation cumulative distribution, we produce equal probability plots for the k and α prediction using regression analysis.

Table 4.5 shows cumulative of rain intensity for the whole year. The data is the output from the MATLAB program. The cumulative rain data are sorted and number of each occurrence of rain intensity is calculated. The highest rain mostly occurred for a few occurrences only while the lower part of the rain intensity occurs frequently. From the calculation of the number of time occur, the number of minutes for each rain

intensity take place is counted. The following equation, Equation (4.2), is used to calculate the percentage of occurrence.

$$Percentage\ of\ occurence\ (\%) = \frac{Number\ of\ minutes\ occured}{((days*months)*hour*minutes)} * 100 \quad (4.2)$$

Table 4.5
Calculation of the whole year rain intensity occurs

Rain Intensity mm/hr	Number of Times Occurrences	Number of minutes attenuation occurred	Percentage of occurances
168	2	2	0.0003858
162	1	3	0.0005787
156	3	6	0.00115741
150	1	7	0.00135031
144	3	10	0.00192901
132	3	13	0.00250772
126	1	14	0.00270062
120	8	22	0.00424383
108	20	42	0.00810185
96	21	63	0.01215278
90	1	64	0.01234568
84	45	109	0.02102623
78	6	115	0.02218364
72	87	202	0.03896605
66	17	219	0.04224537
60	102	321	0.0619213
54	17	338	0.06520062
48	191	529	0.10204475
42	31	560	0.10802469
36	277	837	0.16145833
30	46	883	0.17033179
24	539	1422	0.27430556
18	92	1514	0.29205247
12	1218	2732	0.52700617

Figure 4.7 is the outcome by plotting data from Table 4.5 as a cumulative distribution of rain rate measured for a year.

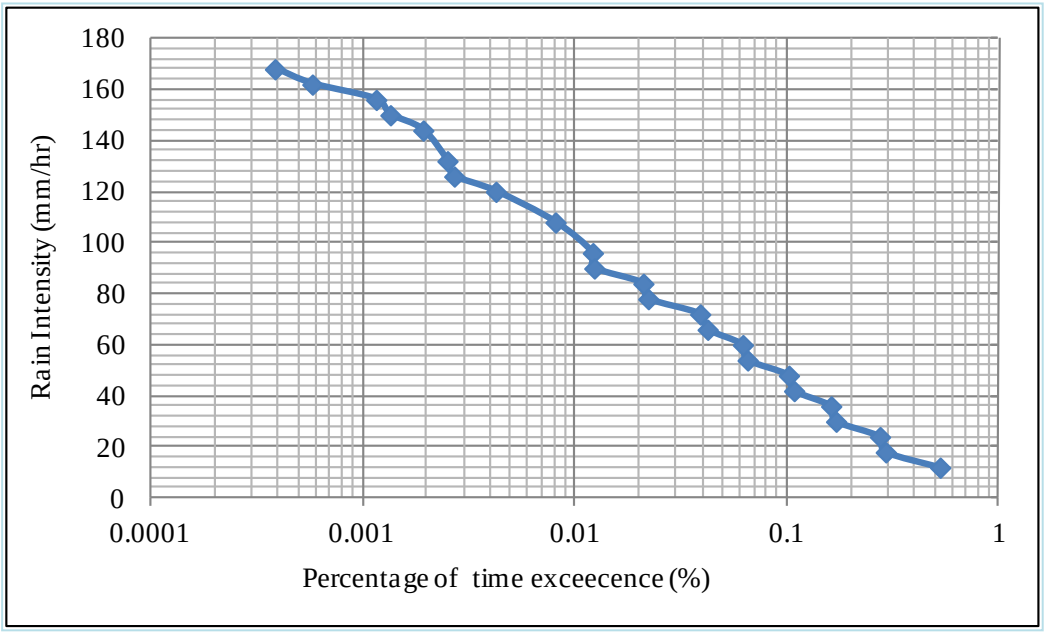

Figure 4.7. Cumulative distribution of rain rate measured for a year

Figure 4.7 shows that the rain rate for the year of 2011 (by considering all heavy rain events), the highest rain intensity can reach up to 168 mm/hr with a percentage of exceeding as 0.0004. ITU-R considered mostly at the 0.01% level. According to our measurement by considering the rain intensity alone, at 0.01%, rain intensity is about 108 mm/hr. The synchronization of rain intensity and rain attenuation implemented by monitoring and measuring power received level on FSO link during rain. Next section, presented explanations about equipment, setup and measurement of attenuation (rain attenuation) on FSO link.

4.5 RAIN ATTENUATION MEASUREMENT

As discussed in section 3.1.2, we monitor the effect of rain intensity and rain attenuation by logging receives level signal of an FSO link during rain events.

A sample of power received level (dBm) monitor and measured during rain events that affected FSO link on 19 May 2011 is as tabulated in Table 4.6

Table 4.6
Sample of power received level during rainfall occur on 19 May 2011

Time (minutes)	Power Received dBm
18:09	-25
18:10	-25
18:11	-25
18:12	-25
18:13	-25
18:14	-25
18:15	-25
18:16	-25
18:17	-25
18:18	-25
18:19	-25
18:20	-26
18:21	-29

From the measurement of power receives level rain attenuation (dB) on an FSO link is extracted using a simple formula as in Equation (4.3)

$$A(t) = A(t_0) - A(t) \tag{4.3}$$

Where $A(t)$ is rain attenuation (dB)

The tabulated data is as shown in Table 4.7

Table 4.7
Sample of rain attenuation calculated from the measured FSO link power received

Time (minutes)	Power Received dBm	Rain Attenuation dB
18:09	-25	1
18:10	-25	1
18:11	-25	1
18:12	-25	1
18:13	-25	1
18:14	-25	1
18:15	-25	1
18:16	-25	1
18:17	-25	1
18:18	-25	1
18:19	-25	1
18:20	-26	2
18:21	-29	5

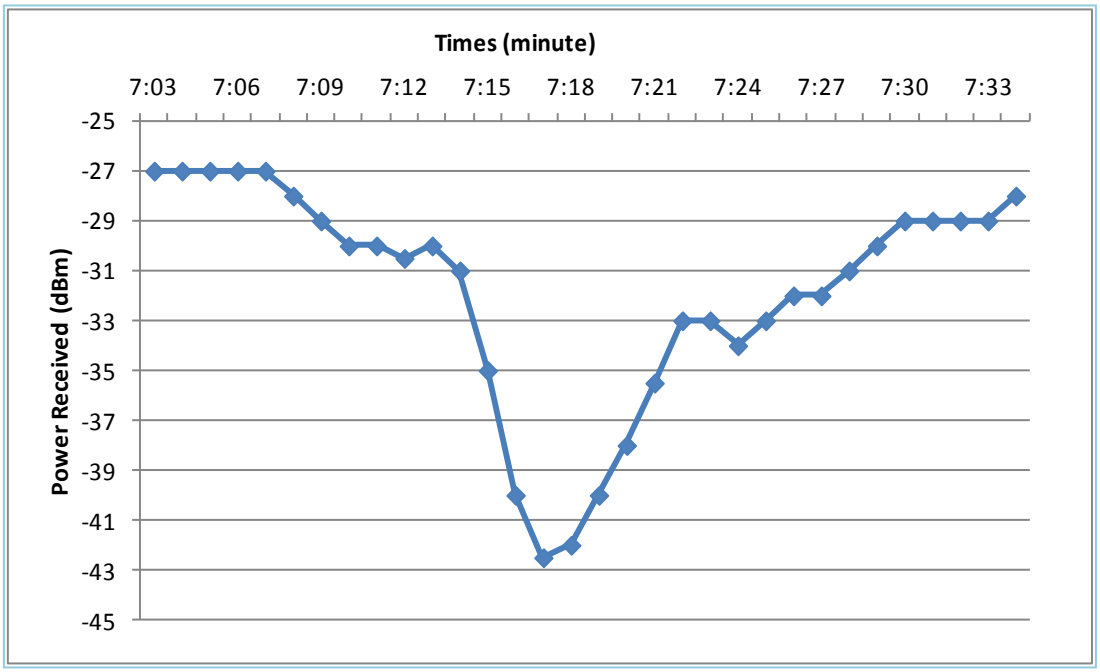

Figure 4.8. Sample 1-day rain attenuation on FSO link on 14 July 2011

The attenuation analyzed at the same time and the same date as the rain intensity with 1-minute integration. From the measured data, we plot cumulative distribution of FSO link attenuation due to rain.

A sample of rain attenuation on an FSO link is as shown in Figure 4.9, the rain attenuation measured on 14 July 2011.

Figure 4.8 shows a sample of attenuation during one rain event on 14 July 2011. The attenuation drops until almost -43 dB for the highest rain intensity on 14 July 2011.

The process is repeated for all one-year FSO link data. Table 4.8 shows the rain attenuation data with the number of times it occurred, number of minutes it occurred and percentage of occurrences.

The highest attenuation is about 21 dB and the lowest attenuation is 1 dB. The highest attenuation mostly occurred for a few occurrences only while the lower part of the rain intensity occurs frequently. From the calculation of the number of time occur, the number of minutes for each rain attenuation occurs is counted. The calculation formula to find percentage of occurrence in the year is as shown in Equation (4.2).

Table 4.8
Calculation of the whole year rain attenuation occurs

Rain Attenuation dB	Number of Times Occurred	Number of minutes attenuation occurred	Percentage of occurances
21	6	6	0.001157407
20	21	27	0.005208333
19.5	2	29	0.005594136
19	6	35	0.006751543
18	11	46	0.008873457
17.5	2	48	0.009259259
17	17	65	0.01253858
16.5	1	66	0.012731481
16	12	78	0.015046296
15	22	100	0.019290123
14.5	2	102	0.019675926
14	36	138	0.02662037
13.5	2	140	0.027006173
13	43	183	0.035300926
12.5	3	186	0.03587963
12	58	244	0.047067901
11.5	10	254	0.048996914
11	67	321	0.061921296
10.5	6	327	0.063078704
10	77	404	0.077932099
9.5	8	412	0.079475309
9	81	493	0.095100309
8.5	9	502	0.09683642
8	93	595	0.114776235
7.5	24	619	0.119405864
7	149	768	0.148148148
6.5	26	794	0.15316358
6	219	1013	0.195408951
5.5	33	1046	0.201774691
5	253	1299	0.250578704
4.5	42	1341	0.258680556
4	418	1759	0.339313272
3.5	55	1814	0.34992284
3	653	2467	0.475887346
2.5	58	2525	0.487075617
2.2	1	2526	0.487268519
2	553	3079	0.593942901
1.5	44	3123	0.602430556
1	377	3500	0.675154321
0.5	17	3517	0.678433642

Table 4.8 show the calculation of a year cumulative distribution of rain attenuation

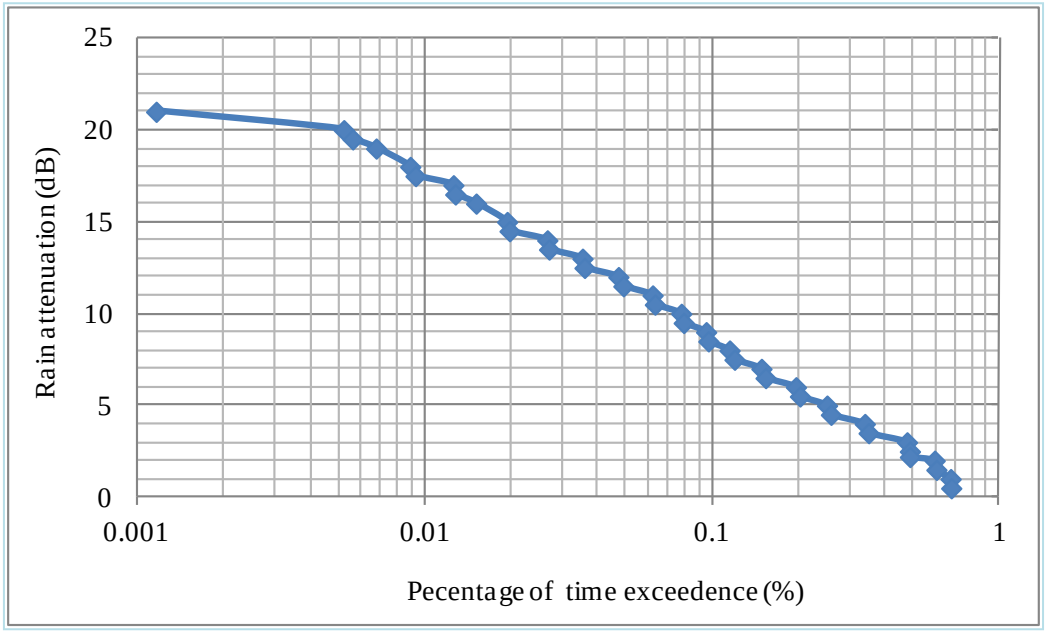

Figure 4.9. Cumulative distribution of rain attenuation measured for a year

Figure 4.9 shows that for the whole year rain attenuation in dB can reach up to 21 dB, which for 0.8 km FSO link will make attenuation of 26.25 dB per kilometre.

A sample of integration of both rain intensity and rain attenuation on the same day of the rain event is as presented in Figure 4.10

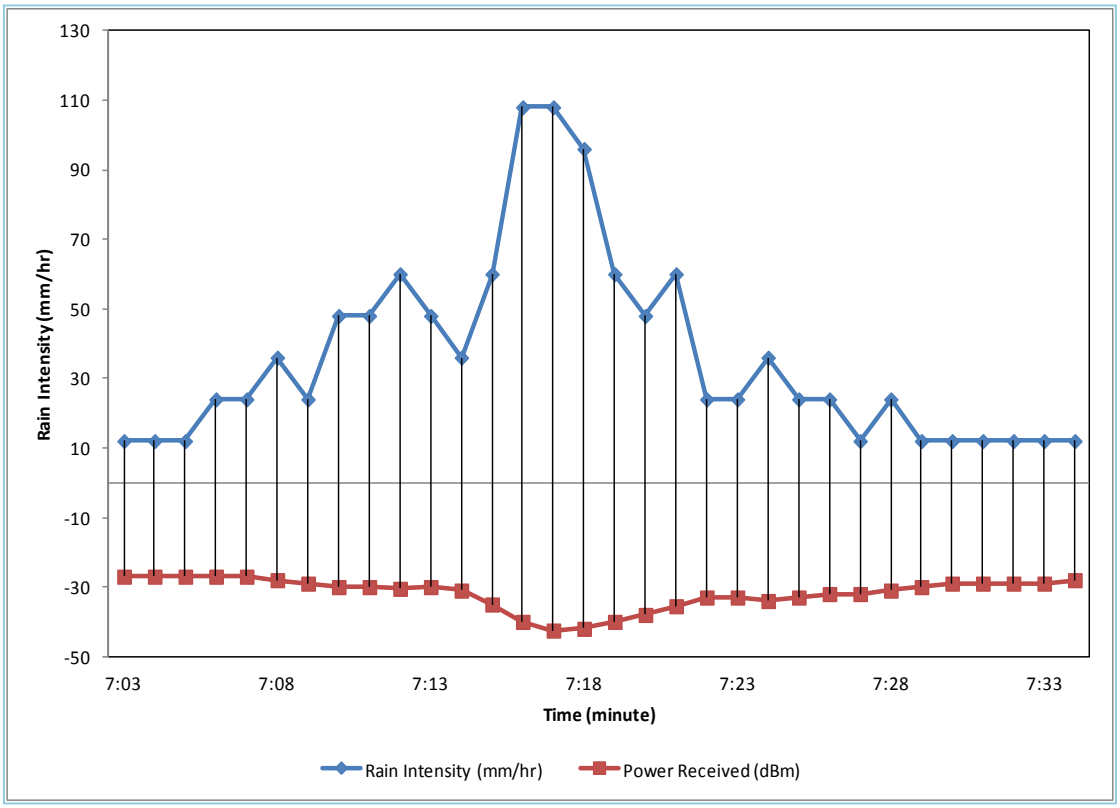

Figure 4.10. Rain intensity and rain attenuation plot for rain event on 14 July 2011

Figure 4.10 shows that the highest rain rate in the sample is around 108 mm/hr with power received level of -43 dBm which give rain attenuation around 17.5 dB and at 0.8 km FSO link will have an attenuation about 21.875 dB/km.

Cumulative distribution of rain rate and rain attenuation is synchronized using equal probability by assumption that rain falls uniformly on the propagation link, Figure 4.12 shows equal probability of rain intensity (mm/hr) and rain attenuation (dB/km). Correlation of equal probability between rain intensity and rain attenuations are as shown in Table 4.9

Table 4.9
Correlation of equal probability between rain intensity (mm/hr) and rain attenuation (dB/km)

%	Rain Intensity (mm/hr)	Rain Attenuation (dB)	Rain Attenuation (dB/km)
0.0010	158	21.2	26.5
0.0013	154	21.1	26.375
0.0015	149	21	26.25
0.0017	146	20.9	26.125
0.0020	144	20.8	26
0.0025	132	20.6	25.75
0.0027	126	20.5	25.625
0.0030	125	20.4	25.5
0.0035	123	20.3	25.375
0.0037	122	20.25	25.3125
0.0040	121	20.2	25.25
0.0045	119	20.1	25.125
0.0047	118	20.05	25.0625
0.0050	117	20	25
0.0055	115	19.75	24.6875
0.0057	114	19.5	24.375
0.0060	113	19.4	24.25
0.0070	111	18.9	23.625
0.0080	108	18.4	23
0.0090	105	18	22.5
0.0100	103	17.5	21.875
0.0130	96	17.2	21.5
0.0150	88	16	20
0.0170	87	15.5	19.375
0.0200	85	15	18.75
0.0230	83	14.5	18.125
0.0250	78	14.2	17.75
0.0270	76	13.5	16.875
0.0300	75	13.2	16.5
0.0330	74	13.1	16.375
0.0350	73	13	16.25
0.0370	71	12.5	15.625
0.0400	69	12.2	15.25
0.0430	66	12.1	15.125
0.0470	63	12	15
0.0500	62	11.5	14.375
0.0600	61	11	13.75
0.0650	56	10.5	13.125
0.0700	53	10.2	12.75
0.0800	51	10	12.5
0.0900	50	9.1	11.375
0.1000	48	8.4	10.5
0.1300	40	7.4	9.25
0.1500	38	7	8.75
0.1700	30	6.3	7.875
0.2000	28	6	7.5
0.2300	26	5.2	6.5
0.2500	24	5	6.25
0.2700	23	4.5	5.625
0.3000	18	4.3	5.375
0.4000	15	3.3	4.125
0.5000	12	2.5	3.125

Rain attenuation in dB/km measurement is on 0.8 km FSO link distance. Plotted data in Table 4.9 is as presented in Figure 4.11.

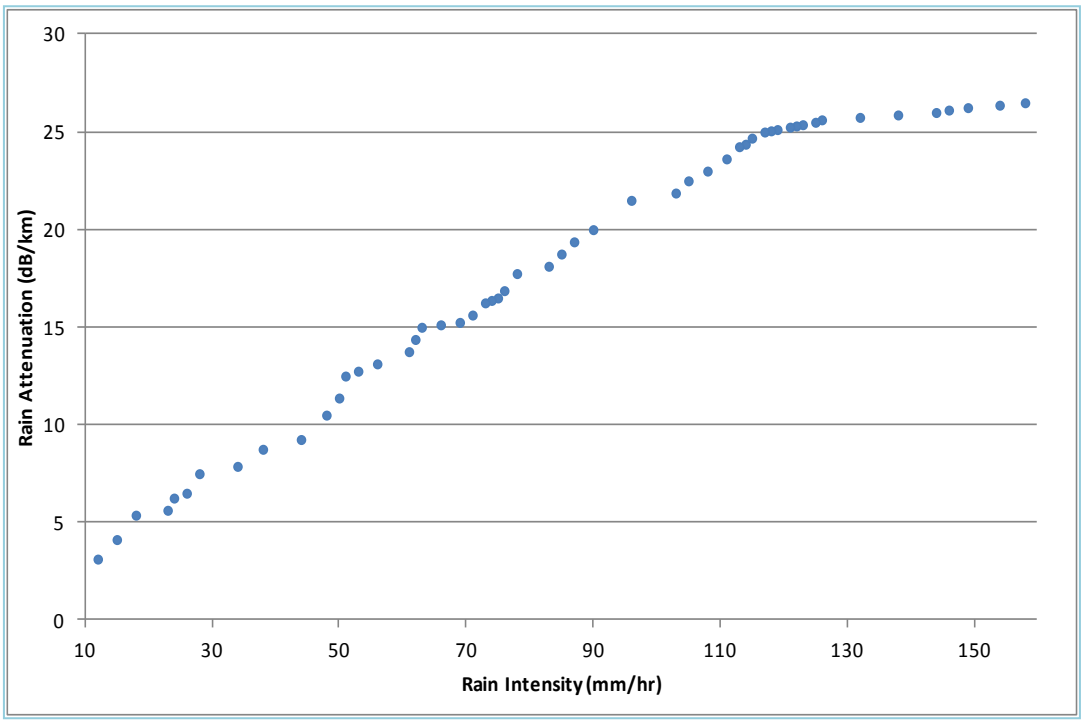

Figure 4.11. Equal probability plot of measured rain intensity (mm/hr) and corresponding rain attenuation (dB/km)

Figure 4.11 shows the plot of rain intensity (mm/hr) versus rain attenuation (dB/km) after equal probability analysis for both parameters. The plot shows that for 0.8 km FSO link range; 158 mm/hr of rain intensity, correspond to 26.5 dB/km rain attenuation.

4.6 PROPOSED NEW VALUES OF SPECIFIC RAIN ATTENUATION PARAMETERS

Available data of specific rain attenuation predictions of k and α values for FSO system based on temperate region. The predicted rain attenuation model of temperate region

cannot represent a valid prediction of tropical region since tropical have higher rain rates comparable to temperate regions.

A best-fit curve plotted and by applying regression analysis, we can derive the value of k and α.

The value of k and α can be derived by regression analysis (Kardi Teknomo's page). Regression analysis is a process of making predictions of some variable, based on the relationship between the dependent variable and an independent variable or set of variables. The actual observed values clustered around the linear regression line or R^2 is a "measure of scatter" around the regression line. The range is from 0 to 1 and the closer R^2 to 1 the better values coincide with the regression line. It means the better the prediction or estimation.

In order to predict accurately specific rain attenuation, we need to examine effective path length of the rainfall on the FSO link. In the following subsection, we present a discussion on rain locality that consists of an effective path length and reduction factor that essential for prediction of rain attenuation.

In Figure 4.12, we plot equal probability of rain intensity measurement corresponding rain attenuation. By fitting and applying regression analysis, we obtained best-fit curve as shown in Figure 4.12. Table 4.10 shows the tabulated of k and α values.

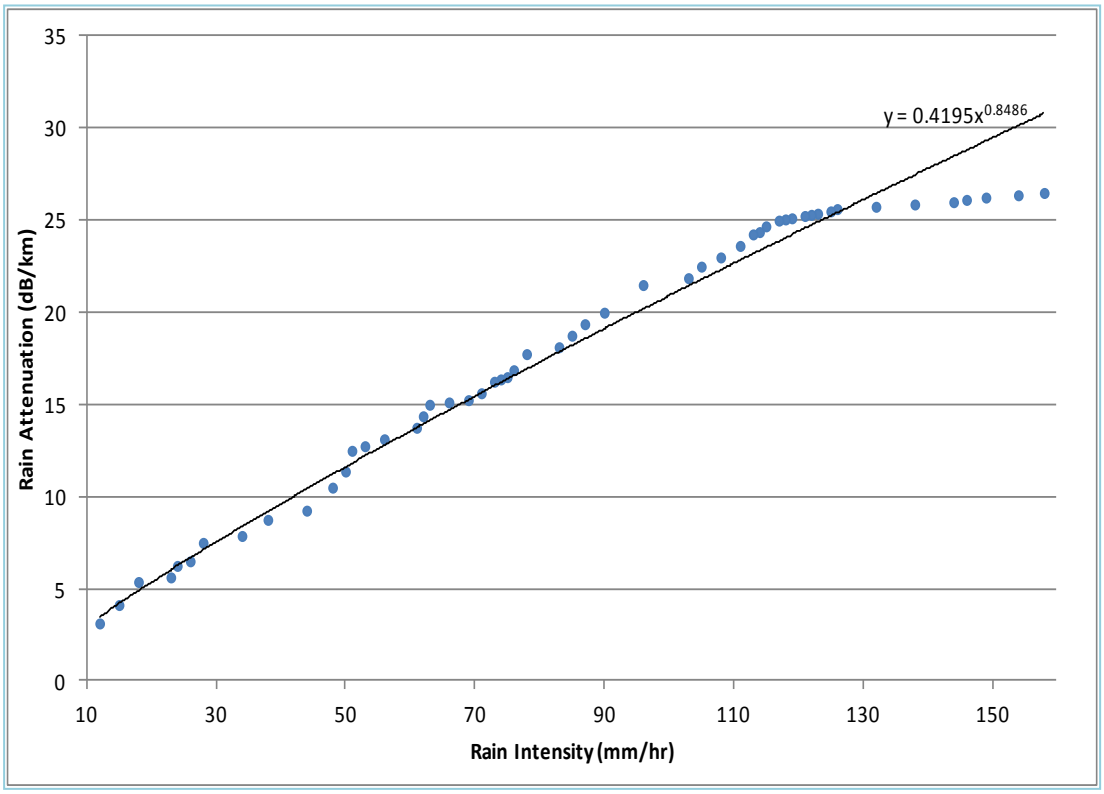

Figure 4.12. Prediction based on modified values of k and α and the measured attenuation

Table 4.10
Modified values of k and α

Model	k	α
Porposed	0.4195	0.8486

The attenuation (dB/km) is in algorithmic function of rain rate and represented as:

$$A = 0.4195R^{0.8486} \tag{4.4}$$

where R is the site rain rate, mm/hr.

The empirical equation in Equation (5.4) represents a tropical region attenuation parameter that would be helpful to the system designer to determine the link margin and attenuation of FSO system due to rain.

4.7 STATISTICAL VERIFICATION OF THE MODEL

Regression analysis applied for a validation of k and α of specific rain attenuation parameters. The type of regression equation that most suitable to describe the relation; depends on the variables considered and with respect to the physic of the processes driving the variables. The most common model used is based on the assumption of a linear relationship between two variables. Such models are called simple linear regression models.

The most common agreement among scientist, engineer, mathematician and statistician is a criterion of the regression best line model should minimize the sum square error (Gerard, 2008). When we square the error, regardless it is positive of negative, the number become positive.

With regression analysis, the actual observed values clustered around the linear regression line or R^2 (coefficient of determination) is a "measure of scatter" around the regression line. The range is from 0 to 1 and the closer R^2 to 1 the better values coincide with the regression line. It means the better the prediction or estimation.

For our application in validating of k and α value, we need to check either linear regression model is appropriate for the data or not. There are two ways of doing it, the first method is by observing the plotted data and the variable needed, however, sometimes observation can be deceiving; by changing the plot's axis the graph will show the data differently . Second method is by assessing the appropriateness of the model by defining residuals and examining residual plots (Stat Trek).

Residual or residual error (ε) is the difference between the observed value of the dependent variable (y) and the predicted value ($\hat{y}$). The equation is as shown,

$$\varepsilon = y - \hat{y} \tag{4.5}$$

Both the sum and the mean of the residuals are equal to zero. That is $\sum \varepsilon = 0$ and $\bar{\varepsilon} = 0$.

Residual plot is a graph that shows the residual on the vertical axis and the independent variable on the horizontal axis. If the points in a residual plot dispersed randomly around the horizontal axis, a linear regression is appropriate for the data; otherwise, a nonlinear model is more appropriate. Calculation of our data giving the following result, non-random: inverted U, suggesting a better fit for a nonlinear model.

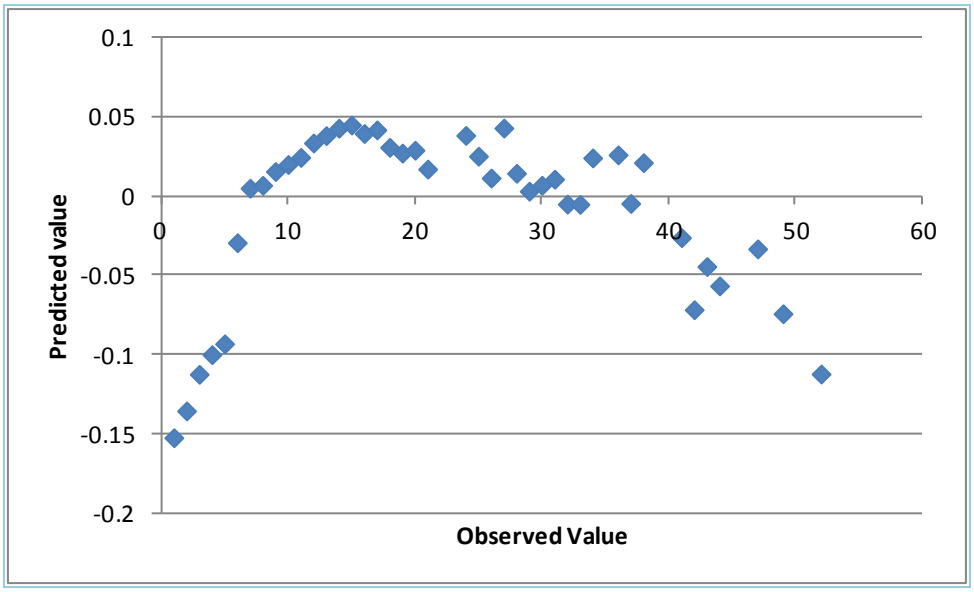

Figure 4.13. Residual plot of an inverted U shape

Since our predicted model is using power law, the appropriate non-linear regression analysis is power regression.

4.7.1 Pearson –r Regression

Although, our analysis requires power regression however, linear regression is applicable. Linear regression (Kardi Teknomo's page) is a method of predicting the value of independent Y, based on the value of an independent variable x.

Linear regression finds the straight line, called the least square regression line or LSRL that best represents observations in a bivariate data set. Definition of bivariate is statistic of distribution involving two random variables and dependent to one another (The free dictionary).

4.7.2 Pearson-r Regression Equation

The linear regression equation is as follows,

$$Y = \beta_0 + \beta_1 X \tag{4.6}$$

Where β_0 is a constant, β_1 is the regression coefficient, X is the value of the independent variable which is rain intensity (mm/hr) and, Y is the value of the dependent variable which is rain attenuation (dB/km).

Given the sample of observation, the linear regression line is estimated by

$$\hat{y} = b_0 + b_1 x \tag{4.7}$$

Where

$$slope, b_1 = \frac{n\sum xy - \sum x \sum y}{n\sum x^2 - (\sum x)^2} \tag{4.8}$$

And

$$intercept, b_0 = \bar{y} - b_1 . \bar{x} \tag{4.9}$$

When the regression parameters (b_0 and b_1) are defines as described above, the regression line has the following properties.

- The line minimizes the sum of squared differences between observed values (the y values) and predicted values (the $\hat{y}$ computed from the regression equation).
- The regression line passes through the mean of the X values ($\bar{x}$) and through the mean of the Y values ($\bar{y}$).
- The regression constant (b_0) is equal to the y intercept of the regression line.
- The regression coefficient (b_1) is the average change in the dependent variable (Y) for 1-unit change in the independent variable (X). It is the slope of the regression line.

Power regression for our analysis, however, needs to be represented by linear regression by converting values of x and y into Ln x and Ln y. A sample of the calculation is as presented in Table 5.11. A complete calculation is in Appendix I.

Table 4.11
Sample of representing power regression with linear regression

x		y	
Rain Intensity		**Rain Attenuation**	
(mm/hr)	**ln x**	**(dB/km)**	**ln y**
158	5.0626	26.50	3.2771
154	5.0370	26.38	3.2724
149	5.0039	26.25	3.2677
146	4.9836	26.13	3.2629
144	4.9698	26.00	3.2581
138	4.9273	25.88	3.2533
132	4.8828	25.75	3.2484
126	4.8363	25.63	3.2436
125	4.8283	25.50	3.2387
123	4.8122	25.38	3.2338
122	4.8040	25.31	3.2313
121	4.7958	25.25	3.2288
119	4.7791	25.13	3.2239

The coefficient of determination (denoted by R^2) is the key output of regression analysis. It is interpreted as the proportion of the variance in the dependent variable that is predictable from the independent variable.

- The coefficient of determination ranges from 0 to 1.
- An R^2 of 0 means that the dependent variable cannot be predicted from the independent variable.
- An R^2 of 1 means the dependent variable can be predicted without error from the independent variable.
- An R^2 between 0 and 1 indicates the extent to which the dependent variable is predicted. An R^2 of 0.10 means that 10 percent of the variance in Y is predictable from X; an R^2 of 0.20 means that 20 percent is predictable; and the closer the value to 1, means our data have been represented with the best prediction model.

The coefficient of determination is the proportion of variance explained by the best line model. It depends on the ratio of sum of square error (SSE) from the regression model and the sum of squares difference around the mean, which is called the sum of square total (SST). SSE and SST can be calculated using the following formula

$$SSE = \sum(y - \hat{y})^2 \tag{4.10}$$

Where $\hat{y}$ is the estimated of y as in Equation (6.7)

While

$$SST = \sum(y - \bar{y})^2 \tag{4.11}$$

Where $\bar{y}$ as the means of y.

The equation of coefficient of determination, R^2 is as shown below

$$R^2 = 1 - \frac{SSE}{SST} \tag{4.12}$$

4.7.3 Validation of k & α Value

Figure 4.14 shows the measured rain intensity and rain attenuation after applying equiprobability analysis.

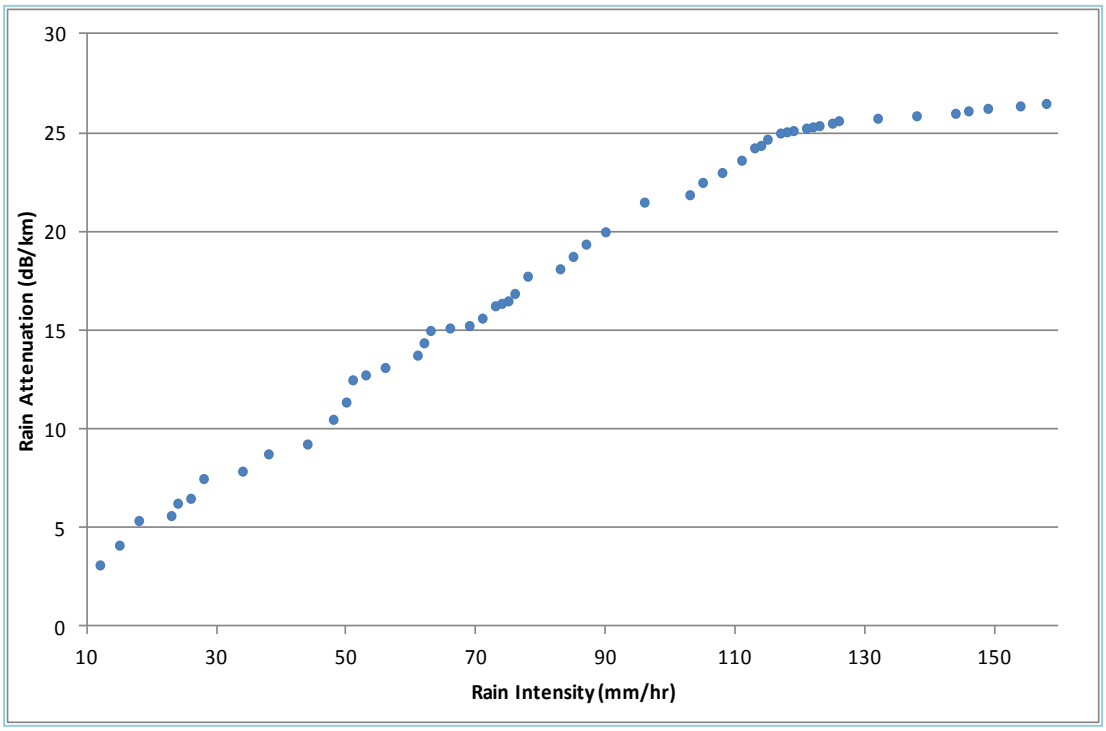

Figure 4.14. Rain Intensity (mm/hr) versus Rain Attenuation (dB/km)

From Figure 4.14 the validation of the data we use power regression or best fit exponential curve (regression exponential curve) (Finite mathematics & Applied calculus).

Steps of validation are as follows

- Converting rain values and rain attenuation to LN values
- Finding summation and average value of x and y
- Determine number of coefficients, n
- Find SSE and SST

- Use Equation (5.12) to find coefficient of determination, R^2

A complete step is as shown in Appendix I. Summary of the output is as tabulated in Table 4.12

Table 4.12
Regression analysis result

Slope	Intercept	Coefficient of determination, R^2
0.8486	-0.8686	0.98906

From the tabulated result, it verifies that the propose value of k and α is highly predicted with the determination of coefficient equal to 0.9891. The closer the value of 1 means our data have been represented with the best prediction model.

4.8 ENHANCEMENT OF PROPOSED K AND α

This section will discuss on the enhancement of the proposed and predicted k and α value as analyzed in the previous section. From Figure 4.15, the data shows that the power regression curvature seems not to bend following the measured data. Therefore, we analyze an enhancement of the proposed k and α to find the best fit for the measured data since in tropical region high rain intensity is crucial in determining the availability of the link.

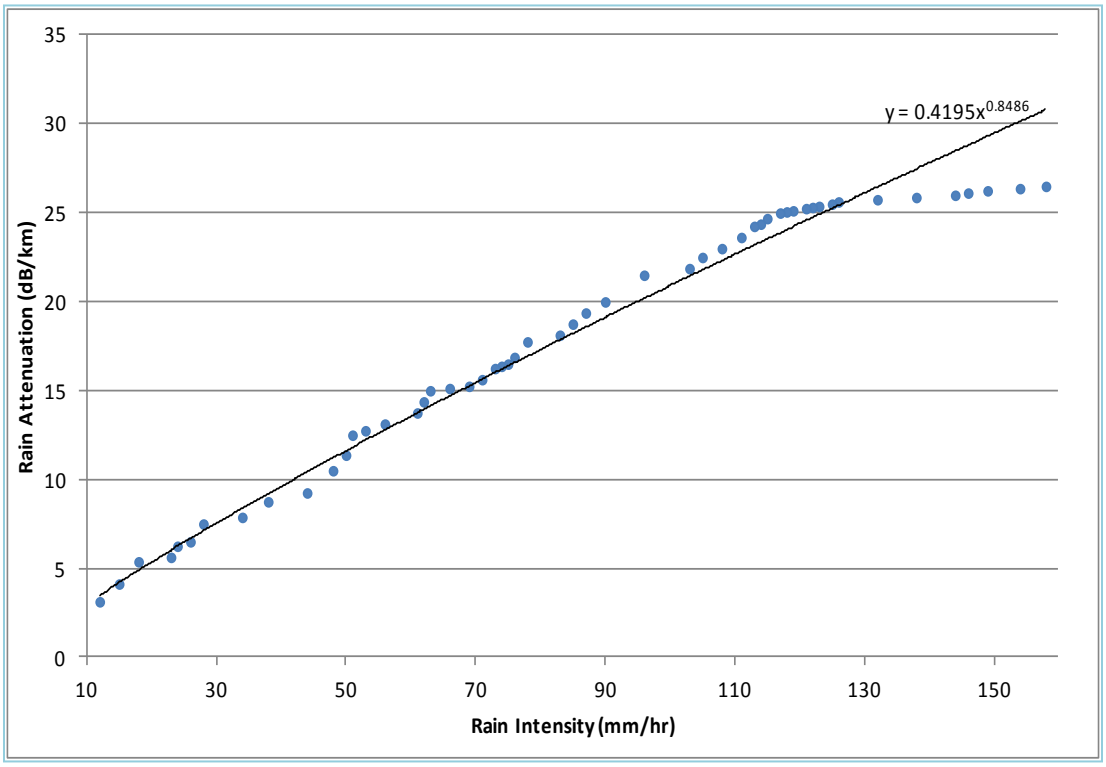

Figure 4.15: Prediction based of k and α from the measured data

The enhancement analysis begins with the fact that the available and accepted k and α value is from temperate region data. Table 4.13 shows the k and α value developed with data from temperate regions. The result of the table shows values of α for all the models are almost at the same range, which is around $\alpha \cong 0.6$.

Table 4.13
Rain attenuation prediction for FSO recommended by ITU-R

Model	Origin	Author	k	α	Note
Carbonneau	France	ITU-R	1.076	0.67	Temperate region
Japan	Japan	ITU-R	1.58	0.63	Temperate region
J.Joss	Switzerland	Bouchet	0.509	0.63	Temperate region
					Drizzle or light rain (R<3.8 mm/hr)
Marshal & Palmer	Canada	Bouchet	0.365	0.63	Temperate region

Mathematically, power value which is α is the factor that determines the curvature of the plot. With that argument, we are trying to find the best-fit line for our measured data by fixing the value of α and calculating the value of k.

The following table illustrates the different values that will be considered in this calculation.

Table 4.14
Different values of α for finding the best-fit line

α	0.63	0.65	0.67	0.73	0.75	0.77	0.83	0.85	0.87	0.90	0.93

By fixing α value, least square fitting power law is used to calculate k. (Weisstein). The equation of least square fitting power law is as in Equation (4.13) – (4.14)

Given $$y = Ax^B \quad (4.13)$$

$$b = \frac{n\sum_{i=1}^{n}(\ln x_i \ln y_i) - \sum_{i=1}^{n}(\ln x_i)\sum_{i=1}^{n}(\ln y_i)}{n\sum_{i=1}^{n}(\ln x_i)^2 - \sum_{i=1}^{n}(\ln x_i)^2} \quad (4.14)$$

$$a = \frac{\sum_{i=1}^{n}(\ln y_i) - b\sum_{i=1}^{n}(\ln x_i)}{n} \quad (4.14)$$

Where B = α and k = A = exp (a)

Details calculation of the procedure is in Appendix J. The following table shows the value of new k as we fix α

Table 4.15
Values of new k and α

α	k
0.63	1.0693
0.65	0.9816
0.67	0.9010
0.73	0.6970
0.75	0.6398
0.77	0.5873
0.83	0.4543
0.85	0.4170
0.87	0.3828
0.90	0.3367
0.93	0.2961

With the new set of k and α, we plot Figure 4.16. The plot is to find the best-fit line for the measured data that will best represent the k and α value for the tropical region with the effect of rain attenuation on FSO link.

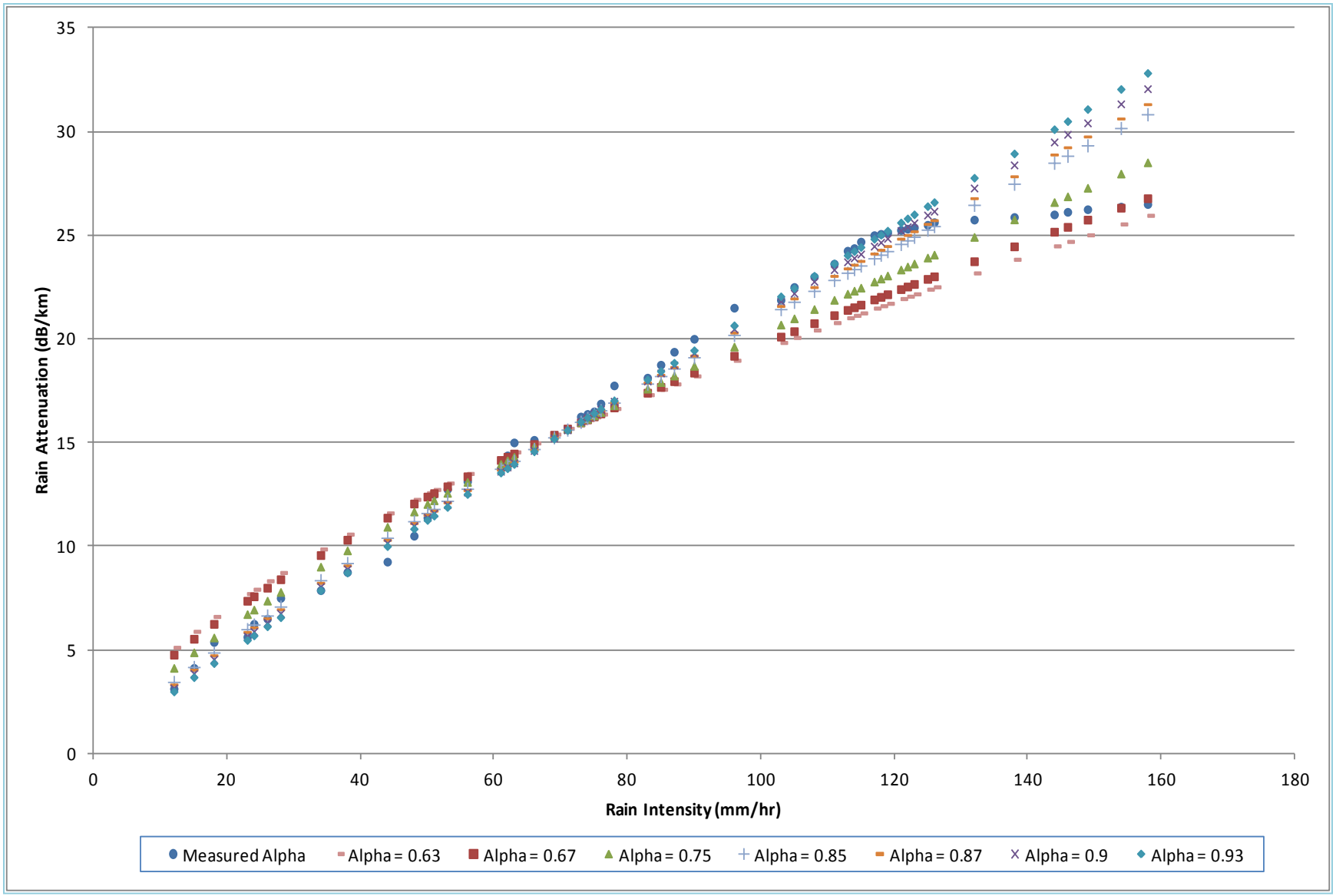

Figure 4.16. Plot of different k and α value

From Figure 4.16 we extract the best-fit plot that matches the measured value strongly. Taking the unrelated values out, we got the following plot in Figure 4.17.

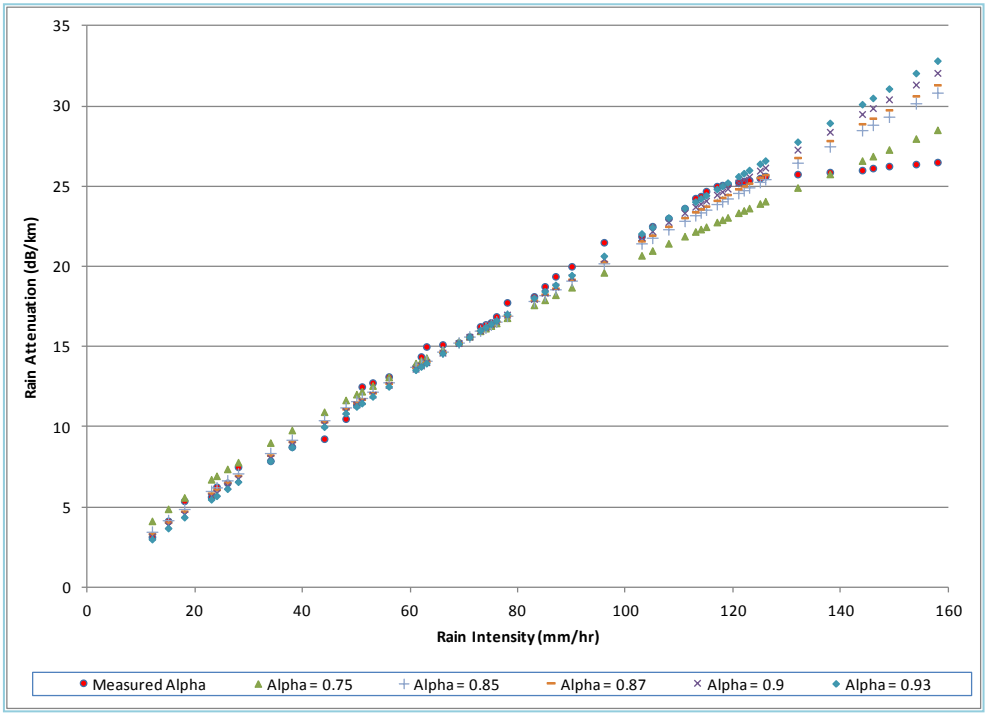

Figure 4.17. Plot of k and α that strongly related to the measured value

From Figure 4.17, there are a few ranges of rain intensity, which can be divided to find the new enhancement of k and α. The division of the rain intensity is as illustrated in Table 4.16.

Table 4.16
Rain intensity for new specific rain parameter prediction

Rain Intensity (mm/hr)
120 - 160
103 - 120
70 - 103
50 - 70
12 - 50

Based on the range as in Table 4.16, the new k and α value are predicted. Figure 4.19, shows the measured data and the closed predicted data that best fit the measured data. From the calculation the best fit for measuring data ranges from 12 mm/hr to 50 mm/hr range is when α = 0.9. The plot of the measured and predicted values is as presented in Figure 4.18. From calculation or taking the regression analysis on the data, it's shown that the new value of predicted k and α is as follows

$$k = 0.3367 \qquad \alpha = 0.9 \qquad (4.15)$$

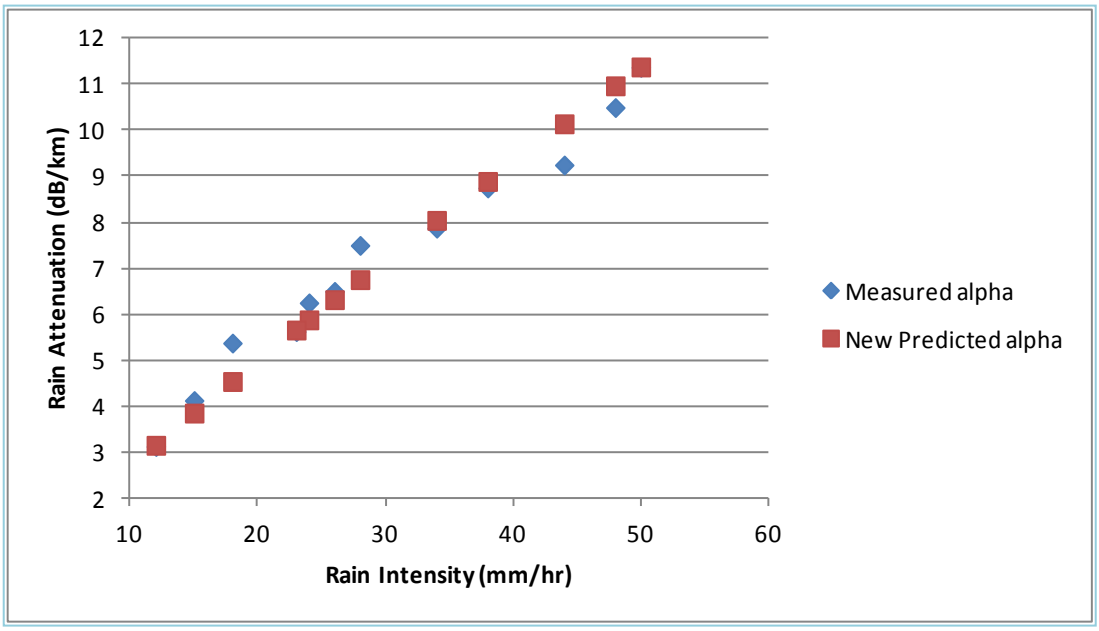

Figure 4.18. Measured and predicted alpha from 12 mm/hr to 50 mm/hr rain intensity

Table 4.17 shows the comparison of the new predicted value with earlier k and α prediction value.

Table 4.17
The RMS comparison of 12 mm/hr to 50 mm/hr rain intensity

Rain intensity mm/hr	Measured Rain Att dB/km	New Prediction Rain Att dB/km	Percentage of error %	First Prediction Rain Att dB/km	Percentage of error %
50	11.375	11.384	0.076	11.601	1.983
48	10.5	10.973	4.504	11.206	6.720
44	9.25	10.146	9.691	10.408	12.519
38	8.75	8.892	1.626	9.190	5.034
34	7.875	8.045	2.162	8.363	6.193
28	7.5	6.755	-9.928	7.092	-5.435
26	6.5	6.320	-2.777	6.660	2.463
24	6.25	5.880	-5.916	6.223	-0.437
23	5.625	5.659	0.610	6.002	6.702
18	5.375	4.539	-15.555	4.875	-9.306
15	4.125	3.852	-6.618	4.176	1.237
12	3.125	3.151	0.837	3.456	10.580
		STD	6.822		6.240
		Mean	1.969		1.801
		RMS	7.100		6.495

According to the evaluation procedure adopted by the ITU-R (ITU-R F.2106-1, 2010) the preferred prediction method is the one producing the smallest RMS value. The result of the analysis for two predicted values shows that the first prediction of k and α is the best to represent the values for 12 mm/hr to 50 mm/hr rain intensity. The value of predicted k and α is as shown

$$k = 0.4195 \qquad \alpha = 0.8486 \qquad (4.16)$$

The second range of rain intensity is from 50 mm/hr to 70 mm/hr. From the calculation the best fit values from 50 mm/hr to 70 mm/hr range is when $\alpha = 0.75$. The plot of the measured and predicted values is as presented in Figure 4.19. From calculation or taking the regression analysis on the data, it's shown that the new value of predicted k and α is as follows

$$k = 0.6398 \qquad \alpha = 0.75 \qquad (4.17)$$

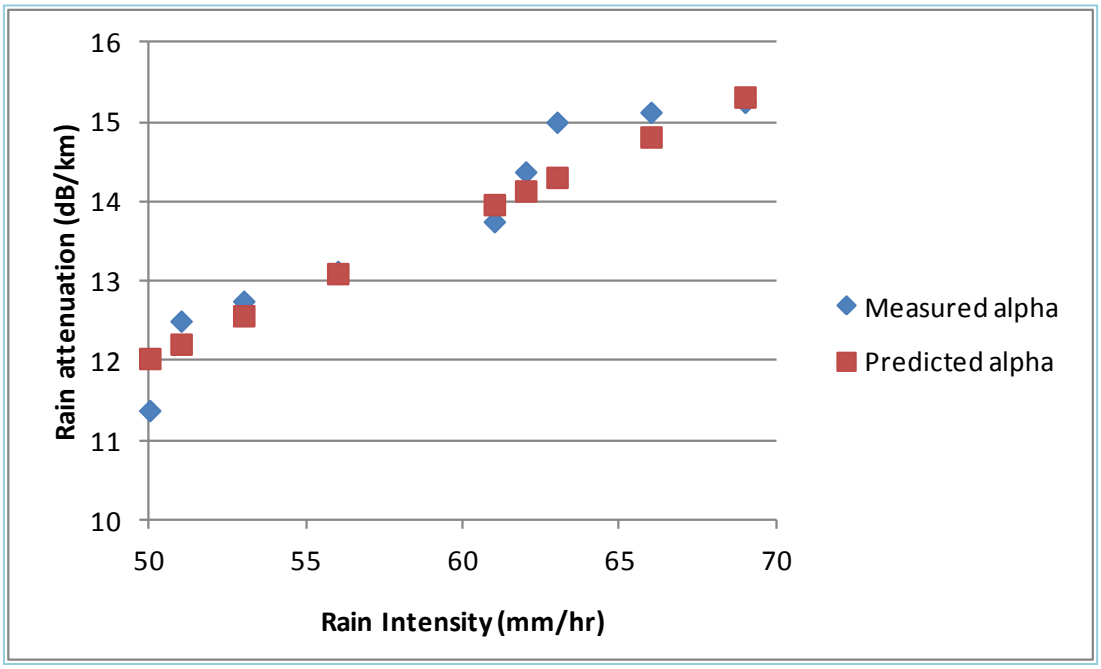

Figure 4.19. Measured and predicted alpha from 50 mm/hr to 70 mm/hr rain intensity

Comparing the new predicted value with earlier k and α prediction value, yield the following result as shown in Table 4.18.

Table 4.18
The RMS comparison of 50 mm/hr to 70 mm/hr rain intensity

Rain intensity mm/hr	Measured Rain Att dB/km	New Prediction Rain Att dB/km	Percentage of error %	First Prediction Rain Att dB/km	Percentage of error %
69	15.25	15.317	0.441	15.247	-0.021
66	15.125	14.815	-2.049	14.682	-2.926
63	15	14.307	-4.620	14.114	-5.906
62	14.375	14.136	-1.660	13.924	-3.139
61	13.75	13.965	1.564	13.733	-0.124
56	13.125	13.097	-0.210	12.772	-2.693
53	12.75	12.568	-1.431	12.189	-4.403
51	12.5	12.210	-2.319	11.797	-5.623
50	11.375	12.030	5.760	11.601	1.983
		STD	2.943		2.680
		Mean	0.981		0.893
		RMS	3.103		2.825

The result shows that α = 0.75 is not the best representation of k and α at this rain intensity range. The best-fit data is for

$$k = 0.4195 \qquad \alpha = 0.8486 \qquad (4.18)$$

which is the value of the first proposed value of k and α.

The next range of rain intensity is from 70 mm/hr to 103 mm/hr. At this range, as in Figure 4.17, the predicted value of k and α does not fit with the measured data. Therefore, regression analysis is used to find k and α value. Figure 4.20 shows the regression method on the data. Table 4.9 show the result of analyzing both predicted value and rain intensity.

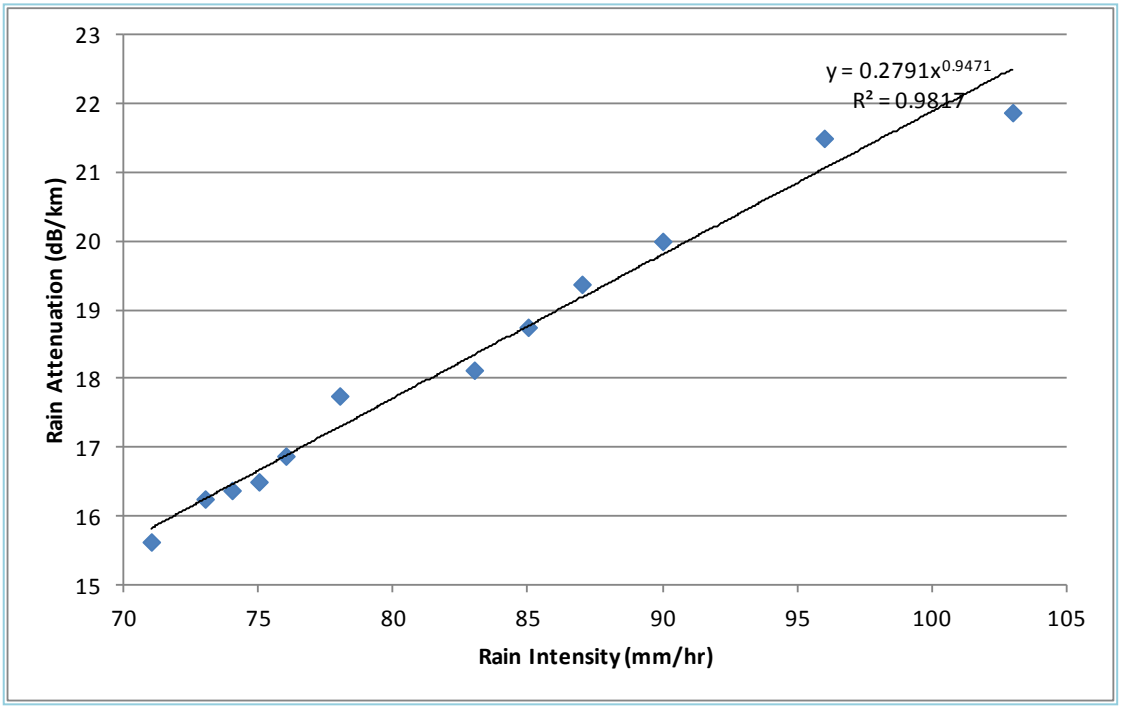

Figure 4.20. Regression analysis of rain intensity from 70 mm/hr to 103 mm/hr

Table 4.19
The RMS comparison of 70 mm/hr to 103 mm/hr rain intensity

Rain intensity mm/hr	Measured Rain Att dB/km	New Prediction Rain Att dB/km	Percentage of error %	First Prediction Rain Att dB/km	Percentage of error %
103	21.875	22.497	2.842	21.420	-2.079
96	21.5	21.046	-2.112	20.178	-6.147
90	20	19.798	-1.010	19.103	-4.485
87	19.375	19.172	-1.045	18.561	-4.200
85	18.75	18.755	0.026	18.199	-2.941
83	18.125	18.337	1.167	17.835	-1.603
78	17.75	17.289	-2.599	16.919	-4.684
76	16.875	16.869	-0.038	16.550	-1.928
75	16.5	16.658	0.959	16.365	-0.820
74	16.375	16.448	0.445	16.179	-1.195
73	16.25	16.237	-0.078	15.994	-1.578
71	15.625	15.816	1.220	15.621	-0.025
		STD	1.519		1.851
		Mean	0.438		0.534
		RMS	1.581		1.926

The result shows that the new propose the value of k and α is best representing the rain attenuation on the link for the rain intensity ranges from 70 mm/hr to 103 m/hr. Therefore the value of k and α is

$$k = 0.2791 \qquad \alpha = 0.9471 \qquad (4.19)$$

Plot in Figure 4.21, is for rain intensity in the range of 103 mm/hr – 120 mm/hr. From Figure 4.18, the fit line with $\alpha = 0.93$ have predicted value that closely fit with measured data. Finding the RMS values for both predicted values giving the following result as shown in Table 4.20.

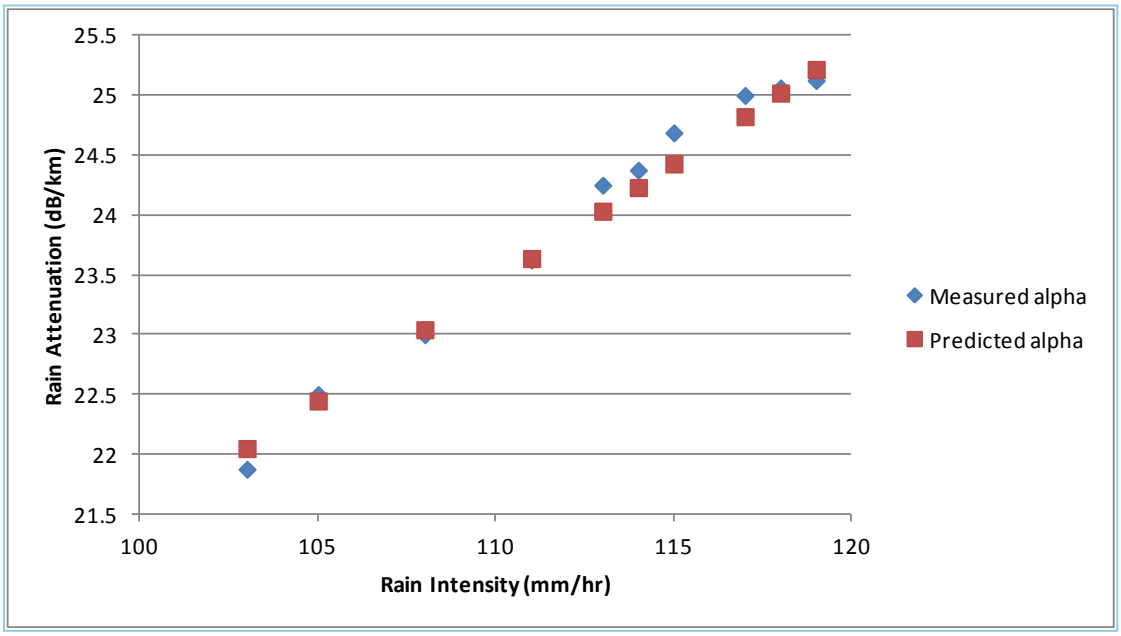

Figure 4.21: Measured and predicted alpha from 103 mm/hr to 120 mm/hr rain intensity

Table 4.20
The RMS comparison of 103 mm/hr to 120 mm/hr rain intensity

Rain intensity mm/hr	Measured Rain Att dB/km	New Prediction Rain Att dB/km	Percentage of error %	First Prediction Rain Att dB/km	Percentage of error %
119	25.125	25.217	0.367	24.213	-3.632
118	25.0625	25.020	-0.169	24.040	-4.081
117	25	24.823	-0.709	23.867	-4.533
115	24.6875	24.428	-1.051	23.520	-4.728
114	24.375	24.230	-0.593	23.346	-4.220
113	24.25	24.033	-0.896	23.173	-4.443
111	23.625	23.637	0.050	22.824	-3.390
108	23	23.042	0.183	22.300	-3.046
105	22.5	22.446	-0.239	21.773	-3.232
103	21.875	22.048	0.793	21.420	-2.079
		STD	0.590		0.822
		Mean	0.187		0.260
		RMS	0.619		0.862

The result shows that the new predicted k and α is the best to represent the values from 103 mm/hr to 120 mm/hr rain intensity ranges. The value of k and α is as follows

$$k = 0.2961 \qquad \alpha = 0.93 \qquad (4.20)$$

Plot in Figure 4.22 is for rain intensity in the range of 120 mm/hr – 160 mm/hr. From Figure 4.18, the predicted value of k and α does not fit with the measured data. Therefore, regression analysis is used to find k and α value. Figure 4.23 shows the regression method on the data. A comparison of both predicted values as shown in Table 4.21.

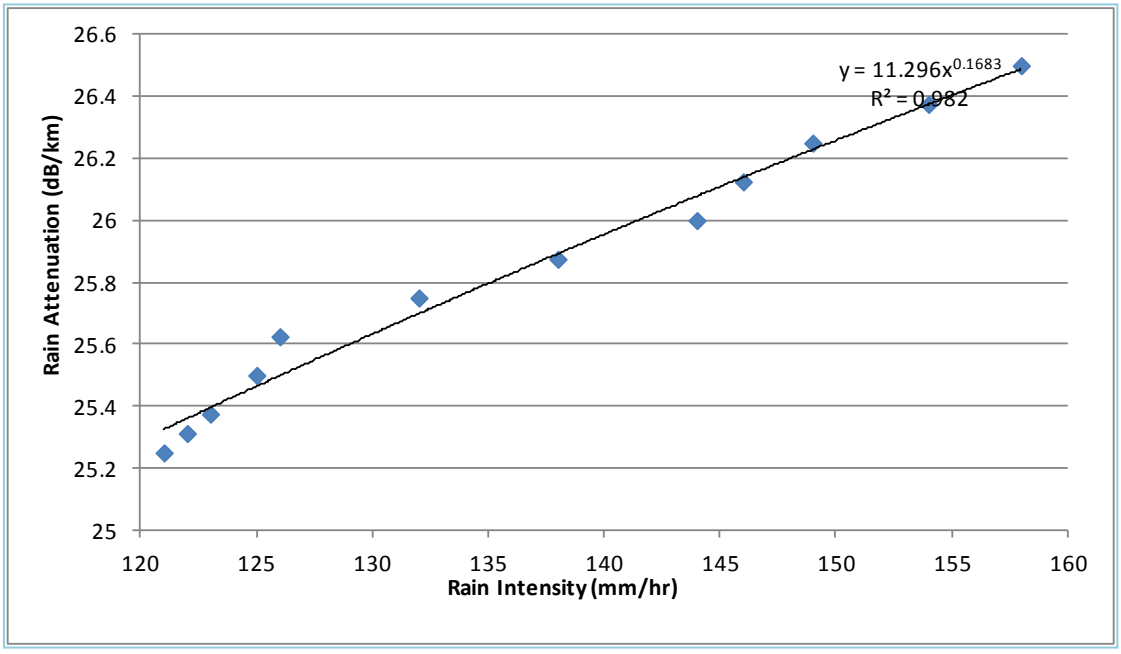

Figure 4.22. Regression analysis of rain intensity of 120 mm/hr to 160 mm/hr

Table 4.21
The RMS comparison of 120 mm/hr to 160 mm/hr rain intensity

Rain intensity mm/hr	Measured Rain Att dB/km	New Prediction Rain Att dB/km	Percentage of error %	First Prediction Rain Att dB/km	Percentage of error %
158	26.5	26.482	-0.066	30.797	16.216
154	26.375	26.368	-0.025	30.134	14.254
149	26.25	26.222	-0.105	29.302	11.627
146	26.125	26.133	0.030	28.801	10.242
144	26	26.072	0.278	28.465	9.483
138	25.875	25.886	0.043	27.456	6.109
132	25.75	25.693	-0.221	26.439	2.677
126	25.625	25.493	-0.516	25.416	-0.816
125	25.5	25.459	-0.162	25.245	-1.001
123	25.375	25.390	0.058	24.901	-1.866
122	25.3125	25.355	0.167	24.730	-2.303
121	25.25	25.320	0.276	24.557	-2.743
		STD	0.221		7.003
		Mean	0.064		2.022
		RMS	0.230		7.289

The best representation of k and α for the 120 mm/hr to 160 mm/hr is

$$k = 11.296 \qquad \alpha = 0.1683 \tag{4.21}$$

A summary table of k and α value of the discussion above is as shown in Table 4.22. Since the value of k and α for 12 mm/hr to 50 mm/hr and 50 mm/hr to 70 mm/hr are the same therefore the range now is considered for 12 mm/hr to 70 mm/hr as presented in Table

Table 4.22
New predicted of k and α

Rain Intensity (mm/hr)	k	α
120 - 160	11.2960	0.1683
103 -120	0.2961	0.9300
70 - 103	0.2791	0.9471
12 - 70	0.4195	0.8486

Therefore, the new equation and range to calculate rain the k and α becomes

For 120 < R (mm/hr) < 160 $A = k_1 R^{\alpha_1}$ (4.22)

For 103 < R (mm/hr) < 120 $A = k_2 R^{\alpha_2}$ (4.23)

For 70 < R (mm/hr) < 103 $A = k_3 R^{\alpha_3}$ (4.24)

For 12 < R_4 (mm/hr) ≤ 70 $A = k_4 R^{\alpha_4}$ (4.25)

Where k_1= 0.4195 and α_1 = 0.8486 , k_2= 0.2791 and α_2 = 0.9471, k_3= 0.2961 and α_3 = 0.93, k_4= 11.296 and α_4 = 0.1683

The analysis is either to determine the enhancement values is better or the single proposed value of k and α is better. In order to do this analysis, the following section will discuss on the validation of the enhancement values.

4.9 STATISTICAL VALIDATION OF ENHANCEMENT K AND α

The validation of the predicted data is analyzed in this section using new k and α. The technique is the same as discussed in section 4.2.3.2 and 4.2.3.3. The complete calculation is in Appendix K. Figure 4.23 shows the summary table of the result.

Table 4.23
Regression analysis result of the enhancement k and α

Slope	Intercept	Coefficient of determination, R^2
0.8407	-0.8334	0.9927

The result in Table 4.23 shows that the predicted value of k and α with variation of rain intensity is highly predicted with the determination of coefficient equal to 0.9927. The result shows that the determination of coefficients, R^2, is closer to 1 indicating the data have represented with the best prediction model.

The validation demonstrated through the prediction error and Root-Mean-Square (RMS) analysis. According to the evaluation procedure adopted by the ITU-R (ITU-R F.2106-1, 2010) the preferred prediction method is the one producing the smallest RMS value. The RMS value is calculated using the method propose by ITU-R F.2106-1 by first finding percentage error. Equation (4.26) shows the calculation Percentage error can be calculated as follows

$$Percentage\ error = \frac{(Predicted\ Attenuation - Measured\ Attenuation}{Measured\ Attenuation} \times 100 \qquad (4.26)$$

RMS is calculated from mean error (μ_e) and standard deviation (σ_e) as shown in Equation (4.27)

$$RMS = \sqrt{\mu_e^2 + \sigma_e^2} \qquad (4.27)$$

In Section 4.2.2 we already propose a single value of k = 0.4195 and α = 0.8486. While is Section 4.3, we proposed a new enhanced value of k and α. Comparing both of proposed k and α, give us the following outcome as presented in Table 4.24

From Table 4.24, it shows the improvement of the proposed k and α values with ranges according to rain intensity that gives lower RMS values comparable to the single k and α value. It means that the complex calculation with different range of k and α give a correct prediction of specific rain attenuation parameters.

Table 4.25 illustrated the comparison at selected rain intensity with single k and α value, variation of the k and α value with ITU-R model (Carbonneau and Japan's model.)

Table 4.24
Prediction error and RMS values of the proposed k and α value

Rain Intensity (mm/hr)	Measured Rain Attenuation (dB/km)	Single value of k and α $0.4195R^{0.8486}$ (dB/km)	Percentage or error (%)	Enhancement of k and α values (dB/km)	Percentage or error (%)
158	26.500	30.797	16.216	26.482	-0.066
154	26.375	30.134	14.254	26.368	-0.025
149	26.250	29.302	11.627	26.222	-0.105
146	26.125	28.801	10.242	26.133	0.030
144	26.000	28.465	9.483	26.072	0.278
138	25.875	27.456	6.109	25.886	0.043
132	25.750	26.439	2.677	25.693	-0.221
126	25.625	25.416	-0.816	25.493	-0.516
125	25.500	25.245	-1.001	25.459	-0.162
123	25.375	24.901	-1.866	25.390	0.058
122	25.313	24.730	-2.303	25.355	0.167
121	25.250	24.557	-2.743	25.320	0.276
119	25.125	24.213	-3.632	25.217	0.367
118	25.063	24.040	-4.081	25.020	-0.169
117	25.000	23.867	-4.533	24.823	-0.709
115	24.688	23.520	-4.728	24.428	-1.051
114	24.375	23.346	-4.220	24.230	-0.593
113	24.250	23.173	-4.443	24.033	-0.896
111	23.625	22.824	-3.390	23.637	0.050
108	23.000	22.300	-3.046	23.042	0.183
105	22.500	21.773	-3.232	22.446	-0.239
103	21.875	21.420	-2.079	22.048	0.793
96	21.500	20.178	-6.147	21.046	-2.112
90	20.000	19.103	-4.485	19.798	-1.010
87	19.375	18.561	-4.200	19.172	-1.045
85	18.750	18.199	-2.941	18.755	0.026
83	18.125	17.835	-1.603	18.337	1.167
78	17.750	16.919	-4.684	17.289	-2.599
76	16.875	16.550	-1.928	16.869	-0.038
75	16.500	16.365	-0.820	16.658	0.959
74	16.375	16.179	-1.195	16.448	0.445
73	16.250	15.994	-1.578	16.237	-0.078
71	15.625	15.621	-0.025	15.816	1.220
69	15.250	15.247	-0.021	15.247	-0.021
66	15.125	14.682	-2.926	14.682	-2.926
63	15.000	14.114	-5.906	14.114	-5.906
62	14.375	13.924	-3.139	13.924	-3.139
61	13.750	13.733	-0.124	13.733	-0.124
56	13.125	12.772	-2.693	12.772	-2.693
53	12.750	12.189	-4.403	12.189	-4.403
51	12.500	11.797	-5.623	11.797	-5.623
50	11.375	11.601	1.983	11.601	1.983
48	10.500	11.206	6.720	11.206	6.720
44	9.250	10.408	12.519	10.408	12.519
38	8.750	9.190	5.034	9.190	5.034
34	7.875	8.363	6.193	8.363	6.193
28	7.500	7.092	-5.435	7.092	-5.435
26	6.500	6.660	2.463	6.660	2.463
24	6.250	6.223	-0.437	6.223	-0.437
23	5.625	6.002	6.702	6.002	6.702
18	5.375	4.875	-9.306	4.875	-9.306
15	4.125	4.176	1.237	4.176	1.237
12	3.125	3.456	10.580	3.456	10.580
		STD	5.854		3.622
		Mean	0.804		0.498
		RMS	5.909		3.656

Table 4.25
Comparison between proposed new enhancement k and α with ITU-R models

			$0.4195R^{0.8486}$		New		$1.076R^{0.67}$		$1.58R^{0.63}$	
	Rain intensity mm/hr	Measured Rain Att dB/km	Predicted Rain Att dB/km	Percentage of error %	Predicted Rain Att. dB/km	Percentage of error %	Carbonneau Rain Att dB/km	Percentage of error %	Japan Rain Att dB/km	Percentage of error %
$R_{0.001}$	158	26.5	30.80	16.22	26.48	-0.07	31.98	20.69	38.35	44.73
$R_{0.003}$	125	25.5	25.24	-1.00	25.46	-0.16	27.34	7.20	33.09	29.77
$R_{0.01}$	103	21.875	21.42	-2.08	22.50	2.84	24.01	9.77	29.29	33.90
$R_{0.03}$	75	16.875	16.36	-3.02	16.42	-2.72	19.41	15.04	23.99	42.14
$R_{0.1}$	48	10.5	11.21	6.72	11.21	6.72	14.40	37.11	18.11	72.44
$R_{0.3}$	18	5.375	4.87	-9.31	4.87	-9.31	7.46	38.82	9.76	81.59
			STD	8.94		5.41		13.62		21.24
			Mean	3.65		2.21		5.56		8.67
			RMS	**9.66**		**5.84**		**14.72**		**22.95**

In Table 4.25 shows the comparison of prediction error and RMS values at selected rain intensity with proposed k and α with other models. The result shows that the predicted with different ranges of k and α value give the lowest RMS values compare to others. The predicted values shows significant improvement in term of prediction error and RMS. Carbonneau and Japan models show that the available prediction values are overestimate for tropical weather condition.

4.10 DIRECT MEASUREMENT VALIDATION

Direct measurement validation means that the validation is performed event by event. The measured rain attenuation is validated by the proposed prediction of attenuation to compare either the prediction value will match with the measured rain attenuation. The prediction of rain attenuation is using the range of values as illustrated in Table 4.22.

Figure 4.23 shows a sample of the plot for direct measurement validation analysis.

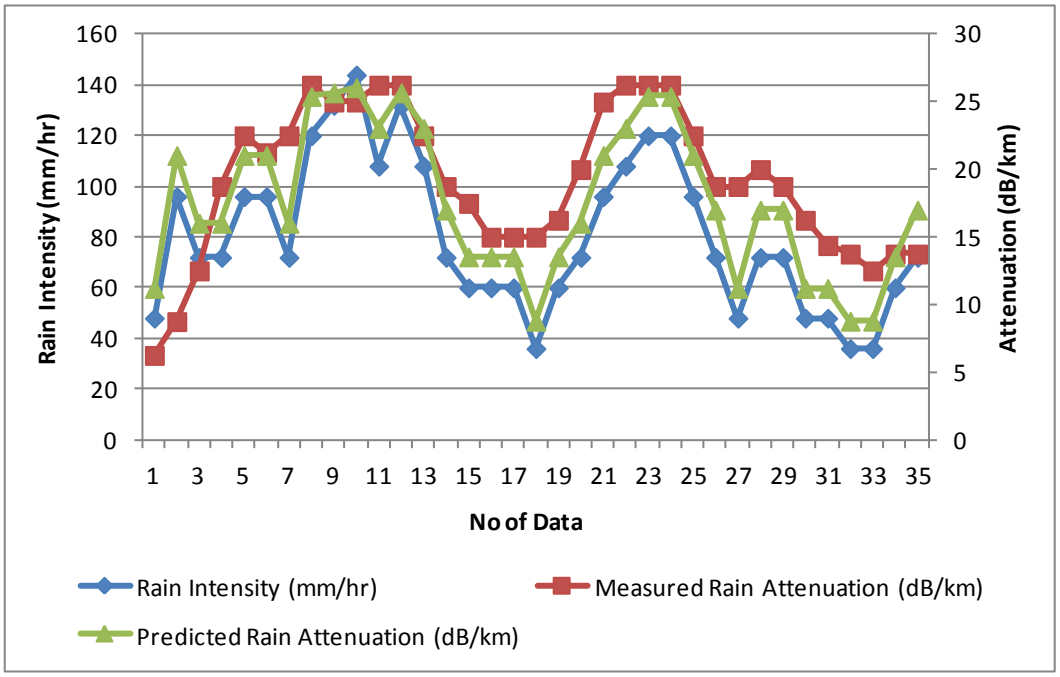

Figure 4.23. Plot of rain intensity, measured rain attenuation and predicted rain attenuation for direct measurement analysis

Figure 4.23 shows the plot of rain intensity data with measured rain attenuation and predicted rain attenuation occurring on 19 May 2011. We perform the analysis of direct measurement by calculating the percentage of error for high peak rain attenuation of measured and predicted values. There are 30 data altogether for this analysis. Table 4.26 shows the result of extracting the peak value of measured rain attenuation and predicted rain attenuation.

From Table 4.26, we extract out the data for high rain attenuation, which mean occurring for 10 dB, and take the average of the error as illustrated in Table 4.27

Table 4.26
Percentage of error calculation of measured and predicted rain attenuation

Observation	Measured	Predicted	Percentage of error
1	10.00	11.206	12.056
2	10.00	8.778	-12.217
3	6.25	8.778	40.453
4	15.00	13.542	-9.722
5	26.25	25.414	-3.184
6	25.00	25.680	2.718
7	25.00	26.058	4.233
8	26.25	25.680	-2.173
9	26.25	25.414	-3.184
10	8.75	11.206	28.063
11	13.75	18.546	34.878
12	4.38	6.223	42.233
13	10.00	7.579	-24.207
14	8.75	8.778	0.323
15	13.75	11.206	-18.505
16	6.25	6.223	-0.437
17	5.00	6.223	24.454
18	25.00	23.034	-7.863
19	3.75	6.223	65.939
20	10.00	11.206	12.056
21	5.00	3.456	-30.888
22	18.75	18.546	-1.089
23	7.50	8.778	17.044
24	21.25	21.046	-0.960
25	23.75	26.072	9.778
26	22.50	21.046	-6.462
27	16.25	18.546	14.128
28	3.75	6.223	65.939
29	5.00	6.223	24.454
30	8.75	6.223	-28.883

Table 4.27
10 dB and above rain attenuation

Observation	Measured	Predicted	Percentage of error
1	10.00	11.206	12.056
2	10.00	8.778	-12.217
3	15.00	13.542	-9.722
4	26.25	25.414	-3.184
5	25.00	25.680	2.718
6	25.00	26.058	4.233
7	26.25	25.680	-2.173
8	26.25	25.414	-3.184
9	13.75	18.546	34.878
10	10.00	7.579	-24.207
11	13.75	11.206	-18.505
12	25.00	23.034	-7.863
13	10.00	11.206	12.056
14	18.75	18.546	-1.089
15	21.25	21.046	-0.960
16	23.75	26.072	9.778
17	22.50	21.046	-6.462
18	16.25	18.546	14.128
		Average	**9.97**

From Table 4.27, by taking the average of the error, we can conclude that for high rain intensity with 10 dB and above attenuation, the error is 10%. If we consider the attenuation of 20 dB and above, the average error is below 5 %. The prediction also presenting a positive and negative error values representing the logical data of the prediction, which at one point the measured is higher than the predicted and at another point the predicted, is higher than the measured since it is point-by-point measurement. By considering point-by-point measurement, it does not reflect the rain intensity occurring along the link therefore average value is the best to represent the analysis.

4.11 BENCHMARKING WITH AVAILABLE PREDICTION AND MEASUREMENT

ITU-R has reported two rain attenuation models, namely Carbonneau and Japan Model (ITU-R 1814, 2007). In tropical region there are two attempts to measure rain attenuation on FSO link conducted in Singapore (Chen, B., 2002) and Indonesia (Bouna et. Al., 2011)

The following section presented a comparison between ITU-R, Singapore, Indonesia and measured model under Malaysia's environment.

4.11.1 Benchmarking with ITU-R model

Figure 4.24 show the benchmarking of our predicted model with ITU-R model.

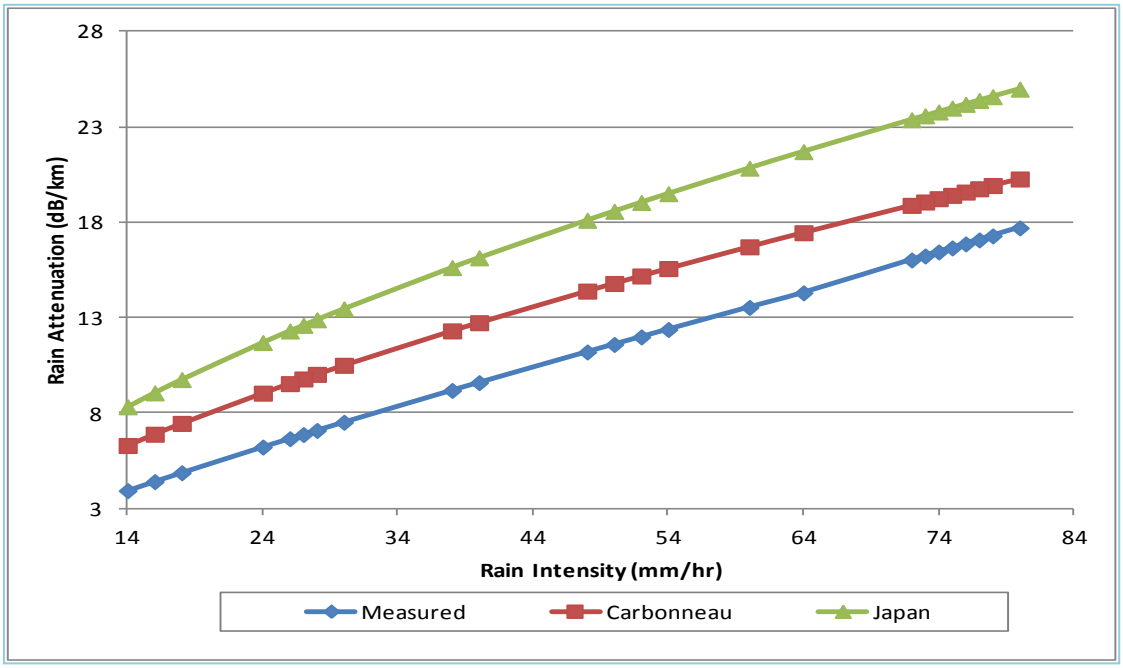

Figure 4.24. Comparison of measured specific rain attenuation with ITU-R model

Figure 5.24 shows the comparison of predicted and proposed specific rain attenuation model with ITU-R model (Carbonneau and Japan models). The

comparison is up to 80 mm/hr since in (ITU-R, 2007) the prediction model is up to 80 mm/hr. The result shows that our measurement is lower than predicted in the in ITU-R. It is due to the fact that, our result is based on direct measurement and correlation between rain intensity and rain attenuation while the ITU-R prediction model is based on drop size distribution analysis. Where k and α in the model are analytically proposed from measured drop size distribution.

4.11.2 Benchmarking with Singapore and Indonesia

The attempt conducted in Singapore and Indonesia is only for the measurement of attenuation on FSO link; and not to develop k and α value. The measurement conducted for a very short period for both attempts. Comparing the data that we directly measured for a year and their measurement gives us the following plot.

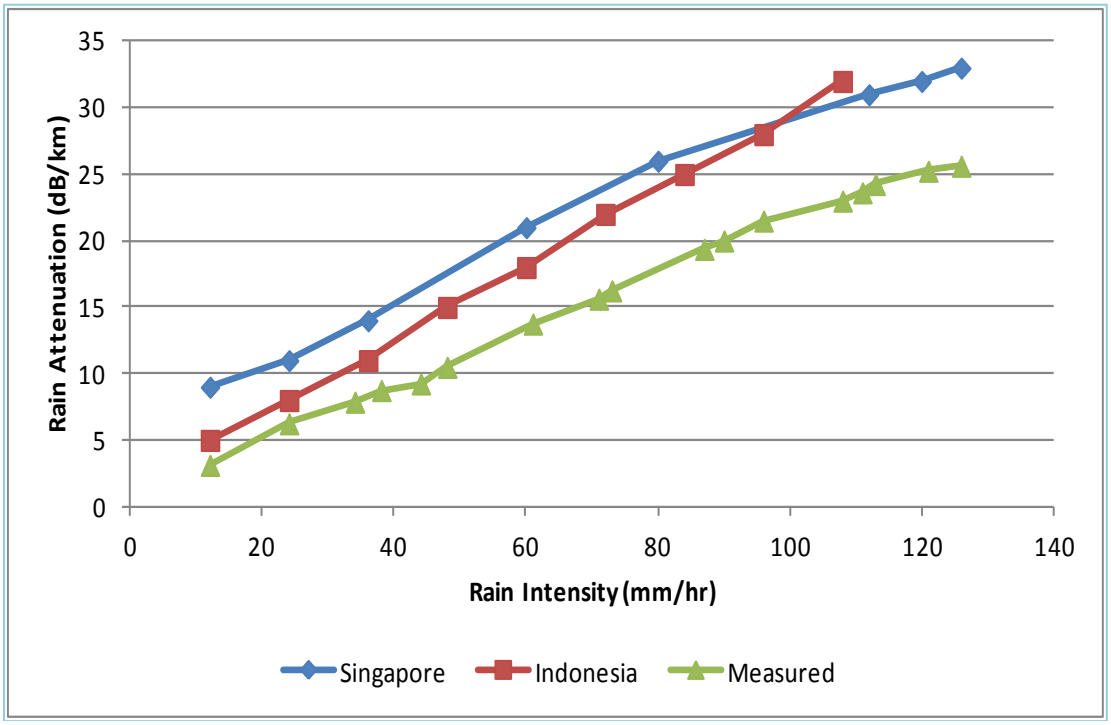

Figure 4.25. Comparison of measured specific rain attenuation with Singapore and Indonesia attempt measurement

Figure 4.26 shows the result of measured and other attempts of measuring the effect of rain on FSO link. Singapore's experiment is based on 3 months of rain attenuation measurement with rain intensity and then the measurement is scaled up to be assumed as one year data using rain data measured from the Singapore Meteorological Department. While for Indonesia the measurement of rain attenuation is collected for a period of 3 months and the link distances is 1.29 meters only. The calculation of the rain attenuation on the link is using a formula of loss and distance. Their measurement is only to analyze the effect of rain on FSO link. Therefore, the result is actually cannot be the benchmarking of our measured one-year rain intensity and rain attenuation.

Although in this section we proposed new specific rain attenuation with the introduction of new k and α value for FSO link attenuation propagating in tropical region, however, there is an unavoidable source of error. The unavoidable source of error comes from loss in the attenuation measurement due to the saturation of receiver sensitivity at the higher rain intensity. Another unavoidable source of error is in the equiprobability calculation due to the receiver saturation also. The equiprobability method might shift, and does not follow a true value of attenuation on the link. It is due to the fact that since the highest attenuation is not correctly capture.

4.12 SUMMARY

The focus of the discussion in this chapter is the predicted values of specific rain attenuation under tropical weather condition. Following the methodology of finding the k and α value, we propose new predicted value region specific rain parameters whereas available values are measured in temperate regions. An enhancement of k and σ is execute in order to have more accurate prediction values of specific rain attenuation,

From the enhancement analysis, a range of rain intensity with different values of k and α is developed to represent proposed and predicted specific rain attenuation of tropical regions. The new range of k and α seem to be a better prediction since the RMS calculated shows the lowest compare to other predicted and available model.

CHAPTER 5

OUTAGE (AVAILABILITY) PREDICTION AND LINK PERFORMANCE ANALYSIS

5.1 INTRODUCTION

One of the important performance parameters in communication is system availability. Definition of system availability is the percentage of time during which the link is operational. System availability is comprised of many factors, including equipment reliability and network design but these are well known and rather quantifiable.

Estimation of the link availability is done by calculating the link budget and determining the link margin for the allowable atmospheric attenuation and by using visibility data.

System availability is the probability that the system worked correctly at the time *t* under defined environmental conditions (EXFO, 2011). There is a statement, (Maxim, 2004) saying that the FSO community uses the term availability to describe the percentage of time that a customer could expect a link to operate in a particular location.

System availability is one of the most important parameters in communication. We can define it as the percentage of time during which the link is operational. In (Sharon, 2003), system availability is the probability that the system works correctly at time t under defined environmental condition. Other researcher in (OptiSystem, 2008), said that FSO community uses the term availability to describe the percentage of time that customers could expect a link to operate in a particular location. In the tropical weather region, rain and haze expected to affect the availability of FSO link.

This chapter will discuss on the availability of an FSO link during clear weather, rain and haze event. Besides that, this chapter also discuss on Bit Error Rate in term of theoretical and simulation analysis. This chapter also covers the experiment on the availability of an FSO link for long distance measurement.

5.2 AVAILABILITY CONSIDERING CLEAR WEATHER

The clear weather condition has been simulated using prediction simulation software for the two sites at International Islamic University Malaysia. From the simulation carry out, we generate the following results that we present in a few plots. The simulation result simulated by fixing the location and varying the link distance. From the simulation result, we plotted in Figure 5.1, FSO link geometrical loss by varying the link distance.

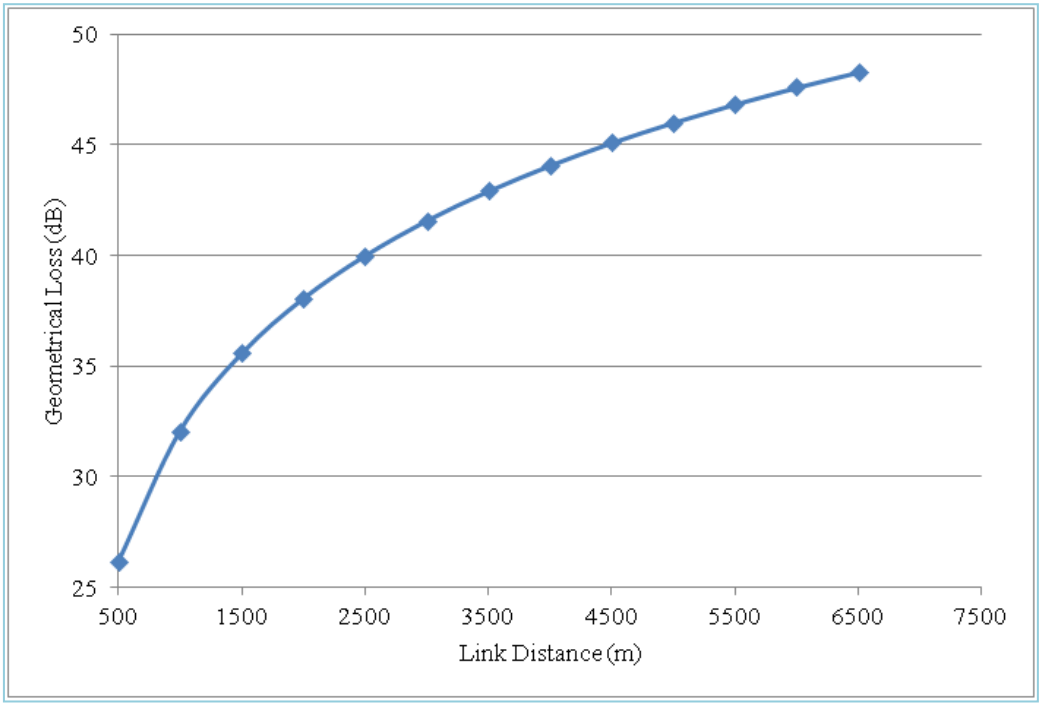

Figure 5.1. Geometrical loss of the link by varying the distance

Figure 5.1 shows that without considering any weather effect the link with -45 dBm sensitivity can go up to 4.5 km before the link is down. The longer the distance the greater geometrical loss will be.

In Figure 5.2 shows the available link margin by increasing FSO link distance.

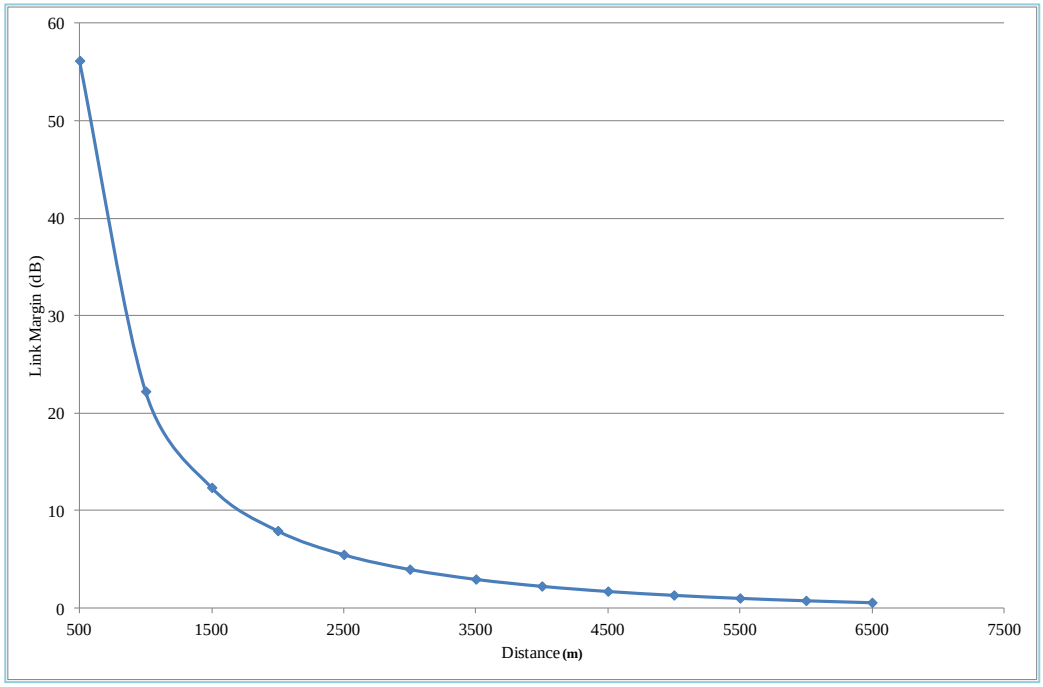

Figure 5.2. Link Margin by varying the distance

Figure 5.2 shows that for each increase of FSO link distance, link margin will decrease. The simulated result show that for the existing FSO link, the link is still working for a range up to 6.5 km in clear weather condition

5.3 AVAILABILITY CONSIDERING RAIN

In the tropical region, high rain intensity is the limiting factor of FSO link availability. The analysis of the availability during the tropical rain event will follow step list out in section 2.4 by (Chen, B.,2002). The analysis begins by finding the available link

margin. The formula to calculate the link margin is as in Equation (3.2) stated in Section 3.4.1. The complete calculation of the link margin with varying distance is in Appendix L. Table 5.1 is the summary table of the calculation result

Table 5.1
Link margin with varying link distance

Link Distance (km)	Link Margin (dB/km)
0.8	43.50
1.0	32.86
1.5	19.56
2.0	13.42
2.5	9.96
3.0	7.77
3.5	6.28
4.0	5.21
4.5	4.40
5.0	3.78
5.5	3.28
6.0	2.88
6.5	2.55
7.0	2.28

The knowledge of the available link margin is used to compare with the desired link availability under the influence of weather condition. First, the analysis is to determine rain attenuation over the link distance for the desired availability. Since for telecommunication operator, the link availability required is from 99.9% to 99.999% while the enterprise user is lower which 99.9% to 99.99% is, the following desired availability, rainfall rate the link must withstand and the rain attenuation for 0.8 km FSO link is presented in Table 5.2. The rainfall the link must withstand is based on the analysis performed in Chapter 4.

Table 5.2
Desired availability, rain rate and rain attenuation the link needs to withstand for 0.8 km link

Desired Availability %	Rainfall Rate Link must withstand mm/hr	Loss due t rain Attenuation (L_R) dB/km
99.995	117	25
99.99	103	21.875
99.95	62	14.275
99.9	48	10.5

Next steps in determining the availability of the link, rain attenuation for transmission of 0.8 km to 2.5 km need to be determined. This can be done by knowing the effective path length of the link by multiplying the reduction factor to the actual link. In Chapter 3, AbdulRahman reduction model is chosen as the model best represents tropical regions. From the analysis in Chapter 3, the following reduction factor values of the required path length using AbdulRahman model is illustrated in Table 5.3

Table 5.3
Reduction factor for transmission link from 0.8 km to 2.5 km

N/P	0.8km	1 km	1.5km	2 k	2.5km
$r_{0.005}$	0.900	0.878	0.827	0.782	0.741
$r_{0.01}$	0.897	0.872	0.823	0.777	0.736
$r_{0.05}$	0.900	0.863	0.807	0.758	0.715
$r_{0.1}$	0.881	0.856	0.799	0.748	0.704

From Table 5.3, overall attenuation due to rain on the FSO link can be determined by multiplying L_R with N and P. Table 5.4 illustrated the value of the overall attenuation due to rain.

Table 5.4
Overall attenuation due to rain on FSO link

Availability	Attenuation at various path length (km)				
%	0.8	1	1.5	2	2.5
99.995	17.993	21.940	31.013	39.096	46.343
99.99	15.701	19.069	27.009	34.003	40.268
99.95	10.274	12.313	17.282	21.650	25.521
99.9	7.404	8.989	12.578	15.715	18.481

From overall attenuation, another 2 dB loss is added due to scintillation. As mentioned in Section 2.4.3.8, if the FSO link is installed outside, 2 dB loss due to scintillation need to be added to the attenuation unless advised otherwise by the vendor. By adding 2 dB loss the overall attenuation will be as presented in Table 5.5

Table 5.5
Overall attenuation due to rain and in addition of 2 dB attenuation due to scintillation

Availability	Attenuation at various path length (km)				
%	0.8	1	1.5	2	2.5
99.995	19.993	23.940	33.013	41.096	48.343
99.99	17.701	21.069	29.009	36.003	42.268
99.95	12.274	14.313	19.282	23.650	27.521
99.9	9.404	10.989	14.578	17.715	20.481

With the result in Table 5.5 and Table 5.1, we can determine either the desired availability is achievable by plotting the link margin and the overall attenuation due to rain. The plot is as shown in Figure 5.3

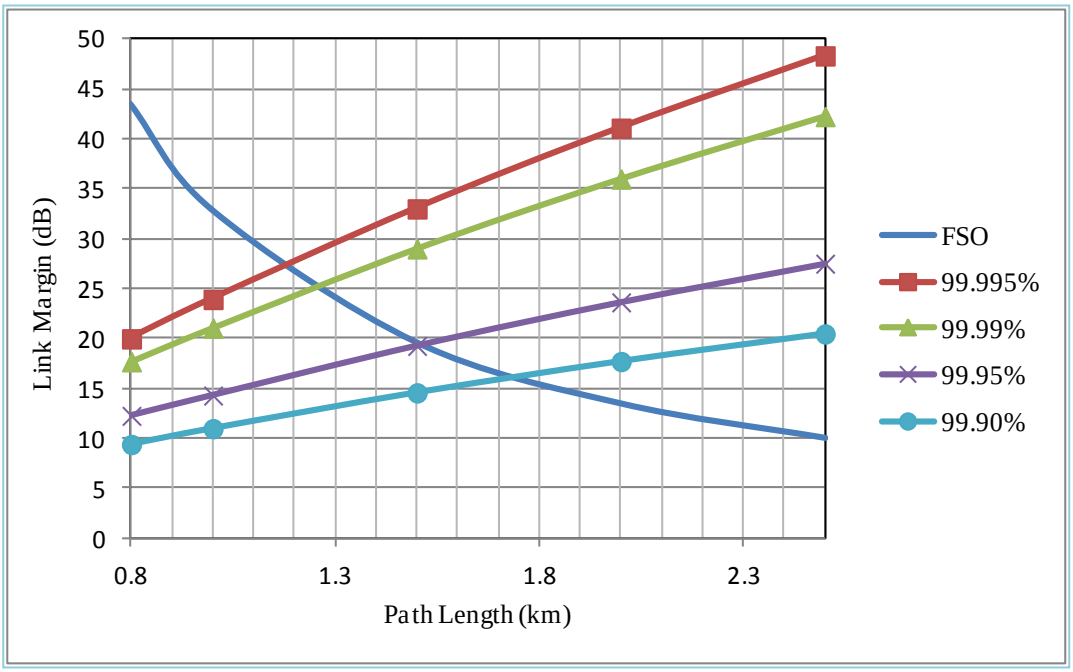

Figure 5.3. Link margin plot versus link availability with varying distance

In Figure 5.3 shows that the link margin curve of FSO intersects the 99.995%, 99.99%, 99.95% and 99.9% availability curves at approximately 1.18 km, 1.25 km, 1.5 km and 1.72 km respectively. These indicate that FSO can provide 99.995% availability or outage of 0.005% when deployed across 1.18 km distance and only 99.95% availability when the link is extended to 1.72 km. In other word, with rain intensity of 103 mm/hr, which is the availability of 99.99%, the link can only operate for 1.25 km link distance and the link only down for 52.54 minutes for the entire year. Although the link is quite short due to the nature of an FSO, which is weather dependent but still the availability of 99.99% is achievable.

5.4 AVAILABILITY CONSIDERING HAZE

Available visibility data are from the Meteorological department which is measured for certain location only especially at the airport. The setup of Visibility meter as

discussed in Chapter 3, section 3.4. The following sub-section will discuss on the data measurement of visibility data.

5.4.1 Measurement of Visibility Data

The measurement of visibility data is as discussed in Chapter 3, section 3.4. Throughout the measurement period, the data available is only for a few months due to the technical problem with the visibility meter itself. Sample data is as in Table 3.9 in Chapter 3, and Table 5.6 is the reproduce again of the data.

Table 5.6
Sample of visibility data logged on 28 Apr 2011

Date	Time	EXCO	Visibility (Km)
4/28/2011	0:00:00	0.239	12.52
4/28/2011	0:00:23	0.239	12.5
4/28/2011	0:00:30	0.239	12.51
4/28/2011	0:00:53	0.24	12.47
4/28/2011	0:01:00	0.242	12.38
4/28/2011	0:01:23	0.247	12.09
4/28/2011	0:01:30	0.249	12.03
4/28/2011	0:01:53	0.248	12.05
4/28/2011	0:02:00	0.247	12.12
4/28/2011	0:02:23	0.241	12.4
4/28/2011	0:02:30	0.24	12.46
4/28/2011	0:02:53	0.24	12.47
4/28/2011	0:03:00	0.241	12.43
4/28/2011	0:03:23	0.245	12.22
4/28/2011	0:03:30	0.247	12.13
4/28/2011	0:03:53	0.25	11.97

In (Kim et. al., 2000), it is stated that the haze occurred when the visibility reach more 1000 meters up to 6000 meters ($1 \text{ km} < V < 6 \text{ km}$), therefore in Table 5.6 the sample data shows no haze condition.

By analyzing available visibility data for February 2011 until May 2011, the condition of the data show the reduction of the visibility due to rain intensity and not hazes condition. A sample data is as shown in Table 5.7 and Table 7.8

Table 5.7
Sample of visibility and corresponding rain intensity logged on 15 February 2011

Time	Visibility (km)	Rain Intensity (mm/hr)
16:30:00	3.13	30
16:31:00	1.35	12
16:32:00	1.42	12
16:33:00	2.38	54
16:34:00	2.50	102
16:35:00	1.59	42
16:36:00	1.40	12
16:37:00	1.77	66
16:38:00	2.00	18
16:39:00	1.90	12
16:40:00	1.72	12
16:41:00	1.17	24
17:33:00	14.22	0
17:34:00	15.68	0
17:35:00	15.80	0
17:36:00	15.76	0
17:37:00	0.82	0
17:38:00	0.82	0
17:39:00	15.90	0
17:40:00	0.82	6
17:41:00	0.82	0
17:42:00	12.68	0
17:43:00	14.08	0
17:44:00	14.22	0

Table 5.8
Sample of visibility and corresponding rain intensity logged on 2 March 2011

Time	Visibility (km)	Rain Intensity (mm/hr)	Time	Visibility (km)	Rain Intensity (mm/hr)
6:47 PM	14.170	0	7:21 PM	1.538	24
6:48 PM	13.667	0	7:22 PM	1.140	12
6:49 PM	14.140	0	7:23 PM	1.058	6
6:50 PM	14.965	0	7:24 PM	1.404	0
			7:25 PM	1.794	6
6:56 PM	9.561	24	7:26 PM	2.260	6
6:57 PM	3.303	42	7:27 PM	2.481	6
6:58 PM	1.263	24	7:28 PM	2.469	6
6:59 PM	0.891	24	7:29 PM	2.115	18
7:00 PM	0.775	36	7:30 PM	1.771	12
7:01 PM	0.579	78			
7:02 PM	0.298	66	7:37 PM	12.047	0
7:03 PM	0.208	54	7:38 PM	13.440	6
7:04 PM	0.210	36	7:39 PM	15.427	0
7:05 PM	0.219	48	7:40 PM	13.640	0
7:06 PM	0.250	60	7:41 PM	11.337	0
7:07 PM	0.272	48	7:42 PM	9.128	0
7:08 PM	0.280	42	7:43 PM	6.419	6
7:09 PM	0.309	54	7:44 PM	3.916	6
7:10 PM	0.344	18	7:45 PM	3.613	6
7:11 PM	0.465	18	7:46 PM	4.044	0
7:12 PM	0.692	18	7:47 PM	4.824	6
7:13 PM	0.829	6	7:48 PM	6.264	0
7:14 PM	1.150	6	7:49 PM	6.261	6
7:15 PM	1.490	6	7:50 PM	5.678	0
7:16 PM	1.918	6	7:51 PM	6.983	0
7:17 PM	2.339	24	7:52 PM	9.740	6
7:18 PM	1.870	30	7:53 PM	11.850	0
7:20 PM	1.634	42	7:54 PM	12.680	0
7:21 PM	1.538	24	7:55 PM	12.703	0

Table 5.7 and Table 5.8 show that the visibility reduced during the rain events. During the non-rain event, the visibility is at its highest value. Due to this result, a conclusion is that the measured visibility cannot represent the presence of haze in the area since the reduction of visibility is not due to the haze but due to the rain. To consider the

availability of the link is by taking into account the haze effect using the available data, the average visibility during the non rainy day is calculated. According to (Kim et al., 2000), the haze is considered to have visibility of 1000 m to 6000 m, therefore, the average visibility of non hazy time is calculated for four months (February 2011 to May 2011). The calculation of the average visibility is 13.412 km. Using the average visibility and multiplying with the link distance, the following Figure 5.4 is plotted.

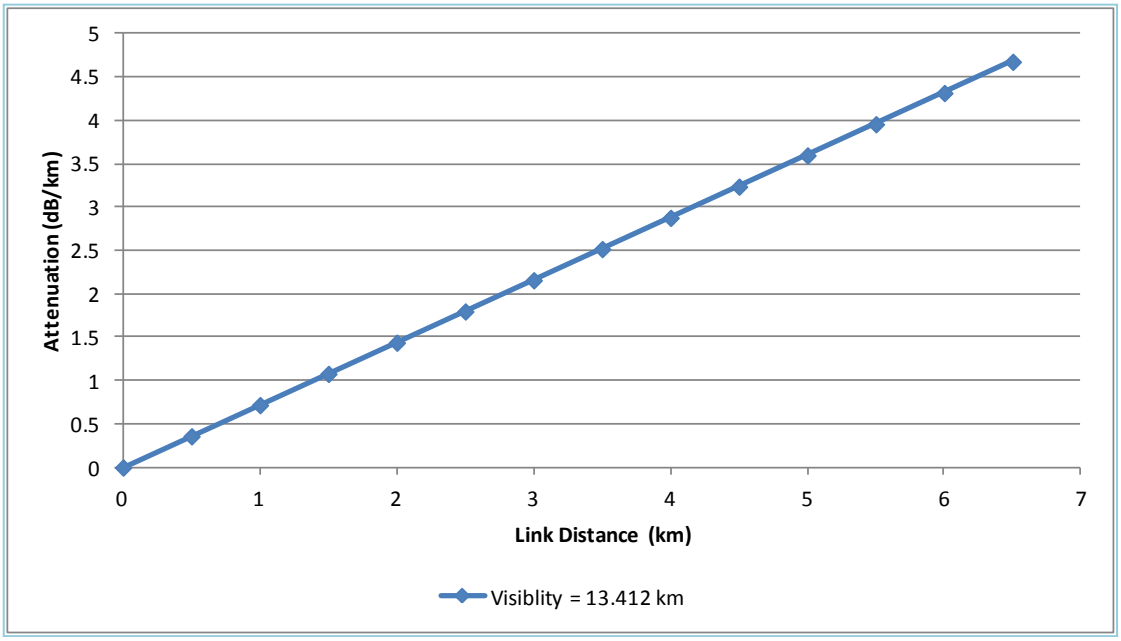

Figure 5.4. The attenuation of fixing the average visibility and varying with link distance

From the plot we can deduce the attenuation for different link distance to be included in the availability calculation. Table 5.9 shows the attenuations associate with the link margin.

Table 5.9 represents a very low attenuation of the haze effect on the link. The attenuation will be used to calculate the availability considering haze and rain.

Table 5.9
Haze attenuation considering different path length

Link Distance (km)	0.8	1	1.5	2	2.5
Attenuation (dB)	0.57545	0.71931	1.07897	1.43862	1.79828

5.4.2 Availability Considering Haze and Rain

In section 5.2, we calculate the outage or availability considering haze. From the calculation, in this section the availability is considering the rain and haze. The haze data are as presented in Table 5.9. We add the haze attenuation to the values in Table 5.5 and Table 5.10 is the illustrated of the new value after the addition.

Table 5.10
Overall attenuation due to rain, scintillation and haze

Availability	**Attenuation at various path length (km)**				
%	**0.8**	**1**	**1.5**	**2**	**2.5**
99.995	20.568	24.660	34.092	42.535	50.142
99.99	18.276	21.788	30.088	37.442	44.066
99.95	12.849	15.032	20.361	25.089	29.319
99.90	9.979	11.708	15.657	19.154	22.280

From Table 5.10, Figure 5.2 shows the plot of the link margin and overall attenuation considering the rain and haze.

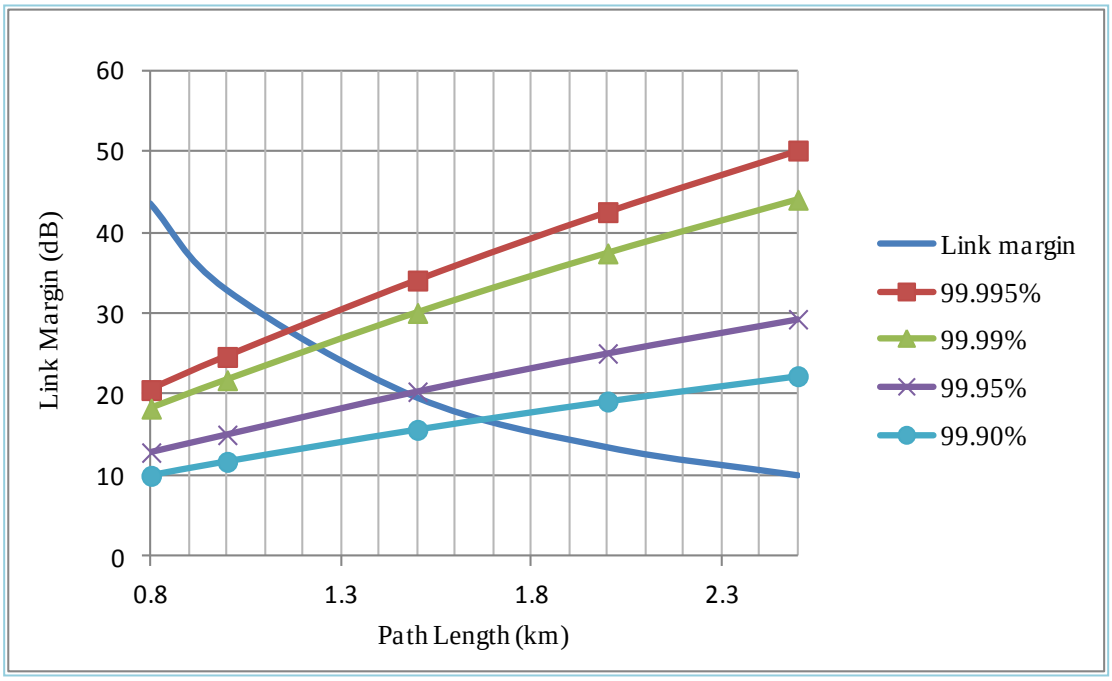

Figure 5.5. Link margin plot versus link availability with varying distance

By adding the haze attenuation to the availability calculation, the following result can be deduced. Since the maximum attenuation added is about 2 dB, therefore the link availability curves does not have a huge effect on it. The link margin curve of FSO intersect with the 99.995%, 99.99%, 99.95% and 99.9% availability curves at approximately 1.15km, 1.22km, 1.46km and 1.68km respectively. The result showing that the effect of haze is very small to the FSO link and can be concluded that there exit no haze event during the measurement period.

After the outage prediction analysis, another section will discuss on the FSO link performance and long distance measurement.

Parameter to measure the performance of a data link is the bit error rate (BER). Unlike any other form of assessment, BER assesses the full end-to-end performance of a system including transmitter, receiver and the medium between the two. BER enables the actual performance of a system in operation to be tested, rather than testing

the component parts and hoping that they will operate satisfactorily when in place. There are two sections in this in this chapter. One section will discuss on performance analyses that focus on signal quality analysis and another section is on field test for long distance FSO link measurement and analysis.

5.5 BIT ERROR RATE MEASUREMENT

Specification and setup of the BER experiment as discussed in Chapter 3, section 3.6. By covering the receiver as mentioned in chapter 4, the BER is measured. With all the procedure and equipment that we have, we are unable to get the result that we need as for the EXFO BER tester, it is designed to test BER for 2 layers which are Ethernet/IPv4/UDP and Ethernet (Kolka et al., 2007). Ethernet/IPv4/UDP is level 4-communication level and Ethernet are level 2-communication level. The BER that we are testing is in the physical layer, which is level 1. With all the attempts that we have tried either on the building site or on field site, we are unable to get the intended result of bit error rate. It might due to the BER tester used is not intended to measure the physical layer bit error rate. Since no experimental measurement is successfully done, the discussion on the BER will be done theory, calculation and simulation.

BER value by it selves does not represent any time. It is only a ratio of numbers of bits sends and receives. A specific BER when related to time can yield a mean time between failures (MTBF) for a digital serial link. This relationship is as presented below

$$\text{MTBF (hours)} = \frac{1}{BER \times bits\ per hour} \tag{5.1}$$

For our FSO equipment, operate at bit rates of 155 Mbits/sec to 1.25Gbits/sec (given by the manufacturer). An operating BER of 10^{-10} for 1.25Gbps data stream would have an MTBF of 0.02 hours. The result is equivalent to detecting an average

of one-bit in error for every 0.02 hours of operation. The same link, at the same BER but operating at 155Mbps would detect an average of one bit in error for every 0.18 hours.

In optical and high-speed communication system, we uses eye diagram for analysis of the system. Eye diagram serves as an additional testing procedure, to analyze the system behaviour. It is accomplished by giving the opportunity to know how much the timing margin is available at the receiver or how much noise the signal can tolerate before there is a significant increase in BER.

One parameter in eye diagram is the measurement of Q-factor. In optical communication, the error rate depends on signal to noise ratio determined by Q-factor (Bloom, 2002).

Q factor is a parameter that directly reflects the Quality of a digital optical communication signal. The higher the value of Q-factor, the quality of the optical signal is better.

5.5.1 Analysis of FSO Signal

The analysis of FSO signal is using OptiSystem Software (Capsoni et al., 2009). The layout design of FSO systems in OptiSystem is as shown in Figure 5.6. Execution of the program for clear weather condition with full specification of our FSO system produce the eye diagram as in Figure 5.7.

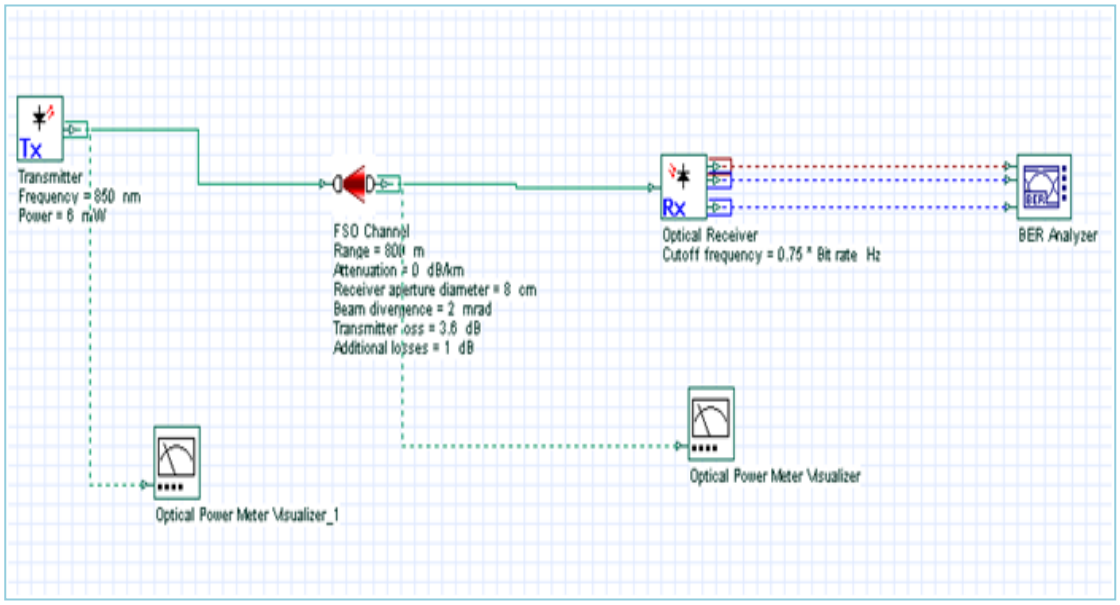

Figure 5.6. Layout of FSO system in OptiSystem

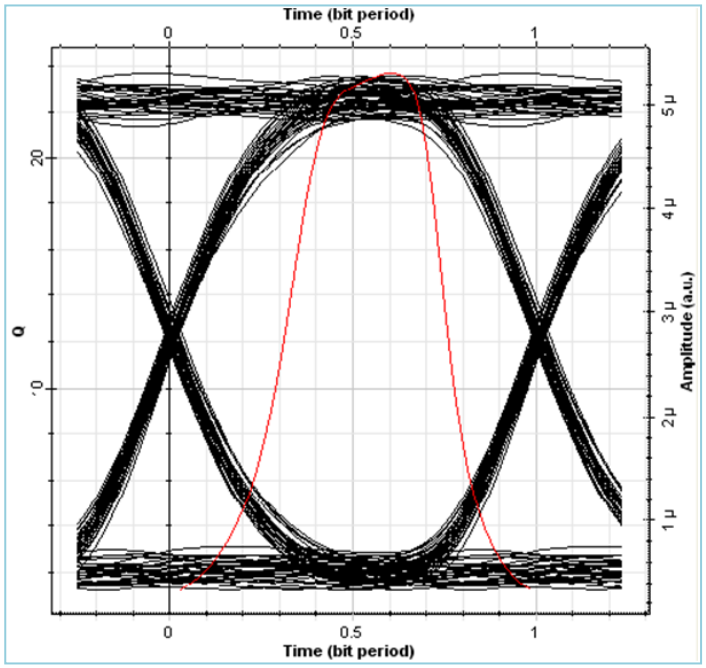

Figure 5.7. Clear weather condition

Plot in Figure 5.7, gives a Q factor of 23 and minimum BER of 10^{-124}, which just indicate that under clear weather condition, for a link of 0.8 km, the FSO signal, work in perfect condition.

The relationship of BER and Q factor is analyzed by varying the input power. Figure 5.8 show two samples of eye diagram for 1 dBm input power and 10 dBm input power. The relationship between BER and Q factor is established as presented in Figure 5.9.

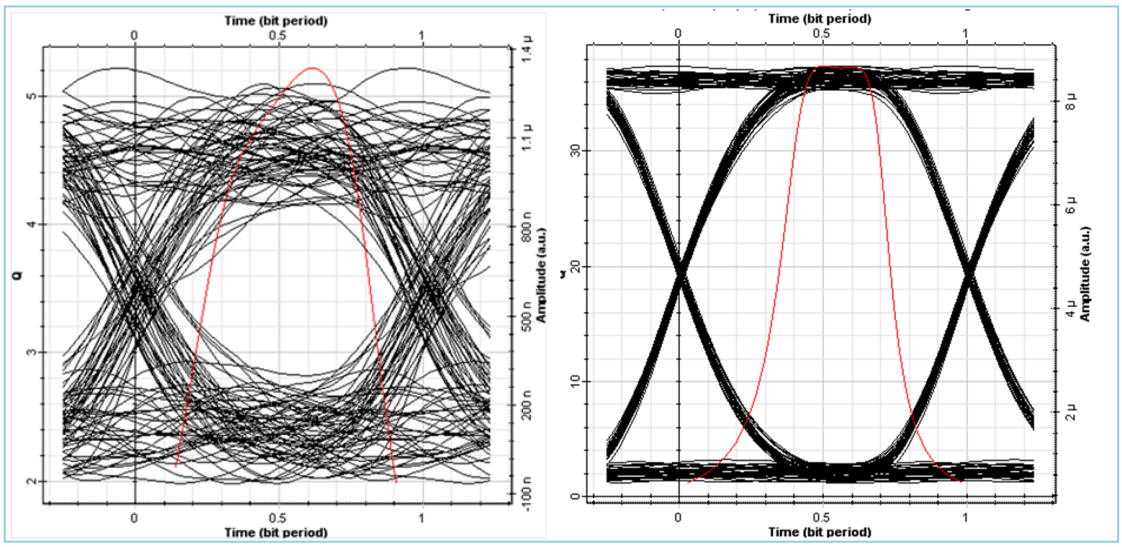

(a) (b)

Figure 5.8. (a) 1 dBm input power (b) 10 dBm input power

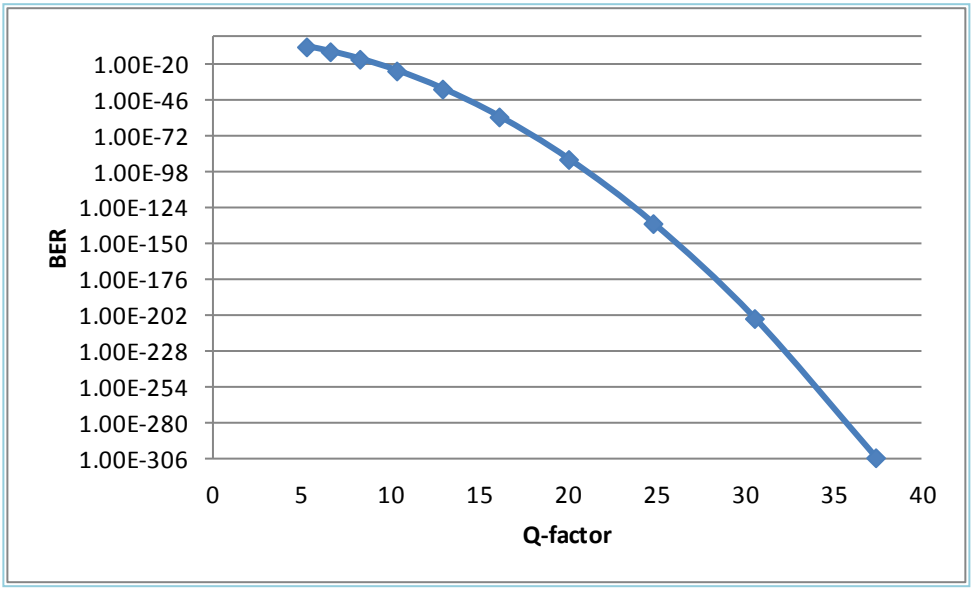

Figure 5.9. BER versus Q-factor for 0.8 km link distance

The plot shows, at 800m FSO link distance and by varying the input power, 2 dBm power requires to achieve an acceptable level of BER around 10^{-10} (given by the manufacturer), with Q-factor of 6. As in the equipment, the input power is around 7 dbm, the Q-factor is about 20, which mean the transmission signal is very good. The effect of rain on the FSO link is analyzed with Q factor analysis as shown in Figure 5.10.

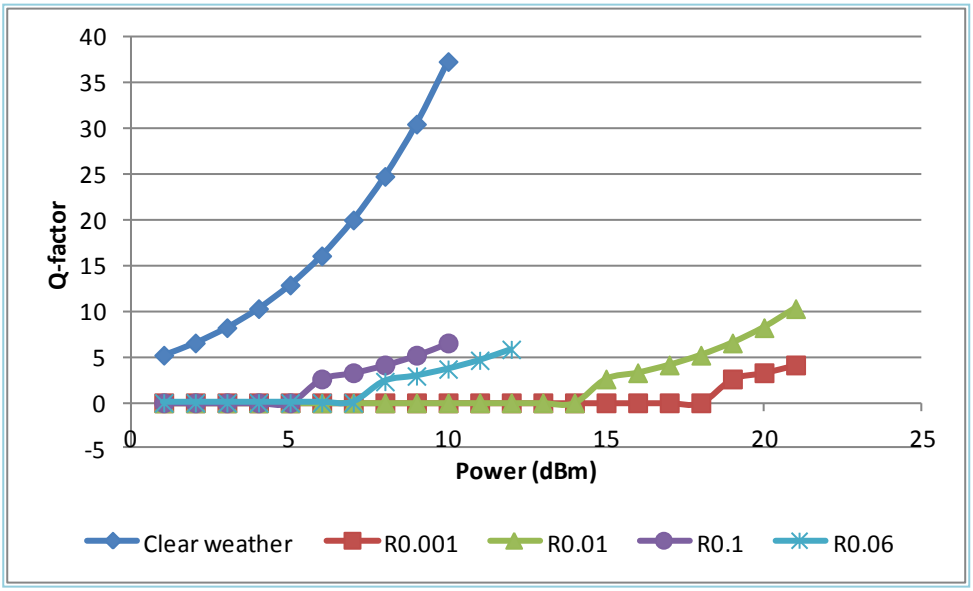

Figure 5.10. Q-factor during clear weather condition and rain attenuation

For clear weather condition at 800 m link, as the input power increase the quality of the signal is better. When we include the attenuation on the link, for rain $R_{0.001}$, with 26.25 dB/km rain attenuation, the signal needs at least 19dBm to operate. $R_{0.01}$ needs 15 dBm to operate on the link of 800m. The input power increases with the increase of the attenuation to establish a good signal during rain event even for a very short distance (800 m)

Rain effect on the link is investigated in term of BER and represented by an eye diagram as in Figure 5.11.

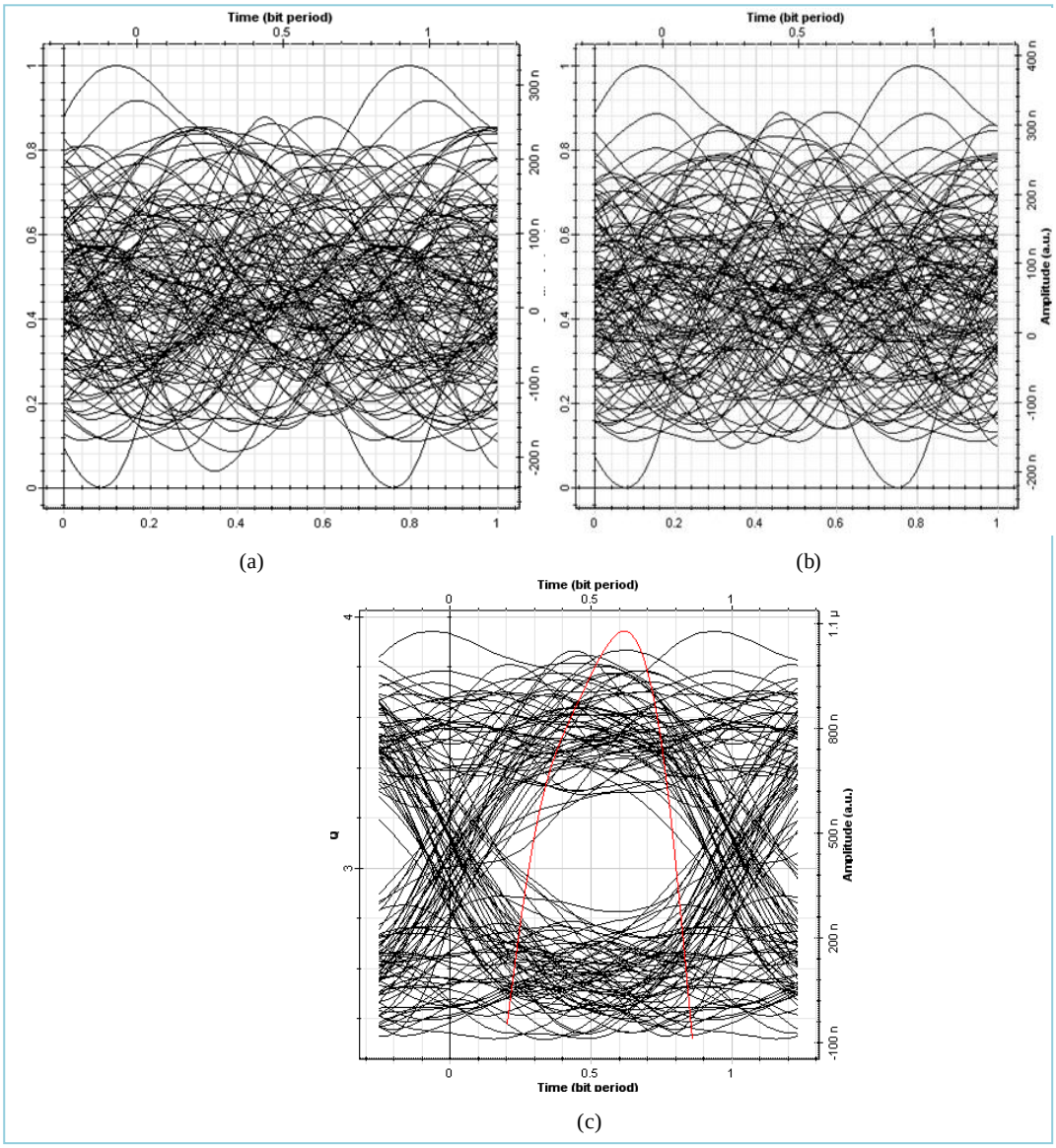

Figure 5.11. Eye diagram of (a) $R_{0.001}$ with 26.25 dB/km attenuation (b) $R_{0.01}$ with 21.25 dB/km attenuation (c) $R_{0.1}$ with 10 dB/km attenuation

Eye diagram showing that during a rain event, the signal is only good at $R_{0.1}$. For $R0_{.001}$ and $R_{0.01}$, the diagram shows there is no opening in the eye of the eye diagram, which indicates the distortion of the signal significantly.

Figure 5.12 shows the simulated result of BER and the rain attenuation effect on the FSO link.

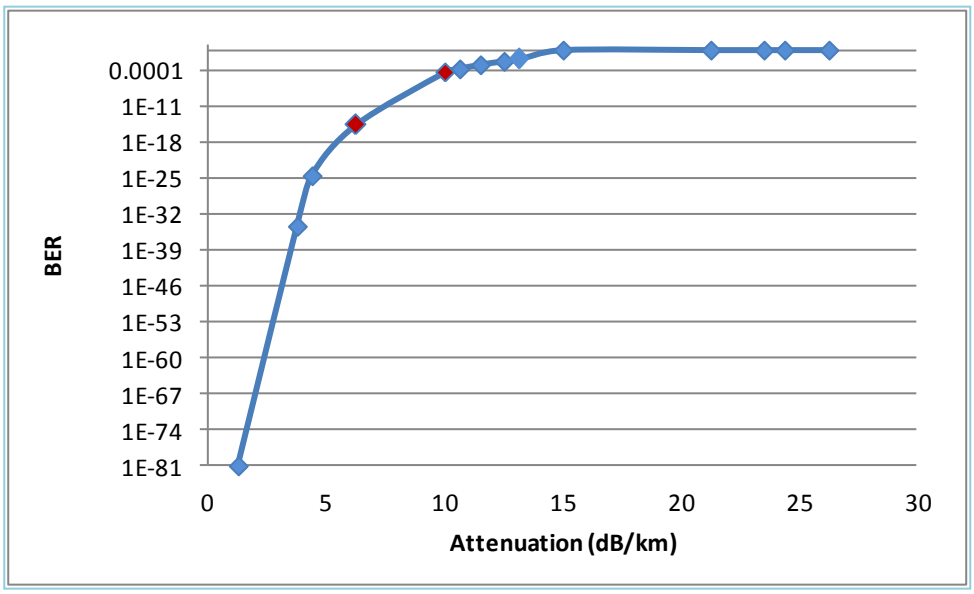

Figure 5.12. BER and rain attenuation effect on the link

Plot of BER versus measured rain attenuation show that, to have an acceptable level of BER (10^{-10}), rainfall is between $R_{0.1}$ and $R_{0.2}$ or between 99.9% and 99.8% availability is achievable (as highlighted difference between the two points). The tolerate attenuation at this availability is between 6.25 - 10 dB/km. Rain intensity is between 30 - 50 mm/hr.

Analysis of signal quality during rain events, sample in term of eye diagram is as illustrated in Figure 5.13 for $R_{0.001}$, $R_{0.06}$, $R_{0.07}$ and $R_{0.1}$.

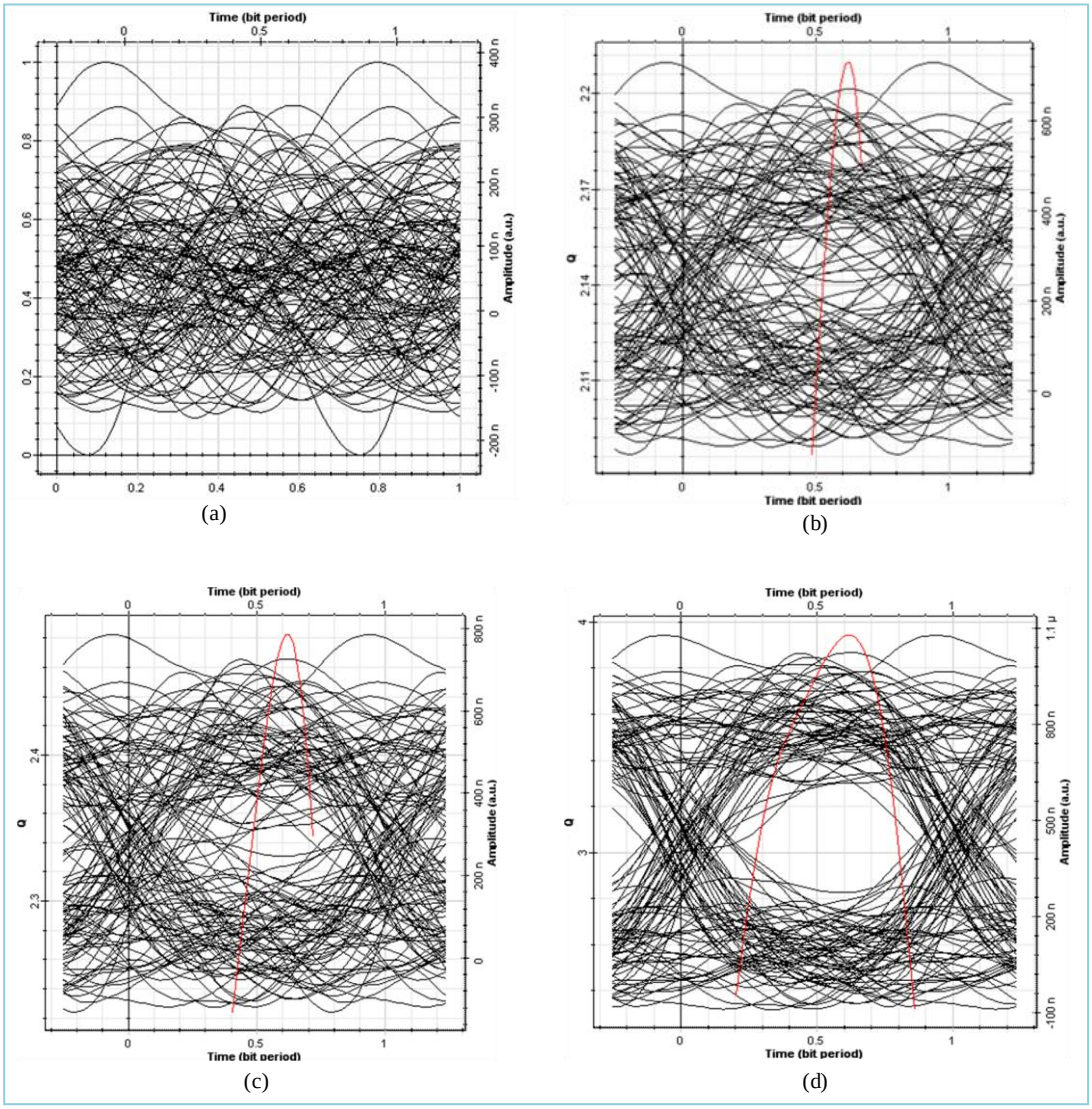

Figure 5.13. Eye diagram of attenuation effect for different intensity as (a) $R_{0.001}$ (b) $R_{0.06}$ (c) $R_{0.07}$ (d)$R_{0.1}$

Plot of Q-factor and rain attenuation based on simulation done as the result shown in Figure 8.8 is as presented in Figure 5.14

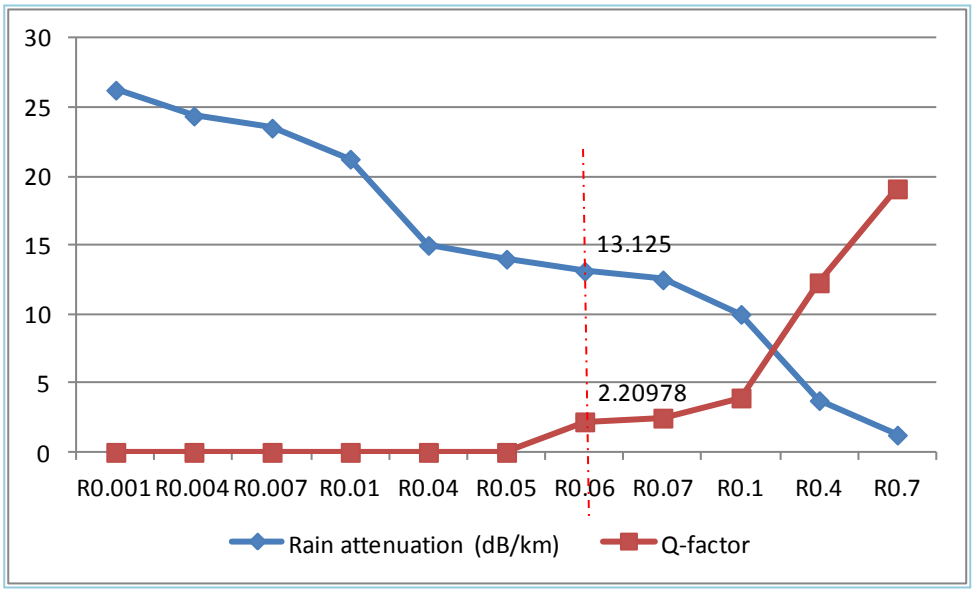

Figure 5.14. Q-factor and different rain attenuation effect

From the plot showing that, the signal is affected badly by rain attenuation of 26.25 dB/km for 800m link and rain $R_{0.001}$. The rain attenuation affects the FSO link and cannot reach even 0.01% or 99.99% availability when under rain attenuation effect. The highest availability can be reached is 99.94% link availability for 800m link.

Figure 5.15 shows a sample analysis result of Q-factor by varying the link distance for a different weather conditions.

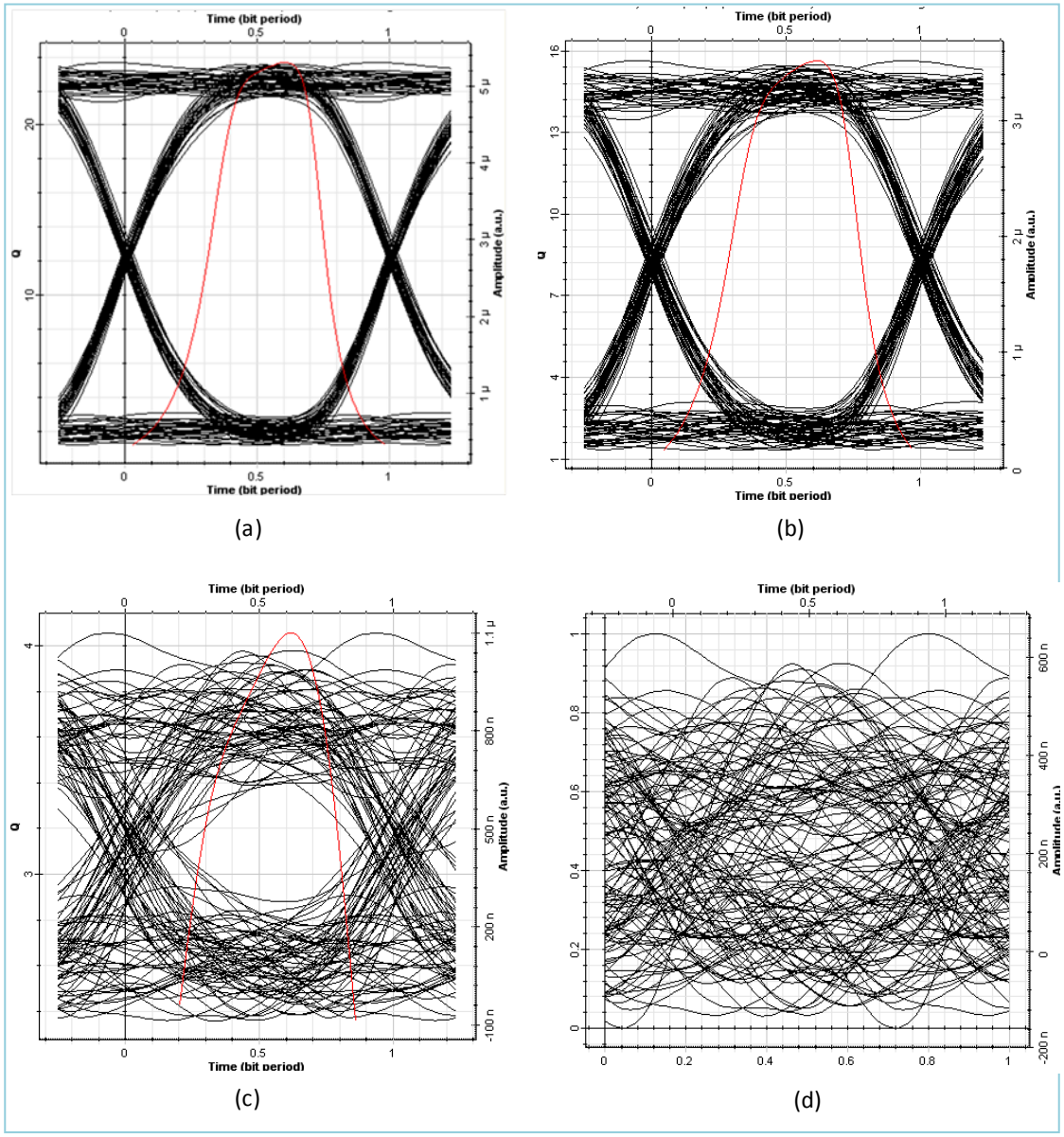

Figure 5.15. Eye diagram of Q-factor with varying distances (a) 800 m (b) 1000 m (c) 2000 m (d) 3000 m

From the simulation of eye diagram, a plot of Q-factor and link distance is a shown in Figure 5.16

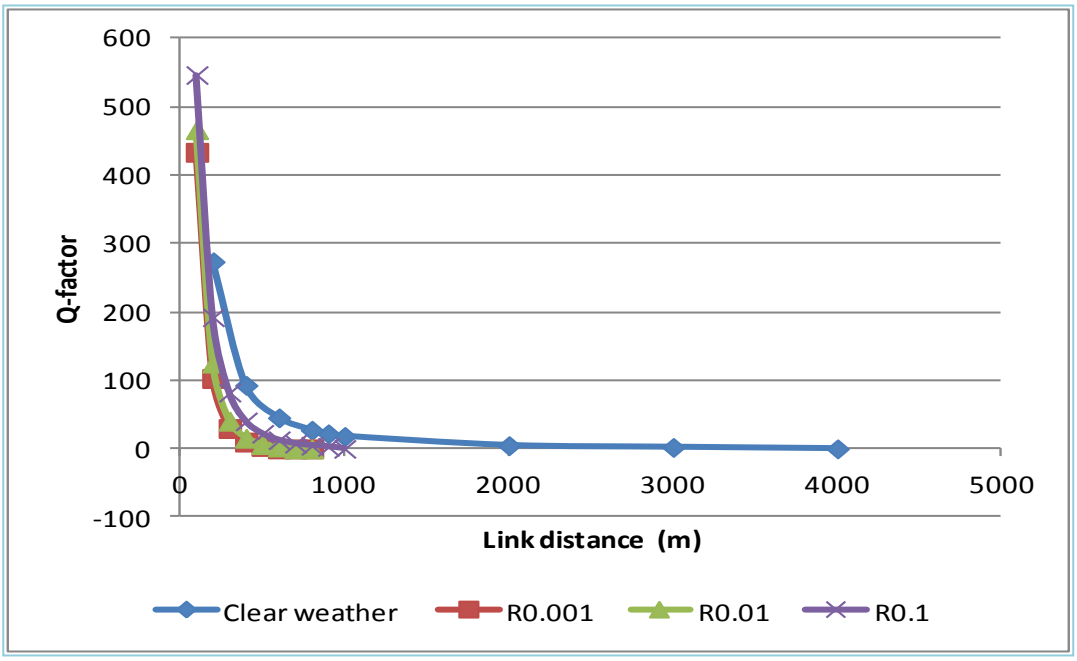

Figure 5.16. Q-factor analysis by varying link distance for different weather conditions

Figure 5.16 representing the comparison of Q-factor in varied link distance for clear weather condition and raining conditions. For clear weather condition, the signal of an FSO link still available up to 4 km. During raining event, however, the signal available for a less than 1 km link distance. To have a clear view on how far the link can actually go for rain event, Figure 5.16 is scaled up for the rain event only and the plot is as presented in Figure 5.17. By scaling up only for a rain event for the analysis of Q-factor and varying link distance; it is clearly shown that for $R_{0.001}$ FSO signal is only available up to 500m, for $R_{0.01}$ FSO signal is available for 600m link distance and for $R_{0.1}$ the signal available up until 900m link distance. Therefore, for 800m link only R0.1 link availability (99.9%) is achievable.

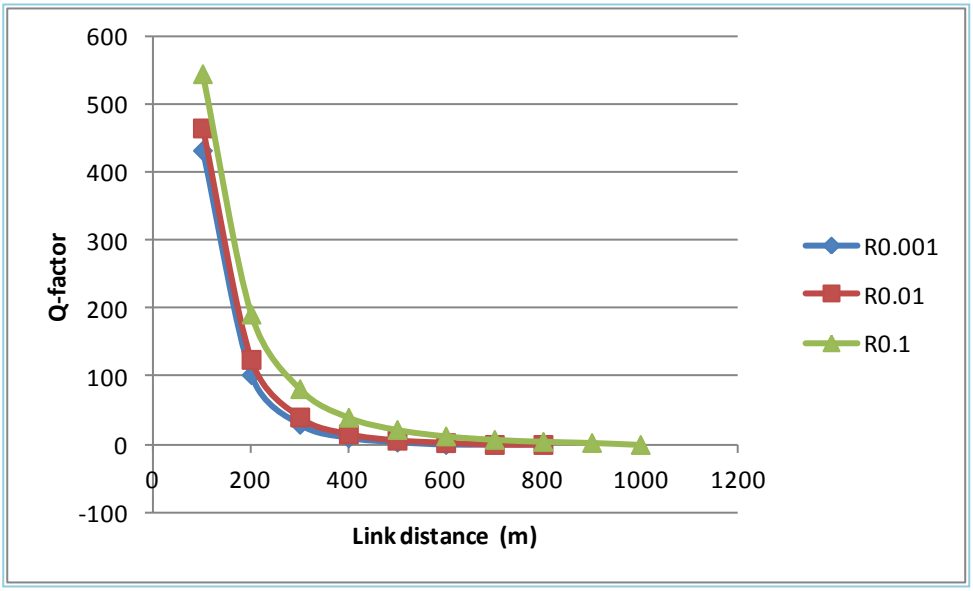

Figure 5.17. Scale up of rain event only for Q-factor analysis

A performance and quality signal of the FSO transmission link under the influence of local weather analyzed and discussed. The discussion and analysis are in term of BER, eye diagram and Q-factor.

In the following sub-section, the discussion is on the performance of the long distance FSO link. Another factor that limits the availability of FSO signal propagation is link distance. The measurement of the availability of the link can be conducting by deployment of a long distance of FSO system. The following sub-section is focused on the discussion of long distance FSO deployment.

5.6 LONG DISTANCE FSO DEPLOYMENT

Factors that affect the received power signal at the receiver which determines the availability of the link depends on several conditions like deployment distance, atmospheric loss, scintillation, pointing loss, geometrical loss, equipment loss and

rainfall,. The longer the link distance also will make the atmospheric effect worsen and the link availability is degraded.

This section will discuss the experiment made for long distance FSO link with our available equipment by taking into consideration of the loss that affects the link. . The experiment conducted for 3 km link range and 6 km link range.

FSO equipment specification needed in the calculation as shown in Table 5.11:

Table 5.11
FSO equipment specifications

Diameter receiver (m)	Diameter transmitter (m)	Beam divergence (mrad)	Sensitivity (dBm)	Power transmit (dBm)
0.08	0.025	2	-45	7.7815

5.6.1 Equations

Equation (5.2), (5.3) and (5.4) are equation used to calculate respective parameters.

Geometrical loss can be expressed as follows :

$$Geometric\ loss,\ P_{geo}\ (dB) = \frac{d_r}{d_t + (\theta L)} \qquad (5.2)$$

Where

d_r = Receive aperture diameter (m)

d_t = Transmit aperture diameter (m)

θ = Beam divergence (mrad)

L = Distance between transceiver (km)

In , power received can be calculated as follows

$$Power\ received\ , P_{rec}\ (dBm) = P_t - Loss_T \qquad (5.3)$$

Where

P_t = Power transmits (dBm)

$Loss_T$ = Total losses

$Loss_T$, total losses are geometric loss and all the losses. For our application, a total loss does not include atmospheric loss (Mie scattering) since the experiment performs under clear weather condition which no present of haze. We also do not consider rain attenuation on the link since there is no rainfall on the experiment day. Therefore, presentation of total loss as shown in Equation (5.4)

$$\text{Total Loss, } Loss_T = Loss_{scin} + Loss_{point} + Loss_{Equip} \qquad (5.4)$$

Where

$Loss_{scin}$ = scintillation loss

$Loss_{point}$ = pointing loss

$Loss_{Equip}$ = equipment loss

Since no measurement carries out for scintillation and pointing loss, we took standard data that widely use in the simulated calculation. In , scintillation loss is taken to be 2dB for FSO equipment installed outdoors. In , pointing loss is 1 dB.

Equipment loss given by the manufacturer is 3.6dB. In summary the data needed in the calculation are as presented in Table 5.12,

Table 5.12
Losses data for simulated calculation

Item	Values
Equipment loss	3.6 dB
Pointing loss	1 dB
Scintillation	2 dB
Total loss	**6.6 dB**

5.7 LONG DISTANCE FSO DEPLOYMENT: RESULT AND ANALYSIS

Using Equation (5.2), (5.3) and (5.4), we calculate power received. The power received signal (dBm) calculated using Equation (5.3). The result of calculation is as tabulated in Table 5.13.

Table 5.13
Power received calculation

d_r m	d_t m	Beam div mrad	Range km	P_{geo} dB	Sensitivity dBm	P_t dBm	$Loss_T$ dB	Power recv dBm
0.08	0.025	2	0.5	22.1527	-45	7.781513	6.6	-20.97116
0.08	0.025	2	1	28.0667	-45	7.781513	6.6	-26.88519
0.08	0.025	2	1.5	31.5527	-45	7.781513	6.6	-30.37119
0.08	0.025	2	2	34.0335	-45	7.781513	6.6	-32.852
0.08	0.025	2	2.5	35.9609	-45	7.781513	6.6	-34.77941
0.08	0.025	2	3	37.5373	-45	7.781513	6.6	-36.35583
0.08	0.025	2	3.5	38.8711	-45	7.781513	6.6	-37.68961
0.08	0.025	2	4	40.0271	-45	7.781513	6.6	-38.84559
0.08	0.025	2	4.5	41.0471	-45	7.781513	6.6	-39.86563
0.08	0.025	2	5	41.9599	-45	7.781513	6.6	-40.77837
0.08	0.025	2	5.5	42.7858	-45	7.781513	6.6	-41.60426
0.08	0.025	2	6	43.5399	-45	7.781513	6.6	-42.35839
0.08	0.025	2	6.5	44.2338	-45	7.781513	6.6	-43.05224
0.08	0.025	2	7	44.8763	-45	7.781513	6.6	-43.69474
0.08	0.025	2	7.5	45.4745	-45	7.781513	6.6	-44.29298

From the calculation of power received as in Table 5.13, we plot it as shown in Figure 5.18. The power received calculated by varying FSO link distance. The experiment performed under clear weather condition for 3 km and 6 km link range. The power received level for 3 km test and 6 km test result is as tabulated in Table 5.14.

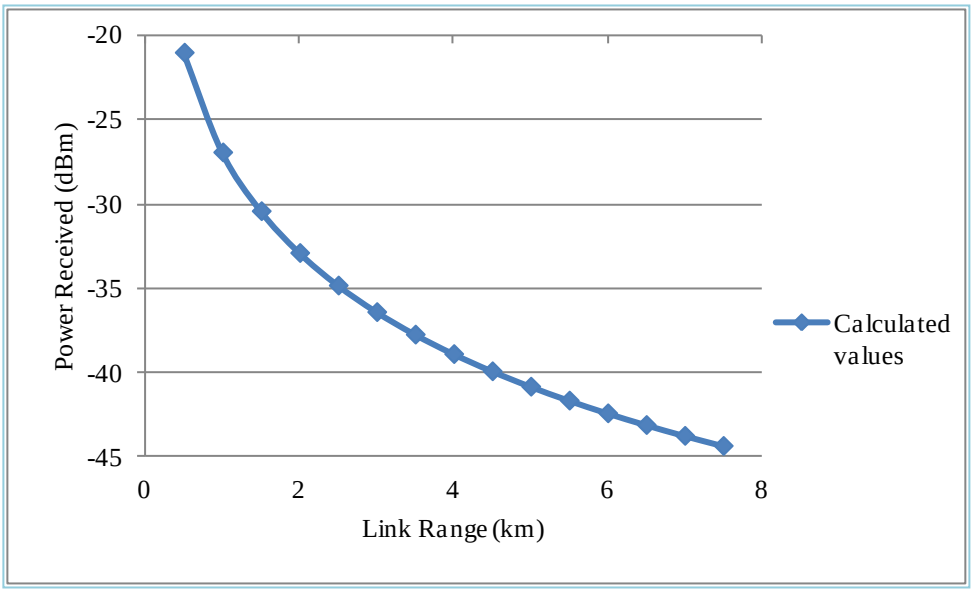

Figure 5.18. Calculated result of power received level (dBm) by varying the link distance

Table 5.14
Measured values for 3 km and 6 km test

Link Range (km)	Power Received (dBm)
3	-36.6
6	-42.9

Figure 5.19 showing the calculated and measured values of the 3 km and 6 km test result. The calculation to determine the availability of a long link range FSO by considering all the parameters that affect power received at the receiver considering clear weather condition. Atmospheric attenuation and rain attenuation will have more effect on the deployment of long distance FSO link. Besides that for long distance FSO link deployment, scintillation and building sway, which cause the pointing loss, also affected the link. Long distance FSO under local weather condition which is clear

weather on the day of the test, showing that the test result strongly agree with the calculated result.

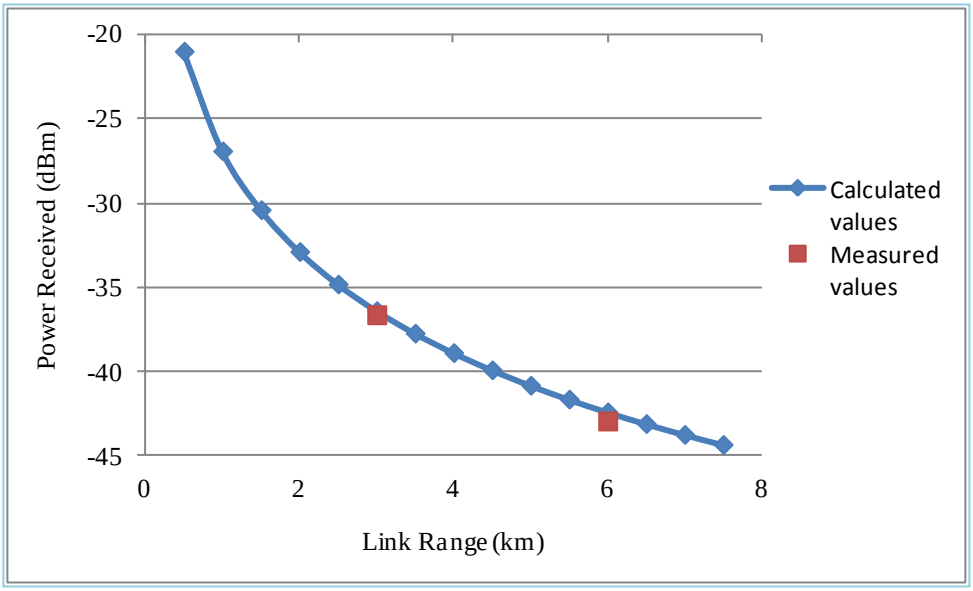

Figure 5.19. Measured and simulated power received level for 3 km and 6 km test

5.8 SUMMARY

Outage prediction and link availability are two parameters to consider when we talk about communication link. This chapter analyzes the framework of outage and availability of an FSO link under tropical weather condition. Analysis and prediction of the link during rain and haze is one of the research objectives. The result shows that in tropical regions, rain intensity plays a major role in the unavailability of an FSO link compare to haze.

This chapter discuss on the result and analysis FSO link performance in term of BER, eye diagram and Q-factor. The analysis showing that rain attenuation is one of the major effects on the establishment and availability of an FSO link in tropical region.

Besides that, the performance and availability of an FSO link also affected by link distance and this proves by field test. we conducted two field tests to measure the performance of an FSO link under tropical clear weather condition. The result shows that for the available FSO the link is available up to about 6 km under clear weather condition.

Next chapter is the last chapter that focus on conclusion of the work and future recommendations.

CHAPTER 6

CONCLUSION & FUTURE WORK

6.1 CONCLUSION

Free Space Optics (FSO) is a promising communication link in the era where higher speed and broader broadband is crucial. Local weather effect, however, is the limiting factor in the accomplishment of FSO link propagation. Since high rain intensity falls almost throughout the year in tropical region, rain is expected be one of the limiting factors. Therefore, the main objective of this research is to predict and propose new specific rain attenuation parameters propagate in tropical region. The motivation of this study is due to the unavailability of specific rain attenuation parameters based on measured data in tropical region. The available and standard use of rain attenuation analysis is based on data measured in temperate regions and mostly is based on a calculation of drop size distribution measurement and not a direct correlation of real data measurement of rain intensity and rain attenuation. The outcome of this main objective is a new value for k and α that, best represent tropical weather climates as discussed in detail in Chapter 4. From the result, we come up with four ranges of rain intensity with difference values of k and α to represent a prediction model. The four ranges of k and α after analyzing give better prediction result which provides the lowest RMS value compare to single k and α and ITU-R; as presented in Table 6.1

In order to have the accurate prediction model, we need to analyze the effective length of the rainfalls on the FSO propagation link. Since there is no formula in FSO to examine rain intensity variation, we perform the mathematical analysis using the available equation in Microwave communication. From the literature review, we

select Abdulrahman Model as the best model that represent reduction factor for a tropical region. The finding of the study, as discussed in Chapter 3, showed that the rain falls uniformly in the link distance less than 1 km. Whereas our FSO link distance under investigation is 0.8 km, meaning that the assumption of rain falls uniformly on the link is valid.

Table 6.1
RMS comparison of predicted and available specific rain attenuation model

	RMS
Ranges of k and α	5.84
Single k and α	9.66
Carbonneau	14.72
Japan	22.95

Another objective of this research is to predict outage or availability of an FSO link under tropical weather condition. The focus of this analysis is on link availability during the presence of rain and haze. The main analysis however is on the availability during rain due to technical problem encounter with visibility data measurement. The analysis shows that in tropical region, rain attenuation is the major effect on FSO link availability, which we discuss in detail in Chapter 5. The result shows that the link availability of 99.995% is achievable but the link distance is only 1.18 km, while for 99.99% availability the link distance is 1.25 km.

FSO link performance and long distance analysis in tropical region is another objective under investigation in this research. This led the study of the performance of FSO signal in term of BER, eye diagram and Q-factor as analyzed in Chapter 5. The analysis showed that, rain is the main limiting factor in tropical weather condition. For long distance analysis, we conducted two field tests for 3 km and 6 km link distance.

Although we performed the test during clear weather condition, the result showed that the theoretical and calculation result is complying with the experimental result. The result showed that under clear weather condition the link can go up to 6 km of link distance however only -42.9 dBm received power available.

6.2 CHALLENGES ENCOUNTERED

One of the challenging tasks of performing this research is due to technical failure of the system and supporting system. Furthermore, the time taken to study and analyze the FSO system is also a challenging factor that somehow delays the analysis of the measured data. The unavailable of raw data processing program, require time to develop a program to process one year of data. Software that can process the data and output a complete result of availability and attenuation will surely expedite the time to process the data and other works related to this study.

6.3 SUGGESTION FOR FUTURE WORK

We encounter a number of open issues and have not been dealt with due to time constraint, constitute continuing work.

6.3.1 Specific Rain Attenuation Prediction

To model and have a concrete result on specific rain attenuation parameters, k and α values, and a longer measurement time of rain data is required. One-year data is a minimum requirement by ITU-R for prediction purpose; however, few more years of data will provide a better result.

6.3.2 Rain Intensity Variation

For terrestrial link in order to analyze effective length, we need to consider a link distance of more than 1 km. Since the distance is expected to give variation in reduction factor. This area can be another research area since for FSO system the reduction factor model does not exist yet.

6.3.3 Outage Prediction

Rain and haze are the two factors to determine the availability of the link. Since both are expecting to be the limiting factor in tropical regions, the analysis is important. Visibility range is the term use for analyzing haze effect. For this purpose, at least a year of visibility data requires to be able to predict the availability of an FSO link due to haze attenuation. Local install visibility meter is a great equipment to measure local visibility distance compared to the standard study using visibility data from the airport area.

6.3.4 Long Distance FSO Link Deployment

Finally, in terms of long distance analysis more than 6 km, more studies and reviews necessary in order to grasp the concept of interfacing the existing FSO system with bigger aperture equipment for longer-range signal detection. One of the ways is by using modified and custom-made interface between FSO link systems and telescope for long distance FSO link deployment. To materialize this, need further and in depth study.

6.4 SIGNIFICANCE OF THE FINDINGS

The key achievements of this research are as follows.

- This research will serve as a base for an FSO designer in designing local FSO link. We have created a framework, which allows analysis on the effect of weather specifically rain intensity effects on FSO link operating in tropical region. Available measured data and models use for FSO analysis are based on temperate region data.
- The result of the research proposed and predicted new specific rain attenuation parameters which develop using locally measured rain intensity and rain attenuation. Whereas the standard used of k and α is based on temperate region data which have a different rain intensity and different method of analyzing and developing k and α. Our analysis used direct and real measurement data on rain intensity and rain attenuation effects on FSO link under tropical weather condition.
- Having variation on specific rain attenuation parameters which yield better prediction result. Variation of specific rain attenuation ensures most of the measurement data is considered and correlated to produce better prediction result.
- These current findings add substantially to the basis of making the deployment of an FSO system as a prominent communication system in Malaysia in particular and in tropical region in general. It is due to the deployment of several of FSO at several places in Malaysia without further analysis on the effect of attenuation on FSO link deployment.
- These findings also enhance our understanding of the reliability and availability of FSO system, FSO parameters that relate to the FSO design and how the local weather condition effect FSO link propagation in term of rain attenuation.

6.5 SUMMARY

In summary, we have laid down the foundation of developing models and analysis base on tropical region with local measured data. We have predicted the availability of an FSO link operating in tropical weather condition. The finding adds substantially to our understanding of weather effect on an FSO link in tropical regions; its serve as a foundation for future studies on FSO link deployment under tropical region weather condition.

BIBLIOGRAPHY

Abdulrahman, A. Y., Rahman, T. A., et al. (2011). Empirically Derived Path Reduction Factor for Terrestrial Microwave Links Operating at 15Gz in Peninsula Malaysia. *J. of Electromagn. Waves and Appl., 25*, 23-37.

Abdulrahman, A. Y., Rahman, T. B. A., et al. (2010). A New Rain Attenuation Conversion Technique for Tropical Regions. *Progress In Electromagnetics Research B, 26*, 53-67.

Aburakawa, Y., & Otsu, T. (2002). *Experimental evaluation of 800-nm band optical wireless link for new generation mobile radio access network*. Paper presented at the Microwave Photonics, 2002. International Topical Meeting on.

Abtahi, M., & Rusch, L. (2006). *Mitigating of scintillation noise in FSO communication links using saturated optical amplifiers*. Paper presented at the MILCOM.

Acampora, A. S., & Krishnamurthy, S. V. (1999). A broadband wireless access network based on mesh-connected free-space optical links. *Personal Communications, IEEE, 6*(5), 62-65.

Achour, M. (2002a). Simulating Atmospheric Free-Space Optical Propagation:Part I, Rainfall Attenuation. *SPIE Proceeding, 3635*.

Achour, M. (2002b). Simulating Atmospheric Free-Space Optical Propagation,Part II: Haze, Fog and Low Clouds Attenuations. *SPIE Proceeding, 4873*.

Akbulut, A., Ilk, H. G., et al. (2005). *Design, availability and reliability analysis on an experimental outdoor FSO/RF communication system*. Paper presented at the Proceedings of 2005 7th International Conference of Transparent Optical Networks 2005.

Akuon, P. O., & Afullo, T. J. O. (2011, 13-15 Sept. 2011). *Path reduction factor modeling for terrestrial links based on rain cell growth*. Paper presented at the AFRICON 2011.

Amandeep, K. V., et al. (2012). Link Margin Optimization of Free Space Optical Link under the Impact of Varying Meteorological Conditions. *International Journal of Engineering Science and Technology, 4*(3), 1120-1125.

Ananda, E. S. (2002). *Free Space Optics (FSO) Links in Singapore: Scintillation Effects*. Nanyang Avenue, Singapore: School of Electrical & Electronic Engineering, Nayang Technological University.

Arun, K. M. (2008). Free-Space Laser Communication. In *Optical Fiber Communication Reports,* (pp. 1-8): Springer.

Assis, M. S. (1990). *Path Length reduction factor for tropical regions.* Paper presented at the URSI Commission F Open Symposium on Regional Factors in Predicting Radiowave Attenuation Due to Rain, Rio de Janeiro, Brazil.

Awan, M. S., Leitgeb, E., et al. (2008). *Evaluation of fog attenuation results for optical wireless links in free space.* Paper presented at the Satellite and Space Communications, 2008. IWSSC 2008. IEEE International Workshop on.

Awan, M. S., Marzuki, et al. (2009). *Weather Effects Impact on the Optical Pulse Propagation in Free Space.* Paper presented at the IEEE 69th Vehicular Technology Conference, 2009, VTC Spring 2009.

Baker, L. (2008). Free Space Optics. Retrieved 11 March, 2009

Bandera, P., & FSona, C. C. (2005). *Defining a Common Standard for Evaluating and Comparing Free-Space Optical Products*: fSona,Communication,Corporation.

Bloom, S. (2002). *The Physics of Free-Space Optics*: White paper,AirFiber, Inc.

Bloom, S., Korevaar, E., et al. (2003). Understanding the performance of Free Space Optics. *Journal of Optical Networking, 2*(6), 178.

Bohren, C. F., & Huffman, D. R. (1983). *Absorption and scattering of light by small particles.* New York: John Wiley and Sons.

Bouchet, O., Marquis, T., et al. (2005). *FSO and Quality of Service Software Prediction.* Paper presented at the Proc. SPIE 5892.

Bouchet, O., Sizun, H., et al. (2006). *Free-Space Optics Propagation and Communication*. UK: ISTE.

Bouna, R. W. L., & Uranus, H. P. (2011). *Analysis of the effect of rainfall intensity in Jakarta and Tangerang to the performance of free space optics communication system*. Paper presented at the International Conference on Electrical Engineering and Informatics (ICEEI), 2011.

Bryant, G. H. (1998). *Rain rate distribution of tropical regions*. Paper presented at the The 2nd African Regional Workshop on Communication (ARWOC2), Kampala, Uganda.

Cablefree. (2000). FSO Technology. Retrieved February 11,2009 from Cablefree Solution Limited. Website: http://www.cablefreesolutions.com/fsotechnology.htm

Capsoni, C., Luini, L., et al. (2009). *A Physically Based Method for the Conversion of Rainfall Statistics From Long to Short Integration Time.* Paper presented at the

Antennas and Propagation (EuCAP), 2010 Proceedings of the Fourth European Conference on, 2010, Bachelona, Spain.

Capsoni, C., Nebulosi, R., et al. (2006). *Attenuation due to rain on FSO.* Paper presented at the XVI Riunione Nazionale di Elettromagnetismo, Genova.

Carbonneau, T. H., & Mecherle, G. S. (2000). SONa beam Optical Wireless Product in Free Space Laser *Proceeding SPIE on Communication Technologies 12 3932*, 45-51.

Carbonneau, T. H., & Wisley, D. R. (1997). Opprtunities and challenges for optical wireless:the competitive advantage of free space telecommunications link in today's crowded marketplace. *Wireless Technologies and Systems: Millimeter Wave and Optical, Proc. SPIE, 3232*, 119-128.

Chabane, M. (2006). *FSO Prediction V3.10 User Guide* (User Manual). Belfort, France: France Telecom R&D.

Chabane, M., Alnaboulsi, M., et al. (2004). A new quality FSO software. *SPIE Journal, Strasbourg*.

Chen, B. (2002). *A Trial-Based Study of Free-Space Optics Systems in Singapore*: Infocomm Development Authority of Singapore, http://www.ida.gov.sg/doc/Technology/Technology_Level2/FSORpt.pdf.

Chinlon, L., Deng, K. L., et al. (2001). *Broadband optical access networks.* Paper presented at the Lasers and Electro-Optics, 2001. CLEO/Pacific Rim 2001. The 4th Pacific Rim Conference.

Colvero, C. P., Cordeiro, M. C. R., et al. (2007, Oct. 29 2007-Nov. 1 2007). *FSO systems: Rain, drizzle, fog and haze attenuation at different optical windows propagation.* Paper presented at the International Conference on Microwave and Optoelectronics, 2007 (IMOC 2007).

Crane, R. K. (1996). *Electromagnetic wave propagation through rain* (A ed.): Wiley-Inter Science Publication, New York, 1996.

Crane, R. K. (2003). *Propagation Handbook for Wireless Communication System Design*: CRC Press, Florida

Crane, R. K., & Robinson, P. C. (1997). ACTS propagation experiment: rain-rate distribution observations and prediction model comparisons. *Proceedings of the IEEE, 85*(6), 946-958.

D'Amico, M., Leva, A., et al. (2003). Free-space optics communication systems: first results from a pilot field-trial in the surrounding area of Milan, Italy. *IEEE Microwave and Wireless Components Letters, 13*(8), 305-307.

Davide, M. F., Incerti, G., et al. (1986). Free Space Optical Technologies. *Journal of the American Society for Information Science, 37*(6), 257-296.

Davidsona, F. M., Bucaillea, S., et al. (2003). Scintillation Measurements of Broadband 980nm Laser Light in Clear Air Turbulence. *Proceedings of the SPIE*.

Davis, C. C., Smolyaninov, I. I., et al. (2003). Flexible optical wireless links and networks. *Communications Magazine, IEEE, 41*(3), 51-57.

Dijk, J., Bruza, I. V., et al. (1983). *Microwave propagation studies, Measurements and eductation in Surabaya, Indonesia*. Surabaya, Indonesia.

Dissanayake, A. W., & Allnutt, J. E. (1992). *Prediction of rain attenuation in low latitude regions.* Paper presented at the Proceeding of URSI Open Symposium, Ravenscar, U.K.

Dordova, L., & Wilfert, O. (2009). *Free space optical link range determination on the basis of meteorological visibility.* Paper presented at the 19th International Conference on Radioelektronika, 2009 (RADIOELEKTRONIKA '09)

Dordova, L., & Wilfert, O. (2010). *Determination of atmospheric transmission media properties in optical spectrum by analysis of optical beam profile.* Paper presented at the 10th International Conference on Laser and Fiber-Optical Networks Modeling (LFNM), 2010

Duncan, W. (2001). *Optical Power Margin or "Fade Margin"*. White Paper Document: Plantree.

EnviroTech Sensors, I. (2008). Sentry Brochure: Sentry™ Visibility Sensor. Retrieved 25 August, 2010

EnviroTech Sensors, I. (2009a). Performance of the Sentry™ Visibility Sensor in Obstructions to Visibility Caused by Blowing Dust & Sand. Retrieved 4 March, 2012

EnviroTech Sensors, I. (2009b). *Sentry Visibility Sensor User's Guide*. Clarksville, U.S.A.: EnviroTech Sensors, Inc.

EXFO. Ethernet Test Set—AXS-200/850. Retrieved 19 August, 2010

EXFO. (2011). Getting Started with the AXS-200/805/855. Retrieved 1 February 2012, 2012

Fatin, H. H., Abu, S. M. S., et al. (2010). Simulation of FSO Transmission at Petaling Jaya due to Attenuations Effect. *ELEKTRIKA - UTM Journal of Electrical Engineering, 12* (1), 30-34.

Fatin, H. M., Abu Sahmah, M. S., et al. (2011). *Effect of Rain Attenuations on Free Space Optic Transmission in Kuala Lumpur.* Paper presented at the International Conference on Advanced Science, Engineering and Information Technology 2011, Hotel Equatorial Bangi-Putrajaya, Malaysia, .

Finite mathematics & Applied calculus Finite mathematics on-line topic: linear and exponential regression. Retrieved 7 June 2012, http://www.zweigmedia.com/RealWorld/calctopic1/regression.html

Florex, S. A. J. (2010). *Circular polarization and availability in free space optics (FSO) communication systems.* Paper presented at the IEEE Latin-American Conference on Communications (LATINCOM), 2010

fSona, C. C. (2001). *Wavelength Selection for Optical Wireless Communications Systems.*

Gagliardi, R. M., & Karp, S. (1995). *Optical Communication* (2nd ed.). New York: John Wiley.

Gebhart, M., Leitgeb, E., et al. (2003). *Atmospheric effects on optical wireless links.* Paper presented at the Proceedings of the 7th International Conference on Telecommunications, 2003 (ConTEL 2003).

Gerard, M. V. (2008). *Excel 2007 for Scientists and Engineer*. Uniontown, OH Holy Macro Books.

Grabner, M., & Kvicera, V. (2007). *On the relation between atmospheric visibility and optical wave attenuation.* Paper presented at the 16th IST Mobile and Wireless Communications Summit, 2007.

Harboe, P. B., & Souza, J. R. (2004). Free Space Optical Communication Systems: A Feasibility Study for Deploymant in Brazil. *Journal of Microwaves and Optoelectronics, 3*(4), 9.

Harris, D. (1995). The attenuation of electromagnetic waves due to atmospheric fog. *International Journal of Infrared and Milimeter Waves, 16*(6), 1091-1108.

Harrold, T. W. (1967). Attenuation of 8.6 mm-wavelength radiation in rain. *Electrical Engineers, Proceedings of the Institution of, 114*(2), 201-203.

Hasan, W. A., Rahim, S. K. A., et al. (2011). Potential interference and rain attenuation at 21.4-22 GHz downlink broadcasting satellite signals. *International Journal of Electronics, 98*(12), 1721-1731.

Henniger, H., & Wilfert, O. (2010). An introduction to Free-space Optical Communications. *Radioengineering, 19*(2), 203-212.

Houze R.A, J. (1997). Stratiform precipitation in regions of convection : A meteorological paradox? *Bull. American Meteorological Society, 78*, 2179-2196.

Hudson Jr, R. D. (1969). *Infrared System Engineering*: Wiley & Sons.

Husagic, A. (2009). *Free Space Optical Link Performance Analysis Under Malaysian Weather Conditions and Its Impact on Quatum Key Distribution* (MScThesis): International Islamic University Malaysia.

Husagic, A., & Al-Khateeb, W. (2008). *Effect of Weather Conditions on Quality of Free Space Optics Links (with focus on Malaysia).* Paper presented at the International Conference on Computer and Communication Engineering 2008 (ICCCE'08), Kuala Lumpur.

Ishii, S., Sayama, S., et al. (2010). Rain Attenuation at Terahertz. *Wireless Engineering and Technology, 1*, 92-95.

Islam, M.R. et all, (2000). *Rain Attenuation Prediction for Terrestrial Microwave Links Based on Rain Rate and Rain Attenuation Measurements in a Tropical Region.* University of Technology Malaysia, Johor Bahru.

ITU-R F.2106-1. (2010) *Fixed service applications using free-space optical links*. International Telecommunication Union.

ITU-R P.530-8, R. (1999). *Propagation Data and Prediction Methods Required for the Design of Terrestrial Line-of-Sight Systems*: International Telecommunication Union.

ITU-R P.530-13, R. (2009). *Propagation data and prediction methods required for the design of terrestrial line-of-sight systems*: International Telecommunication Union.

ITU-R P.618-6, R. (1999). *Propagation Data and Prediction Methods Required for the Design of Earth-Space Telecommunication System*: International Telecommunication Union.

ITU-R P.837-5, R. (2007). *Characteristics of precipitation for propagation modeling*.

ITU-R P.838, R. (2005). *Specific attenuation model for rain for use in prediction methods*: International Telecommunication Union.

ITU-R P.1814, R. (2007). *Prediction methods required for the design of terrestrial free-space optical links*: International Telecommunication Union.

ITU-R P.1817, R. (2007). *Propagation data required for the design of terrestrial free-space optical links*: International Telecommunication Union.

Jafri Din. (1997). *Influence of rainfall drop size distribution on attenuation at mocrowave frequencied in a tropical region.* University Technology Malaysia.

Joss, J., Thams, J. C., et al. (1968). *The variation of raindrops size distribution at Lacarno.* Paper presented at the Proc. of International Conference on Cloud Physics, Toronto (Canada).

Kardi Teknomo's page. What is regression model? Retrieved 6 June 2012, http://people.revoledu.com/kardi/tutorial/Regression/WhatIsRegression.html

Karimi, M., & Nasiri-Kenari, M. (2009). BER Analysis of Cooperative Systems in Free-Space Optical Networks. *Lightwave Technology, Journal of, 27*(24), 5639-5647.

Ken, K. (2003). Introduction to RF Simulation and its application. Designer's Guide Consulting, Inc., Retrieved on November 3, 2009. Website: www.designers-guide.org

Khamis, N. H. H. (2005). *Path Reduction Factor for Microwave Terrestrial Links Derived from the Malaysian Meteorological Radar Data.* Universiti Teknologi Malaysia, Skudai.

Khamis, N. H. H., Din, J., et al. (2005). *Rainfall Rate from Meteorological Radar Data for Microwave Applications in Malaysia.* Paper presented at the 13th IEEE International Conferance Jointly held with the IEEE 7th Malaysia International Conference on Communication, 2005 Malaysia.

Khamis, N. H. H., Din, J., et al. (2004). *Determination of rain cell size distribution for microwave link design in Malaysia.* Paper presented at the RF and Microwave Conference, 2004. RFM 2004. Proceedings.

Khamis, N. H. H., Din, J., et al. (2005). *Analysis of rain cell size distribution from meteorological radar data for rain attenuation studies.* Paper presented at the Asia-Pacific Conference on Applied Electromagnetics, 2005 (APACE 2005)

Kidouchim, I. (2007). Introduction to FSO Technology: Wireless Product Division, MRV. Retrieved on 14 Jun 2010, www.systemsupportsolutions.com/.../Introduction_to_FSO_Technology.pps

Kim, I. I., & Korevaar, E. (2001). Availability of free-space optics (FSO) and hybrid FSO/RF systems. *Proceedings of SPIE, 4530*, 84–95.

Kim, I. I., McArthur, B., et al. (2000). Comparison of laser beam propagation at 785 nm and 1550 nm in fog and haze for optical wireless communications. *Optical Wireless Communications III, Proc. SPIE, 4214*, 26-37.

Kim, I. I., Mitchell, M., et al. (1999). Measurement of scintillation for free-space laser communication at 785 nm and 1550 nm. *Optical Wireless Communications II, Proc. SPIE., 3850*, 49-62.

Kim, I. I., Stieger, R., et al. (1998). Wireless optical transmission of Fast Ethernet, FDDI, ATM, and ESCON protocol data using the TerraLink laser communication system. *Opical Engineering, 37*, 3143-3455.

Kolka, Z., Wilfert, O., et al. (2007). Reliability of Digital FSO Links in Europe. *Int. Journal of Electronics,Circuits and Systems, 1*(4), 236-239.

Korevaar, E., Kim, I. I., et al. (2003). Atmospheric Propagation Characteristics of Highest Importance to Commercial Free Space Optics. *Proc. of SPIE, 4976*, 1-12.

Kruse et al, P. W. (1962). *Element of Infrared Technology: Generation, Transmission, and Detection*. New York: Wiley.

Kvicala, R., Kvicera, V., et al. (2007). BER and Availability Measured on FSO link. *Radioengineering, 16*(3), 6.

Laws, J. O., & Parson, D. A. (1943). The relation of raindrops size distribution to intensity. *Trans. Amer. Geophys. Union, 24*, 452-460.

Le-Minh, H., Ghassemlooy, Z., et al. (2010). *Experimental study of bit error rate of free space optics communications in laboratory controlled turbulence*. Paper presented at the IEEE GLOBECOM Workshops (GC Wkshps), 2010

Leitgeb, E., Awan, M. S., et al. (2009). *Current Optical Technologies for Wireless Access*. Paper presented at the 10th International Conference on Telecommunications (ConTEL 2009), Zagreb, Croatia.

Leitgeb, E., Awan, M. S., et al. (2009). *Investigations on Free-Space optical links within SatNEx II*. Paper presented at the Antennas and Propagation, 2009. EuCAP 2009. 3rd European Conference on.

Leitgeb, E., Bregenzer, J., et al. (2002). *Free space optics - extension to fiber-networks for the "last mile"*. Paper presented at the The 15th Annual Meeting of the IEEE on Lasers and Electro-Optics Society, 2002 (LEOS 2002)

Leitgeb, E., Muhammad, S. S., et al. (2005). *Reliability of FSO links in next generation optical networks*. Paper presented at the Proceedings of 2005 7th International Conference on Transparent Optical Networks, 2005

Lightpointe. Flightstrata: http://www.lightpointe.com/products/fs_155.cfm.

Lightpointe. (2009a). *How to Design a Reliable FSO System*: Lightpointe White Paper Series.

Lightpointe. (2009b). *What is Free Space Optics (FSO)?* : Lighpointe White Paper.

Lin, S. H. (1977). Nationwide long term rain statistics and emperical calculation of 11 GHz microwave rain attenuation. *The Bell System Technical Journal, 56*(9), 1581-1604.

Loschnigg, M., Mandl, P., et al. (2009). *Long-term performance observation of a Free Space Optics link*. Paper presented at the Telecommunications, 2009. ConTEL 2009. 10th International Conference on.

Mandeep, J. S., Ooi Wen, H., et al. (2011). *Modified ITU-R rain attenuation model for equatorial climate*. Paper presented at the IEEE International Conference on Space Science and Communication (IconSpace), 2011, Penang.

Mandeep, J. S., & Tanaka, K. (2007). Effect of Atmospheric Parameters on Satellite Link. *International Journal of Infrared and Millimeter Waves, 28*(10), 789-795.

Mandeep, J. S. a. J. E. A. (2007). Rain attenuation predictions at Ku-band in south east Asia countries. *Progress In Electromagnetics Research, PIER, 76*, 65-74.

Marshall, J. S., & Palmer, W. M. (1948). The distribution of raindrops with size. *Journal of Meteorology, 5*(4), 165-166.

Maxim, I. D. (2004). Physical Layer Performance: Testing the Bit Error Ratio (BER). Retrieved 1 May, 2012

Middleton, W. E. K. (1952). *Vision tahrough the Atmosphere*: University of Toronto Press.

Moupfouma, F. (1984). Improvement of a rain attenuation prediction method for terrestrial microwave links. *IEEE Transactions on Antennas and Propagation, 32*(12), 1368-1372.

Moupfouma, F. (1985). Model of rainfall-rate distribution for radio system design. *Microwaves, Antennas and Propagation, IEE Proceedings H, 132*(1), 39-43.

Moupfouma, F. (2009). Electromagnetic waves attenuation due to rain: A prediction model for terrestrial or L.O.S SHF and EHF radio communication links. *J. Infra, Milli., Tetrahertz Waves, 30*(6), 622-632.

Muhammad, S. S., Kohldorfer, P., et al. (2005). *Channel modeling for terrestrial free space optical links*. Paper presented at the Proceedings of 2005 7th International Conference on Transparent Optical Networks, 2005.

Naboulsi, M. A., Sizun, H., et al. (2004). Fog attenuation prediction for optical and infrared waves. *Optical Engineering, 43*(2), 319-329.

Naboulsi, M. A., Sizun, M., et al. (2003). Propagation of optical and infrared waves in the atmosphere. *SPIE Journal*.

Nadeem, F., Kvicera, V., et al. (2009). Weather effects on hybrid FSO/RF communication link. *Selected Areas in Communications, IEEE Journal on, 27*(9), 1687-1697.

Naimullah, B. S., Othman, M., et al. (2008). *Comparison of wavelength propagation for Free Space Optical Communications*. Paper presented at the Electronic Design, 2008. ICED 2008. International Conference on.

Naimullah, B. S. S., Hitam, S., et al. (2007). *Analysis of the Effect of Haze on Free Space Optical Communication in the Malaysian Environment*. Paper presented

at the Proceedings of the 2007 IEEE International Conference on Telecommunications, Penang, Malaysia.

Nazmi, A. M., Amr, S. E., et al. (2012). Pointing Error in FSO Link under Different Weather Conditions. *International Journal of Video & Image Processing and Network Security (IJVIPNS-IJENS), 12*(01).

NexSens Technology. iChart Environmental software. http://nexsens.com/featured/nexsens_ichart_f.htm

Ojo, J. S., Ajewole, M. O., et al. (2008). Rain Rate and Rain Attenuation Prediction for Satellite Communication in KU and KA Bands over Nigeria. *Progress In Electromagnetics Research B, 5*, 207-223.

Olsen, R. L., Rogers, D., et al. (1978). The aRb Relation in the Calculation of Rain Attenuation. *Antennas and Propagation, IEEE Transactions on, 26*(2), 318-329.

OptiSystem. (2008). *Optical Communication System Design Software : Modulation Formats*: OptiWave Design System for Photonics.

Pan, Q. W., & Bryant, G. H. (1994). Effective rain-cell diameters and rain-column heights in the tropics. *Electronics Letters, 30*(21), 1800-1802.

Paraboni, A., Riva, C., et al. (1997). *Radiowave propagation in the hopics for satellite and*
terrestrial applications". Paper presented at the African Regional Workshop in Microwave Communications, University of Dar-es-Salaam, Tanzania.

Perez Garcia, N. A., & da Silva Mello, L. A. R. (2004). Improved method for prediction of rain attenuation in terrestrial links. *Electronics Letters, 40*(11), 683-684.

Plank, T., Czaputa, M., et al. (2011). *Wavelength selection on FSO-links.* Paper presented at the Proceedings of the 5th European Conference on Antennas and Propagation (EUCAP).

Pontes, M. S., da Silva Mello, L. A. R., et al. (2007). *Modeling of effective rainfall rate and rain attenuation in terrestrial links in the tropics.* Paper presented at the 6th International Conference on Information, Communications & Signal Processing, 2007.

Popoola, W. O., Ghassemlooy, Z., et al. (2009). *Atmospheric channel effects on terrestrial free space optical communication links.* Paper presented at the 3rd International Conference on Computers and Artificial Intelligence (ECAI 2009), ROMÂNIA.

Prokes, A. (2009). Atmospheric effects on availability of free space optics systems. *Optical Engineering, 48*(6), 10.

Ramasarma, V. (2002). Free Space Optics: A Viable Last-Mile Solution. *Bechtel Telecommunications Technical Journal*, 22-30.

Ricklin, J. C., Hammel, S. M., et al. (2006). Atmospheric channel effects on free-space laser communication. *Journal of Optical and Fiber Communications Reports, 3*, 111-158.

Robeiro, W., & Tan, R. (2006). Free Space Optical Laser Communication Link. *Journal for the Advancement of Science and Arts, 1*, 20-52.

Sandalidis, H. G., Tsiftsis, T. A., et al. (2008). BER Performance of FSO Links over Strong Atmospheric Turbulence Channels with Pointing Errors. *IEEE Communications Letters, 12*(1), 44-46.

Saquib, N., Sabbir Rahman Sakib, M., et al. (2010). *Free space optical connectivity for last mile solution in Bangladesh.* Paper presented at the 2nd International Conference on Education Technology and Computer (ICETC), 2010

Shahrul Kamal, A. R. (2000). *Rain attenuation study over terrestrial and earth-satellite Links in Malaysia*: Wireless Communication Research Laboratory University Technology Malaysia.

Sharon, W. (2003). Optical receiver performance evaluation. Retrieved 5 June, 2012, http://www.maxim-ic.com/app-notes/index.mvp/id/1938

Singh, M. K., Kapoor, V., et al. (2011a, 24-25 Feb. 2011). *Bit Error Rate Analysis of Free Space Optical Link Using Different Optical Windows.* Paper presented at the International Conference on Devices and Communications (ICDeCom) 2011.

Singh, M. K., Kapoor, V., et al. (2011b). Power Budget Performances of Free Space Optical Link using Direct Line of Sight Propagation. *Special Issue of International Journal of Computer Applications (0975 – 8887) on Electronics, Information and Communication Engineering - ICEICE 3*.

Silva Mello, L. A. R., Pontes, M. S., et al. (2007). Prediction of rain attenuation in terrestrial links using full rainfall rate distribution. *Electronics Letters, 43*(25), 1442-1443.

Silva Mello, L. A. R., Pontes, M. S., et al. (2007). *New method for the prediction of rain attenuation in terrestrial links using the concept of effective rainfall rate.* Paper presented at the Microwave and Optoelectronics Conference, 2007. IMOC 2007. SBMO/IEEE MTT-S International.

Silva Mello, L. A. R., Pontes, M. S., et al. (2006). *Modeling of effective rainfall rate based on attenuation measurements in converging terrestrial links.* Paper presented at the First European Conference on Antennas and Propagation, 2006. EuCAP 2006. .

Šporik, J., & Tejkal, V. (2010). *The increase of availability of FSO link by reducing the distance of FSO's Heads.* Paper presented at the Proceedings of the 16th

conference STUDENT EEICT 2010, Faculty of Information Technology, Brno University of Technology.

Srinivasan, R., & Sridharan, D. (2010). *The climate effects on line of sight (LOS) in FSO communication*. Paper presented at the 2010 IEEE International Conference on Computational Intelligence and Computing Research, India.

Stat Trek, R. j. What is linear regression? Retrieved 7 June 2012, http://stattrek.com/regression/influential-points.aspx?tutorial=ap

Suriza, A. Z., Md. Rafiqul, I., et al. (2011). Analysis of Rain Effects on Terrestrial Free Space Optics Based on Data Measured in Tropical Climate. *IIUM Engineering Journal 12*(5), 45-51.

Szajowski, P. F., Nykolak, G., et al. (1998). 2.4-km free-space optical communication 1550-nm transmission link operating at 2.5 Gb/s: experimental results. *Optical Wireless Communication, Proc. SPIE., 3532*, 29-40.

The free dictionary. Retrieved 7 June 2012, http://www.thefreedictionary.com/bivariate

Tom, G., Joel, B., et al. (2005). Analysis of Free Space Optics as a Transmission Technology. Retrieved 7 January 2010

Tropos, N. (2007, July 2007). Receive Sensitivity: A Practical Explanation. Retrieved 19 Jan 2011, http://www.tropos.com/pdf/technology_briefs/tropos_techbrief_rx_sensitivity.pdf

Tusubira, F. F., & Kyeyune, A. (2003). *Modeling and model verification for rain-induced attenuation on a line-of-sight link at Ku-band*. Paper presented at the Antennas and Propagation, 2003. (ICAP 2003). Twelfth International Conference on (Conf. Publ. No. 491).

Vitasek, J., Latal, J., et al. (2011). *Atmospheric turbulences in Free Space Optics channel*. Paper presented at the 34th International Conference on Telecommunications and Signal Processing (TSP), 2011

Wainright, E., Hazem, H. R., et al. (2005). Wavelength Diversity in Free-Space Optics to Alleviate Fog Effects *Proceedings of SPIE on Free-Space Laser Communication Technologies XVII 5712*, 110-118.

Weichel, H. (1990). *Laser Beam Propagation in the Atmosphere*. Bellingham, WA: SPIE Optical Engineering Press.

Weisstein, E. W. Least Squares Fitting--Power Law. Retrieved http://mathworld.wolfram.com/LeastSquaresFittingPowerLaw.html, 2012

Wikipedia. Alhazen. Retrieved 11 Febuary 2011

Wikipedia. Atmosphere of Earth. Retrieved 17 Jan , http://en.wikipedia.org/wiki/Atmosphere_of_Earth, 2011

Willebrand, H., & Ghuman, B. S. (2001). *Free-Space Optics: Enabling Optical Connectivity in Today's Network*. Indianapolis, Indiana: Sams Publishing.

Yagasena, A. & Hassan, S.I.S. (2000). *Worst-month rain attenuation statistic for satellite-Earth link design at Ku-band in Malaysia*. Proceeding TENCON 2000, Vol 1, 122 – 125.

YOUNG, R. M. Tipping Bucket Rain Gauge. http://www.youngusa.com/products/3/18.html

Zhang, W., & Moayeri, N. (1999). Power-Law Parameters of Rain Specific Attenuation. Retrieved 09 March, 2011

Zhou, X. X., Lee, Y. H., et al. (2009). *Conversion model of one-minute rainfall rate distribution in Singapore*. Paper presented at the IEEE Antennas and Propagation Society International Symposium, 2009 (APSURSI '09).

Zhuanhong, J., Qingling, Z., et al. (2006). *Atmospheric Attenuation Analysis in the FSO Link*. Paper presented at the International Conference of Communication Technology 2006 (ICCT'06), Guilin, Chine.

APPENDIX A

155E FLIGHTSTRATA SPECIFICATION

UNIT SPECIFICATIONS	FLIGHTSTRATA 155E
Recommended Operational Ranges	2,000 Meters (Approximately 6,600 Feet)
Description	Four-Beam Optics System with Auto Tracking and Auto Power Control
Receiver/Transmitter(s)	Four receivers, four transmitters
Dimensions (WxHxL) (12.6x11.7x24.4 in)	321x297.5x620 mm
Unit Weight	11.1 kg (24.4 lbs)
Operating Voltage	90 to 240 V (50/60 Hz) or +/– 48 V DC
Operating Temperature	-25 C to 60 C (-13 F to 140 F)
Humidity Range	Up to 95% non-condensing
Power Consumption Max	40 W
Immune to EMI & RF Interference	Yes
Built-In Alignment Telescope	Yes
Built-In Defroster	Yes
SNMP Management	Optional

FREE SPACE SPECIFICATIONS	
Bit Rate	1.5Mbps to 155Mbps
Free-Space Optical Transmitter	VCSEL
Free-Space Wavelength	850 nm
Optical Receiver	Si APD
Receive Power Indicator	10-level bar graph
Status Indicator (LED)	Power, TX Data, LOS, Overload, Data In, Data Out

SINGLEMODE FIBER INTERFACE FSA 155E	
Protocol	Transparent
System Interface	SC Connector
Interface Wavelength	1270 to 1350 nm

Optical Receive Power	-8 to -31 dBm -3 to -20 dBm
LASER CLASSIFICATION	
IEC/EN 60825-1/A2	Class 1M

APPENDIX B

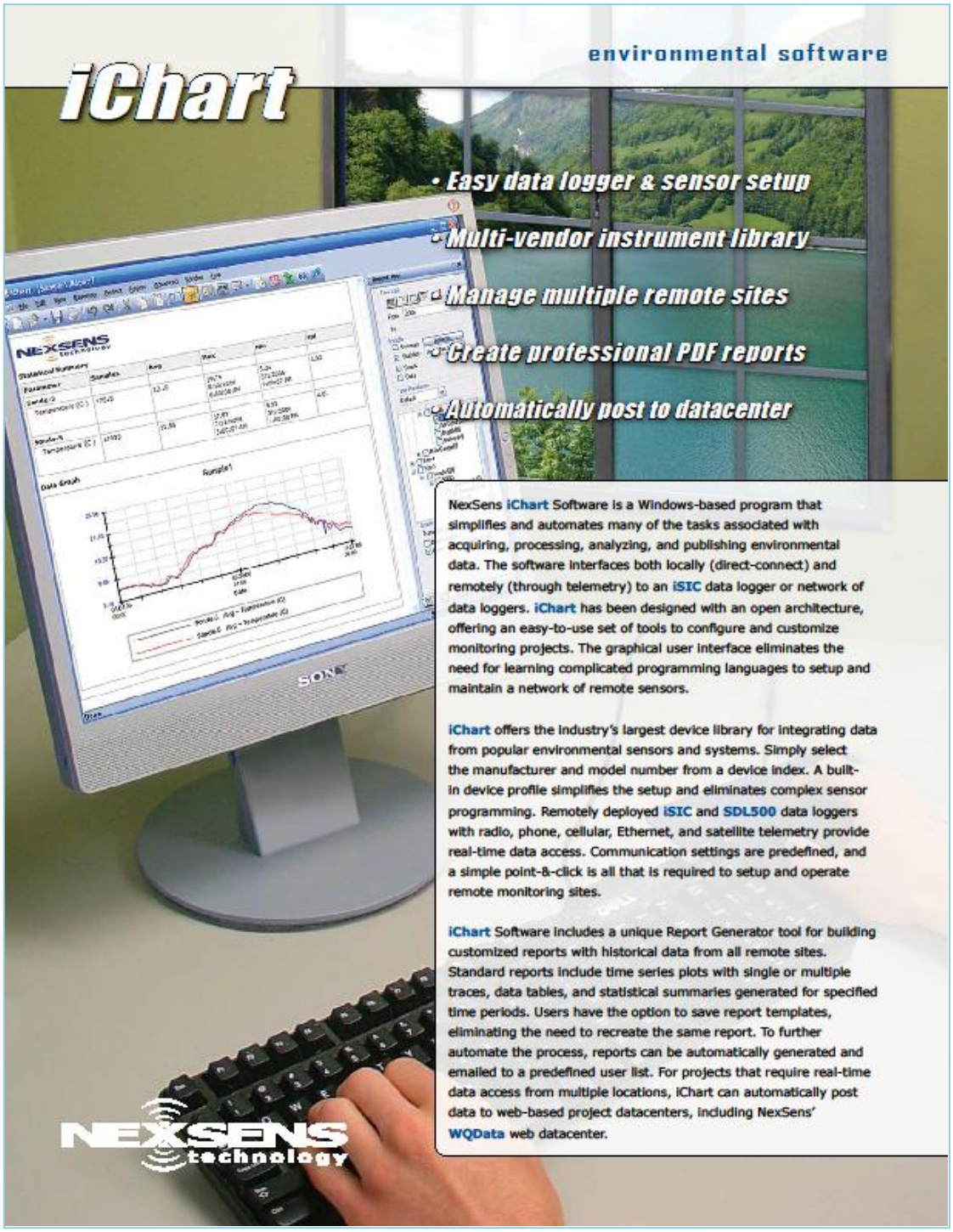
environmental software
iChart
• Easy data logger & sensor setup
• Multi-vendor instrument library
• Manage multiple remote sites
• Create professional PDF reports
• Automatically post to datacenter
NexSens iChart Software is a Windows-based program that simplifies and automates many of the tasks associated with acquiring, processing, analyzing, and publishing environmental data. The software interfaces both locally (direct-connect) and remotely (through telemetry) to an iSIC data logger or network of data loggers. iChart has been designed with an open architecture, offering an easy-to-use set of tools to configure and customize monitoring projects. The graphical user interface eliminates the need for learning complicated programming languages to setup and maintain a network of remote sensors.
iChart offers the industry's largest device library for integrating data from popular environmental sensors and systems. Simply select the manufacturer and model number from a device index. A built-in device profile simplifies the setup and eliminates complex sensor programming. Remotely deployed iSIC and SDL500 data loggers with radio, phone, cellular, Ethernet, and satellite telemetry provide real-time data access. Communication settings are predefined, and a simple point-&-click is all that is required to setup and operate remote monitoring sites.
iChart Software includes a unique Report Generator tool for building customized reports with historical data from all remote sites. Standard reports include time series plots with single or multiple traces, data tables, and statistical summaries generated for specified time periods. Users have the option to save report templates, eliminating the need to recreate the same report. To further automate the process, reports can be automatically generated and emailed to a predefined user list. For projects that require real-time data access from multiple locations, iChart can automatically post data to web-based project datacenters, including NexSens' WQData web datacenter.
NEXSENS technology

iChart

environmental software

notable features

Device Library	Select sensor manufacturer and model number from a device index. A built in device profile offers relevant information to simplify sensor setup
Unattended Access	Remotely deployed iSIC data loggers with radio, phone, cellular, Ethernet, and satellite telemetry are interrogated at predefined time-based intervals
Centralized Database	Includes a common data entry portal with both manual and automatic import from a variety of industry-standard data formats
Data Processing	Standard data reports include time series plots with single or multiple traces, data tables, and statistical summaries generated for specified time periods
Data Review	Automatic Report Generator tool can be set to generate PDF reports at a user-defined time interval and send them via email to a predefined user list
Data Visualization	Includes functions and interactive tools for analyzing historical data, modeling, simulating systems, and developing statistical algorithms
Data Filtering	Data filtering can be set to automatically or manually eliminate erroneous points in datasets
Data Replication	Can be configured to automatically replicate and store all data into an ODBC compatible database using a standard Windows ODBC connection
Publish & Export	Automatic website creation and WQData web datacenter offers an interactive, multi-level user interface for real-time data
Alarming	Automated alarming tools with multi-user call lists, pre-configured reason codes, and easy-to-use acknowledgement menus ensure timely alarm notification
Database Integration	Industry-standard database technology with multiple levels of redundancy to ensure maximum data integrity

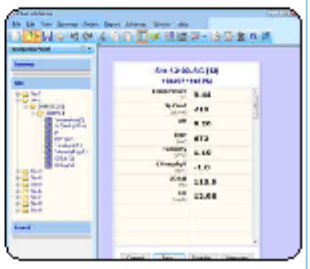

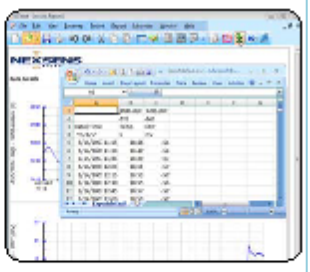

parts list

Part #	Description
1001	iChart Software for Windows-based computers
WQData	Annual web-based datacenter hosting service

NEXSENS technology

937.426.2703
8am to 7pm EST, Monday-Friday

937.426.1125
24 hours a day, every day

NexSens Technology, Inc.
PO Box 151
Alpha, OH 45301-0151

info@nexsens.com

nexsens.com

APPENDIX C


Reliable Rainfall
Measurement
YOUNG
YOUNG
Model 52202
Tipping Bucket Rain Gauge

YOUNG

Model 52202 Tipping Bucket Rain Gauge

The YOUNG Tipping Bucket Rain Gauge meets the specifications of the World Meteorological Organization (WMO).

The design uses a proven tipping bucket mechanism for simple and effective rainfall measurement. The bucket geometry and material are specially selected for maximum water release, thereby reducing contamination and errors.

Catchment area of 200 cm^2 and measurement resolution of 0.1 mm meet the recommendations of the WMO. Extensive use of molded thermoplastic components ensures maximum performance and value. Leveling screws and bullseye level are built-in for easy and precise adjustment in the field. Measured precipitation is discharged through a collection tube for verification of total rainfall. Model 52202 is heated for operation in cold temperatures. An unheated version, 52203, is available for use in moderate climates.

Specifications

Size:
18 cm dia. x 30 cm high, (39 cm high with mounting base)

Catchment Area:
200 cm^2

Resolution:
0.1 mm per tip

Accuracy:
2% up to 25 mm/hr
3% up to 50 mm/hr

Output:
Magnetic reed switch (N.O.), rating 24VAC/DC 500mA

Operating Temperature:
-20°C to +50°C (heated)

Power:
18 Watts for heater only

Mounting:
Clamp for 1" (1.34" dia.) iron pipe
or 3 bolts on 160mm dia. circle

Other:
Leveling adjustment,
thermostatic control for heater,
intake screen

Ordering Information — MODEL

TIPPING BUCKET RAIN GAUGE (HEATED) 52202
TIPPING BUCKET RAIN GAUGE (UNHEATED) 52203

YOUNG
R.M. YOUNG COMPANY
2801 Aero-Park Drive
Traverse City, Michigan 49686 U.S.A.
TEL: (616) 946-3980 FAX: (616) 946-4772
E-mail: met.sales@youngusa.com
Web Site: www.youngusa.com

APPENDIX D

CASELLA RAIN GAUGE SPECIFICATION

Specification	TIPPING BUCKET RAIN GAUGE
Bucket sizes	0.1, 0.2 or 0.5mm
Aperture	400cm²
Accuracy	±1% @ 1 litre/hr
Weight	2.5kg
Ordering information	
0.1mm Tipping Bucket Rain Gauge (light rainfall)	102471E
0.2mm Tipping Bucket Rain Gauge (moderate rainfall)	100000E
0.5mm Tipping Bucket Rain Gauge (heavy rainfall)	100579E

Specification	200CM TIPPING BUCKET RAIN GAUGE
Bucket size	0.2 mm
Aperture	200 cm²
Accuracy	±1% at 25mm/hr
Capacity	Unlimited
Transducer	Magnet/Reed switch
Operating temperature range	1°C to 85°C
Output	Contact closure
Weight	3.2 kg
Reed Switch Details	
Double pole relay for attachment to 2 separate logging devices. Switching contact closure time is typically less than 100 milli-seconds for 0.2 mm of rain.	
Maximum current rating	500 mA
Breakdown voltage	400 V.D.C. minimum
Contact resistance	150 mΩ
Insulation resistance	10⁹ Ω (100 GΩ)
Capacitance open contacts	0.2 pF
Life	10⁸ operations.
Ordering information	
200cm Tipping Bucket Rain Gauge	100504D

APPENDIX E

E.1. Matlab programming

```
function varargout = Rain_Intensity(varargin)
% RAIN_INTENSITY M-file for Rain_Intensity.fig
%      RAIN_INTENSITY, by itself, creates a new RAIN_INTENSITY or
raises the existing
%      singleton*.
%
%      H = RAIN_INTENSITY returns the handle to a new RAIN_INTENSITY
or the handle to
%      the existing singleton*.
%
%      RAIN_INTENSITY('CALLBACK',hObject,eventData,handles,...) calls
the local
%      function named CALLBACK in RAIN_INTENSITY.M with the given
input arguments.
%
%      RAIN_INTENSITY('Property','Value',...) creates a new
RAIN_INTENSITY or raises the
%      existing singleton*.  Starting from the left, property value
pairs are
%      applied to the GUI before Rain_Intensity_OpeningFunction gets
called.  An
%      unrecognized property name or invalid value makes property
application
%      stop.  All inputs are passed to Rain_Intensity_OpeningFcn via
varargin.
%
%      *See GUI Options on GUIDE's Tools menu.  Choose "GUI allows
only one
%      instance to run (singleton)".
%
% See also: GUIDE, GUIDATA, GUIHANDLES

% Edit the above text to modify the response to help Rain_Intensity

% Last Modified by GUIDE v2.5 29-Jun-2011 18:49:13

% Begin initialization code - DO NOT EDIT
gui_Singleton = 1;
gui_State = struct('gui_Name',       mfilename, ...
                   'gui_Singleton',  gui_Singleton, ...
                   'gui_OpeningFcn', @Rain_Intensity_OpeningFcn, ...
                   'gui_OutputFcn',  @Rain_Intensity_OutputFcn, ...
                   'gui_LayoutFcn',  [] , ...
                   'gui_Callback',   []);
if nargin && ischar(varargin{1})
    gui_State.gui_Callback = str2func(varargin{1});
end

if nargout
    [varargout{1:nargout}] = gui_mainfcn(gui_State,
varargin(Mandeep));
else
```

```
    gui_mainfcn(gui_State, varargin(Mandeep));
end
% End initialization code - DO NOT EDIT


% --- Executes just before Rain_Intensity is made visible.
function Rain_Intensity_OpeningFcn(hObject, eventdata, handles,
varargin)
% This function has no output args, see OutputFcn.
% hObject    handle to figure
% eventdata  reserved - to be defined in a future version of MATLAB
% handles    structure with handles and user data (see GUIDATA)
% varargin   command line arguments to Rain_Intensity (see VARARGIN)

% Choose default command line output for Rain_Intensity
handles.output = hObject;
y = imread('iium_logo.jpg');
axes(handles.axes1)
imshow(y);
% Update handles structure
guidata(hObject, handles);

% UIWAIT makes Rain_Intensity wait for user response (see UIRESUME)
% uiwait(handles.figure1);


% --- Outputs from this function are returned to the command line.
function varargout = Rain_Intensity_OutputFcn(hObject, eventdata,
handles)
% varargout  cell array for returning output args (see VARARGOUT);
% hObject    handle to figure
% eventdata  reserved - to be defined in a future version of MATLAB
% handles    structure with handles and user data (see GUIDATA)

% Get default command line output from handles structure
varargout{1} = handles.output;


% --- Executes on button press in import1.
function import1_Callback(hObject, eventdata, handles)
% hObject    handle to import1 (see GCBO)
% eventdata  reserved - to be defined in a future version of MATLAB
% handles    structure with handles and user data (see GUIDATA)
[handles.FileName1, PathName1] = uigetfile('*.txt','Select the Raw
Data for Format 1');
set(handles.Format1,'String',handles.FileName1);

guidata(hObject,handles)



% --- Executes on button press in Analyze1.
function Analyze1_Callback(hObject, eventdata, handles)
% hObject    handle to Analyze1 (see GCBO)
% eventdata  reserved - to be defined in a future version of MATLAB
% handles    structure with handles and user data (see GUIDATA)
%Importing raw data into MATLAB
[date, data] = textread(handles.FileName1,'%s %s','delimiter', ' ');
```

```
rdata = zeros(length(data),4);
rdata1 = num2str(rdata);
for i=1:length(data)
    data_temp = cell2mat(data(i,1));
    if(length(data_temp)<10)
        rdata1(i,(11-length(data_temp)):10) = data_temp(1,:);
    else
        rdata1(i,1:length(data_temp)) = data_temp(1,:);
    end
end

date1 = zeros(length(date),4);
date2 = num2str(date1);
for i=1:length(data)
    date_temp = cell2mat(date(i,1));
    if(length(date_temp)<10)
        date2(i,(11-length(date_temp)):10) = date_temp(1,:);
    else
        date2(i,1:length(date_temp)) = date_temp(1,:);
    end
end

%Extracting number of days
for i=1:length(date)
    [months(i) days(i) year(i)] = strread(date2(i,:), '%s %u %s',
'delimiter' , '-');
end
handles.count1=1;
for i=1:length(days)-1
    if(days(i) ~= days(i+1))
        handles.count1 = handles.count1 + 1;
        m_days(handles.count1) = i;
    end
end
set(handles.days1,'String',num2str(handles.count1));

%Extracting rain intensity data
for i=1:length(rdata1)
    [time(i) r_intensity(i)] = strread(rdata1(i,:), '%s %.2f',
'delimiter', ',');
end

%Detecting orphanage rain intensity for every day #
m_days2 = [m_days length(rdata1)];
for i=1:length(m_days2)-1
        dayN(i,:) = [(m_days2(i)+1) m_days2(i+1)];
end
%Check 3 values before and after for zeros indicating orphanage
r_check = r_intensity;
for i=1:length(dayN)
    for n=(dayN(i,1)+4):dayN(i,2)-4
        if(r_check(n-3)== 0 && r_check(n-2)== 0 && ...
                r_check(n-1)== 0 && r_check(n+1)== 0 && ...
                r_check(n+2)== 0 && r_check(n+3)== 0)
            r_check(n) = 0;
        end
    end
end

%Calculating rain intensity according to day #
```

```
for i=1:length(dayN)
    for m=dayN(i,1):dayN(i,2)-1
        handles.data_intensity1(m) = r_check(m+1) - r_check(m);
    end
    handles.day_intensity1(i) = length(handles.data_intensity1);
end

%Sorting the intensity values and calculate the frequency of
occurence
data_sort = sort(handles.data_intensity1,'descend');
data_sort1 = data_sort.*60;
count_Freq = 1;
for i=1:length(data_sort1)-1
    if((data_sort1(i) - data_sort1(i+1)) > 0.005)
        fsort_val(count_Freq) = data_sort1(i);
        count_Freq = count_Freq + 1;
        fsort_occurence(count_Freq) = i;
    end
end
fsort_occurence2 = [fsort_occurence length(data_sort1)];
for i=1:length(fsort_occurence2)-1
    handles.fsort_oc(i) = fsort_occurence2(i+1) -
fsort_occurence2(i);
end

data_check = zeros(length(handles.data_intensity1),2);
data_check(:,1) = r_check(1:length(handles.data_intensity1));
data_check(:,2) = handles.data_intensity1;

%csvwrite('check_data1.csv',data_check);
%winopen('check_data1.csv');

%Summation of fsort and graph
for i=1:length(fsort_val)
    if (fsort_val(i) > 0)
        handles.fsort_val2(i) = fsort_val(i);
    end
end
sum = 0;
for i=1:length(handles.fsort_val2)
    handles.fsort_oc2(i) = handles.fsort_oc(i) + sum;
    sum = sum + handles.fsort_oc(i);
end

handles.log_out1 = (handles.fsort_oc2 ./ (handles.count1 * 24 * 60))
.* 100;

guidata(hObject,handles)

% --- Executes on button press in Graph1.
function Graph1_Callback(hObject, eventdata, handles)
% hObject    handle to Graph1 (see GCBO)
% eventdata  reserved - to be defined in a future version of MATLAB
% handles    structure with handles and user data (see GUIDATA)
%set(handles.axes2, 'Visible', 'on');
axes(handles.axes2)
%plot(handles.fsort_oc2,handles.fsort_val2);
plot(handles.log_out1,handles.fsort_val2);
set(handles.axes2,'XScale','log');
```

```
grid on;
xlabel('% of exceeded');
ylabel('Rain Intensity (mm/hr)');

guidata(hObject,handles)




% --- Executes on button press in import2.
function import2_Callback(hObject, eventdata, handles)
% hObject    handle to import2 (see GCBO)
% eventdata  reserved - to be defined in a future version of MATLAB
% handles    structure with handles and user data (see GUIDATA)
[handles.FileName2, PathName2] = uigetfile('*.txt','Select the Raw
Data for Format 1');
set(handles.Format2,'String',handles.FileName2);

guidata(hObject,handles)

% --- Executes on button press in Analyze2.
function Analyze2_Callback(hObject, eventdata, handles)
% hObject    handle to Analyze2 (see GCBO)
% eventdata  reserved - to be defined in a future version of MATLAB
% handles    structure with handles and user data (see GUIDATA)
%Importing raw data into MATLAB
[date, data] = textread(handles.FileName2,'%s %s','delimiter', ' ');
rdata = zeros(length(data),4);
rdata1 = num2str(rdata);
for i=1:length(data)
    data_temp = cell2mat(data(i,1));
    if(length(data_temp)<10)
        rdata1(i,(11-length(data_temp)):10) = data_temp(1,:);
    else
        rdata1(i,1:length(data_temp)) = data_temp(1,:);
    end
end

date1 = zeros(length(date),4);
date2 = num2str(date1);
for i=1:length(data)
    date_temp = cell2mat(date(i,1));
    if(length(date_temp)<10)
        date2(i,(11-length(date_temp)):10) = date_temp(1,:);
    else
        date2(i,1:length(date_temp)) = date_temp(1,:);
    end
end

%Extracting number of days
for i=1:length(date)
    [months(i) days(i) year(i)] = strread(date2(i,:), '%s %u %s',
'delimiter' , '/');
end
handles.count2=1;
for i=1:length(days)-1
    if(days(i) ~= days(i+1))
        handles.count2 = handles.count2 + 1;
        m_days(handles.count2) = i;
```

```
    end
end
set(handles.days2,'String',num2str(handles.count2));

%Extracting rain intensity data
for i=1:length(rdata1)
    [time(i) r_intensity(i)] = strread(rdata1(i,:), '%s %.2f',
'delimiter', ',');
end

%Detecting orphanage rain intensity for every day #
m_days2 = [m_days length(rdata1)];
for i=1:length(m_days2)-1
        dayN(i,:) = [(m_days2(i)+1) m_days2(i+1)];
end
%Check 3 values before and after for zeros indicating orphanage
r_check = r_intensity;
for i=1:length(dayN)
    for n=(dayN(i,1)+4):dayN(i,2)-4
        if(r_check(n-3)== 0 && r_check(n-2)== 0 && ...
                r_check(n-1)== 0 && r_check(n+1)== 0 && ...
                r_check(n+2)== 0 && r_check(n+3)== 0)
            r_check(n) = 0;
        end
    end
end

%Calculating rain intensity according to day #
for i=1:length(dayN)
    for m=dayN(i,1):dayN(i,2)-1
        handles.data_intensity2(m) = r_check(m+1) - r_check(m);
    end
    handles.day_intensity2(i) = length(handles.data_intensity2);
end

%Sorting the intensity values and calculate the frequency of
occurence
data_sort = sort(handles.data_intensity2,'descend');
data_sort1 = data_sort.*60;
count_Freq = 1;
for i=1:length(data_sort1)-1
    if((data_sort1(i) - data_sort1(i+1)) > 0.005)
        fsort_val(count_Freq) = data_sort1(i);
        count_Freq = count_Freq + 1;
        fsort_occurence(count_Freq) = i;
    end
end
fsort_occurence2 = [fsort_occurence length(data_sort1)];
for i=1:length(fsort_occurence2)-1
    handles.fsort_oc12(i) = fsort_occurence2(i+1) -
fsort_occurence2(i);
end

%Summation of fsort and graph
for i=1:length(fsort_val)
    if (fsort_val(i) > 0)
        handles.fsort_val22(i) = fsort_val(i);
    end
end
sum = 0;
```

```
for i=1:length(handles.fsort_val22)
    handles.fsort_oc22(i) = handles.fsort_oc12(i) + sum;
    sum = sum + handles.fsort_oc12(i);
end

handles.log_out2 = (handles.fsort_oc22 ./ (handles.count2 * 24 * 60))
.* 100;

guidata(hObject,handles)

% --- Executes on button press in Graph2.
function Graph2_Callback(hObject, eventdata, handles)
% hObject    handle to Graph2 (see GCBO)
% eventdata  reserved - to be defined in a future version of MATLAB
% handles    structure with handles and user data (see GUIDATA)
%set(handles.axes2, 'Visible', 'on');
axes(handles.axes2)
plot(handles.log_out2,handles.fsort_val22);
set(handles.axes2,'XScale','log');
grid on;
xlabel('% of exceeded');
ylabel('Rain Intensity (mm/hr)');

guidata(hObject,handles)



% --- Executes on button press in Combine.
function Combine_Callback(hObject, eventdata, handles)
% hObject    handle to Combine (see GCBO)
% eventdata  reserved - to be defined in a future version of MATLAB
% handles    structure with handles and user data (see GUIDATA)
handles.data_intensityUpdate = [handles.data_intensity1
handles.data_intensity2];

%Sorting the intensity values and calculate the frequency of
occurence
data_sort = sort(handles.data_intensityUpdate,'descend');
data_sort1 = data_sort.*60;
count_Freq = 1;
for i=1:length(data_sort1)-1
    if((data_sort1(i) - data_sort1(i+1)) > 0.005)
        fsort_val(count_Freq) = data_sort1(i);
        count_Freq = count_Freq + 1;
        fsort_occurence(count_Freq) = i;
    end
end
fsort_occurence2 = [fsort_occurence length(data_sort1)];
for i=1:length(fsort_occurence2)-1
    handles.fsort_ocUpdate1(i) = fsort_occurence2(i+1) -
fsort_occurence2(i);
end

%Summation of fsort and graph
for i=1:length(fsort_val)
    if (fsort_val(i) > 0)
        handles.fsort_valUpdate(i) = fsort_val(i);
    end
end
```

```
sum = 0;
for i=1:length(handles.fsort_valUpdate)
    handles.fsort_ocUpdate2(i) = handles.fsort_ocUpdate1(i) + sum;
    sum = sum + handles.fsort_ocUpdate1(i);
end

handles.countFinal = handles.count1 + handles.count2;

handles.log_outFinal = (handles.fsort_ocUpdate2 ./
(handles.countFinal * 24 * 60)) * 100;

axes(handles.axes2)
plot(handles.log_outFinal,handles.fsort_valUpdate);
set(handles.axes2,'XScale','log');
grid on;
xlabel('% of exceeded');
ylabel('Rain Intensity (mm/hr)');

figure()
plot(handles.log_outFinal,handles.fsort_valUpdate);
set(gca, 'XScale', 'log');
grid on;
xlabel('% of exceeded');
ylabel('Rain Intensity (mm/hr)');


%length(handles.fsort_valUpdate)
%length(handles.fsort_ocUpdate1)
%length(handles.fsort_ocUpdate2)

handles.output = zeros(length(handles.fsort_valUpdate),4);
handles.output(:,1) = handles.fsort_valUpdate';
handles.output(:,2) =
handles.fsort_ocUpdate1(1,1:length(handles.fsort_valUpdate))';
handles.output(:,3) = handles.fsort_ocUpdate2';
handles.output(:,4) = handles.log_outFinal';

guidata(hObject,handles)

% --- Executes on button press in Reset.
function Reset_Callback(hObject, eventdata, handles)
% hObject    handle to Reset (see GCBO)
% eventdata  reserved - to be defined in a future version of MATLAB
% handles    structure with handles and user data (see GUIDATA)
%set(handles.axes2, 'Visible', 'off');
set(handles.Format1,'String', 'Import File 1');
set(handles.Format2,'String', 'Import File 2');
set(handles.FileName, 'String', 'data.csv');
set(handles.days1, 'String', ' ');
set(handles.days2, 'String', ' ');
clear all;

% --- Executes on button press in ExportCSV.
function ExportCSV_Callback(hObject, eventdata, handles)
% hObject    handle to ExportCSV (see GCBO)
% eventdata  reserved - to be defined in a future version of MATLAB
% handles    structure with handles and user data (see GUIDATA)
FName = get(handles.FileName, 'String');
csvwrite(FName, handles.output);
```

```
guidata(hObject,handles)

% --- Executes on button press in Close.
function Close_Callback(hObject, eventdata, handles)
% hObject    handle to Close (see GCBO)
% eventdata  reserved - to be defined in a future version of MATLAB
% handles    structure with handles and user data (see GUIDATA)
close all




function FileName_Callback(hObject, eventdata, handles)
% hObject    handle to FileName (see GCBO)
% eventdata  reserved - to be defined in a future version of MATLAB
% handles    structure with handles and user data (see GUIDATA)

% Hints: get(hObject,'String') returns contents of FileName as text
%        str2double(get(hObject,'String')) returns contents of
FileName as a double


% --- Executes during object creation, after setting all properties.
function FileName_CreateFcn(hObject, eventdata, handles)
% hObject    handle to FileName (see GCBO)
% eventdata  reserved - to be defined in a future version of MATLAB
% handles    empty - handles not created until after all CreateFcns
called

% Hint: edit controls usually have a white background on Windows.
%       See ISPC and COMPUTER.
if ispc && isequal(get(hObject,'BackgroundColor'),
get(0,'defaultUicontrolBackgroundColor'))
    set(hObject,'BackgroundColor','white');
end
```

APPENDIX F


Sentry™
Visibility Sensor
Now with 24 month factory warranty!
Rain
Snow
Fog
Smoke
Dust
- - - Key Features - - -
Factory adjustable visibility ranges
Proven 42-degree forward scatter angle
Compact, lightweight package
Flexible output options
Ice-resistant "look down" geometry
Simple installation & maintenance
EnviroTech Sensors Inc.
www.envirotechsensors.com

Sentry™ Visibility Sensor

Measures atmospheric visibility (meteorological optical range) by determining the amount of light scattered by particles (smoke, dust, haze, fog, rain, & snow) in the air that pass through the optical sample volume. A 42-degree forward scatter angle is used to ensure performance over a wide range of particle sizes. MOR is calculated by converting the received signal strength (extinction coefficient, σ) using Koschmeider's formula, MOR (Km) = 3/σ.

Performance in all weather conditions is achieved with an integrated sensor design that keeps all sensor cabling internal to the sensor for complete protection against the weather. The sensor is made from anodized aluminum and rugged, UV-resistant fiberglass enclosures rated to IP66. Based on the proven field experience of the NWS and FAA, the sensor uses a "look down" geometry to reduce window contamination and clogging from blowing snow. The optical windows have continuous duty anti-dew heaters and optional thermostatically controlled external hood heaters are available for protection in extreme environments. All power and signal lines to the Sentry™ are protected with surge and EMI filtering to help guarantee uninterrupted service for the life of the sensor.

Installation and maintenance are simple with the Sentry™. A mounting flange located on the bottom of the Main Enclosure Box mates with a user supplied 1-1/2 inch IPS mounting pipe. Power and signal cables are installed through waterproof cable glands on the bottom of the Main Enclosure Box to terminal boards for simple but reliable connections.

Calibration of the Sentry™ in the field is as simple as attaching a factory supplied calibration fixture and following a procedure that takes less than 30 minutes. Semiannual calibration is recommended.

Specifications

Performance

Visibility Range: 30m - 16 km standard; 10m - 10 km optional

Accuracy: +/- 10% RMSE

Time Constant: 60 sec

Scatter Angle: 42 deg nominal

Source: 880 nm LED

Outputs: 0-10 VDC analog standard

Output Options:

- 0-5 VDC analog
- 4-20 ma single ended or isolated
- Relays - Control (up to 2), diagnostic, or latching
- Serial RS-232, RS-422, or RS-485
- Wireless RF Modem

Extinction Range: 100 – 0.1863 km^{-1} standard; 300 – 0.30 km^{-1} optional

Power

AC Version: 100-240 VAC, 24 VA Nominal; 75 VA w/ Hood Heaters

DC Version: 10-36 VDC, 6 VA Nominal; 18 VA w/ Hood Heaters

Physical

Weight: 8 kg (18 lb)

Dimensions: 889 mm W x 292 mm H x 305 mm D (35 in x 11.5 in x 12 in)

Mounting: Nominal 40 mm ISO pipe, 48 mm OD max (1-1/2" IPS pipe, 1.9 inch OD max) or Nominal 25 mm ISO pipe, 33 mm OD max (1" IPS pipe, 1.3 inch OD max)

Environmental

Operating Temperature: -40 to 60 C

Operating Humidity: 0-100%

Protection: IP66 (NEMA-4X)

CE This equipment is in compliance with the essential requirements and other provisions of Low Voltage Directives 73/23/EEC and 89/336/EEC as amended by Directive 93/68/EEC.

Airport

Coastal/Maritime

- Applications for the Sentry™ Visibility Sensor -

Roads/Bridges

Tunnels

Ordering Information

Sentry™ Visibility Sensor Model SVS1-xx-y-H-P

Where "xx" = mains voltage (AC = 100-240 VAC, DC = 10-36 VDC)

"y" = output option (Select from Options Brochure or Price List)

"H" = hood heaters (Blank = none, H = yes)

"P" = mounting flange (Blank = 1-1/2", P = 1")

- See Option & Accessory Brochure and Price List for more information -

- List any optional range requirements on the purchase order -

EnviroTech Sensors Inc.

P.O. Box 794
Clarksville, MD 21029 USA
Phone: 410.531.8596 / Fax: 410.531.7010
www.envirotechsensors.com

3/08

APPENDIX G

ETHERNET TEST SET

AXS-200/850

part of the SharpTESTER Access Line

NETWORK TESTING–ACCESS

Features/Benefits

- User-definable RFC 2544 test routines
- Bit-error-rate testing (BERT) up to layer 4
- Pass/fail results (LED indicators) with user-defined thresholds
- Configurable VLAN and Q-in-Q capability
- QoS, ToS and diffserv capabilities
- Intelligent network autodiscovery for simplified loopback testing
- Compact, rugged, lightweight unit

www.EXFO.com
Telecom Test and Measurement

EXFO
EXPERTISE REACHING OUT

Simplifying Ethernet Testing

Part of EXFO's wide-ranging Ethernet test offering, the AXS-200/850 Ethernet Test Set delivers comprehensive test functionalities without the typical complexity associated with Ethernet/IP testing. Whether for installing, turning up or maintaining Ethernet and IP services, the AXS-200/850 is ready to perform. Thanks to a feature set that includes RFC 2544, BERT, as well as IP connectivity tools such as ping and Traceroute, this lightweight, handheld unit provides front-line technicians with all the tools they need to get through their test cycles quickly and efficiently.

Quick Access to Test Results

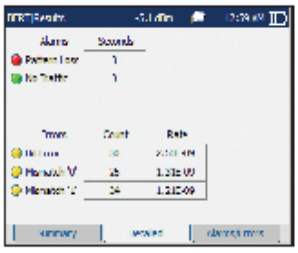

Ethernet alarms/errors

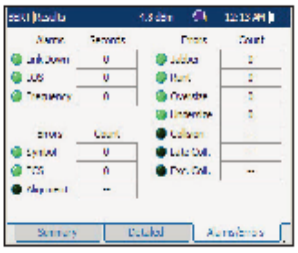

BERT errors.

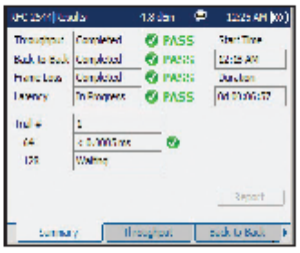

RFC 2544 results.

Key Features

Bit-error-rate testing (BERT)	BERT up to layer 4 with a wide range of standard and customizable patterns.
RFC 2544	Industry-standard range of tests: throughput, back-to-back, frame loss and latency.
VLAN with Q-in-Q	Encapsulates up to two VLAN layers for all tests including the modification of VLAN ID, priority, type and drop eligibility.
Traffic generation	Increases or decreases the bandwidth and frame size in real time.
Intelligent autodiscovery	Finds multiple remote AXS-200/850 units and loop them up or down for loopback testing.
Smart Loopback	Loopbacks incoming test traffic up to layer 4.
Optical power measurement	Optical power readings available during all testing phases.
Interoperability with Packet Blazer units	Interoperates with EXFO's Packet Blazer Ethernet test module series–the FTB-8510, FTB-8510B, FTB-8510G, FTB-8120NGE and FTB-8130NGE.

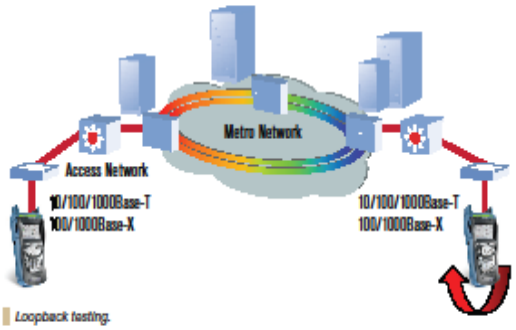

Loopback testing.

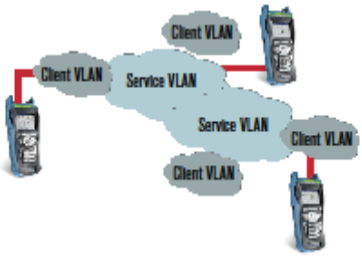

Q-in-Q testing.

www.EXFO.com

APPENDIX H

H.1. 0.1 mm/tip and 0.2 mm/tip resolution rain gauge measurement comparison

There are thirty (30) data presented in this section as a verification of the technical flaw on using 0.1 mm per tip resolution over 0.2 mm per tip resolution rain gauge as the rain intensity measurement.

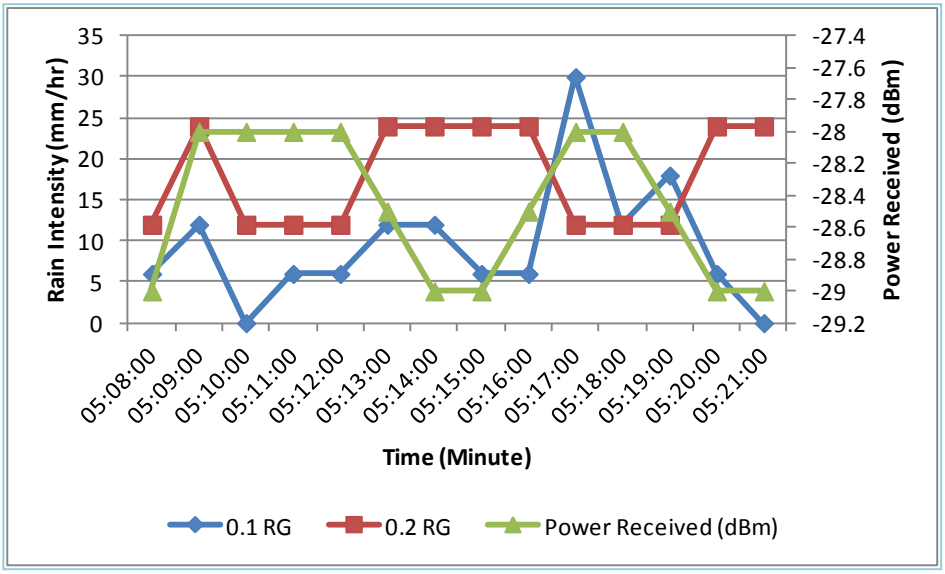

Figure H.1: Comparison data of 8 March 2011

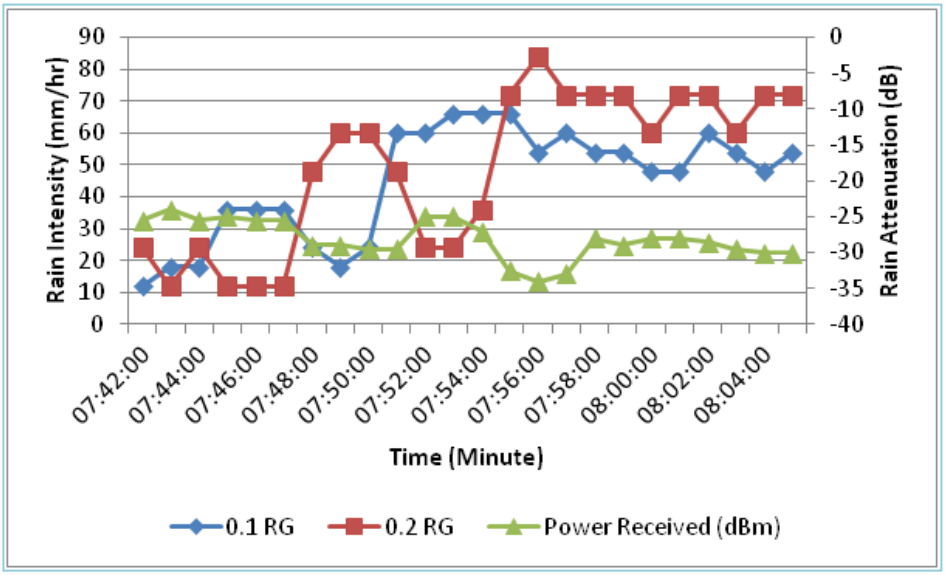

Figure H.2: Comparison data of 16 March 2011

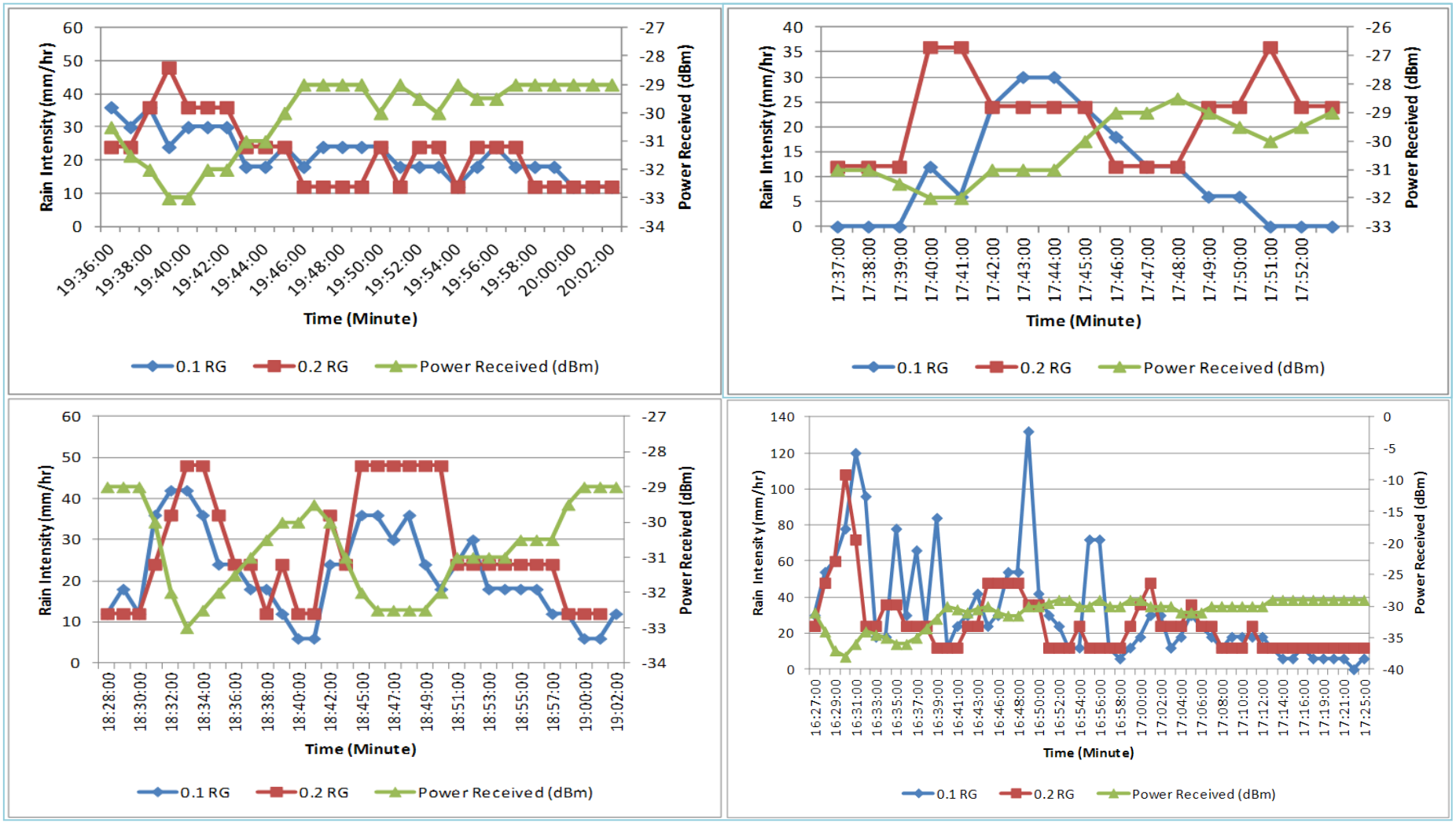

Figure H.3: Comparison data of 14 April, 20 April, 2 May and 3 May 2011 respectively

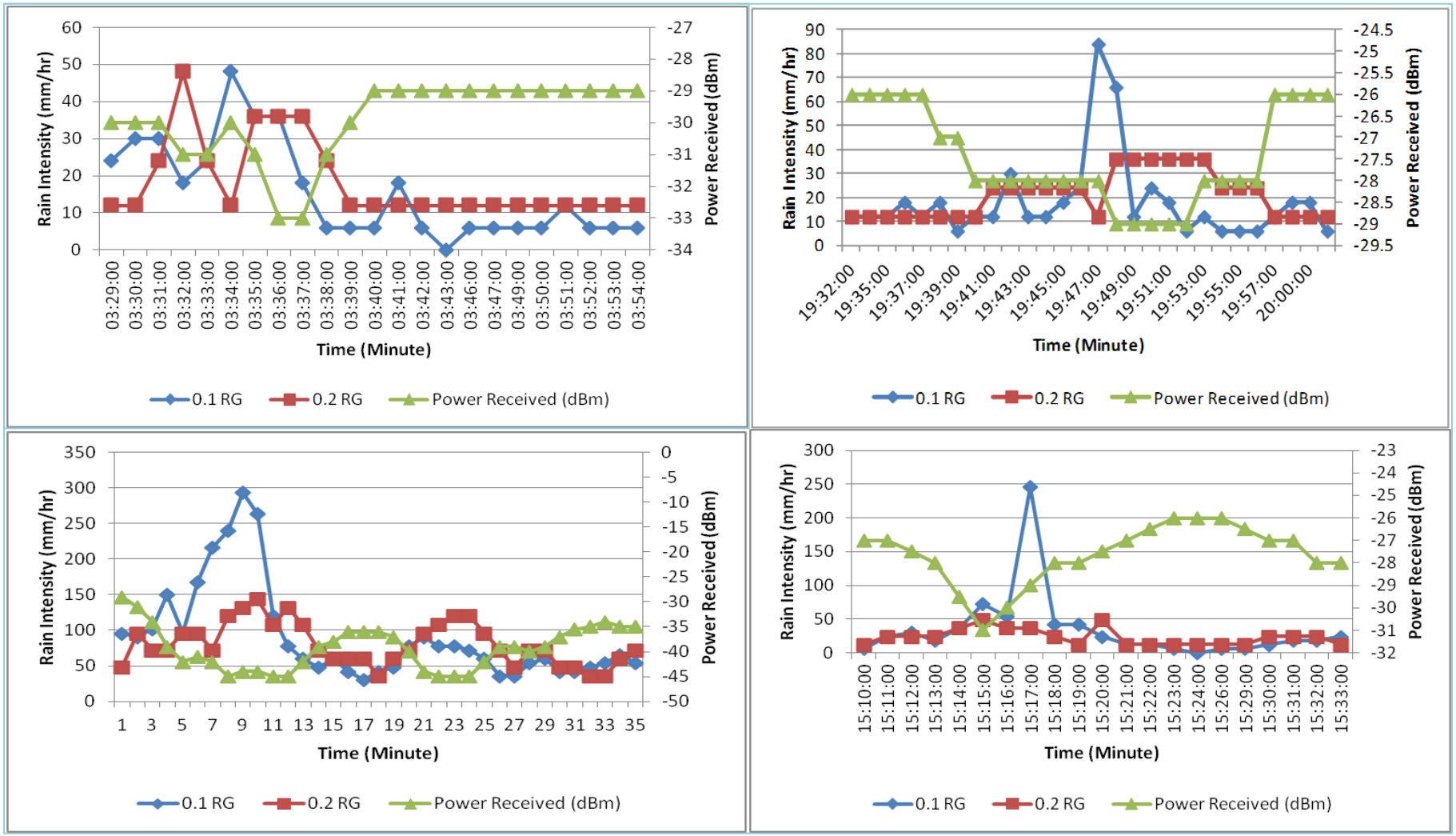

Figure H.4: Comparison data of 4 May, 18 May, 19 May and 20 May 2011 respectively

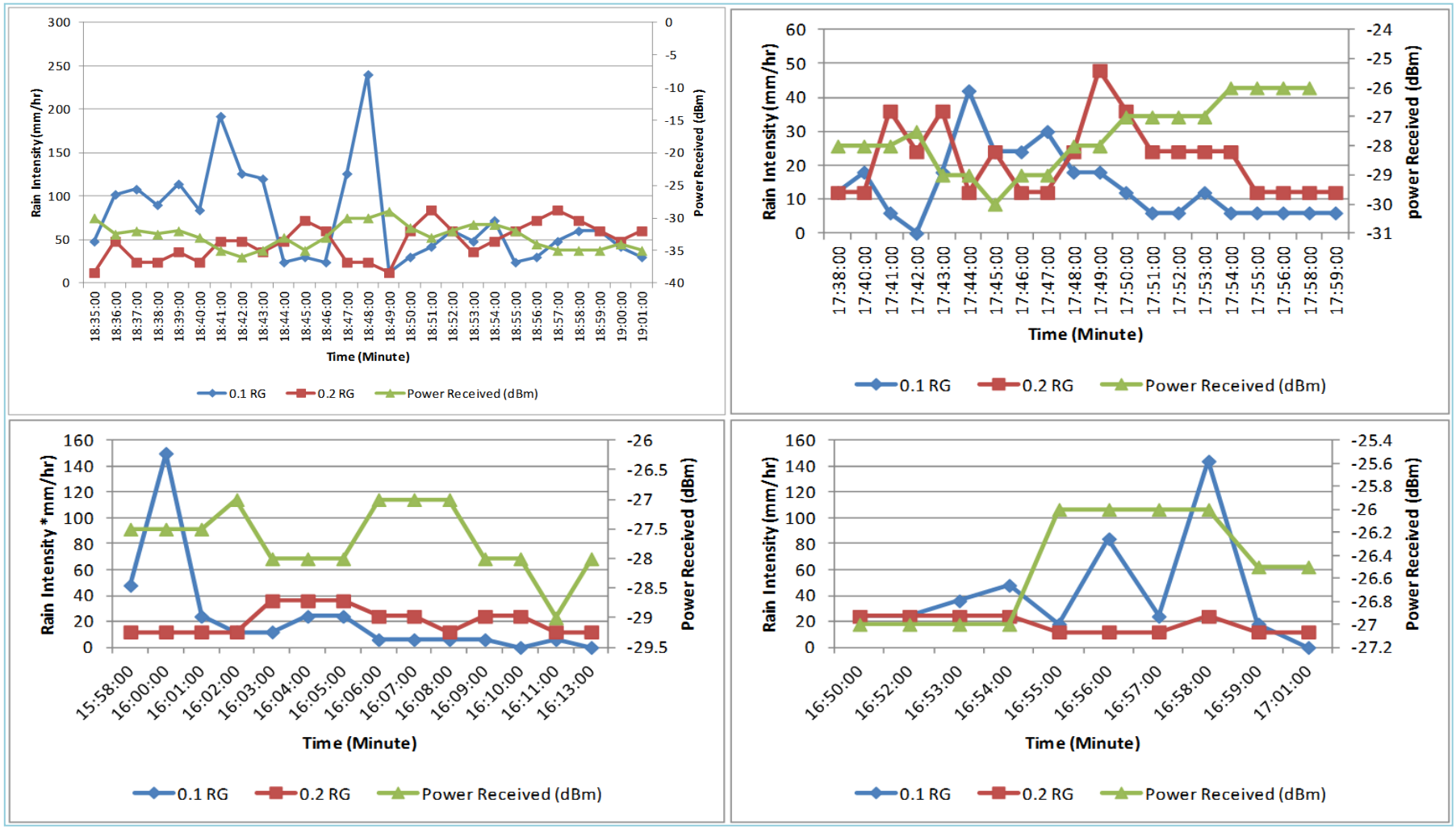

Figure H.5: Comparison data of 15 July, 4 August, 14 August and 15 August 2011 respectively

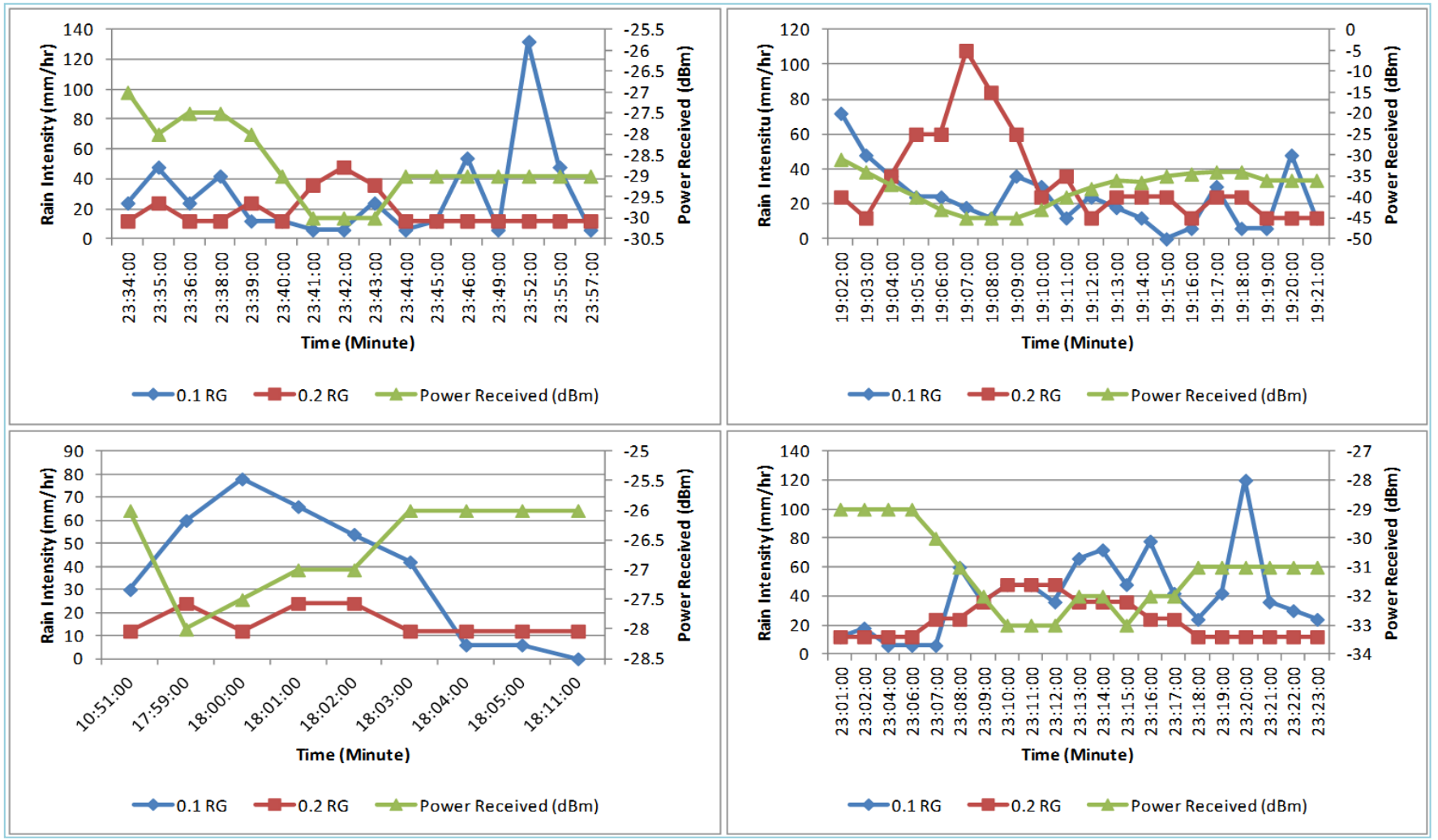

Figure H.6: Comparison data of 19 August, 20 August, 21 August and 10 September 2011 respectively

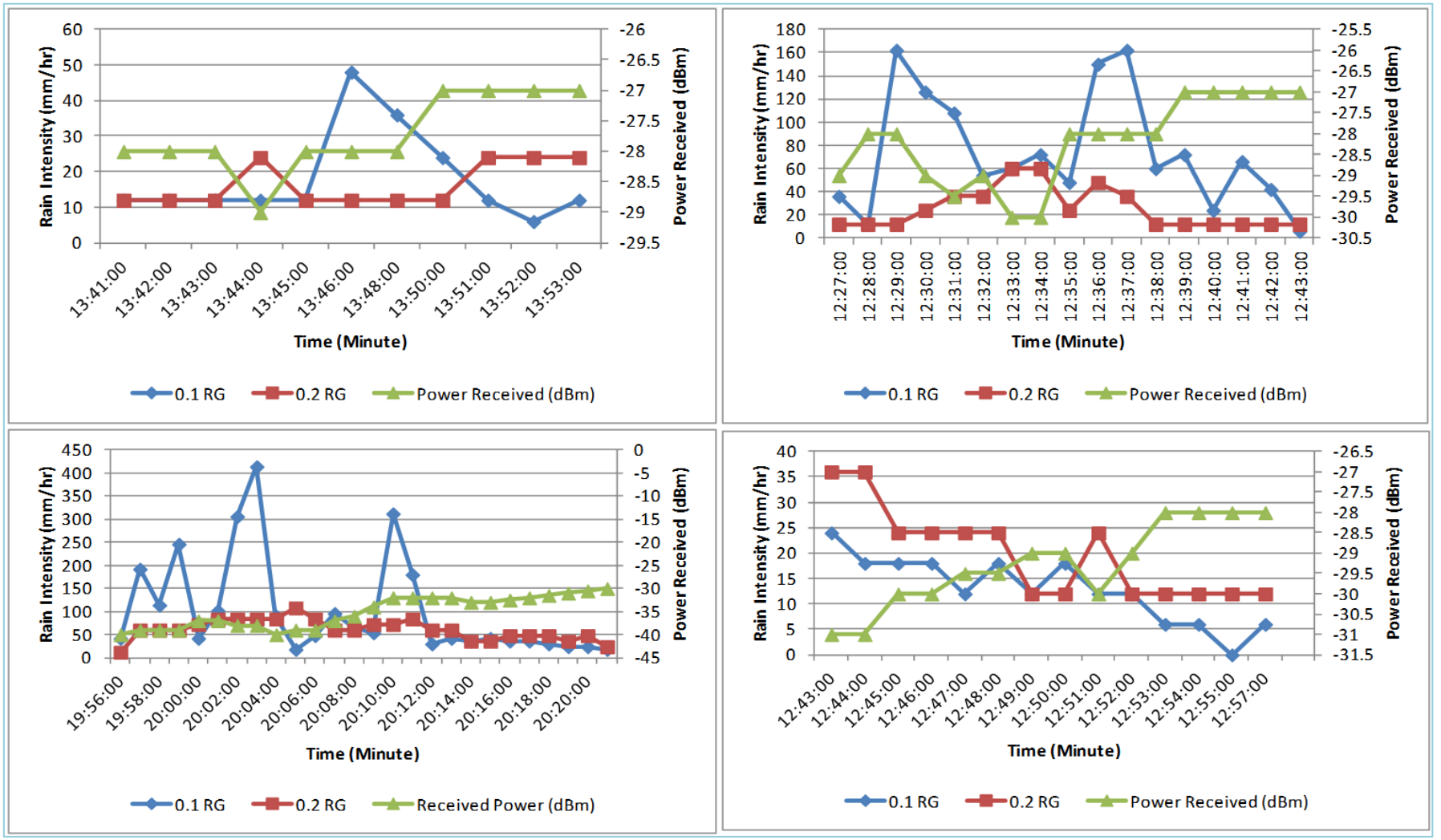

Figure H.7: Comparison data of 11 September, 12 September, 13 September t and 14 September 2011 respectively

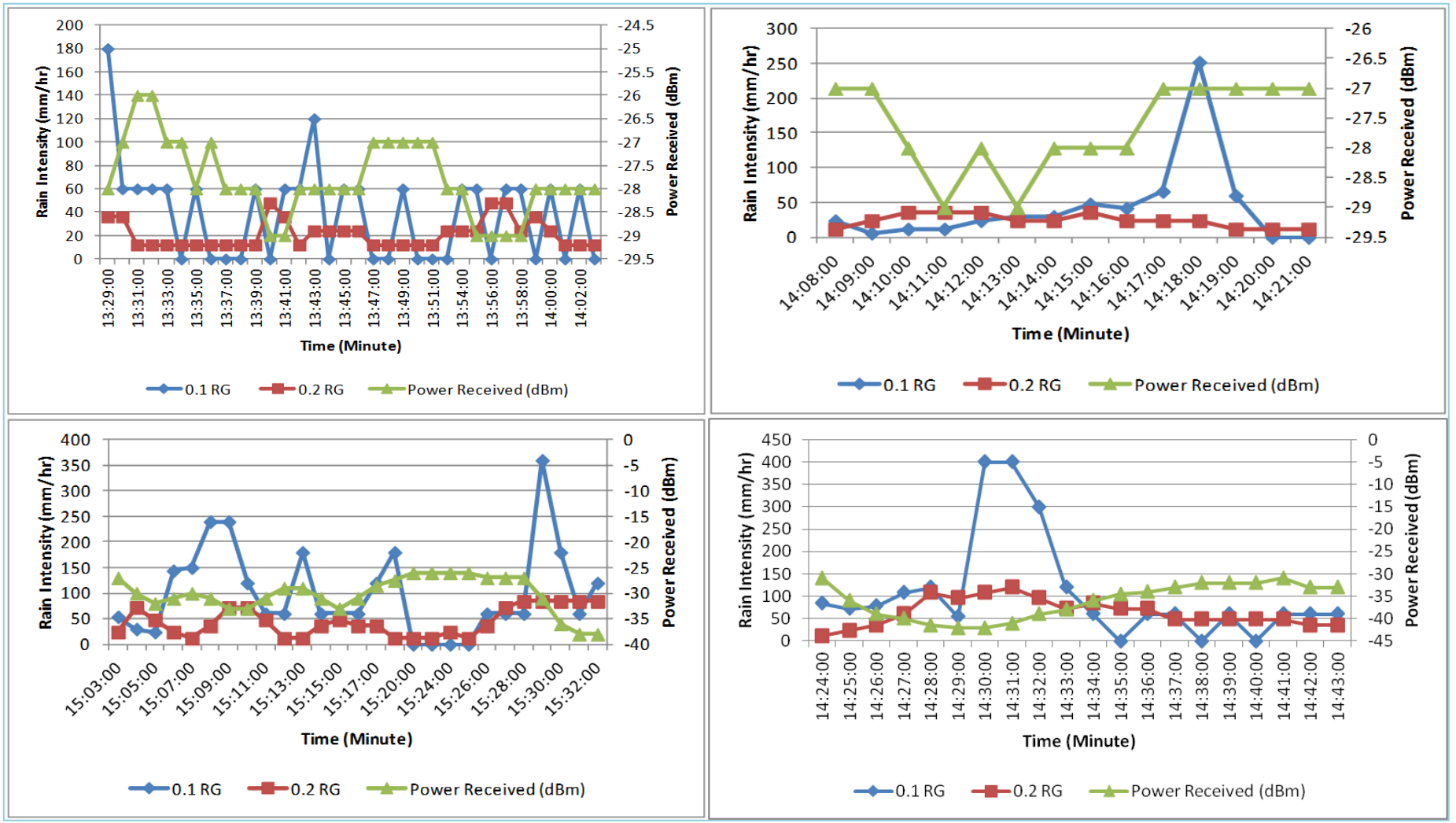

Figure H.8: Comparison data of 4 October, 5 October, 7 October and 15 October 2011 respectively

Figure H.9: Comparison data of 17 October, 2 November, 4 November and 13 November 2011 respectively

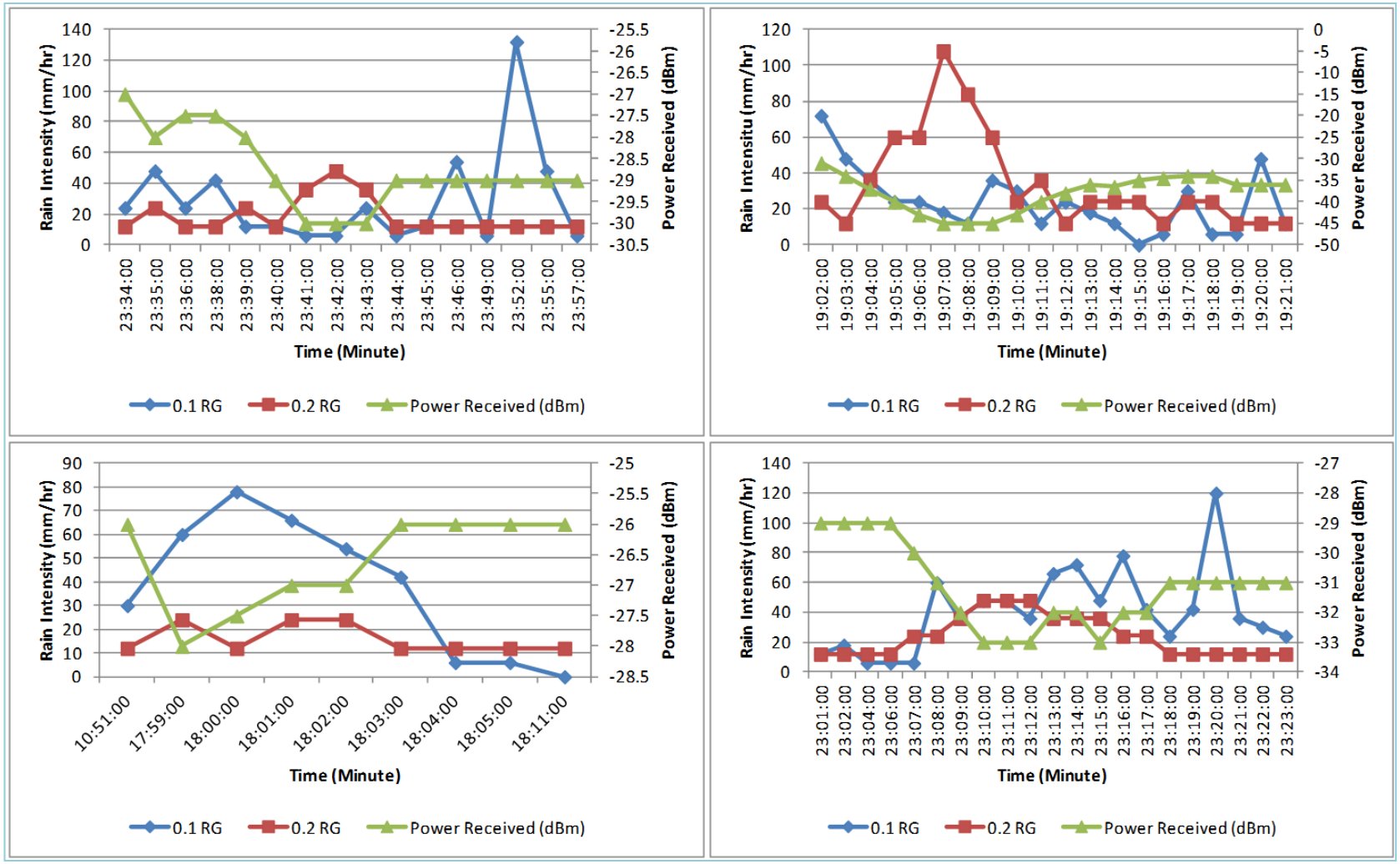

Figure H.6: Comparison data of 19 August, 20 August, 21 August and 10 September 2011 respectively

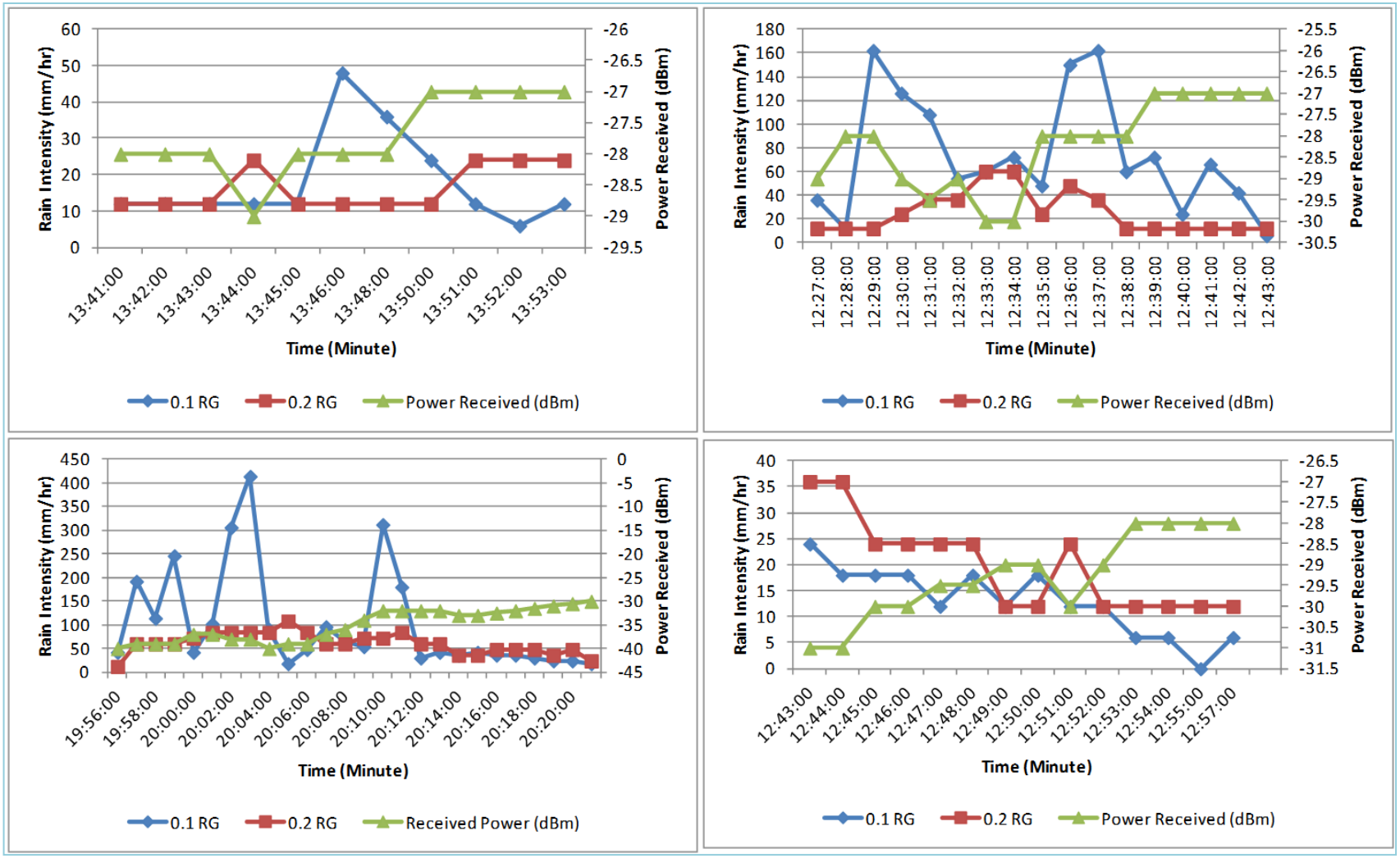

Figure H.7: Comparison data of 11 September, 12 September, 13 September t and 14 September 2011 respectively

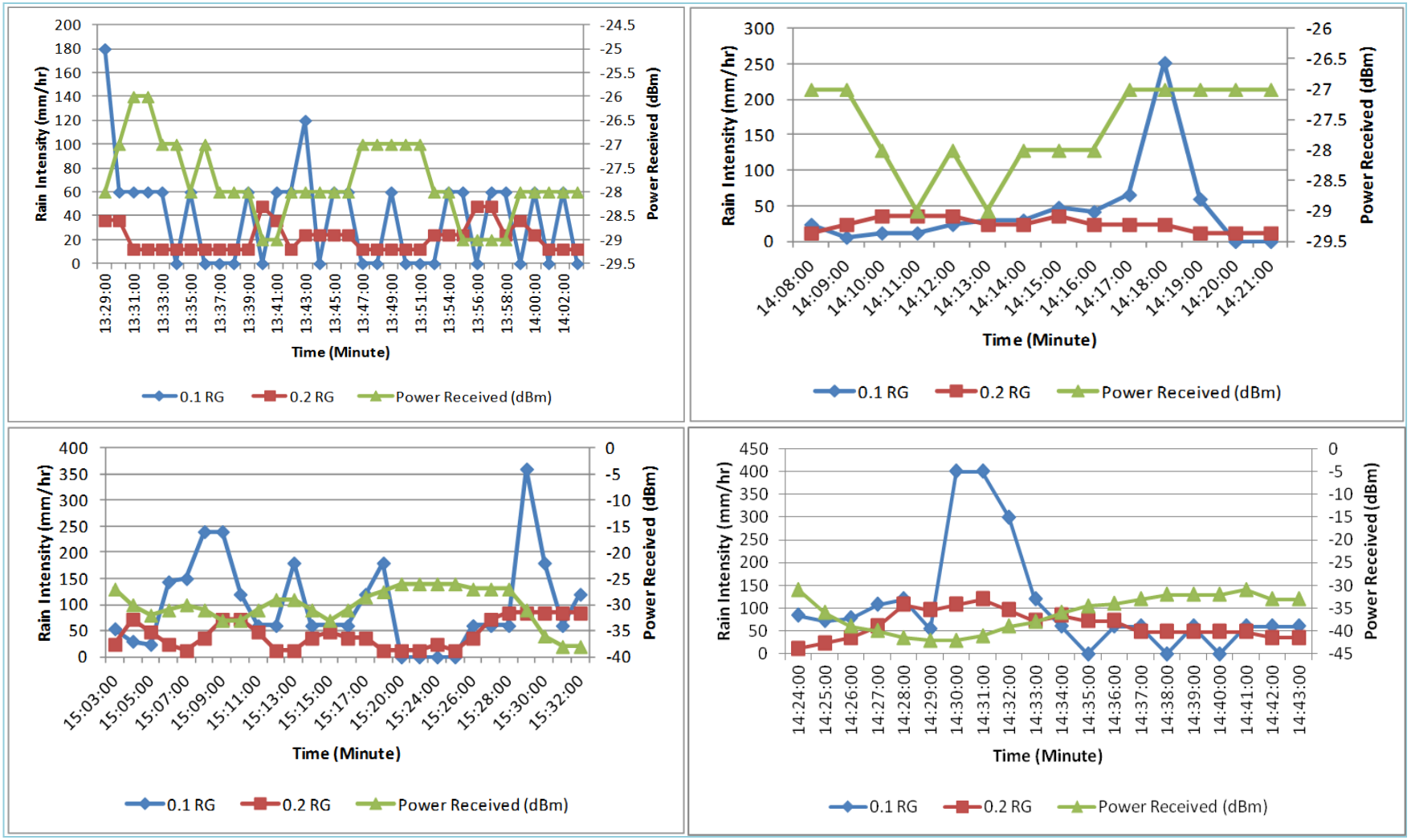

Figure H.8: Comparison data of 4 October, 5 October, 7 October and 15 October 2011 respectively

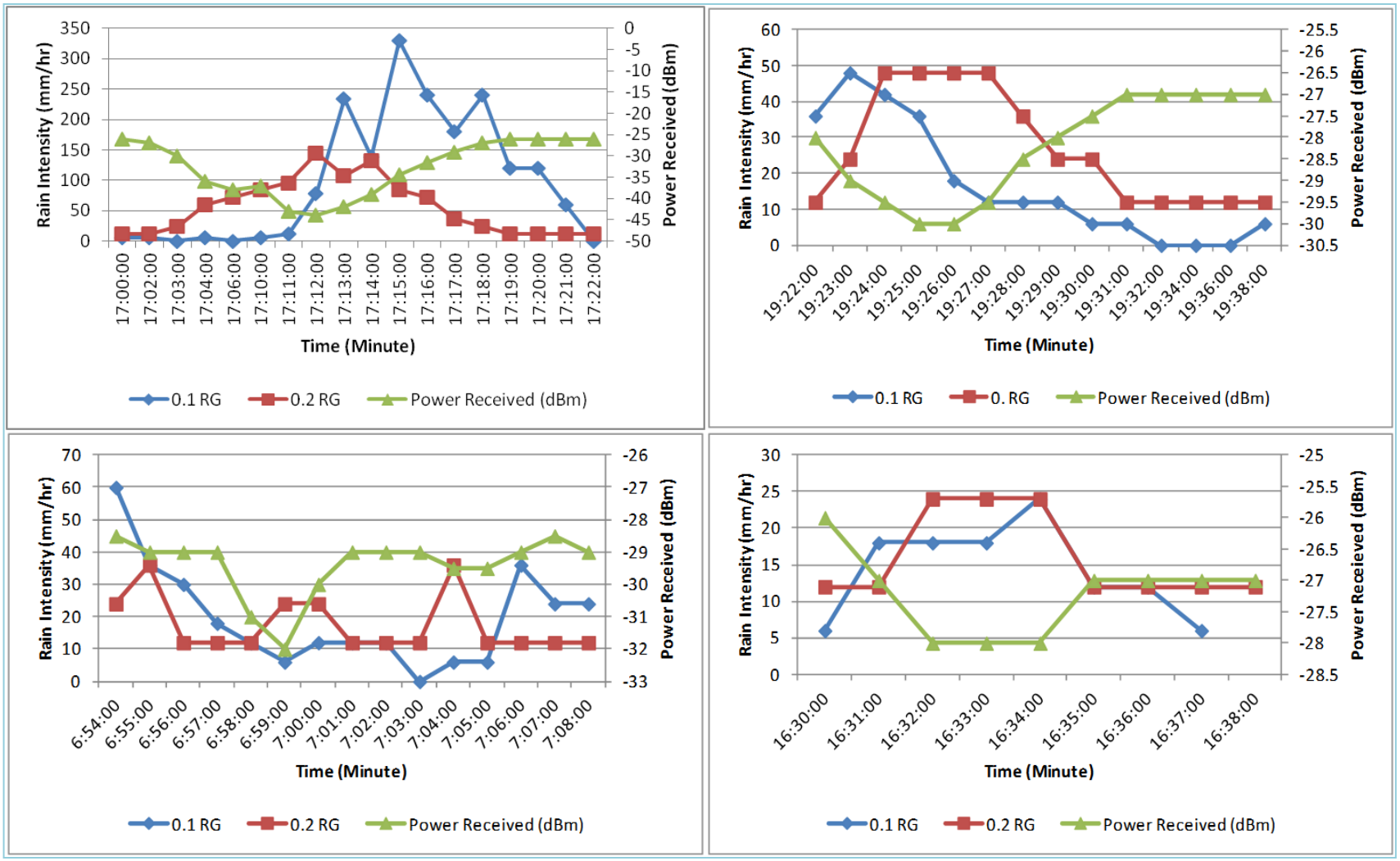

Figure H.9: Comparison data of 17 October, 2 November, 4 November and 13 November 2011 respectively

Table J.3(a): Calculation of predicted rain attenuation with varying k and α

Rain Intensity (mm/hr)	Measured Rain Attenuation (dB/km)	Predicted Rain Attenuation $A=1.2158R^{0.6}$ (dB/km)	Predicted Rain Attenuation $A=1.0693R^{0.63}$ (dB/km)	Predicted Rain Attenuation $A=0.7757R^{0.65}$ (dB/km)	Predicted Rain Attenuation $A=0.9010R^{0.67}$ (dB/km)	Predicted Rain Attenuation $A=0.7925R^{0.7}$ (dB/km)	Predicted Rain Attenuation $A=0.6398R^{0.75}$ (dB/km)
158	26.50	25.3546	25.9569	20.8363	26.7809	27.4195	28.5126
154	26.38	24.9675	25.5410	20.4919	26.3247	26.9317	27.9695
149	26.25	24.4779	25.0154	20.0569	25.7490	26.3166	27.2856
146	26.13	24.1810	24.6969	19.7935	25.4004	25.9446	26.8725
144	26.00	23.9817	24.4832	19.6169	25.1668	25.6953	26.5960
138	25.88	23.3770	23.8355	19.0816	24.4593	24.9410	25.7605
132	25.75	22.7618	23.1772	18.5382	23.7416	24.1769	24.9158
126	25.63	22.1353	22.5078	17.9860	23.0130	23.4023	24.0615
125	25.50	22.0297	22.3951	17.8931	22.8905	23.2721	23.9181
123	25.38	21.8175	22.1687	17.7065	22.6444	23.0109	23.6305
122	25.31	21.7109	22.0550	17.6128	22.5209	22.8797	23.4863
121	25.25	21.6040	21.9409	17.5188	22.3971	22.7483	23.3417
119	25.13	21.3890	21.7117	17.3300	22.1483	22.4844	23.0518
118	25.06	21.2810	21.5966	17.2352	22.0235	22.3520	22.9063
117	25.00	21.1726	21.4811	17.1401	21.8982	22.2192	22.7606
115	24.69	20.9547	21.2490	16.9491	21.6467	21.9527	22.4682
114	24.38	20.8452	21.1324	16.8532	21.5204	21.8189	22.3215
113	24.25	20.7352	21.0155	16.7569	21.3938	21.6847	22.1745
111	23.63	20.5143	20.7804	16.5636	21.1393	21.4154	21.8795
108	23.00	20.1798	20.4247	16.2712	20.7548	21.0085	21.4344
105	22.50	19.8416	20.0654	15.9760	20.3667	20.5983	20.9863
103	21.88	19.6139	19.8238	15.7775	20.1060	20.3229	20.6858
96	21.50	18.8029	18.9640	15.0720	19.1799	19.3459	19.6222
90	20.00	18.0887	18.2084	14.4528	18.3682	18.4914	18.6950
87	19.38	17.7245	17.8237	14.1378	17.9557	18.0577	18.2257
85	18.75	17.4789	17.5644	13.9257	17.6781	17.7661	17.9105
83	18.13	17.2309	17.3029	13.7118	17.3983	17.4725	17.5935
78	17.75	16.6004	16.6387	13.1691	16.6889	16.7288	16.7925
76	16.88	16.3437	16.3686	12.9486	16.4010	16.4274	16.4685
75	16.50	16.2143	16.2326	12.8376	16.2561	16.2758	16.3057
74	16.38	16.0843	16.0959	12.7261	16.1105	16.1236	16.1424
73	16.25	15.9535	15.9585	12.6140	15.9643	15.9707	15.9785
71	15.63	15.6898	15.6817	12.3883	15.6700	15.6632	15.6491
69	15.25	15.4231	15.4019	12.1603	15.3728	15.3530	15.3173
66	15.13	15.0172	14.9766	11.8140	14.9217	14.8826	14.8150
63	15.00	14.6038	14.5440	11.4621	14.4638	14.4058	14.3070
62	14.38	14.4643	14.3981	11.3435	14.3096	14.2454	14.1364
61	13.75	14.3239	14.2514	11.2243	14.1545	14.0841	13.9650
56	13.13	13.6074	13.5039	10.6173	13.3663	13.2657	13.0974
53	12.75	13.1652	13.0435	10.2441	12.8822	12.7642	12.5676
51	12.50	12.8648	12.7312	9.9911	12.5544	12.4251	12.2102
50	11.38	12.7129	12.5733	9.8633	12.3890	12.2540	12.0302
48	10.50	12.4053	12.2541	9.6051	12.0547	11.9088	11.6674
44	9.25	11.7743	11.6004	9.0769	11.3720	11.2051	10.9303
38	8.75	10.7828	10.5770	8.2519	10.3081	10.1122	9.7922
34	7.88	10.0867	9.8612	7.6764	9.5679	9.3548	9.0085
28	7.50	8.9775	8.7259	6.7662	8.4008	8.1660	7.7878
26	6.50	8.5871	8.3278	6.4480	7.9939	7.7532	7.3667
24	6.25	8.1844	7.9183	6.1211	7.5765	7.3307	6.9375
23	5.63	7.9781	7.7088	5.9541	7.3635	7.1156	6.7195
18	5.38	6.8869	6.6057	5.0772	6.2482	5.9936	5.5911
15	4.13	6.1733	5.8889	4.5098	5.5298	5.2755	4.8765
12	3.13	5.3997	5.1166	3.9009	4.7619	4.5126	4.1251

Table J.3(b): Calculation of predicted rain attenuation with varying k and α

Rain Intensity (mm/hr)	Measured Rain Attenuation (dB/km)	Predicted Rain Attenuation $A=0.5873R^{0.77}$ (dB/km)	Predicted Rain Attenuation $A=0.5165R^{0.8}$ (dB/km)	Predicted Rain Attenuation $A=0.4170R^{0.85}$ (dB/km)	Predicted Rain Attenuation $A=0.38R28^{0.87}$ (dB/km)	Predicted Rain Attenuation $A=0.3367R^{0.9}$ (dB/km)
158	26.50	28.9618	29.6480	30.8315	31.3187	32.0652
154	26.38	28.3956	29.0460	30.1668	30.6277	31.3337
149	26.25	27.6830	28.2891	29.3322	29.7608	30.4166
146	26.13	27.2528	27.8325	28.8294	29.2388	29.8649
144	26.00	26.9649	27.5271	28.4934	28.8900	29.4964
138	25.88	26.0956	26.6056	27.4810	27.8398	28.3880
132	25.75	25.2175	25.6761	26.4621	26.7837	27.2747
126	25.63	24.3302	24.7381	25.4361	25.7214	26.1563
125	25.50	24.1814	24.5809	25.2644	25.5437	25.9694
123	25.38	23.8829	24.2658	24.9204	25.1878	25.5952
122	25.31	23.7332	24.1078	24.7481	25.0095	25.4078
121	25.25	23.5833	23.9496	24.5756	24.8311	25.2203
119	25.13	23.2826	23.6324	24.2299	24.4736	24.8448
118	25.06	23.1318	23.4734	24.0567	24.2946	24.6568
117	25.00	22.9807	23.3141	23.8833	24.1154	24.4687
115	24.69	22.6776	22.9947	23.5358	23.7563	24.0919
114	24.38	22.5256	22.8346	23.3617	23.5765	23.9033
113	24.25	22.3733	22.6743	23.1874	23.3965	23.7145
111	23.63	22.0678	22.3526	22.8381	23.0358	23.3364
108	23.00	21.6071	21.8680	22.3124	22.4932	22.7680
105	22.50	21.1434	21.3807	21.7845	21.9486	22.1980
103	21.88	20.8327	21.0543	21.4313	21.5844	21.8171
96	21.50	19.7337	19.9016	20.1868	20.3024	20.4780
90	20.00	18.7770	18.9001	19.1092	19.1939	19.3224
87	19.38	18.2932	18.3944	18.5664	18.6360	18.7418
85	18.75	17.9685	18.0553	18.2030	18.2628	18.3536
83	18.13	17.6421	17.7147	17.8383	17.8883	17.9644
78	17.75	16.8179	16.8557	16.9206	16.9471	16.9875
76	16.88	16.4849	16.5090	16.5511	16.5684	16.5949
75	16.50	16.3176	16.3350	16.3658	16.3785	16.3983
74	16.38	16.1498	16.1605	16.1802	16.1884	16.2014
73	16.25	15.9815	15.9856	15.9941	15.9979	16.0042
71	15.63	15.6433	15.6342	15.6209	15.6159	15.6090
69	15.25	15.3029	15.2809	15.2461	15.2325	15.2127
66	15.13	14.7880	14.7471	14.6808	14.6546	14.6161
63	15.00	14.2676	14.2083	14.1116	14.0734	14.0168
62	14.38	14.0929	14.0276	13.9210	13.8788	13.8164
61	13.75	13.9176	13.8463	13.7299	13.6839	13.6157
56	13.13	13.0306	12.9307	12.7672	12.7027	12.6070
53	12.75	12.4897	12.3735	12.1835	12.1085	11.9975
51	12.50	12.1252	11.9985	11.7915	11.7100	11.5893
50	11.38	11.9417	11.8099	11.5947	11.5100	11.3846
48	10.50	11.5722	11.4304	11.1993	11.1084	10.9739
44	9.25	10.8223	10.6618	10.4009	10.2985	10.1473
38	8.75	9.6670	9.4819	9.1823	9.0653	8.8930
34	7.88	8.8736	8.6747	8.3540	8.2292	8.0459
28	7.50	7.6414	7.4267	7.0831	6.9502	6.7559
26	6.50	7.2175	6.9992	6.6506	6.5163	6.3200
24	6.25	6.7861	6.5651	6.2132	6.0779	5.8808
23	5.63	6.5674	6.3453	5.9925	5.8570	5.6598
18	5.38	5.4378	5.2154	4.8654	4.7322	4.5393
15	4.13	4.7255	4.5076	4.1669	4.0380	3.8523
12	3.13	3.9795	3.7706	3.4470	3.3255	3.1514

APPENDIX K

Table K.1: Coefficient determination, R^2 calculation of enhancement k and α

	x Rain Intensity (mm/hr)	ln x	y Rain Attenuation (dB/km)	ln y	xy	x2	ŷ	SSE	SST	y2
	158	5.0626	26.4825	3.2765	16.5875	25.6299	3.4229	0.0215	0.2615	10.7353
	154	5.0370	26.3684	3.2722	16.4818	25.3709	3.4014	0.0167	0.2571	10.7071
	149	5.0039	26.2224	3.2666	16.3460	25.0395	3.3736	0.0115	0.2515	10.6708
	146	4.9836	26.1328	3.2632	16.2625	24.8363	3.3565	0.0087	0.2481	10.6484
	144	4.9698	26.0722	3.2609	16.2059	24.6990	3.3449	0.0071	0.2458	10.6333
	138	4.9273	25.8861	3.2537	16.0318	24.2778	3.3092	0.0031	0.2387	10.5866
	132	4.8828	25.6931	3.2462	15.8507	23.8418	3.2718	0.0007	0.2315	10.5380
	126	4.8363	25.4928	3.2384	15.6618	23.3896	3.2327	0.0000	0.2240	10.4872
	125	4.8283	25.4586	3.2371	15.6295	23.3126	3.2260	0.0001	0.2227	10.4785
	123	4.8122	25.3896	3.2343	15.5642	23.1571	3.2124	0.0005	0.2202	10.4610
	122	4.8040	25.3547	3.2330	15.5312	23.0786	3.2056	0.0008	0.2189	10.4521
	121	4.7958	25.3196	3.2316	15.4980	22.9996	3.1986	0.0011	0.2176	10.4431
	119	4.7791	25.7935	3.2501	15.5327	22.8400	3.1846	0.0043	0.2352	10.5633
	118	4.7707	25.5882	3.2421	15.4672	22.7594	3.1775	0.0042	0.2275	10.5114
	117	4.7622	25.3827	3.2341	15.4012	22.6783	3.1704	0.0041	0.2199	10.4592
	115	4.7449	24.9716	3.2177	15.2680	22.5144	3.1559	0.0038	0.2049	10.3539
	114	4.7362	24.7659	3.2095	15.2007	22.4316	3.1485	0.0037	0.1974	10.3007
	113	4.7274	24.5601	3.2011	15.1330	22.3482	3.1411	0.0036	0.1901	10.2472
	111	4.7095	24.1482	3.1842	14.9961	22.1797	3.1261	0.0034	0.1756	10.1392
	108	4.6821	23.5297	3.1583	14.7874	21.9224	3.1031	0.0030	0.1546	9.9746
	105	4.6540	22.9102	3.1316	14.5743	21.6593	3.0794	0.0027	0.1343	9.8068
	103	4.6347	22.4967	3.1134	14.4296	21.4807	3.0632	0.0025	0.1213	9.6931
	96	4.5643	20.6515	3.0278	13.8199	20.8333	3.0041	0.0006	0.0690	9.1675
	90	4.4998	19.4484	2.9678	13.3544	20.2483	2.9498	0.0003	0.0411	8.8076
	87	4.4659	18.8448	2.9362	13.1130	19.9443	2.9213	0.0002	0.0293	8.6215
	85	4.4427	18.4416	2.9146	12.9486	19.7372	2.9017	0.0002	0.0223	8.4949
	83	4.4188	18.0377	2.8925	12.7813	19.5262	2.8817	0.0001	0.0162	8.3663
	78	4.3567	17.0250	2.8347	12.3499	18.9809	2.8295	0.0000	0.0048	8.0354
	76	4.3307	16.6186	2.8105	12.1716	18.7553	2.8076	0.0000	0.0021	7.8990
	75	4.3175	16.4152	2.7982	12.0812	18.6407	2.7965	0.0000	0.0011	7.8300
	74	4.3041	16.2115	2.7857	11.9899	18.5250	2.7852	0.0000	0.0004	7.7602
	73	4.2905	16.0077	2.7731	11.8977	18.4080	2.7738	0.0000	0.0001	7.6899
	71	4.2627	15.5994	2.7472	11.7106	18.1704	2.7504	0.0000	0.0003	7.5473
	69	4.2341	15.2468	2.7244	11.5353	17.9277	2.7264	0.0000	0.0017	7.4222
	66	4.1897	14.6824	2.6866	11.2561	17.5532	2.6890	0.0000	0.0062	7.2181
	63	4.1431	14.1141	2.6472	10.9676	17.1656	2.6499	0.0000	0.0139	7.0075
	62	4.1271	13.9237	2.6336	10.8692	17.0332	2.6365	0.0000	0.0173	6.9358
	61	4.1109	13.7329	2.6198	10.7697	16.8993	2.6228	0.0000	0.0211	6.8633
	56	4.0254	12.7716	2.5472	10.2535	16.2035	2.5509	0.0000	0.0475	6.4883
	53	3.9703	12.1886	2.5005	9.9277	15.7632	2.5046	0.0000	0.0700	6.2525
	51	3.9318	11.7971	2.4679	9.7032	15.4593	2.4723	0.0000	0.0884	6.0903
	50	3.9120	11.6005	2.4511	9.5886	15.3039	2.4556	0.0000	0.0986	6.0077
	48	3.8712	11.2056	2.4164	9.3544	14.9862	2.4213	0.0000	0.1216	5.8390
	44	3.7842	10.4080	2.3426	8.8647	14.3201	2.3481	0.0000	0.1786	5.4876
	38	3.6376	9.1904	2.2182	8.0688	13.2320	2.2249	0.0000	0.2992	4.9203
	34	3.5264	8.3627	2.1238	7.4892	12.4352	2.1314	0.0001	0.4113	4.5104
	28	3.3322	7.0924	1.9590	6.5278	11.1036	1.9681	0.0001	0.6498	3.8377
	26	3.2581	6.6601	1.8961	6.1778	10.6152	1.9058	0.0001	0.7552	3.5953
	24	3.1781	6.2227	1.8282	5.8101	10.1000	1.8385	0.0001	0.8778	3.3423
	23	3.1355	6.0020	1.7921	5.6191	9.8313	1.8028	0.0001	0.9468	3.2116
	18	2.8904	4.8748	1.5841	4.5786	8.3542	1.5967	0.0002	1.3949	2.5093
	15	2.7081	4.1760	1.4294	3.8708	7.3335	1.4434	0.0002	1.7843	2.0431
	12	2.4849	3.4556	1.2400	3.0813	6.1748	1.2558	0.0002	2.3260	1.5376
Sum	**4490**	**226.849**	**945.0287718**	**146.552**	**644.9724**	**992.0113**		**0.109615**	**14.99495**	**420.2304**
Average	**84.71698113**	**4.28017**	**17.83073154**	**2.765131**						
count n =	**53**					**slope**	**Intercept**		**So: R2**	
						0.840739	**-0.83337**		**0.99269**	

APPENDIX L

L.1: Calculation of Link Margin

Table L.1: Calculation of link margin with varying link distance

T (dBm)	N_T	T_{total} (dBm)	S_r (dBm)	A (m^2)	N_R	A_{total} (m^2)	θ (mrad)	d (km)	L_G (dB)	L_F (dB)	LM dB	LM dB/km
7.7815	4	13.8021	-45	0.0050	4	0.0201	2	0.5	15.9176	4	38.8845	77.7690
7.7815	4	13.8021	-45	0.0050	4	0.0201	2	0.8	20.0000	4	34.8021	43.5026
7.7815	4	13.8021	-45	0.0050	4	0.0201	2	1	21.9382	4	32.8639	32.8639
7.7815	4	13.8021	-45	0.0050	4	0.0201	2	1.5	25.4600	4	29.3421	19.5614
7.7815	4	13.8021	-45	0.0050	4	0.0201	2	2	27.9588	4	26.8433	13.4217
7.7815	4	13.8021	-45	0.0050	4	0.0201	2	2.5	29.8970	4	24.9051	9.9620
7.7815	4	13.8021	-45	0.0050	4	0.0201	2	3	31.4806	4	23.3215	7.7738
7.7815	4	13.8021	-45	0.0050	4	0.0201	2	3.5	32.8196	4	21.9826	6.2807
7.7815	4	13.8021	-45	0.0050	4	0.0201	2	4	33.9794	4	20.8227	5.2057
7.7815	4	13.8021	-45	0.0050	4	0.0201	2	4.5	35.0025	4	19.7997	4.3999
7.7815	4	13.8021	-45	0.0050	4	0.0201	2	5	35.9176	4	18.8845	3.7769
7.7815	4	13.8021	-45	0.0050	4	0.0201	2	5.5	36.7455	4	18.0567	3.2830
7.7815	4	13.8021	-45	0.0050	4	0.0201	2	6	37.5012	4	17.3009	2.8835
7.7815	4	13.8021	-45	0.0050	4	0.0201	2	6.5	38.1965	4	16.6056	2.5547
7.7815	4	13.8021	-45	0.0050	4	0.0201	2	7	38.8402	4	15.9620	2.2803
7.7815	5	14.7712	-44	0.0050	5	0.0251	3	7.5	41.9922	4	12.7791	1.7039
7.7815	6	15.5630	-43	0.0050	6	0.0302	4	8	44.2597	4	10.3033	1.2879
7.7815	7	16.2325	-42	0.0050	7	0.0352	5	8.5	46.0550	4	8.1775	0.9621
7.7815	8	16.8124	-41	0.0050	8	0.0402	6	9	47.5552	4	6.2572	0.6952
7.7815	9	17.3239	-40	0.0050	9	0.0452	7	9.5	48.8522	4	4.4717	0.4707
7.7815	10	17.7815	-39	0.0050	10	0.0503	8	10	50.0000	4	2.7815	0.2782

Where

T	= Transmission Power (dBm)	- Supplied by vendor
N_T	= No of Transmitters	- Supplied by vendor
T_{Total}	= Total Transmitted Power (dBm)	- Calculation $-T + 10Log_{10}*(N_T)$
S_r	= Receiver Sensitivity (dBm)	- Supplied by vendor
A	= Receiver Aperture Area (m^2)	- Supplied by vendor
N_R	= No of Receivers	- Supplied by vendor
A_{Total}	= Total Receiver Area (m^2)	- Calculation $A^* N_R$
θ	= Beam Divergence (mrad)	- Supplied by vendor
d	= Link Distance (km)	- User requirement
L_G	= Geometric Loss (dB)	- Calculation - $-10\log_{10}[4A_{Total}/\pi(d\theta)^2$
L_F	= Fixed System Loss (dB)	- Supplied by vendor